

# **Role of BRD4 and histone acetylation in estrogen receptor-positive breast cancers**

**Dissertation**

for the award of the degree  
“Doctor rerum naturalium (Dr. rer. nat.)“  
of the Georg-August-Universität Göttingen

Submitted by  
**Sankari Nagarajan**

born in  
**Villupuram, India**

Göttingen, 2015

## Thesis Supervisor:

Prof. Dr. Steven A. Johnsen

## Doctoral Committee:

Prof. Dr. Steven A. Johnsen (Reviewer)

Clinic for General, Visceral and Pediatric Surgery

University Medical Center Göttingen

Prof. Dr. Dieter Kube (Reviewer)

Dept. of Haematology and Oncology

University Medical Center Göttingen

Dr. Halyna Shcherbata

Max-Planck Institute of Biophysical Chemistry

Am Fassberg, Göttingen

Date of oral examination: 18 May, 2015

# Affidavit

I hereby declare that the PhD thesis entitled “Role of BRD4 and histone acetylation in estrogen receptor-positive breast cancers” was written independently and with no other sources and aids than quoted.

---

Sankari Nagarajan

March, 2015

Göttingen

# Table of contents

<b>List of Abbreviations</b>	I
<b>List of Figures</b>	IX
<b>Summary</b>	X
<b>1. Introduction</b>	
<b>1.1. Breast cancers and hormone dependency</b>	1
<b>1.2. Estrogen receptor</b>	1
1.2.1. Structure of estrogen receptor	2
1.2.2. Mechanism of estrogen receptor mediated transcription	3
1.2.2.1. Estrogen response elements	4
1.2.2.2. FOXA1 is a pioneer factor for ER $\alpha$ activity	4
1.2.2.3. Transcriptional coactivators of estrogen induction	6
1.2.2.4. Long range chromosomal interactions	8
1.2.2.5. Transcription complex assembly and disassembly	12
1.2.3. Dysregulation of estrogen receptor activity for breast cancer therapy	13
<b>1.3. Nucleosomal organization and histone modifications</b>	15
1.3.1. Histone code and cross-talk	15
1.3.2. Histone acetylation in estrogen induced transcription	16
1.3.3. Epigenetic readers and BRD4	18
1.3.3.1. Structure of BRD4 and development of BRD4 inhibitors	19
1.3.3.2. BRD4 in regulating gene transcription	21
1.3.3.3. BRD4 in cancer	24
1.3.4. Histone ubiquitination in breast cancer	25
<b>1.4. Enhancer RNAs in regulating transcription</b>	27

## **2. Publications**

2.1. Publication I	30
Bromodomain protein BRD4 is required for estrogen receptor-dependent enhancer activation and gene transcription	
2.1.1. Supplementary information	54
2.2. Publication II	88
H4K12ac is regulated by estrogen receptor-alpha and is associated with BRD4 function and inducible transcription	
2.2.1. Supplementary information	107
<b>3. Discussion</b>	<b>112</b>
<b>4. Reference</b>	<b>126</b>
<b>5. Acknowledgements</b>	<b>145</b>
<b>6. Curriculum Vitae</b>	<b>147</b>

## List of Abbreviations

%	Percentage
(NH <sub>4</sub> ) <sub>2</sub> SO <sub>4</sub>	Ammonium Sulphate
µg	Microgram
µl	microliter
µM	micromolar
18 SrRNA	Ribosomal RNA with Sedimentation rate 18S
3C	Chromosomal Conformation Capture
A549	Adenocarcinomic human alveolar basal epithelial cells
<i>ACTB</i>	Coding gene for beta- actin
AF1/2	Activation Function-1/2
AIB1	Amplified In Breast Cancer-1
ANOVA	Analysis of Variance
AP2γ	Activating enhancer binding Protein 2 Gamma
AR	Androgen receptor
ATAD5	ATPase family, AAA domain containing-5
ATM	Ataxia Telangiectasia Mutated
ATR	Ataxia Telangiectasia and Rad3 related
BAF	BRG1- or BRM-associated factors
bam	Binary Version of sam files
<i>BCL2</i>	B-cell CLL/lymphoma 2
BD1	Bromodomain-1
BD2	Bromodomain-2
BET	Bromodomain and Extraterminal Domain
BID	Basic Interaction Domain
bigwig	Binary Version of wiggle files
BRD1/2/3/4	Bromodomain-containing protein 1/2/3/4
BRDT	Bromodomain-containing protein testis-specific
BRG1	Brahma-Related Gene-1
BRM	Brahma
C57BL/6	C57 black 6 mice
<i>CA12</i>	Carbonic Anhydrase XII

CARM1	Coactivator-associated Arginine Methyltransferase-1
CBP	cAMP-response element-binding protein (CREB) binding protein
CCND1	Cyclin D1
CDK8/9	Cyclin-Dependent Kinase-8/9
cDNA	Complementary DNA
CHD4	Chromodomain and Helicase containing protein-4
ChIA-PET	Chromatin Interaction Analysis by Paired-End Tag Sequencing
ChIP	Chromatin Immunoprecipitation
ChIP-3C	ChIP coupled with 3C
ChIP-seq	ChIP-coupled with next generation sequencing
c-MYC	avian Myelocytomatosis viral oncogene homolog
CO <sub>2</sub>	Carbon-dioxide
CPRIT	Cancer Prevention Research Institute of Texas
CSS	Charcoal-Stripped Serum
CTCF	CCCTC-binding Factor
CTD	Carboxy-Terminal Domain
CTSD	Cathepsin D
<i>CXCL12</i>	Chemokine (C-X-C motif) Ligand 12
DBD	DNA Binding Domain
<i>DHFR</i>	Dihydrofolate Reductase
DHS	DNase I-hypersensitivity sites
DMEM	Dulbecco- Minimum Essential medium
DMSO	Dimethyl sulfoxide
DNA	Deoxyribonucleic acid
DNase-seq	Sequencing of DNA samples after DNase treatment
DNMT1	DNA methyltransferase-1
dNTP	Deoxyribo Nucleotide Tri Phosphate
DRB	5,6-Dichloro-1-beta-D-ribofuranosylbenzimidazole
DSIF	DRB sensitivity Inducing factor
E2	Estrogen
EDTA	Ethylene Diamine Tetra Acetic Acid
EGF	Epidermal Growth Factor
EMBO	European Molecular Biology Organization

ER+	Estrogen Receptor-positive
ERBB2	v-erb-b2 avian Erythroblastic leukemia viral oncogene homolog 2
ERE	Estrogen Response Element
eRNA	Enhancer RNA
ER $\alpha$	Estrogen Receptor-Alpha
ER $\beta$	Estrogen Receptor-Beta
ES	Enrichment Score
ESR1	Estrogen Receptor-Alpha gene
ESR2	Estrogen Receptor-Beta gene
ET	Extra-terminal Domain
exp.	Expression
FAIRE	Formaldehyde-Assisted Isolation of Regulatory Elements
FDR	False Discovery Rate
FISH	Fluorescence <i>in-situ</i> Hybridization
<i>FOSL1</i>	FBJ murine osteosarcoma viral oncogene homolog-Like Antigen-1
FOXA1	Forkhead box-containing protein-A1
G3	Grading system-3 of tumors
<i>GAPDH</i>	Glyceraldehyde 3-Phosphate Dehydrogenase
GATA3	GATA binding protein-3
GCN5	General Control Nonderepressible-5
GLTSCR1	Glioma Tumor Suppressor Candidate Region gene-1
GnRH	Gonadotropin-Releasing Hormone
<i>GREB1</i>	Growth Regulation by Estrogen in Breast cancer-1
GRIP1	Glucocorticoid Receptor-Interacting Protein 1
GRO-seq	Global Run-on Assay coupled with sequencing
GSEA	Gene Set Enrichment Analysis
H1299	Human non-small cell lung carcinoma cell line from the lymph node
H2Bub1	Histone H2B monoubiquitination at Lys 120
H3K18ac	Histone H3 acetylation at lysine 18
H3K27ac	Histone H3 acetylation at Lys 27
H3K27me3	Histone H3 trimethylation at Lys 27
H3K36me3	Histone H3 trimethylation at lysine 36
H3K4me1	H3 monomethylation at Lys 4



H3K4me2	Histone H3 dimethylation at lysine 4
H3K4me3	Histone H3 trimethylation at Lys 4
H3K79me3	Histone H3 trimethylation at lysine 79
H3R2/17/26	Histone H3 Arginine residues 2/17/26
H3S10ph	Histone H3 phosphorylation at serine 10
H4K12ac	Histone H4 acetylation at Lys 12
H4K16ac	Histone H4 acetylation at Lys 16
H4K5	Histone H4 lysine 5
H4K8	Histone H4 lysine 8
H4R3	Histone H4 Arginine residue 3
HAT	Histone Acetyl Transferase
HDAC	Histone Deacetylase
HER2/EGFR	Human Epidermal growth factor Receptor-2
HEXIM	HEXAmethylene bisacetamide Inducible protein
hg19	Human Genome Project version 19
hGH	human Growth Hormone
HNF3 $\alpha$	Hepatocyte Nuclear factor-3 alpha
<i>HNRNPK</i>	Heterogeneous Nuclear Ribo Nucleo Protein K
hr	hour
HS2	DNase Hyper-Sensitivity site-2
HSC70	Heat Shock Protein-70 kDa
HSD	Honest Significant Difference
IBET	Inhibitor of BET
ICI	ICI-182,780
IgG	Immunoglobulin G
Il1b	Interleukin-1 beta
JMJD6	Jumonji-domain containing histone demethylase-6
JQ1	named after Dr. Jun Qi
kb	kilo base pairs
kg	kilogram
<i>KLF4/10</i>	Kruppel-like factor 4
LARP7	La Related Protein-7
LBD	Ligand Binding Domain

LCR	Locus Control Region
LiCl	Lithium Chloride
LNA	Locked Nucleic Acids
M	Molar
MACS	Model-based Analysis of ChIP-seq
Mad211	Mitotic Arrest Deficient Yeast, Homolog-2-Like 1
MAPK	Mitogen-Activated Protein kinase
Mb	Million base pairs
MCF10A	Michigan Cancer Foundation-10A
MCF7	Michigan Cancer Foundation-7
MED1	Mediator complex Protein-1
mg	milligram
MgCl <sub>2</sub>	Magnesium Chloride
ml	milliliter
MLL/COMPASS	Mixed Lineage Leukemia Complex of Proteins Associated with Set-1
mM	millimolar
MOF	Males absent On the First
mRNA-seq	Next generation sequencing of mRNA samples
MSK1/2	Mitogen- and Stress-activated protein Kinase-1/2
<i>MYB</i>	avian Myeloblastosis viral oncogene homolog
NaCl	Sodium Chloride
NCBI	National Center for Biotechnology Information
NCOR1/2	Nuclear Corepressor-1/2
NELF	Negative Elongation Factor
NES	Normalized Enrichment Score
NFAT	Nuclear Factor of Activated T-cells
NF-κB	Nuclear Factor 'kappa-light-chain-enhancer' of activated B-cells
ng	nanogram
NIH	National Institute of Health
NLS	Nuclear Localization Signal
nM	nanomolar
NMC	NUT midline carcinoma

---

NP-40	Nonidet P40
NPS	N-terminal Cluster of Phosphorylation Sites
NRIP1	Nuclear Receptor Interacting Protein 1
NSD3	Nuclear SET Domain-Containing Protein-3
NTD	N-terminal Domain
NuRD	Nucleosome Remodeling and Deacetylase
NUT	Nuclear Protein in Testis
OTX015	Oncoethix-015
OVCAR3	Ovarian Carcinoma-3
<i>P2RY2</i>	Purinergic Receptor P2Y, G-protein coupled, 2
p300	E1A binding protein p300
PBS	Phosphate-Buffered Saline
PBX1	Pre-B-cell leukemia homeobox-1
PCA	Principal Component Analysis
PCAF	p300/CBP-Associated Factor
PCR	Polymerase Chain Reaction
PGR	Progesterone Receptor
PID	P-TEFb Interacting Domain
PR	Progesterone Receptor
PRMT1/4	Protein Arginine Methyltransferase-1/4
P-TEFb	positive Transcription Elongation Factor-b
p-value	probability value of rejecting a null-hypothesis
qPCR	Quantitative Polymerase Chain Reaction
RAD21	Double-Strand-Break Repair Protein
Ran	RAS Oncogene Family
Rel.	Relative
<i>RET</i>	Receptor Tyrosine Kinase
RIPA	Radio-Immunoprecipitation buffer
RNA	Ribonucleic Acid
RNA-seq	Next generation sequencing of RNA samples
RNAPII	RNA Polymerase II
RNAPII P <sub>Ser2</sub>	Phosphorylation of RNAPII serine 2 residues
RNF20/40	Ring Finger Protein-20/40

---

RPLP0	Ribosomal Protein, Large, P0
SAGA	Spt-Ada-Gcn5 acetyltransferase
sam	Sequence Alignment/Map
SD	Standard Deviation
SDS	Sodium dodecyl Sulphate
SDS-PAGE	Sodium dodecyl Sulphate- Polyacrylamide Gel Electrophoresis
SERM	Selective Estrogen Receptor Modulator
SERPINE1	Serpin Peptidase Inhibitor, clade E, member 1
SGC	Structural Genomics Consortium
<i>SIAH2</i>	Seven In Absentia Homolog-2
siBRD4	BRD4 siRNA
siCont	Negative Control siRNA
siRNA	small interfering RNA
<i>SMAD7</i>	Mothers Against Decapentaplegic, Drosophila Homolog-7
SMC1/3	Structural Maintenance of Chromosomes-1/3
Spt6	Suppressor of Ty 5 Homolog-6
SRC1/2/3	Steroid Receptor Coactivator-1/2/3
STAG1	Stromal Antigen-1
SUPT4H	Suppressor of Ty 5 Homolog-4
SUPT5H	Suppressor of Ty 5 Homolog-5
SUPT6H	Suppressor of Ty 5 Homolog-6
SUV39H1	Suppressor of Variegation 3-9 Homolog 1
SWI/SNF	SWItch/Sucrose NonFermentable
TAFII250	TATA box binding protein (TBP)-associated factor, 250kDa
Taq	<i>Thermus aquaticus</i>
TBP	TATA box Binding Protein
TE	Tris-EDTA
<i>TFF1</i>	Trefoil Factor-1
TGF- $\alpha$	Transforming Growth Factor alpha
TGF- $\beta$ 1	Transforming Growth Factor beta1
<i>TMPRSS3</i>	Transmembrane Protease, Serine 3
TR	Transcribed Region
TSS	Transcription Start Site

U2OS	U-2 Osteosarcoma
UCSC	University of California - Santa Cruz
USP22	Ubiquitin-specific Protease 22
v/v	volume/volume
Veh	Vehicle
w/v	weight/volume
WAC	WW domain-containing Adapter protein
WB	Western Blot
WHSC1	Wolf-Hirschhorn Syndrome Candidate-1
WHSC1L1	Wolf-Hirschhorn Syndrome Candidate-1-Like-1
wig	Wiggle
wt.	weight
XBP1	X-box binding protein 1

# List of Figures

## 1. Introduction

Figure 1.1	Structure of estrogen receptor- $\alpha$ (ER $\alpha$ )	3
Figure 1.2	Association of pioneer factor and transcriptional cofactors in ER $\alpha$ -regulated transcription	7
Figure 1.3	Commonly studied histone modifications and their correlation with transcriptional activation or repression	16
Figure 1.4	Structure of BRD4 with its interacting proteins	20
Figure 1.5	Regulation of BRD4 and histone marks in coordinating transcriptional activation	22

## 2.1. Publication I

Figure 2.1.1	BRD4 perturbation impairs E2-induced gene expression	33
Figure 2.1.2	Inhibition and knockdown of BRD4 affect proliferation and uterine growth	36
Figure 2.1.3	BRD4 occupies promoters and correlates with active transcription	37
Figure 2.1.4	BRD4 binds to ER <sup>+</sup> enhancers after ER $\alpha$ recruitment and H3K27ac and regulates eRNA synthesis	41

## 2.2. Publication II

Figure 2.II.1	H4K12ac correlates with BRD4 binding in estrogen-induced transcription	93
Figure 2.II.2	H4K12ac correlates with BRD4 binding in estrogen-induced enhancer function	95
Figure 2.II.3	H4K12ac correlates with BRD4 function in regulating gene expression	96
Figure 2.II.4	H4K12ac positively correlates with gene expression	98
Figure 2.II.5	H4K12ac depends upon ER $\alpha$ activity	99

## 3. Discussion

Figure 3.1	Mechanism of histone acetylation and BRD4 in regulating estrogen-induced transcription	112
Figure 3.2	Therapeutic targeting of the ER $\alpha$ -regulated transcriptional pathway by the inhibitors	123

## Summary

The estrogen receptor- $\alpha$  (ER $\alpha$ ) acts as a nuclear transcription factor to promote estrogen-induced transcription and plays a central role in the progression of ER-positive tumors. ER $\alpha$  binds to the consensus DNA elements referred to as Estrogen Response Elements (EREs) which act as enhancers mostly occupying distal regions. In our study, we show that Bromodomain-containing protein, BRD4 depletion/inhibition regulates estrogen-induced transcription by affecting RNA polymerase II (RNAPII) and histone monoubiquitination in ER-positive MCF7 cells. Furthermore, BRD4 controls the proliferation of breast and endometrial cancer cell lines *in vitro* and estrogen-dependent uterine growth *in vivo*. Genome-wide studies demonstrate the increased occupancy of BRD4 near transcriptional start sites (TSS) upon estrogen stimulation and BRD4 inhibition decreases estrogen-stimulated H2B monoubiquitination across gene bodies substantially on the genes which display estrogen-induced *de novo* polymerase recruitment. Consistently, BRD4 binding correlates with active transcriptional marks on the promoters. Moreover, BRD4 also occupies ER $\alpha$  and FOXA1-bound distal elements after the appearance of ER $\alpha$ , H3K27ac and Cohesin. Interestingly, BRD4 inhibition regulates the RNAPII recruitment as well as phosphorylation on distal regions and inhibits the production of enhancer RNAs (eRNAs). Altogether these findings establish a specific coactivator function of BRD4 in estrogen-dependent transcription (Nagarajan et al., 2014).

BRD4 binds to the acetylated chromatin preferentially on histone H4 at Lys 5, 8, 12 and 16 residues. In our study, we also show that the presence of H4K12ac correlates with BRD4 occupancy during estrogen-driven transcription. Consistent with BRD4 binding, H4K12ac occupancy increases adjacent to estrogen-induced gene promoters and distal ER $\alpha$ -bound regions. H4K12ac is correlated with eRNA transcription and RNAPII occupancy on enhancers. Surprisingly, H4K12ac occupancy is increased in ER-positive cell lines compared to ER-negative cell lines and estrogen promotes global acetylation of H4K12ac in ER-positive cells. Notably, estrogen-induced H4K12ac occupancy is highly dependent on ER $\alpha$  expression and activity. Altogether these findings confirm the importance of H4K12ac and BRD4 in ER $\alpha$ -induced transcription and provide a strong rationale for the development of

potential therapeutic approaches for targeting histone acetylation and BRD4 in ER $\alpha$ -positive breast tumors (Nagarajan et al., 2015).



# 1. Introduction

## 1.1. Breast cancers and hormone dependency

Breast cancer is the second most frequently diagnosed cancer and the leading cause of cancer-related death in women reported in the global cancer statistics for the year 2012 (Ferlay et al., 2015). Occurrence of breast cancer is well-correlated with lifestyle and is most prevalent in more developed regions of the world. Other than the environmental factors and lack of physical activity as being some of many risk factors, breast cancer can be hereditary and highly influenced by age and hormonal status in women.

Estrogen, which is a primary female sex hormone, plays an important role in the normal development of reproductive organs like breast, ovaries and uterus in women. It plays a central role in the development of the mammary gland during ductal elongation, side branching and lactational differentiation after puberty (Briskin and O'Malley, 2010). Dysregulation in its signaling can lead to development of breast cancer. The importance of hormones in breast cancers was initially identified due to the studies using ovariectomy (removal of ovaries) in an advanced breast cancer patient (Beatson, 1896). Moreover, the risk for breast cancer in women increases at the late menarche and early menopause stages reflecting the role of estrogen in cancer progression (Russo and Russo, 2006). Around two-thirds of breast cancers are estrogen receptor-positive. Estrogen mainly affects the proliferation of breast epithelial cells via promoting the transcription of various cell cycle-regulatory genes, which could act as tumor promoters and repressing genes, which negatively regulate cell proliferation (Cicatiello et al., 2010). Thus estrogen elicits its major endocrine effect by transcriptional regulation of gene expression.

## 1.2. Estrogen receptor

Estrogen mediates transcriptional activity via binding to the estrogen receptor (ER), which belongs to subfamily-3 of nuclear steroid receptors. ER acts mostly as a ligand-dependent nuclear transcription factor which can bind to DNA after estrogen activation and regulate transcription. Estrogen receptor exists as two isoforms referred to as ER $\alpha$  encoded by the *ESR1* gene and ER $\beta$  encoded by the *ESR2*

gene. These isoforms are very similar in structure. Similar to ER $\alpha$ , ER $\beta$  is also shown to be important for the development of female reproductive organs, but its role in mammary glands is poorly established. In contrast to ER $\alpha$ , it is differentially distributed in tissues like testis, thymus, spleen and ovaries (Mosselman et al., 1996). In the breast, expression and function of ER $\alpha$  is associated with epithelial cells and ER $\beta$  with stromal cells. Importantly in breast cancer cells, these receptors were also shown to possess opposite functions - where ER $\beta$  can inhibit ER $\alpha$  function (Omoto et al., 2003; Peng et al., 2003). Extensive research on ER $\alpha$  greatly allowed us to understand its role in the context of gene induction mechanisms in breast development and tumorigenesis (Green and Carroll, 2007).

### 1.2.1. Structure of estrogen receptor

The structure of estrogen receptor is conserved across various nuclear receptors (Sommer and Fuqua, 2001; Kumar et al., 2011). It possesses three structural domains: N-terminal domain (NTD), DNA-binding domain (DBD) and ligand-binding domain (LBD), where the functional domains of the receptor are referred to as A to H (Figure 1.1). The transcriptional activity of ER is determined by the presence of Activation Function domains AF1/2. Domains A and B are located in the NTD and constitute the AF1 domain, which functions in a hormone-independent manner. These domains also show high variability among all the steroid receptors. ER $\beta$  has a shorter NTD than ER $\alpha$  and displays only 15% homology in this domain. The DBD (C-domain) binds to DNA through its two zinc finger motifs. The first zinc finger located in the N-terminal region exerts an important function of allowing the nuclear receptor to bind to the consensus DNA sequence called the Estrogen Response Element (ERE) which consists of mostly a 13 bp palindromic motif GGTCAnnnTGACC. The second zinc finger regulates protein-DNA interactions which could be non-specific. ER further possesses a dimerization domain which allows it to form homo- or heterodimers after estrogen activation and bind to EREs. This domain importantly exerts more than 95% homology between ER $\alpha$  and ER $\beta$ . The D domain, otherwise called the hinge region contains a nuclear localization signal and also elicits coregulator binding property. E and F domains contain the LBD and are present in the C-terminal domain of the receptor. The LBD contains the structural pocket for the binding of estrogen and exhibits around 55% homology between the two ER isoforms. Moreover, these allow transcriptional coactivators or

repressors to bind. The LBD also has various other important functional domains including a nuclear localization signal, a dimerization domain, and binding sites for coregulators and referred to as AF2. Therefore, this domain is considered to be very important for the estrogen-dependent transcriptional activity.

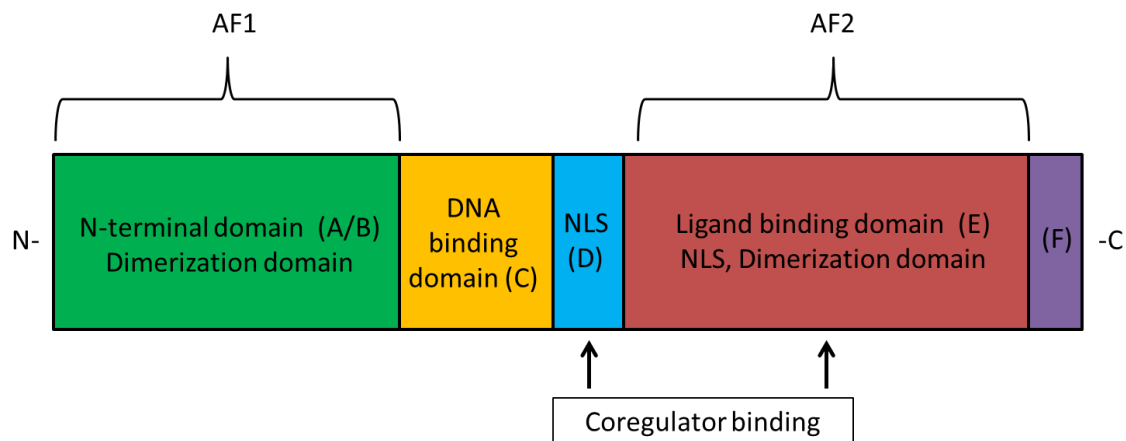


**Figure 1.1. Structure of estrogen receptor- $\alpha$  (ER $\alpha$ ).** The functional domains are shown according to their location and as A-F within brackets. The domains which interact with transcriptional coregulators are denoted with arrows as coregulator binding. Parentheses denote the activation function domains AF1 and AF2 (adapted from Sommer and Fuqua, 2001; Kumar et al., 2011).

### 1.2.2. Mechanism of estrogen receptor-mediated transcription

After estrogen stimuli, estrogen receptor executes the following subsequent processes to exert its transcriptional activity:

- Receptor dimerization
- Binding of the receptor to EREs
- Recruitment of coactivators and histone-modifying enzymes

Upon estrogen-activation, ER $\alpha$  undergo structural changes which promote dimerization. Reports show that ER $\beta$  can also heterodimerize with ER $\alpha$  (Cowley et al., 1997; Pace et al., 1997). Interestingly, ER $\alpha$  dominates its transcriptional role during heterodimerization with ER $\beta$  and this leads to the transcriptional activation (Cowley et al., 1997; Pace et al., 1997; Li et al., 2004). The resulting ER $\alpha$  homo- or heterodimers get recruited to EREs to control target gene transcription.

### 1.2.2.1. Estrogen response elements

The transcriptional activity of ER $\alpha$  is carried out by binding of the dimerized receptor to EREs after estrogen stimulation. These DNA elements are widely conserved among several vertebrates. Importantly, they act as transcriptional enhancers which could be present as regulatory elements frequently located far away from gene promoters. These regions are occupied with transcriptional coactivators and active histone marks and enhance transcriptional activation in a cell-specific manner (Heintzman et al., 2009; Heinz et al., 2015). These regions are particularly interesting in the context of ER $\alpha$ -regulated transcription as they are mostly distal. Only around 3-4 % of ER $\alpha$  binding sites occupy the promoter proximal regions or gene-bodies (Carroll et al., 2006; Li et al., 2013). The rest of them are located distal to gene promoters and appear to regulate the transcription of these genes. Distal ER binding sites are frequently considered as enhancers. Studies show that distal EREs influence the estrogen-induced transcription in an efficient manner comparing to EREs which are located close to the promoters (Pan et al., 2008). Altogether these studies suggest that distal ER $\alpha$  binding sites function as *bona fide* enhancers to promote estrogen-responsive transcription.

### 1.2.2.2. FOXA1 is a pioneer factor for ER $\alpha$ activity

Pioneer factors are very important in facilitating ER $\alpha$  binding to ERE in a chromatin context. Pioneer factors are DNA binding proteins which can bind to the condensed chromatin efficiently and enable ATP-independent chromatin remodeling. The DNA binding domain of these proteins contains winged helices which resemble histone H1 (Clark et al., 1993). This allows the pioneer factors to bind to the major groove of DNA even in a condensed chromatin state. However, unlike histone proteins, these factors don't compact the chromatin due to the absence of four basic amino acid sequences within the winged-helix domain compared to H1 and they associate with chromatin with their C-terminal domains binding to H3 and H4 histones (Cirillo et al., 1998, 2002). Importantly, the Forkhead box-containing family of proteins (FOX) are among the predominant pioneer factors which determine tissue specific-transcription (Kato and Kato, 2004). FOXA factors were identified initially as activators of liver-specific gene expression in rat and hence also referred to as Hepatocyte Nuclear Factor (HNF).

FOXA1 (HNF3 $\alpha$ ) was found to be associated with breast cancer prognosis and is predominantly expressed in luminal type A breast cancers. This has been implicated for ER $\alpha$  expression and activity (Nakshatri and Badve, 2007; Hu et al., 2014). Moreover, FOXA1 is mutated or amplified as a focal region in 1.8% of breast cancers (Robinson et al., 2013). Reports using chromatin immunoprecipitation assays coupled with sequencing (ChIP-seq) confirmed the involvement of FOXA1 protein in estrogen-regulated transcription (Hurtado et al., 2011). Motif analysis of estrogen receptor binding sites revealed an enrichment of FOXA1 binding motifs in regions bound by ER $\alpha$ . Around 50% of the ER $\alpha$  binding sites are also bound by FOXA1 in different ER $\alpha$ -positive breast cancer cell lines. Notably, upon depletion of FOXA1, ER $\alpha$  recruitment is significantly decreased on a large fraction of EREs identified in ER $\alpha$ -positive MCF7 breast cancer cells. Consistently, around 95% of estrogen-induced genes are affected by FOXA1 knockdown. These findings show that FOXA1 is required for the binding of ER $\alpha$  on the EREs and regulate estrogen-mediated transcription. Other pioneer factors like PBX1, TLE, AP2 $\gamma$  and GATA3 can also associate with FOXA1 and influence ER $\alpha$  binding directly (Jozwik and Carroll, 2012; Theodorou et al., 2013).

Consistent with a role in promoting ER $\alpha$  activity, FOXA1 knockdown exhibited decreased estrogen-induced proliferation of ER $\alpha$ -positive cell lines. Tamoxifen belongs to the Selective Estrogen Receptor Modulator (SERM) family of drugs commonly used as a chemotherapeutic agent against ER $\alpha$ -positive breast cancers. Notably, 93% of tamoxifen-induced ER $\alpha$  binding sites in tamoxifen-sensitive cells overlap with those induced by estrogen. These sites also show the requirement of FOXA1 for the binding of ER $\alpha$ . Furthermore, around 55% of the unique ER $\alpha$ -binding sites in tamoxifen-resistant cells interestingly are co-occupied with FOXA1 and ER $\alpha$  binding requires FOXA1 in these regions. Consistently, overexpression of ER $\alpha$  and FOXA1 in ER-negative cells including the osteosarcoma cell line U2OS and ovarian cancer cell line OVCAR3 enable ER $\alpha$  binding to EREs bound in FOXA1/ER $\alpha$ -positive cells. Moreover, FOXA1 maintains an open chromatin state for ER $\alpha$  to bind and ER $\alpha$  binding is less on the regions which are not already open and not bound by FOXA1. FOXA1 is also responsible for the maintenance of open chromatin on the promoters of estrogen-activated genes. These studies show that FOXA1 is very

important for determining overall ER $\alpha$  binding in ER $^+$  cells and thus estrogen-dependent transcription (Hurtado et al., 2011).

### 1.2.2.3. Transcriptional coactivators of estrogen induction

Upon binding to EREs, ER can recruit several transcriptional coregulators including the p160 family of coactivators, cAMP-response element-binding protein (CREB) binding protein (CBP), p300, p300/CBP-Associated Factor (PCAF), chromatin remodeling complexes like SWItch/Sucrose NonFermentable (SWI/SNF) complex or BRG1- or BRM-associated factors (BAF), histone methyltransferases like Coactivator-associated Arginine Methyltransferase-1 or Protein Arginine Methyltransferase-4 (CARM1/PRMT4) and PRMT1. The recruitment of these cofactors relies upon the activation function domains of ER $\alpha$  (Figure 1.2) (Sommer and Fuqua, 2001; Green and Carroll, 2007).

AF1 and AF2 can regulate transcription independently as well as synergistically. Moreover, these domains determine the agonist or antagonist activities of anti-estrogens by associating with distinct transcriptional complexes in a context- and tissue-specific manner. Both of these domains exhibit binding with important transcriptional cofactors of estrogenic activity like Steroid Receptor Coactivator-1 (SRC-1) and exert cell type-specific activity. The structure of ER $\alpha$  LBD containing the AF2 domain and bound with 17  $\beta$ -estradiol (estrogen-E2) or tamoxifen has been characterized (Wrenn and Katzenellenbogen, 1993; Green and Carroll, 2007). This contains 12  $\alpha$ -helices named as H1-H12 and interestingly both estrogen and tamoxifen bind to the same helical pocket of ER $\alpha$ . However, upon estrogen binding, helices 3, 4, 5 and 12 undergo conformational changes to interact with proteins which contain LXXLL motifs including the p160 coactivators SRC1, amplified in breast cancer-1 (AIB1) or SRC3 and Glucocorticoid Receptor-Interacting Protein-1 (GRIP1) or SRC2. LXXLL motif is commonly called the nuclear Receptor Interaction Domain (RID). Contradictorily, when tamoxifen binds to ER $\alpha$  the helical pocket, helix H12 is placed in a conformation such that ER $\alpha$  no longer recognizes LXXLL-containing proteins, but interacts with proteins containing an LXXML motif (Shiau et al., 1998). This interrupts the interaction of ER $\alpha$  with p160 family of proteins and promotes ER $\alpha$  binding to transcriptional corepressors like Nuclear Corepressor-1/2 (NCOR1/2). Thus, binding of estrogen and tamoxifen to ER $\alpha$

exhibits different structural changes which promote differential transcriptional activity in a ligand-specific manner.

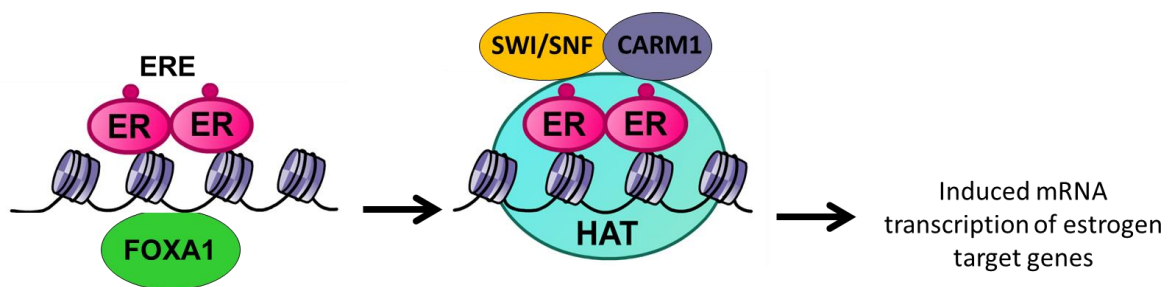


**Figure 1.2. Association of pioneer factor and transcriptional cofactors in ER $\alpha$ -regulated transcription.** Binding of FOXA1 on Estrogen Response Elements (EREs) facilitates the binding of ER $\alpha$  dimers which further leads to the recruitment of Histone Acetyltransferases (HATs), SWItch/Sucrose NonFermentable (SWI/SNF) complex and CARM1 to promote transcription.

Acetylation of histones appears to play a vital role of promoting transcriptional activation by recruiting several transcription factors and chromatin remodeling complexes. This further facilitates chromatin opening to promote transcription. Histone acetylation is mediated by Histone Acetyl-Transferases (HATs). Some of the notable HATs are CBP, p300 and PCAF. Interestingly, SRC1 also possesses intrinsic histone acetyltransferase activity (Spencer et al., 1997). These acetylate histones H3 and H4 at several residues and facilitate transcriptional activation. Importantly, CBP and p300 are involved in catalyzing histone acetylation which is associated with ER $\alpha$ -induced transcriptional activity. Recent cryo-electron microscopy studies validate the presence of p300 in the active ER $\alpha$ -coactivator complex (Yi et al., 2015). Furthermore, CBP/p300 and PCAF form a complex with p160 coactivators. This helps in the recruitment of the whole coactivator complex to EREs and induce estrogen-responsive transcription (Kamei et al., 1996; Korzus et al., 1998; Kim et al., 2001; Demarest et al., 2002). These factors can also interact with ER $\alpha$  in its AF1 and/or AF2 domain. Eventually, this facilitates their synergistic regulation of ER $\alpha$ -mediated transcription (Webb et al., 1998; Kobayashi et al., 2000). Moreover, acetylation of chromatin adjacent to estrogen-induced promoter of TFF1 facilitates the binding of TATA box Binding Protein (TBP) which further recruits other transcription factors on promoters for activating transcription (Sewack et al., 2001). Importantly, CBP and p300 are shown to be highly expressed in breast cancers and high expression of p300 is well-correlated with the poor prognosis of patients with

breast cancer (Hudelist et al., 2003; Xiao et al., 2011). These factors along with p160 proteins are also shown to be involved in ER $\alpha$ -dependent gene induction in tamoxifen-resistant breast cancers which express ER, Human Epidermal Growth Factor Receptor 2 (HER2/EGFR) and ER $\alpha$ -associated coactivator AIB1/SRC3 (Shou et al., 2004). All these findings demonstrate that HATs play an essential role in the activation of gene expression under estrogen-stimulation by interacting with ER $\alpha$ .

In addition to histone acetylation, histone methylation has a crucial function in ER $\alpha$ -induced transcription. Some of the histone methyltransferases methylate arginine residues on histones. For example, CARM1 was shown to methylate arginine residues 2, 17 and 26 of histone H3 (H3R2, H3R17 and H3R26), whereas PRMT1 was shown to methylate histone H4 at arginine 3 (H4R3). The role of these enzymes and their respective marks appears to be very important for estrogen-regulated transcription (Bauer et al., 2002; Ma et al., 2001; Métivier et al., 2003; Schurter et al., 2001; Wagner et al., 2006). Furthermore, CARM1 was found to be recruited directly by ER $\alpha$  and p160 proteins and it cooperates with p160 and p300 proteins to synergistically induce estrogen-stimulated transcription (Chen et al., 1999, 2000). Importantly, during estrogen response, CARM1 was also shown to recruit the SWI/SNF complex proteins (Brahma-Related Gene-1 (BRG1) and BRG1- or BRM-associated factor-57 (BAF57)) which can bind to acetylated chromatin to regulate chromatin remodeling (Xu et al., 2004). BRG1 and BAF57 are important for mediating estrogen-stimulated transcription due to their interaction with ER $\alpha$ -AF2 as well as with p160 cofactors (Belandia et al., 2002; García-Pedrero et al., 2006). All these studies establish the critical role of transcriptional cofactors and histone marks and understanding their importance would strengthen our knowledge on the molecular mechanisms involved in ER $\alpha$ -induced gene expression.

#### **1.2.2.4. Long range chromosomal interactions**

ER $\alpha$  primarily occupies regions distal to the promoters of estrogen-responsive genes and highly influences their transcription. This suggests that these enhancer and promoter regions are somehow linked to each other. Moreover, the presence of several enhancers near individual estrogen-regulated genes suggests that these regions can also be linked to each other despite of the linear distance between them in order to regulate transcription in a coordinated manner (Lovén et al., 2013).



Recent technological advances in the analysis of long range chromosomal interactions improved the concept of chromosomal looping which is thought to be important in mediating enhancer and promoter interactions (Liu and Cheung, 2014). Variations of the Chromosomal Conformation Capture (3C) assay which utilizes the principle of proximity ligation supported the importance of enhancer-promoter interactions by DNA looping for several estrogen-responsive genes including *CXCL12*, *PGR*, *SIAH2*, *GREB1*, *TFF1*, *CA12*, *P2RY2*, *ERBB2*, *CTSD* and *BCL2* (Barnett et al., 2008; Bonéy-Montoya et al., 2010; Bretschneider et al., 2008; Dekker, 2006; Fullwood et al., 2009; Hurtado et al., 2008; Pan et al., 2008; Perillo et al., 2008; Prenzel et al., 2011, 2012; Theodorou et al., 2013; Zhang et al., 2010). ChIP coupled with 3C (ChIP-3C) experiments display that ER $\alpha$  is mainly involved in promoting long-range chromosomal interactions and estrogen and anti-estrogens stimulate and perturb intra-chromosomal loops respectively, to control the expression of *NRIP1* and *TFF1* (Carroll et al., 2005; Pan et al., 2008).

Genome-wide studies of these long range interactions were facilitated by the development and implementation of Chromatin Interaction Analysis by Paired-End Tag Sequencing (ChIA-PET), which is an advanced version of the ChIP-3C assay. These studies show that ER $\alpha$  mediates long-range chromosomal interactions, where 86% of these regions were in the range of 10 to 100 kb, 13% in the range of 100 kb to 1 Mb and < 1% longer than 1 Mb. The data from these studies also denote that there are several ER $\alpha$ -binding anchor regions which constitute complex interactions to regulate a single gene by promoting proximity with the promoter. These intra-chromosomal interactions were also partially verified by Fluorescence *in-situ* Hybridization (FISH) experiments. Around 60% of the estrogen-upregulated genes were found to be located between anchor regions and are associated with the occupancy of RNA polymerase II (RNAPII) across gene bodies. Interestingly, most of the estrogen-downregulated genes were observed in the looped DNA around the anchors around 20 kb or away (Fullwood et al., 2009). This could also explain a possibility of how estrogen receptor can differentially regulate gene expression.

Notably, several transcriptional cofactors have been shown to be involved in the process of mediating interactions between enhancers as well as enhancer-

promoter regions and thus facilitate the transcription of estrogen-dependent genes. ChIA-PET studies identified the role of a pioneer factor, Activating enhancer binding Protein 2 gamma (AP-2 $\gamma$ ), to be involved in the regulation of ER $\alpha$ -dependent transcription via facilitating intra-chromosomal loops between different ER $\alpha$  binding sites (Tan et al., 2011). AP-2 $\gamma$  binds to AP-2 motifs adjacent to EREs and regulates estrogen-induced transcription. Furthermore, binding of ER $\alpha$  to EREs was found to be dependent on the recruitment of AP-2 $\gamma$ . Interestingly, depletion of AP-2 $\gamma$  highly perturbs estrogen-stimulated interactions between promoter-enhancer and enhancer-enhancer regions of the *RET* and *GREB1* genes. Around 50% of the ER $\alpha$  binding sites are colocalized with AP-2 $\gamma$  which is similar to FOXA1 binding. Moreover, one-third of the EREs possess both FOXA1 and AP-2 $\gamma$  binding and approximately 14% of EREs are bound only by AP-2 $\gamma$ . These results further suggest that FOXA1 is not the only critical factor which is needed for ER $\alpha$  recruitment to EREs (Carroll et al., 2005; Jozwik and Carroll, 2012). Furthermore, the regions which were shown to be involved in the intra-chromosomal looping in the previously described ChIA-PET analyses (Fullwood et al., 2009) are mainly co-occupied by ER $\alpha$ , FOXA1 and AP-2 $\gamma$  (Tan et al., 2011). All these findings suggest the importance of FOXA1 and AP-2 $\gamma$  in mediating ER $\alpha$ -dependent long range interactions.

Recently, GATA binding protein-3 (GATA3) was found to occupy EREs prior to FOXA1 binding and this controls the ability of ER $\alpha$  to mediate the chromatin looping (Theodorou et al., 2013). Depletion of GATA3 prior to estrogen treatment leads to a genome-wide redistribution in the binding of transcriptional cofactors and histone marks associated with gene activity. Upon GATA3 knockdown, ER $\alpha$  binds to distinct regions other than its consensus ER $\alpha$  binding sites. Moreover, GATA3 alone facilitates intra-chromosomal interactions and affects *TFF1* gene expression without the involvement of ER $\alpha$ .

Furthermore, recent studies elucidated the role of CCCTC-binding Factor (CTCF) and Cohesin in mediating long-range interactions in the context of estrogen-dependent transcription (Schmidt et al., 2010). The CTCF protein is a highly conserved insulator protein and is associated with the maintenance of facultative heterochromatin, inter- and intra-chromosomal looping and global chromatin

architecture (Phillips and Corces, 2009; Narendra et al., 2015; Vietri Rudan et al., 2015). In ER-positive cells, genome-wide studies show that CTCF binding is not affected by estrogen or tamoxifen treatment and functions prior to FOXA1 binding (Zhang et al., 2010; Ross-Innes et al., 2011). An interesting study using 3C assay in the *TFF1* locus showed that CTCF acts as the upstream regulator prior to FOXA1 in the recognition of boundaries for the looping anchor regions which are not present in the estrogen-independent breast cancer cells. This would suggest a possibility that CTCF controls the cell type-specific occurrence of chromatin looping and specifically marks transcriptionally active regions (Zhang et al., 2010).

The Cohesin complex has been implicated not only in holding sister chromatids together during mitosis, but also in facilitating or maintaining chromosomal looping during interphase (Rhodes et al., 2011). Cohesin is made up of four subunits including Structural Maintenance of Chromosomes-1 and 3 (SMC1, SMC3), which together form a ring-like structure to link two or more chromatids, and RAD21 and Stromal Antigen-1 (STAG1) which form the basis of the ring structure. Various studies show that coordinated function of CTCF and Cohesin are involved in the regulation of insulator function across the chromosomes and thereby influence higher order chromatin looping (Rhodes et al., 2011). Notably, Cohesin recruitment is found to be increased after estrogen treatment on EREs specifically and also promotes the looping between distal regulatory regions (Li et al., 2013). Moreover, we showed that depletion of the Cohesin subunit SMC3 rapidly downregulates the expression of *ESR1* (Prenzel et al., 2012). Interestingly, the regions which are co-bound with ER $\alpha$  and Cohesin and not with CTCF mainly function in long-range interactions and regulate ER $\alpha$ -dependent transcriptional pathways (Schmidt et al., 2010). Additionally, a minor subset of regions occupied with CTCF, ER $\alpha$  and FOXA1 are *bona fide* enhancers of ER $\alpha$ -induced transcription (Ross-Innes et al., 2011). These studies show that CTCF and Cohesin complex can function distinctly according to the cell-specific scenarios in mediating chromosomal looping which could actively participate in transcriptional regulation. Furthermore, Mediator complex has been implicated both in transcriptional initiation as well as long-range chromosomal interactions together with the Cohesin complex in pluripotency and in estrogen-mediated transcription (Kagey et al., 2010; Prenzel et al., 2012; Allen and Taatjes, 2015). Altogether, these findings suggest an important role of the Cohesin

complex in facilitating intra-chromosomal interactions during estrogen-dependent gene induction.

#### 1.2.2.5. Transcription complex assembly and disassembly

Estrogen receptor-mediated transcription involves complex and dynamic events in order to control transcription. Two important studies show that ER $\alpha$ -induced transcription of *TFF1* gene involves the association and disassociation of several transcriptional coactivators (Shang et al., 2000; Métivier et al., 2003). This results in a rapid increase and a dynamic decrease in transcription in order to efficiently respond to the estrogen stimuli. These transcriptional bursts contain six important phases which happen according to the duration of estrogen stimuli (Shang et al., 2000; Métivier et al., 2003; Green and Carroll, 2007).

Initially, pioneer factors like FOXA1, AP-2 $\gamma$ , GATA3 or CTCF bind to chromatin in order to denote the proper sites for ER $\alpha$  binding prior to estrogen treatment (I). During the response to estrogen treatment, prior binding of pioneer factors helps in the recruitment of ER $\alpha$  and p160 cofactors to promote transcription. HATs like p300, CBP and PCAF are also recruited by ER $\alpha$  and p160 factors to the EREs during this phase. This leads to histone acetylation (II). Subsequent recruitment of histone methyltransferases leads to histone methylation and RNAPII and its transcriptional cofactors are recruited to promoters which are brought in proximity to EREs by chromosomal looping to promote transcription. Additional HATs like General Control Nonderepressible-5 (GCN5) are also recruited to promote further acetylation on other specific residues (III). Increased acetylation and methylation lead to the efficient binding of the SWI/SNF complex proteins BRG1 and Brahma (BRM) to EREs as well as promoters. Altogether these events stabilize transcriptional activation. Over time, the expression of estrogen-induced genes can be reduced due to the decrease in the stimuli or the turn-over in the assembly of the activator proteins and the histone marks. The turnover of the activation complex is a rate-limiting step and is required for the activation of subsequent rounds of transcription. Furthermore, deacetylation by HDACs and demethylation by various histone demethylases are important to promote further acetylation and methylation for the next rounds of transcriptional response (IV). The next events occur at this phase along with arginine methylation via PRMT1 or CARM1 and recruitment of new

cofactors (V). The cycle resumes as in phase III with subsequent histone acetylation and methylation (VI). Overall these events facilitate the dynamic assembly and disassembly of cofactors in order to stabilize the estrogen-induced transcription and to provide a temporal response for estrogen stimuli. Altogether, these also suggest that a rapid turnover of histone marks and cofactors are essential for regulating the transcriptional response in ER $\alpha$ -regulated gene expression.

### 1.2.3. Dysregulation of estrogen receptor activity for breast cancer therapy

ER $\alpha$  plays a central role in a large fraction of breast cancers. Expression of ER $\alpha$  predicts the response to hormonal therapies (Lumachi et al., 2013). Hence, ER $\alpha$  is the major therapeutic clinical target in ER-positive breast cancer. These cancers are treated by one of the following three endocrine therapeutic approaches: (i) ovarian suppression by the administration of gonadotropin-releasing hormone (GnRH) agonists, (ii) selective estrogen receptor modulators (SERMs) or downregulators and (iii) aromatase inhibitors which perturb estrogen production. ICI182780 or Fulvestrant is the only approved ER $\alpha$  downregulator for breast cancer patients. This compound rapidly promotes ER $\alpha$  degradation by the ubiquitin-proteasome system (Wakeling and Bowler, 1992). Most commonly used drugs against ER-positive breast cancers are SERMs like tamoxifen and raloxifene. These drugs affect cell proliferation via their competitive binding to ER, induce different conformational changes in ER structure and promote transcriptional repression in breast cancer cells by recruiting repressors. Importantly, these inhibit ER $\alpha$  in a cell-type specific manner. While tamoxifen and raloxifene inhibit the proliferation of ER-positive breast cancer cells, they function like estrogen to preserve the bone mineral density. However, tamoxifen but not raloxifene activates the proliferation in other estrogen responsive tissues or organs such as the uterus. Thus, tamoxifen treatment has the major disadvantage of increasing the risk of endometrial cancer progression. Raloxifene has the advantage that it exhibits antiestrogenic activity on both the breast and uterus while acting estrogenic in the bone. Clinical trials showed that this drug can be used for patients with invasive breast cancers and osteoporosis as effectively as tamoxifen (Vogel et al., 2006).

Although tamoxifen frequently shows positive effects on ER $\alpha$ -positive tumors, at least 30% of ER-positive breast cancer patients develop tamoxifen-resistant

tumors over time. Several mechanisms were proposed to be important for the progression to tamoxifen resistance (Sommer and Fuqua, 2001). In tamoxifen-resistant breast cancer cells, ER $\alpha$  and FOXA1 were shown to possess unique binding sites and their differential binding predicts the survival and metastatic status of the patients (Hurtado et al., 2011; Ross-Innes et al., 2012). In addition to the classical ligand-dependent activation of ER $\alpha$  by estrogen, ER $\alpha$  can also be activated by phosphorylation events via the signaling of growth factor receptors like EGFR/HER1, HER2, Insulin-like Growth Factor-I Receptor (IGF-IR), etc.,. During tamoxifen resistance, HER1-HER2 heterodimers and IGF-IR mediate ER $\alpha$  phosphorylation via Mitogen-Activated Protein kinase (MAPK) pathways. This thereby promotes the ability of ER $\alpha$  to regulate transcription (Lee and Yee, 1995; Tzeng and Klinge, 1996; Casa et al., 2008). Moreover, these receptors promote cell proliferation by the activation of several downstream pathways like MAPK. Consistently, the expression of IGF-IR is correlated with the tamoxifen resistance in breast cancers (Nicholson et al., 2004). EGF induces distinct ER $\alpha$  binding to 67% of classical estrogen-induced binding sites while also inducing binding to other unique sites which are proposed to confer tamoxifen resistance to ER-positive tumors which overexpress HER2. The gene signature regulated by EGF-induced ER $\alpha$  is correlated with HER2 overexpression and with poor outcome in breast cancer patients (Lupien et al., 2010). Tumors with estrogen receptor-positive/progesterone receptor-negative (ER+/PR-) which overexpress HER1/2 show robust resistance to tamoxifen and are more aggressive (Arpino et al., 2005). Thus, HER2 seems to be a critical determinant of tamoxifen resistance (Britton et al., 2006). Several mutations in ER $\alpha$  were also found to be associated with tamoxifen resistance. The mutations in the activator function domains or phosphorylation sites of ER $\alpha$  can lead to its constitutive activity in a ligand-independent manner thus driving tamoxifen resistance (Sommer and Fuqua, 2001; Lumachi et al., 2013).

However, 1/3 of the breast cancers are not driven by ER $\alpha$ . Reports show that the triple negative breast cancers (lacking expression of ER $\alpha$ , PR and HER2) have poor overall and disease-free survival rates whereas ER+/PR+ cancers have a better survival rate (Onitilo et al., 2009). The similar observation was also found with FOXA1 status where ER-/FOXA1- patients possess 3.6% increased risk of cancer recurrence comparing to ER and FOXA1-positive cancer patients (Albergaria et al.,

2009). This suggests that ER $\alpha$  status is an indicator of the overall response for endocrine therapy and decreased risk in the progression of aggressive tumors, and dysregulation of ER $\alpha$  can lead to a poorer prognosis. However, the normal and tumorigenic activity of ER $\alpha$  seems to possess contradictory roles in mammary epithelium and breast cancer development. Considering the importance of ER $\alpha$ -driven transcription in the proliferation and hormone dependency/independency in breast cancer, an extensive understanding of the molecular mechanisms of the ER $\alpha$ -mediated transcriptional pathways can help in the discovery of potential specific therapeutic targets against breast cancers.

### **1.3. Nucleosomal organization and histone modifications**

Gene transcription is highly influenced by the organization of DNA into chromosomes. The DNA of a human cell covers approximately 2 meters of length. However, this DNA becomes highly condensed and organized in order to fit into the nucleus by associating with histone proteins. Histones belong to highly conserved proteins which exist in five different types H1, H2A, H2B, H3 and H4. Two H2A-H2B and H3-H4 heterodimers form a nucleosomal core particle by forming an octamer covering 147 bp of DNA and H1 binds to the linker DNA between each nucleosome. Higher order organization of the nucleosomes leads to highly condensed chromatin and chromosomes (Luger et al., 1997; Ramakrishnan, 1997). Interestingly, histone proteins, in general, elicit major topological and functional effects which influence transcriptional status (Mariño-Ramírez et al., 2005).

#### **1.3.1. Histone code and cross-talk**

Histone proteins undergo various post-translational modifications like acetylation, methylation, phosphorylation, ubiquitination, etc., These marks are highly implicated in the coordinative regulation of transcription along with transcription factors. The presence of various histone marks is correlated with an active or repressed transcriptional status and are described as active marks or repressive marks respectively (Zhou et al., 2011; Shlyueva et al., 2014) (Figure 1.3). For example, histone trimethylation on H3 at Lys 4 (H3K4me3) is described to be involved in the active transcription marking the active promoters while monomethylation (H3K4me1) marks enhancers. Histone acetylation on H3 at Lys 27

(H3K27ac) serves as an active mark for both promoters and enhancers whereas methylation of Lys 27 (H3K27me3) is linked with transcriptional repression. Furthermore, several marks like H3K36me3, H3K79me3 and H2B monoubiquitination (H2Bub1) are correlated with transcriptional elongation. The diverse functions of histone modifications highly support the establishment of histone marks-mediated cross-talks. This has led to the histone code hypothesis which states that the presence of various different histone modifications is associated with and influences the transcriptional activity of the genome (Strahl and Allis, 2000; Jenuwein and Allis, 2001). Notably, several histone marks have been shown to be associated with estrogen-induced transcription.

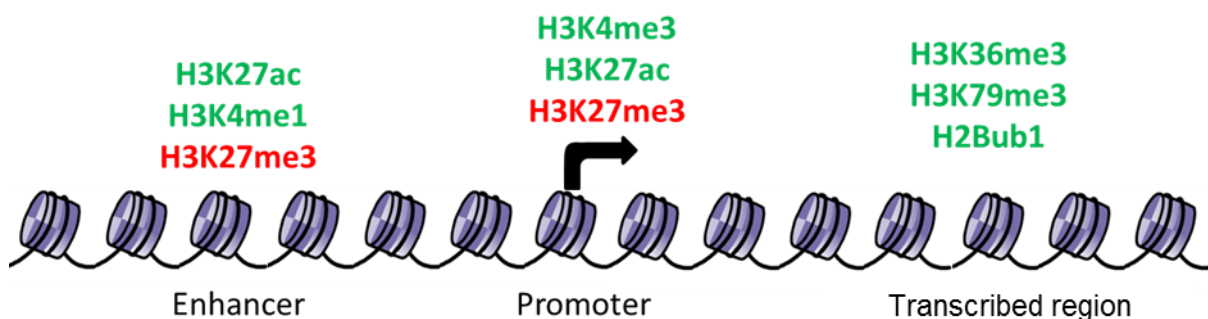


**Figure 1.3. Commonly studied histone modifications and their correlation with transcriptional activation or repression.** Marks which are marked with green are considered as active and red as repressive marks of transcription. Elongation-associated marks are mentioned adjacent to the promoter in the direction of transcription.

### 1.3.2. Histone acetylation in estrogen induced transcription

Histone acetylation is generally associated with active transcription. Histone acetylation facilitates the activation of transcription largely by recruiting several sequence-specific transcriptional factors and chromatin remodeling complexes (Allfrey et al., 1964; Grunstein, 1997; Struhl, 1998; Clayton et al., 2006). This modification is catalyzed by HATs and removed by Histone Deacetylases (HDACs). In various contexts, histone acetylation and deacetylation have been shown to be important for fine tuning the transcriptional activity and for temporal response in stimuli-induced transcription, especially in estrogen-mediated transcription (Kim et al., 2001; Sun et al., 2001). Several HATs are identified as transcriptional coactivators of estrogen-dependent gene expression and implicated in the cyclic



assembly of transcription complexes along with ER $\alpha$  (Shang et al., 2000; Métivier et al., 2003; Green and Carroll, 2007; Yi et al., 2015). These interact with ER $\alpha$  to form an active complex which leads to induced histone acetylation after estrogen treatment (Kim et al., 2001; Sun et al., 2001; Yi et al., 2015).

Histone deacetylation was also shown to regulate estrogen receptor-dependent transcription and has been suggested as a potential target for combination therapy together with anti-estrogens. For instance, several HDAC inhibitors downregulate the expression of ER $\alpha$  and sensitize the cells to tamoxifen treatment (Hodges-Gallagher et al., 2006; Biçaku et al., 2008; Thomas et al., 2011). However, in ER-negative breast cancer cells, administration of HDAC inhibitors, LBH589 and entinostat, reactivates ER $\alpha$  expression by releasing the binding of DNMT1 (DNA methyltransferase-1), H3K9 methyltransferase SUV39H1 and HDAC1 from the *ESR1* promoter and restores sensitivity to tamoxifen and aromatase inhibitors (Zhou et al., 2007; Sabnis et al., 2011). Furthermore, use of Vorinostat, another HDAC inhibitor, may be effective in patients who developed resistance against tamoxifen (Munster et al., 2011). Furthermore, HDAC inhibition by PCI-24781 kills breast cancers cells by downregulating the expression of AKT and thus inhibiting hormone-independent activity of ER $\alpha$  (Thomas et al., 2013).

Association of histone acetylation also occurs on on ER $\alpha$ -bound enhancers. In particular, H3K27ac is associated with active promoters and enhancers. Interestingly, this mark occupies found to occupy 23% of ER $\alpha$ -bound enhancers along with H3K4me1 (Li et al., 2013). Several studies demonstrated an increase of H3K27ac upon estrogen treatment at ER $\alpha$  binding sites (Lupien et al., 2009; Hah et al., 2013). Additionally, marks like H3K18ac and H4K12ac were also shown to be increased on EREs after estrogen treatment (Lupien et al., 2009). These were also upregulated on the EGF-responsive ER $\alpha$  binding sites, supporting a role in the ligand-independent function of ER $\alpha$  and in hormone-refractory breast cancers (Lupien et al., 2010). Furthermore, H4K12ac is recognized by Bromodomain-containing protein BRD4, which belongs to the bromodomain and extraterminal domain (BET) containing family of proteins, and recently implicated in tamoxifen-resistant breast cancers (Feng et al., 2014).

### 1.3.3. Epigenetic readers and BRD4

Transcriptional activation is facilitated by histone acetylation (Allfrey et al., 1964; Grunstein, 1997; Struhl, 1998; Clayton et al., 2006). Several histone-modifying complexes and chromatin-remodeling factors bind to the acetylated chromatin through specific protein domains called bromodomains. These domains were initially identified from a protein Brahma which belongs to *Drosophila* SWI/SNF complex and binds to acetylated lysine residues of histone tails (Tamkun et al., 1992). Bromodomains are highly conserved and are interestingly found in many HAT proteins including PCAF, TAFII250, CBP/p300 and GCN5 (Muller et al., 2011; Filippakopoulos and Knapp, 2014; Hohmann and Vakoc, 2014). Thus, in addition of containing acetyltransferase activity, HATs frequently possess bromodomains which bind to acetylated chromatin and further promote additional acetylation events. Moreover, some transcriptional co-activators including bromodomain-containing proteins BRD2/3/4/T and subunits of chromatin remodeling SWI/SNF complex including Brg1, Brm, BRD7 and BRD9 also possess bromodomains. Among these proteins, double bromodomain containing protein, BRD4 and SWI/SNF complex proteins are currently recognized as the potential therapeutic targets against various cancers.

Apart from its association with mitosis, BRD4 has mainly been studied for its role in transcription by regulating promoter and enhancer activity by binding to acetylated histone H4 at Lys 5,8,12 and 16 residues (Chiang, 2009; Zippo et al., 2009; Zhang et al., 2012a; Lovén et al., 2013). Recent evidence suggests that BRD4 recognizes poly-acetylated and phosphorylated histones in adjacent residues with an higher affinity than single acetylated sequences (Filippakopoulos et al., 2012). This study also showed that specificity of each bromodomain for recognizing acetylated residues is different between bromodomains within the same protein, where the first bromodomain (BD1) of BRD4 preferentially binds to poly-acetylated histone peptides of H4K5, 8, 12 and 16 while the second bromodomain (BD2) binds preferentially to acetylated H4K12 and 16 and histone H3. This suggests a strong cross-talk between adjacent histone acetylation and phosphorylation marks which regulate binding of bromodomains to chromatin to influence their transcriptional activity.

### 1.3.3.1. Structure of BRD4 and development of BRD4 inhibitors

BRD4 is the prototype of the BET family of proteins which contains two bromodomains, an extra-terminal domain and a C-terminal Positive Transcription Elongation Factor-b (P-TEFb) interaction domain (PID) (Figure 1.4). BRD4 exists as two different isoforms including a full-length transcript and a shorter form which lacks the PID (Chiang, 2009). Among these domains, the bromodomains are functionally important for BRD4 to elicit its transcriptional activity via binding to acetylated lysine residues of histones thereby facilitating BRD4 recruitment to chromatin. Additionally, the extra-terminal domain promotes protein-protein interactions with several transcription factors and histone modifiers including the Chromodomain and Helicase-containing protein CHD4 which belongs to the Nucleosome Remodeling and Deacetylase (NuRD) complex, RNA splicing-associated Jumonji-domain containing histone demethylase JMJD6, H3K36 methyltransferase NSD3 or WHSC1L1, GLTSCR1 which is a tumor suppressor, and ATAD5 which might be involved in ATM/ATR-driven DNA damage response (Rahman et al., 2011; Liu et al., 2013). The PID domain of BRD4 plays an essential role in transcription via its interaction with P-TEFb. However, recent studies show that bromodomains can also interact with acetylated P-TEFb complex proteins (Schröder et al., 2012). Triacetylated Cyclin T1 was shown to interact with bromodomains, however it also requires interaction with PID for its activation.

The evolutionarily conserved bromodomain is made up of four helices  $\alpha Z$ ,  $\alpha A$ ,  $\alpha B$  and  $\alpha C$ . These helices are linked by two loops called as ZA and BC which are similar in charge and amino acid length. These surround the acetyl-lysine binding pocket, which is hydrophobic and binds to chromatin via interaction with its conserved Asn residue. Interestingly, a recent study demonstrate the association of two acetyl-lysine residues with a single bromodomain (Morinière et al., 2009; Filippakopoulos et al., 2012; Filippakopoulos and Knapp, 2014). Structural and biochemical analyses on BD1 of BRDT describe that after the anchoring of the first acetyl-lysine residue to the hydrophobic pocket, hydrogen bonds form a network with the second acetyl-lysine moiety. Subsequent binding of two acetyl-lysine residues determines the specificity of BRD4 to bind to particular histone acetylation and stabilizes the protein domains (Morinière et al., 2009; Filippakopoulos et al., 2012).

Even though the structure of bromodomains is highly similar among its family of proteins, the regions covering the surface of the pocket and loops are highly variable which enables the development of specific inhibitors against individual bromodomain-containing proteins.

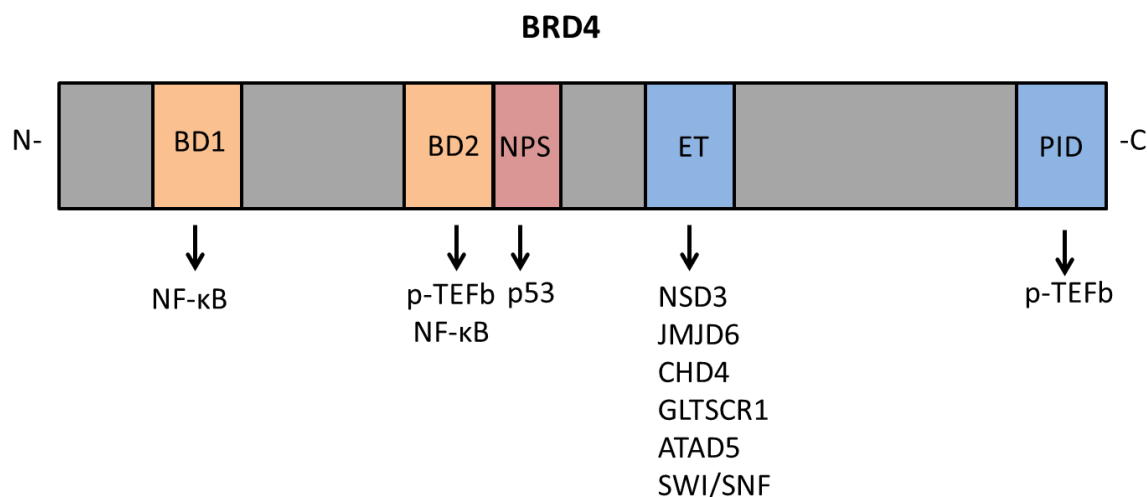


**Figure 1.4. Structure of BRD4 with its interacting proteins.** BD1 and BD2 represent first and second bromodomains respectively. ET – Extra-Terminal domain; PID – P-TEFb Interaction Domain. NPS – N-terminal Cluster of Phosphorylation Sites. The regions of BRD4 where various transcriptional cofactors interact with are shown with arrows (Modified from Schröder et al., 2012).

Various small molecule inhibitors against BET family of proteins with high affinity towards BRD4 have been reported. These competitively bind to the acetyl-lysine binding pocket of BRD4 and displace BRD4 from the chromatin and inactivate its function in transcriptional regulation. They function by mimicking the acetyl-lysine residue in forming hydrogen bonds with Asn residue of the hydrophobic pocket of the bromodomain (Filippakopoulos et al., 2010). The acetyl-lysine mimics belong to the chemical structure-based classes of thienodiazepines (for e.g. JQ1, OTX015) (Filippakopoulos et al., 2010; Coude et al., 2013), benzodiazepines (I-BET762 or GSK525762A) (Mirguet et al., 2013), benzotriazepine (I-BET151) (Dawson et al., 2011), dihydroquinazoline-one (PFI-1) (Picaud et al., 2013a), quinazolone (RVX-208) (Picaud et al., 2013b), etc., (Filippakopoulos and Knapp, 2014). The most commonly used BRD4 inhibitor in transcriptional research is JQ1 (Filippakopoulos et al., 2010). This inhibitor is used commonly as a highly specific BET domain inhibitor against BRD1/2/3/4/T; however it binds to the acetyl-lysine binding pockets of both BD1 and BD2 of BRD4 with high affinity. The “open source” availability of this compound from

the research groups of Bradner and Knapp have rapidly facilitated a large number of studies using JQ1 in the potential treatment of various diseases including cancer (Muller et al., 2011; Barbieri et al., 2013; Filippakopoulos and Knapp, 2014).

### 1.3.3.2. BRD4 in regulating gene transcription

Activation of transcription by BRD4 requires an extensive histone cross-talk. Binding of BRD4 to the chromatin is facilitated by the coordination of acetylation and phosphorylation events on histones (Filippakopoulos et al., 2012). A cross-talk mediated by H3S10ph which leads to gene activation in *trans* was established for the *FOSL1* gene upon serum induction (Figure 1.5) (Zippo et al., 2009). In order to respond to serum induction, a number of dynamic events occur in the chromatin context. Initially, H3S10ph is stimulated on the *FOSL1* promoter and enhancer regions. Depending upon the context, phosphorylation on these regions can be catalyzed by different kinases. Promoter-occupied H3S10ph is mediated by MSK1/2 and enhancer-associated H3S10ph by PIM-1. This subsequently provides a phospho/acetyl platform in the chromatin. The acetyl-phosphorylation on enhancers specifically induces the recruitment of 14-3-3 proteins which promotes the binding of a histone acetyltransferase, Males absent On the First (MOF). As a result, MOF acetylates H4K16ac leading to serum-stimulated acetylation on enhancers. This, in turn, allows efficient BRD4 binding to the chromatin.

A number of studies describe the binding of BRD4 on enhancers as well as promoters, but the possibility of BRD4 in bringing these regions proximal to each other via chromosomal looping is still not clear (Liu et al., 2013). Importantly, the association of BRD4 with acetylated chromatin recruits P-TEFb to the chromatin and this enables transcriptional activation. P-TEFb complex contains Cyclin-Dependent kinase (CDK9) and Cyclin T1/T2 and in most cases, this is associated with an inactive complex containing the 7SK small nuclear ribonucleoprotein complex, La Related Protein-7 (LARP7) and HEXamethylene bisacetamide Inducible protein (HEXIM) proteins. Further biochemical analyses of BRD4 and P-TEFb interaction suggest that BRD4 efficiently interacts with P-TEFb via its second bromodomain BD2 and PID and interaction with PID releases P-TEFb from the inactive complex. Thus, active P-TEFb associates with chromatin via interaction with BRD4 (Ai et al., 2011; Yang et al., 2005; Patel et al., 2013; Schröder et al., 2012).

P-TEFb elicits its positive effect on transcription via CDK9-mediated phosphorylation of Negative Elongation Factor (NELF), Suppressor of Ty 5 Homolog-5 (SUPT5H) and serine 2 of the RNAPII C-terminal tail in their heptad repeats. SUPT4H and SUPT5H constitute the 5,6-Dichloro-1-beta-D-ribofuranosylbenzimidazole (DRB) Sensitivity-Inducing Factor (DSIF) and are associated both with paused polymerase as well as active transcription. Importantly, NELF is involved in the pausing of RNAPII around 40 bp proximal to the promoter regions. This event is referred as promoter proximal pausing of RNAPII and is proposed to affect the efficient transcription of full-length transcripts. Hence, NELF, when bound to DSIF, inhibits the positive function of SUPT5H on transcription. Phosphorylation of the NELF-E subunit by CDK9 releases NELF from the chromatin and allows SUPT5H to exhibit its positive role on transcription activation (Yamaguchi et al., 1999; Ping and Rana, 2001; Peterlin and Price, 2006; Patel et al., 2013). Interestingly, the HEXIM and NELF complex proteins have been shown to regulate estrogen-induced transcription (Aiyar et al., 2004; Ogba et al., 2008; Ketchart et al., 2011).

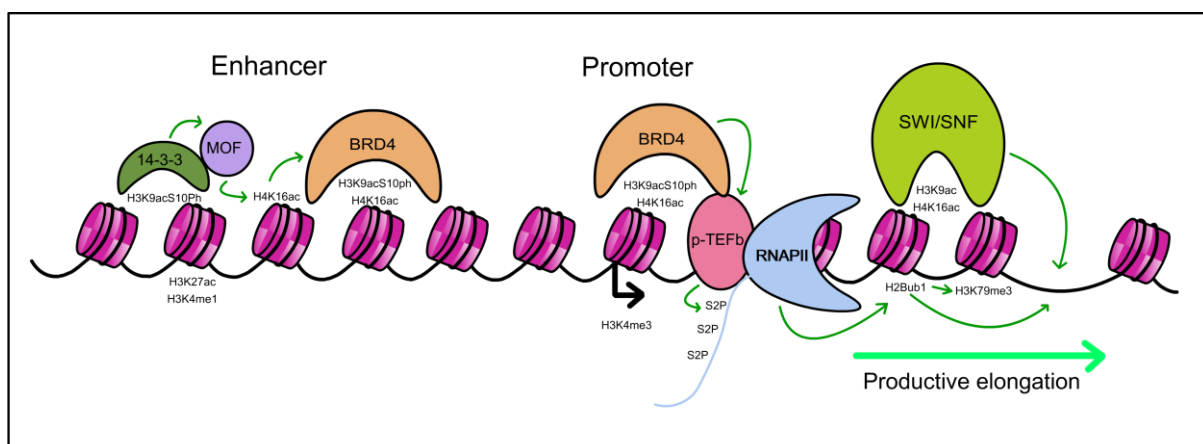


**Figure 1.5. Regulation of BRD4 and histone marks in coordinating transcriptional activation.** MOF - Males absent on the First; BRD4 – Bromodomain-containing protein-4; P-TEFb – positive Transcription Elongation Factor b; RNAPII – RNA Polymerase II; S2P – RNAPII Serine 2 phosphorylation; SWI/SNF - SWIItch/Sucrose NonFermentable complex.

Phosphorylation of RNAPII at serine 2 residues (RNAPII P<sub>Ser2</sub>) within its C-terminal heptapeptide repeats is associated with transcriptional elongation. This further serves to promote histone H2B monoubiquitination which facilitates opening of chromatin and enables transcriptional elongation (Pavri et al., 2006; Minsky et al.,

2008; Pirngruber et al., 2009a, 2009b). Moreover, H2Bub1 further controls the recruitment of Mixed Lineage Leukemia Complex of Proteins Associated with Set 1 (MLL/COMPASS) complex to promote H3K4me3, potentially providing an additional mechanism for its role in transcriptional activation (Dover et al., 2002; Johnsen, 2012).

Additionally, in the context of ER $\alpha$ -regulated transcription in tamoxifen-resistant breast cancers, BRD4 was reported to recruit WHSC1, which helps in the methylation of H3K36, further associating with transcriptional elongation (Feng et al., 2014). Moreover, another recent study uncovered an interaction of BRD4 with SWI/SNF complex subunits and BRD4 inhibition by JQ1 or BRG1 depletion both regulated the expression of a subset of genes via their recruitment to chromatin in an independent manner (Shi et al., 2013). Thus, activation of BRD4 requires the coordination of acetylation and phosphorylation and this subsequently leads to ubiquitination and methylation of histones and the recruitment of transcription-associated proteins to favor transcription.

Several recent studies have shown that BRD4 inhibition by JQ1 reverses the effects of dysregulation of various cell and lineage-specific transcription-factor associated pathways like p53, NF- $\kappa$ B, GATA4, Calcineurin-NFAT, c-MYC, etc., (Delmore et al., 2011; Ott et al., 2012; Wu et al., 2013; Anand et al., 2013; Zou et al., 2014). Furthermore, a direct interaction of p53 and NF- $\kappa$ B with BRD4 was also studied (Wu et al., 2013; Zou et al., 2014).

The acetylation of the Rel-A subunit of NF- $\kappa$ B was shown to be recognized by the bromodomains of BRD4. This stabilizes NF- $\kappa$ B and its activity and is important for NF- $\kappa$ B-driven transcription during tumorigenesis in lung cancer cells (Zou et al., 2014). Recent biochemical studies on the interaction of BRD4 and p53 identified two novel domains in BRD4 called as N-terminal cluster of Phosphorylation Sites (NPS) which contains putative phosphorylation sites and Basic Interaction Domain (BID) with several conserved basic amino acids (Wu et al., 2013). These domains are located downstream of BD2 of BRD4. The NPS contains several acidic residues and tends to interact with the positively charged BRD4-BD2. This competitively interrupts the binding of BD2 to the chromatin. Moreover, p53 association with chromatin is inhibited by its binding to the BID of BRD4. Interestingly, Casein Kinase-2 mediated

phosphorylation of NPS leads to an intramolecular contact switch of interaction from NPS-BD2 to NPS-BID. This subsequently allows the BD2 to associate with chromatin and also leads to the binding of p53 to NPS. Thus, this phosphorylation-dependent switch in BRD4 facilitates p53-dependent transcription. These studies further denote that the association of BRD4 with transcription factors is essential for BRD4-assisted transcriptional activation.

### 1.3.3.3. BRD4 in cancer

BRD4 was initially identified via its association with cancer in NUT midline carcinoma (NMC) which affects adjacent parts of the respiratory tract (French et al., 2001). This is a highly aggressive and poorly differentiated cancer with 75% of cases possessing a translocation of *BRD4* (t(15;19)) with the Nuclear protein in Testis (*NUT*) gene leading to the transcription of a BRD4-NUT fusion protein. This promotes tumorigenesis by interrupting the differentiation of epithelial cells. BRD3-NUT and BRD4-NUT depletion in these cells led to squamous cell differentiation and cell cycle arrest (French et al., 2008). The importance of BRD4 in the progression of several cancers like leukemia, lymphoma and solid tumors have also been studied (Zuber et al., 2011; Herrmann et al., 2012; Lockwood et al., 2012; Chapuy et al., 2013; Asangani et al., 2014; Bhadury et al., 2014; Feng et al., 2014; Fiskus et al., 2014; Sahai et al., 2014; Wang et al., 2015; Hu et al., 2015; Baratta et al., 2015).

Notably, BRD4 has been implicated in the progression of breast cancer. Xenograft studies of mouse mammary tumor cell lines which contain a deletion of C-terminal proline-rich region containing the PID of Brd4 promoted metastasis and stem cell-like conversion (Alsarraj et al., 2011). Consistently, overexpression of Brd4 led to reduced invasiveness and pulmonary metastasis and decreased tumor growth (Crawford et al., 2008). Brd4 deletion also promoted the expression of a subset of genes which is associated with poor outcome in human breast cancer, especially G3 grade tumors (Alsarraj et al., 2011). Consistently, a deeper analysis of BRD4-regulated gene signatures also predicted better survival and outcome in breast cancer patients, particularly ER-positive breast cancers. Furthermore, a recent study demonstrated that BRD4 is a central transcriptional coactivator for androgen receptor-induced transcription in castration-resistant prostate cancer, which supports a role of BRD4 in nuclear receptor-driven transcription (Asangani et al., 2014).



Consistently, BRD4 was shown to be essential for ER $\alpha$ -dependent transcription induction in tamoxifen-resistant breast cancers (Feng et al., 2014). Thus, understanding the molecular mechanism behind the association of BRD4 with estrogen-induced transcription is essential for the potential establishment of BRD4 as a specific therapeutic target for ER $\alpha$ -positive breast cancer.

#### 1.3.4. Histone ubiquitination in breast cancer

Histone modifications are coordinated with one another to facilitate a given transcriptional outcome. They provide a specific platform for the binding of transcription factors which control transcription. However, significant topological changes of chromatin structure also occur during transcription. One of the modifications which influences chromatin organization is histone H2B monoubiquitination. H2Bub1 occurs at lysine 123 in yeast and lysine 120 in mammals and introduces an 8.5 kD ubiquitin moiety into the chromatin which appears to physically open the chromatin structure (Fierz et al., 2011; Johnsen, 2012).

H2B monoubiquitination has been shown to be associated with transcriptional elongation and occupy gene bodies (Pavri et al., 2006; Minsky et al., 2008). This modification is mediated by the obligate heterodimeric E3 ubiquitin ligase complex RNF20/40. Recruitment of RNF20/40 complex and H2Bub1 occupancy is facilitated by P-TEFb complex (Pirngruber et al., 2009a). The kinase activity of CDK9 promotes phosphorylation of RNAPII at Ser2 residues which serves as an active mark for transcriptional elongation and provides a specific platform for an adaptor protein, WW domain-containing adapter protein WAC (Zhang and Yu, 2011). The WW domain present in the N-terminal tail of WAC directly recognizes CDK9-mediated RNAPII Ser2P while the C-terminal coiled coil domain directly interacts with the RNF20/40 complex. Subsequently, this leads to H2B monoubiquitination (Pirngruber et al., 2009a; Karpiuk et al., 2012). These show that the P-TEFb complex functions together with RNF20/40 complex to promote histone monoubiquitination to facilitate transcriptional elongation.

A number of studies have suggested a role of P-TEFb and H2B monoubiquitination in the regulation of estrogen-induced transcription (Wittmann et

al., 2005; Ogba et al., 2008; Ketchart et al., 2011; Prenzel et al., 2011; Mitra et al., 2012; Sengupta et al., 2014). Notably, CDK9 and Cyclin T1 were shown to form a complex with ER $\alpha$  which is further increased after estrogen treatment (Sharp et al., 2006; Mitra et al., 2012). This complex was also shown to release the transcriptional pausing of the estrogen-dependent *MYB* proto-oncogene. Consistently, flavopiridol (a relatively specific CDK9 inhibitor) and DRB inhibit *MYB* expression (Mitra et al., 2012). Induced expression of another estrogen-responsive oncogene *MYC* is associated with tamoxifen-resistant cell lines. Interestingly, the expression of CDK9 is also elevated in these cell lines, where it was shown to promote RNAPII P-Ser2 on the *MYC* gene and thereby facilitate estrogen-independent proliferation (Sengupta et al., 2014).

In addition to these findings, Cyclin T1 was also reported to interact with ER $\alpha$  where its activity is negatively regulated by HEXIM1, which is a component of the inactive 7SK/P-TEFb complex (Wittmann et al., 2005). Estrogen-induced transcription of *TFF1* and *CCND1* is inhibited by HEXIM1 (Ogba et al., 2008). Moreover, HEXIM1 recruitment is increased during tamoxifen treatment to inhibit ER $\alpha$ -responsive transcription and its lower expression is associated with tumor recurrence after tamoxifen treatment, indicating a potential role in tamoxifen-resistant breast cancer (Ketchart et al., 2011). Consistently, Ser2-phosphorylation of RNAPII is important in the dynamic events of estrogen-induced transcription by regulating transcriptional elongation (Kininis et al., 2009). Altogether these studies suggest the physical and functional interaction of P-TEFb complex with ER $\alpha$  to be essential for the regulation of estrogen-responsive transcription.

Notably, H2Bub1 was shown to be important for estrogen-induced transcription (Prenzel et al., 2011). In this study, RNF40 depletion reduced the expression of estrogen-induced genes *CXCL12*, *GREB1* and *TFF1*. These studies demonstrate that the inhibition of proteasomal activity regulates estrogen signaling, most likely via depletion of nuclear ubiquitin pool. This further results in a rapid loss of H2Bub1 which affects estrogen-induced transcription. Furthermore, RNF20 has been suggested to be a potential tumor suppressor. RNF20 depletion increases the EGF-induced migration of breast epithelial cells. RNF20 promoter hypermethylation and loss of H2Bub1 is associated with breast cancer progression (Shema et al.,

2008; Prenzel et al., 2011). Consistent with the finding of yeast SPT6 being a transcriptional activator of ER $\alpha$ -dependent transcription (Baniahmad et al., 1995), a recent study showed that SUPT6H promotes H2B monoubiquitination and estrogen-stimulated transcription (Bedi et al., 2015). This study demonstrated that SUPT6H is required for the expression of RNF40 and forms a complex with both RNF40 and ER $\alpha$ . Consistently, SUPT6H protein levels correlated positively correlated with H2Bub1 levels and inversely with breast cancer malignancy.

A recent interesting report reveals that SWI/SNF complex, which is also shown to be important for estrogen-regulated transcription, can bind to H2Bub1 modified chromatin directly and its recruitment depends upon RNF20 (Shema-Yaacoby et al., 2013). Moreover, this study shows that the expression of H2Bub1-dependent genes is regulated by the SWI/SNF complex. This is consistent with the interaction of BRD4 and SWI/SNF complex to regulate the expression of a similar subset of genes (Shi et al., 2013). Thus, BRD4, H2Bub1 and the SWI/SNF complex may cooperate in estrogen-stimulated transcription.

#### **1.4. Enhancer RNAs in regulating transcription**

The regulation of mRNA expression by enhancers is coordinated by long-range chromosomal interactions, enhancer-associated histone modifications and transcriptional machinery which can function to link enhancers with promoters. Interestingly, enhancer transcription was discovered recently and shown to be essential for enhancer activity. These non-coding transcripts are referred to as enhancer RNAs (eRNAs) (Lam et al., 2014). Widespread transcription of eRNAs was recently observed via the advancement in the nuclear run-on assays and a few studies demonstrate the characteristics of eRNAs (Kim et al., 2010; Li et al., 2013). eRNAs typically range in size from 500 to 5000 bp and could be transcribed in both directions (Li et al., 2013). These transcripts are dynamically associated with promoting mRNA expression in various cell-specific contexts, especially in androgen and estrogen-responsive transcription (Kim et al., 2010; Wang et al., 2011; Hah et al., 2013; Li et al., 2013; Kaikkonen et al., 2013; Hsieh et al., 2014; Ilott et al., 2014; Arner et al., 2015).

The transcription of enhancer RNAs is correlated with the occupancy of RNAPII on the promoters which are looped to enhancers via long-range interactions and could thus represent transcriptional noise (Natoli and Andrau, 2012; Lam et al., 2014). Several studies were conducted to understand the functions of eRNA in the context of mRNA transcriptional regulation. A classical Locus Control Region (LCR), which has more recently been described as a “super enhancer”, constitutes a set of enhancer regions controlling a single gene expression. A DNase Hyper-Sensitivity site HS2 which is located within the LCR of  $\beta$ -globin gene was shown to be important for the enhancer activity of LCR. Interestingly, this site possesses a transcriptional start site and the introduction of a lac operator/R repressor complex downstream of HS2 in a reporter construct blocks its enhancer activity (Tuan et al., 1992; Ling et al., 2004). Furthermore, insertion of a transcriptional termination site into the LCR of the human Growth Hormone (hGH) gene also regulates hGH expression (Ho et al., 2006).

Recent evidences further verified the importance of eRNAs in the transcriptional regulation of estrogen-responsive transcription (Hah et al., 2013; Li et al., 2013). Notably, estrogen-induced eRNAs were identified in MCF7 cells from parallel studies by Rosenfeld and Kraus groups (Hah et al., 2013; Li et al., 2013). eRNA transcription was shown to be dependent upon ER $\alpha$  binding to EREs. Furthermore, utilization of chimeric eRNA designed to bind to an estrogen-induced promoter specifically shows that the presence of the eRNA transcript is essential for the stimulation of estrogen-induced transcription of the cognate target gene. Moreover, specific estrogen-induced eRNA depletion using small interfering RNAs (siRNAs) or Locked Nucleic Acids (LNA) regulates the transcription of respective estrogen-driven genes. This study also shows that eRNAs induce estrogen-induced chromatin looping and the Cohesin complex physically stabilizes the looping by its interaction with eRNA (Li et al., 2013).

Lee Kraus and his colleagues (Hah et al., 2013) showed that estrogen-upregulated eRNAs are associated with enhancer-specific active transcriptional complexes including ER $\alpha$ , FOXA1, p300/CBP, RNAPII which demonstrate DNase hypersensitivity, histone marks like H3K27ac and H3K4me1 and estrogen-induced chromatin looping. Moreover, the presence of eRNA transcription is predictive of *de*

*novo* enhancer activity (Kaikkonen et al., 2013). The kinetics of eRNA transcription was shown to occur very rapidly supporting the dynamic nature of estrogen-induced transcription. Importantly, flavopiridol treatment inhibited eRNA synthesis without affecting the formation of the initial active transcriptional complex forming events on enhancers including looping. However, this result is contradictory to the studies from the Rosenfeld group which reported a role of eRNAs in mediating Cohesin recruitment and chromatin looping (Hah et al., 2013). Furthermore, in another system, CDK9 and BRD4 inhibition was shown to inhibit eRNA transcription from *de novo* enhancers, and enhancer transcription, and not the transcript itself is important for H3K4me2 deposition (Kaikkonen et al., 2013). Additionally, a recent report demonstrated that BRD4, in general, helps in the elongation of eRNA transcripts by allowing RNAPII to travel through the acetylated enhancer regions (Kanno et al., 2014). This study also showed that eRNA transcription can be inhibited by JQ1 without significantly affecting the association of BRD4 and P-TEFb around the TSS of BRD4-dependent genes such as *Myc* and *Klf4*. Altogether these studies suggest an important role of eRNA transcription which could be coordinated by BRD4 and CDK9 during estrogen-induced transcription.

## 2. Publications

### 2.1. Publication I

#### **Bromodomain protein BRD4 is required for estrogen receptor-dependent enhancer activation and gene transcription**

##### **Citation**

Sankari Nagarajan, Tareq Hossan, Malik Alawi, Zeynab Najafova, Daniela Indenbirken, Upasana Bedi, Hanna Taipaleenmäki, Isabel Ben-Batalla, Marina Scheller, Sonja Loges, Stefan Knapp, Eric Hesse, Cheng-Ming Chiang, Adam Grundhoff, Steven A. Johnsen

Bromodomain Protein BRD4 Is Required for Estrogen Receptor-Dependent Enhancer Activation and Gene Transcription

*Cell Reports*, Volume 8, Issue 2, p460–469, 24 July 2014

<http://dx.doi.org/10.1016/j.celrep.2014.06.016>

##### **Own contribution**

Experiments and data analyses for accomplishing all figures 1, 2A, 3 and 4 and all the supplementary figures, data analyses for figure 2B-D, all the bioinformatic analyses, complete figure arrangement and contribution in writing the manuscript.

## Summary

The estrogen receptor  $\alpha$  (ER $\alpha$ ) controls cell proliferation and tumorigenesis by recruiting various cofactors to estrogen response elements (EREs) to control gene transcription. A deeper understanding of these transcriptional mechanisms may uncover therapeutic targets for ER $\alpha$ -dependent cancers. We show that BRD4 regulates ER $\alpha$ -induced gene expression by affecting elongation-associated phosphorylation of RNA polymerase II (RNAPII) and histone H2B monoubiquitination. Consistently, BRD4 activity is required for proliferation of ER+ breast and endometrial cancer cells and uterine growth in mice. Genome-wide studies revealed an enrichment of BRD4 on transcriptional start sites of active genes and a requirement of BRD4 for H2B monoubiquitination in the transcribed region of estrogen-responsive genes. Importantly, we demonstrate that BRD4 occupancy on distal EREs enriched for H3K27ac is required for recruitment and elongation of RNAPII on EREs and the production of ER $\alpha$ -dependent enhancer RNAs. These results uncover BRD4 as a central regulator of ER $\alpha$  function and potential therapeutic target.

## Introduction

Estrogen receptor-positive (ER+) breast cancers represent a significant challenge to modern health care. ER $\alpha$ -dependent transcription in these cancers potentiates cell proliferation and malignancy. Estrogen (E2) binding leads to conformational changes within ER $\alpha$  that promote dimerization, binding to estrogen response elements (EREs), and subsequent cofactor recruitment (Deroo and Korach, 2006). Binding of ER $\alpha$  to EREs is promoted by the pioneer factor, Forkhead protein FOXA1 (HNF3 $\alpha$ ) (Carroll et al., 2005; Hurtado et al., 2011). ER $\alpha$  also functions along with Cohesin (Schmidt et al., 2010) to facilitate long-range chromosomal interactions between EREs (Fullwood et al., 2009).

The regulation of transcriptional elongation plays an essential role in E2-dependent gene transcription. This is largely regulated by the activity of the Positive Transcription Elongation Factor-b (P-TEFb) complex (Peterlin and Price, 2006). P-TEFb promotes elongation in part by relieving negative regulation by phosphorylating negative elongation factor (NELF) and dichloro-1- $\beta$ -D-ribofuranosylbenzimidazole

(DRB)-sensitivity inducing factor (DSIF) complexes. Pausing of RNA polymerase II (RNAPII) by NELF just downstream of the transcriptional start site (TSS) is a critical determinant of ER $\alpha$ -dependent transcription (Aiyar et al., 2004). P-TEFb also phosphorylates Ser2 (p-Ser2) within the heptapeptide repeat of the RNAPII carboxy-terminal domain (CTD). This in turn promotes elongation-associated histone modifications including histone H2B monoubiquitination (H2Bub1) (Karpiuk et al., 2012; Pirngruber et al., 2009a), which is required for E2-dependent transcription (Bedi et al., 2015; Prenzel et al., 2011). Consistently, E2-dependent transcription was shown to be regulated at a post-RNAPII recruitment step involving increased RNAPII p-Ser2 by P-TEFb (Kininis et al., 2009).

The Bromodomain-containing Protein 4 (BRD4) binds to acetylated histones at both enhancers and promoters and recruits P-TEFb to support lineage-specific gene transcription (Zippo et al., 2009; Zhang et al., 2012a). Importantly, inhibition of BRD4 by pan-bromodomain and extraterminal domain (BET) inhibitors such as JQ1 (Filippakopoulos et al., 2010), PFI-1 (Picaud et al., 2013a), and IBET revealed the involvement of BRD4 in various cancers in animal models (Herrmann et al., 2012; Lockwood et al., 2012; Ott et al., 2012; Zhang et al., 2012b; Zuber et al., 2011). Moreover, a BRD4-dependent gene expression signature was reported to be a positive predictor of breast cancer survival (Crawford et al., 2008) and has been implicated as an inherent susceptibility gene for metastasis in breast cancers (Alsarraj et al., 2011).

Recent findings describe a role for enhancer RNA (eRNA) production from ER $\alpha$ -bound enhancers during E2-regulated transcription (Hah et al., 2013; Li et al., 2013). eRNAs are noncoding RNAs that promote transcription by an unknown mechanism (Kim et al., 2010). Interestingly, cyclin-dependent kinase 9 (CDK9) is required for E2-regulated eRNA synthesis (Hah et al., 2013).

In this study, we investigated a role for BRD4 as a transcriptional cofactor of ER $\alpha$ -induced transcription by regulating transcriptional elongation and revealed its recruitment both to gene promoters as well as FOXA1-ER $\alpha$ -bound enhancers in ER+ breast cancer cells. Moreover, we demonstrate that distal EREs that produce eRNAs are enriched for BRD4 occupancy and uncover a role for BRD4 in eRNA synthesis.



## Results

### BRD4 regulates E2-induced transcriptional activity in ER+ cancers

To analyze the importance of BRD4 in ER $\alpha$ -dependent gene regulation, we performed mRNA sequencing (mRNA-seq) analyses in ER+ breast cancer cells following E2 stimulation in cells depleted for BRD4 or treated with the BRD4 inhibitor, JQ1 (Figure 2.I.S1A). Heatmap analysis shows a nearly global decrease of E2-stimulated gene expression following BRD4 depletion and inhibition (Figure 2.I.1A and 2.I.S1C), whereas the effects of BRD4 perturbation in this time frame were less apparent for E2-downregulated genes (Figure 2.I.S1D). The inhibition of E2-induced transcription by BRD4 perturbation was further verified for representative E2-upregulated genes (Figure 2.I.S1B).

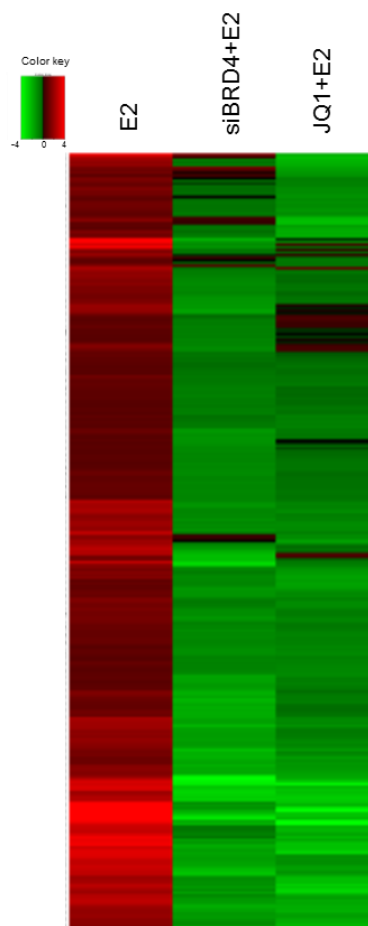


**Figure 2.I.1A. BRD4 perturbation impairs E2-induced gene expression.** Heatmap made with log<sub>2</sub>-fold changes from mRNA-seq of MCF7 cells. E2 denotes siCont and E2-treated samples relative to cells transfected with siCont and Veh treated. siBRD4+E2 denotes siBRD4 and E2-treated samples

relative to siCont with E2 induction. JQ1+E2 denotes siCont, JQ1, and E2-treated samples relative to siCont with E2 induction. Only E2-upregulated genes R1.5-fold are shown. Adjusted p value is  $\leq 0.05$ .

NAME	E2 vs Veh	E2 vs siBRD4 E2	E2 vs JQ1 E2
WILLIAMS_ESR1_TARGETS_UP	0.8538	0.8092	0.6459
FRASOR_RESPONSE_TO ESTRADIOL_UP	0.8055	0.7825	0.7205
MASSARWEH_RESPONSE_TO ESTRADIOL	0.7883	0.7095	0.7155
BHAT_ESR1_TARGETS_NOT_VIA_AKT1_UP	0.7774	0.7605	0.6174
DUTERTRE ESTRADIOL_RESPONSE_6HR_UP	0.7442	0.7127	0.6159
PID_HNF3A_PATHWAY	0.6805	0.5973	0.5821
STEIN_ESR1_TARGETS	0.6797	0.6764	0.5274
MASSARWEH_TAMOXIFEN_RESISTANCE_DN	0.6537	0.5733	0.5469
CREIGHTON ENDOCRINE THERAPY RESISTANCE 4	0.6317	0.5407	0.5104

**Figure 2.I.1B. BRD4 perturbation impairs E2-induced gene expression.** GSEA of mRNA expression data from RNA-seq. The table shows the enrichment score for the topmost estrogen-related pathways in each condition. Nominal p value is  $\leq 0.05$ , FDR  $\leq 25\%$ .

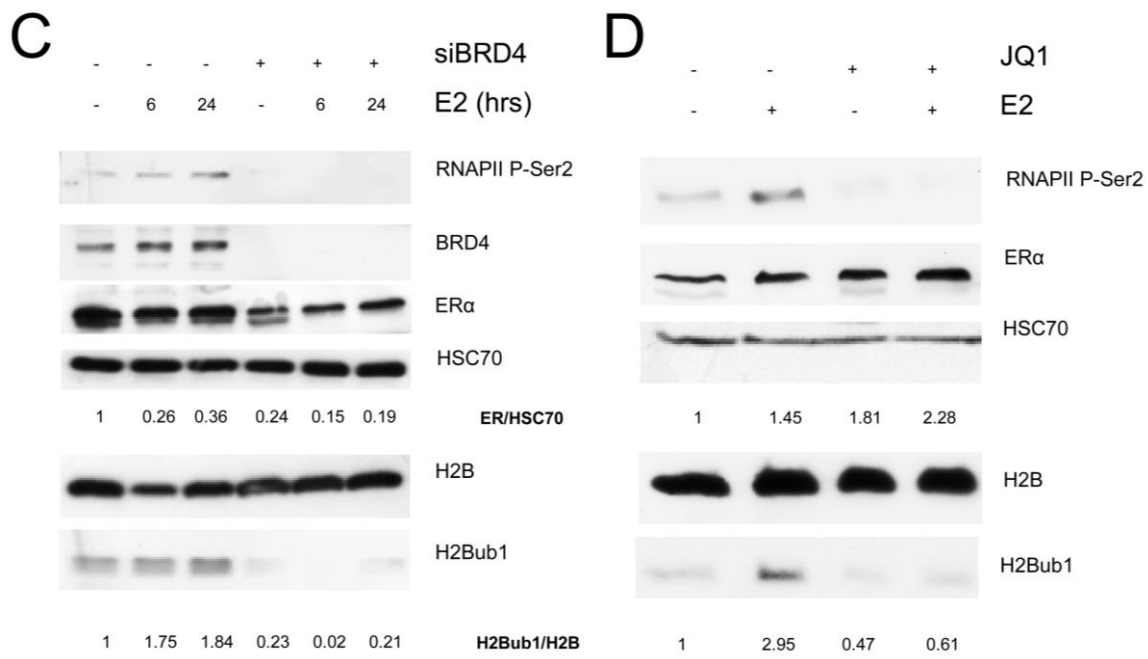


**Figure 2.I.1C,D. BRD4 perturbation impairs E2-induced gene expression, RNA polymerase Ser2 phosphorylation, and H2Bub1.** Western blot analyses with specific antibodies on whole MCF7 protein extracts after transfection with negative control (-) or siBRD4 with 6 or 24 hr of E2 induction (C) or DMSO (-) or JQ1 and/or E2 induction for 24 hr (D). Relative quantified values of H2Bub1 normalized with H2B and ERα with HSC70 are indicated under the respective blots.

Strikingly, in addition to the known targets of BRD4 such as cell proliferation-specific and tumor necrosis factor-nuclear factor  $\kappa$ B target genes (Mochizuki et al., 2008; Zou et al., 2014), gene set enrichment analyses (GSEAs) identified multiple

E2- and ER $\alpha$ -related pathways as being significantly enriched following BRD4 knockdown or inhibition under vehicle (Veh) as well as E2-treated conditions (Figure 2.I.1B, 2.I.S1E, and 2.I.S1F). Similar effects were also seen in the ER $^+$  Ishikawa endometrial cancer cell line (Figure 2.I.S1G), whereas BRD4 depletion had little or no effect on transforming growth factor  $\beta$ 1 (TGF- $\beta$ 1)-induced gene expression (Figure 2.I.S1H). Together, these findings indicate a specific and central role for BRD4 in regulating E2-induced transcription in ER $^+$  cancers.

### **BRD4 regulates RNAPII phosphorylation and H2Bub1**

Given the importance of BRD4 in controlling RNAPII elongation (Liu et al., 2013; Patel et al., 2013), and the established roles for RNAPII p-Ser2 (Kininis et al., 2009) and H2Bub1 (Prenzel et al., 2011) in E2-induced gene transcription, we examined whether BRD4 depletion or inhibition affects RNAPII p-Ser2 or H2Bub1. Interestingly, both RNAPII p-Ser2 and H2Bub1 substantially increased upon E2 treatment, and depletion or inhibition of BRD4 decreased their levels under basal as well as E2-induced conditions (Figure 2.I.1C, 2.I.1D, and 2.I.S1J). Similar effects were also observed in Ishikawa and H1299 cells upon BRD4 depletion (Figure 2.I.S1I).

### **BRD4 regulates ER $\alpha$ -dependent cell proliferation and uterine growth**

In order to investigate the physiological function of BRD4 in controlling ER $\alpha$  activity, we examined cell proliferation after knockdown or inhibition of BRD4 in both MCF7 and Ishikawa cells. Notably, consistent with gene expression results (Figure 2.I.1A, 2.I.1B, and 2.I.S1B–S1F), BRD4 perturbation decreased cell proliferation in a manner similar to the pure anti estrogen ICI182780 both in the presence and absence of E2 (Figure 2.I.2A, 2.I.S2A, and 2.I.S2B).

Decreased uterine weight is a hallmark of diminished estrogen signaling in vivo. Consistent with in vitro experiments, JQ1-injected mice demonstrated a substantial decrease in uterine growth (Figure 2.I.2B) and uterine wet weight (Figure 2.I.2C), without significant changes in total body weight (Figure 2.I.S2C). Gene expression analyses confirmed decreased expression of E2-dependent genes in uteri from JQ1-injected mice (Figure 2.I.2D), confirming a central role for BRD4 in controlling E2-induced proliferation and growth both in vitro and in vivo.

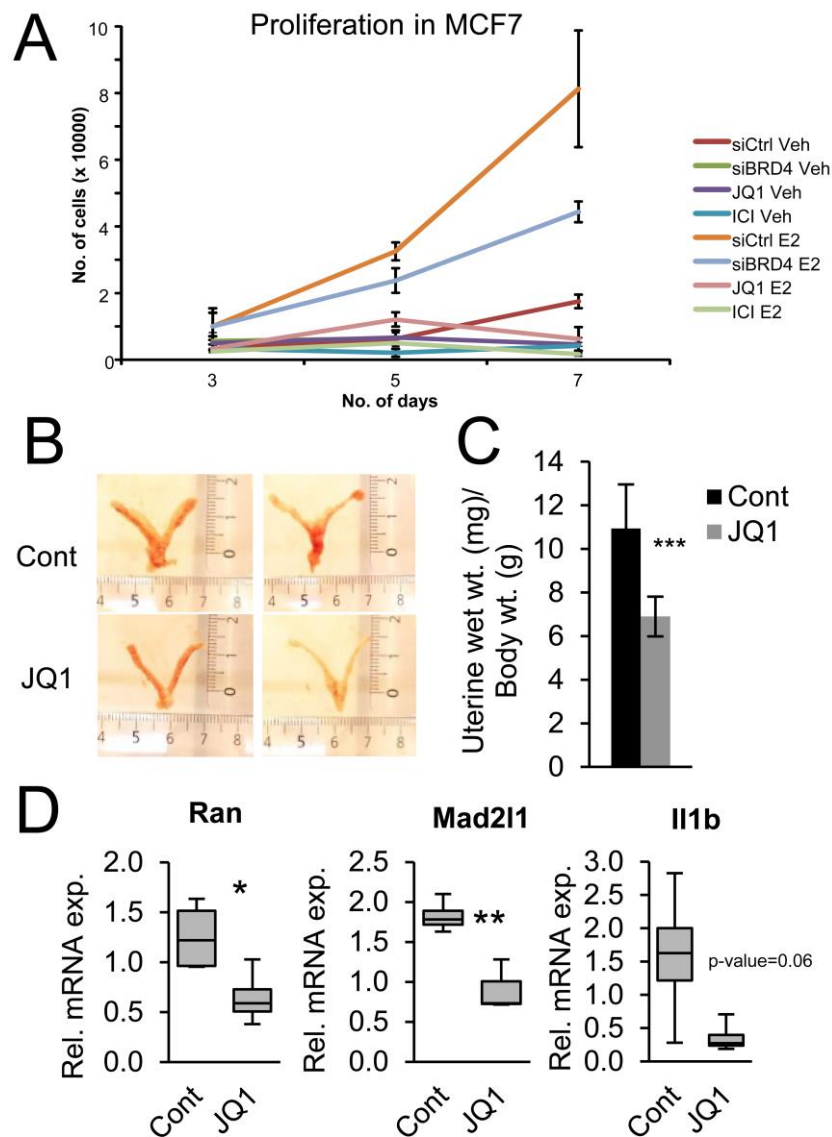


**Figure 2.I.2. Inhibition and knockdown of BRD4 affect proliferation and uterine growth.** (A) Cell proliferation assays in MCF7 cells upon E2 as well as basal conditions under negative siCont, siBRD4, JQ1, and ICI182780 treatment. (B–D) Three-week-old mice injected with Veh (Cont [control]) and JQ1 for 3 weeks were dissected, and uteri were analyzed for their size (B) and wet weight (wt.) (C). \*\*\* $p \leq 0.001$ . Data are represented as mean  $\pm$  SD ( $n = 8$ ). (D) Single-gene expression analyses of E2-induced genes (Ran, Mad2I1, and Il1b) after Veh (cont) or JQ1-injected mouse uteri. \* $p \leq 0.05$ ; \*\* $p \leq 0.01$ . The data are represented as median  $\pm$  SD ( $n = 4$ ). Rel. mRNA exp., relative mRNA expression.

### BRD4 occupancy is associated with an active epigenetic context and transcription

To gain mechanistic insight into the function of BRD4 and H2Bub1 in ER $\alpha$ -regulated transcription, we performed genome-wide chromatin immunoprecipitation

(ChIP) and sequencing (ChIP-seq) analyses. Consistent with its role in E2-induced gene transcription, genome-wide profiling and single-gene analyses revealed increased BRD4 occupancy slightly downstream of the TSS and continuing into the transcribed region of E2-induced genes (Figure 2.I.3A, 2.I.3B, and 2.I.S3A–S3G). This occupancy is decreased upon JQ1 treatment (Figure 2.I.S3B). Conversely, E2 reduced BRD4 recruitment on E2-repressed genes (Figure 2.I.S3D and 2.I.S3F). Consistent with a previous study by (Minsky et al., 2008)), H2Bub1 preferentially occupied gene bodies (Figure 2.I.3C, 2.I.3D, and 2.I.S3H–S3L). Notably, E2 treatment increased H2Bub1 levels on E2-stimulated genes significantly, and this effect was reduced by JQ1 treatment (Figure 2.I.3C, 2.I.S3I, and 2.I.S3K–S3M). Interestingly, the effect of JQ1 on H2Bub1 occupancy was most pronounced on genes exhibiting de novo RNAPII recruitment, such as GREB1 and TFF1, but less on RNAPII-recruited and -preloaded and -constitutively bound genes like XBP1 (Figure 2.I.S3K and 2.I.S3N).

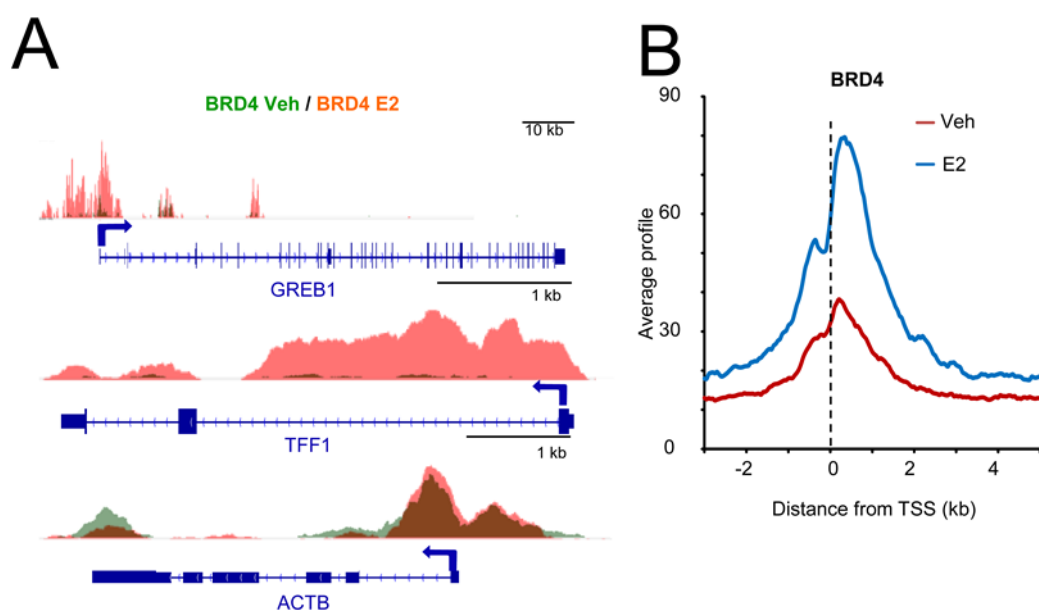


**Figure 2.I.3A,B. BRD4 occupies promoters and correlates with active transcription.** (A) Genomic binding profiles of BRD4 on E2-induced genes (GREB1 and TFF1) and a housekeeping gene (ACTB). Red indicates E2-treated and green indicates Veh-treated conditions. (B) Aggregate plots showing genomic binding profiles of BRD4 on E2-upregulated gene-specific TSS upon Veh and E2-treated conditions. x axis shows the distance from the TSS of E2-upregulated genes in kilobase pairs. y axis shows the average BRD4 signal of the reads normalized per hundred million base pairs. TSS is marked with a black dotted line.

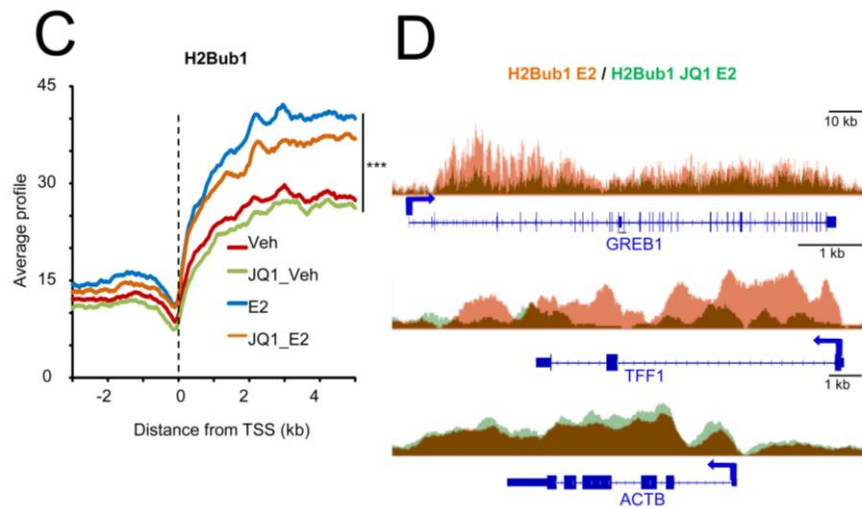


**Figure 2.1.3C,D. BRD4 occupies promoters and correlates with active transcription.** (C) Aggregate plots showing genomic profiles of H2Bub1 on E2-upregulated genes upon Veh, JQ1, as well as Veh (JQ1 Veh), E2, and JQ1 as well as E2 (JQ1 E2)-treated conditions. Weighted averages for each E2-upregulated gene, 1.5–2.5 kb downstream of each TSS, were used to calculate the p values using ANOVA with multiple-regression model. \*\*\* $p \leq 0.001$ . (D) Genomic profiles of H2Bub1 on GREB1, TFF1, and ACTB. Red indicates E2-treated and green indicates JQ1 as well as E2 (JQ1 E2)-treated conditions.

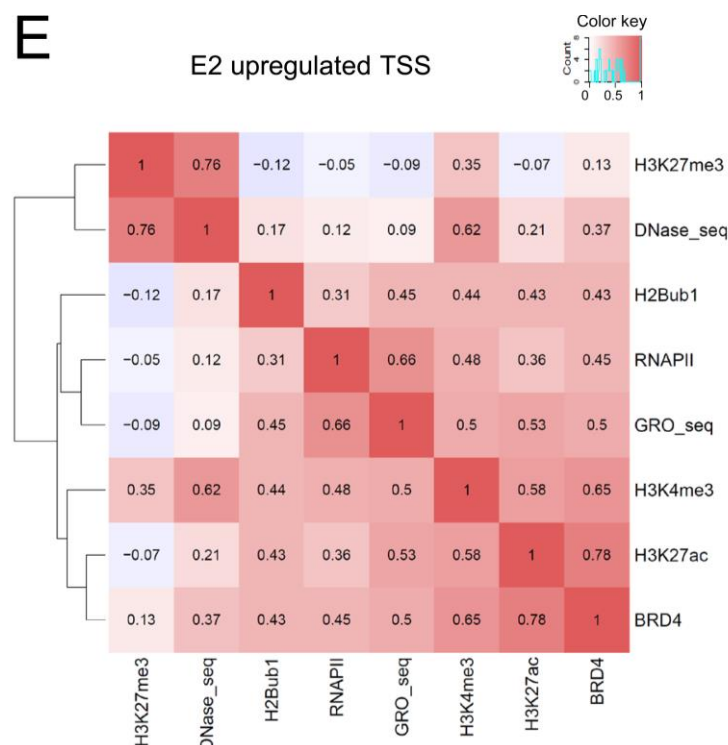


**Figure 2.1.3E. BRD4 occupies promoters and correlates with active transcription.** Correlation plot on E2-regulated gene-specific TSS +3 kb showing the association of BRD4, H3K27ac, H3K4me3, nascent RNA transcription (GRO-seq), RNAPII, H2Bub1, and DNase I-hypersensitivity sites (DNase-seq) and H3K27me3.

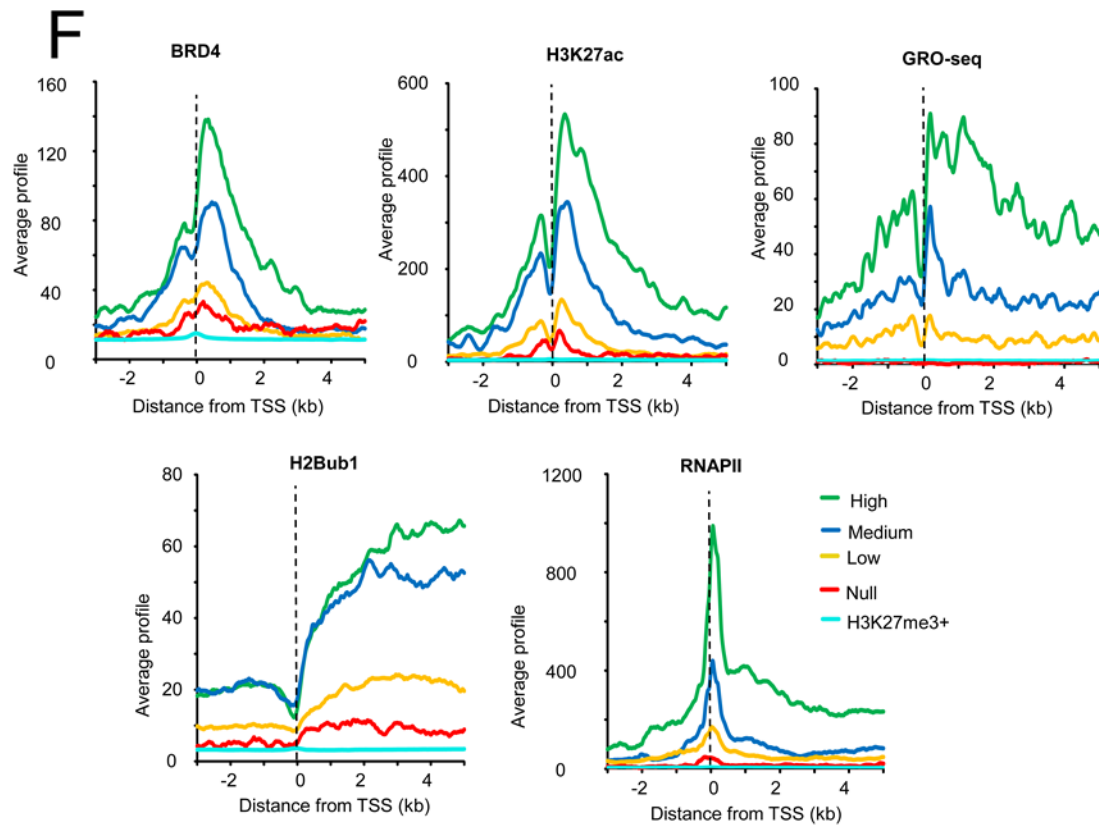


**Figure 2.1.3F. BRD4 occupies promoters and correlates with active transcription.** Aggregate plot analyses of BRD4, H3K27ac, RNAPII, and H2Bub1 on GRO-seq-based groups (high, medium, low, and null), at specific TSSs on E2-regulated genes. “High” group corresponds to E2-upregulated TSS having a weighted average of GRO-seq signal from E2-treated MCF7 cells  $>0.3$ , “medium”  $>0.15 <0.3$ , “low”  $>0 <0.15$ , and “null” with no value of average. A class of H3K27me3-positive summits was examined as a negative control of active transcription.

Correlation and aggregate plots confirmed an association of BRD4 and active transcription on E2-induced TSSs (Figure 2.1.3E, 2.1.3F, and 2.1.S3O–S3R). Moreover, BRD4 occupancy positively correlated with histone marks H3K27ac and H3K4me3, which are hallmarks of active transcription, as well as RNAPII, H2Bub1, and DHSs (DNase I-hypersensitivity sites), but not with H3K27me3 (Figure 2.1.3E and 2.1.S3O). Similarly, H2Bub1 also correlated with transcription, H3K4me3, BRD4, H3K27ac, and RNAPII (Figure 2.1.3E and 2.1.S3O). Grouping of TSSs according to the level of nascent RNA expressed (high, medium, low, and null) and aggregate plot and heatmap analyses revealed a clear association of BRD4, H3K27ac, H3K4me3, RNAPII, and H2Bub1 occupancy as well as DHSs and gene transcription (Figure 2.1.3F and 2.1.S3P–S3R).

## **BRD4 functions downstream of ER $\alpha$ , H3K27ac, and Cohesin**

Because BRD4 inhibition prevents E2-dependent gene induction without appreciably affecting ER $\alpha$  protein levels (Figure 2.I.1D and 2.I.S4A), we also examined the effects of JQ1 treatment on the recruitment of ER $\alpha$  and the Cohesin subunit RAD21. Single-gene analyses of ER $\alpha$  binding suggested that ER $\alpha$  binding is not affected at specific EREs after BRD4 inhibition (Figure 2.I.4A and 2.I.S4B). Consistent with a recent report describing an effect of BRD4 inhibition on androgen receptor (AR) recruitment (Asangani et al., 2014), genome-wide analyses confirmed that JQ1 treatment decreases ER $\alpha$  binding at most EREs (Figure 2.I.4B, 2.I.S4D, and 2.I.S4E). However, these effects are only partial, and substantial levels of ER $\alpha$  are still bound to EREs after JQ1 treatment (Figure 2.I.S4F). Consistent with the recent studies that BRD4 does not promote chromosomal looping between enhancers and promoters (Liu et al., 2013), RAD21 binding to three different EREs known to serve as hubs for ER $\alpha$ -dependent looping (Fullwood et al., 2009) was unaffected by JQ1 treatment (Figure 2.I.S4C). Interestingly, whereas BRD4 binding correlated with H3K27ac (Figure 2.I.3E) (Zhang et al., 2012a), BRD4 inhibition did not influence the E2-induced H3K27ac on individual E2-regulated enhancers and promoters (Figure 2.I.4C and 2.I.S4H). These results suggest that BRD4 is recruited to E2-regulated genes subsequent to ER $\alpha$  binding, histone acetylation, and Cohesin recruitment.

## **BRD4 occupies enhancers and regulates eRNA synthesis by affecting RNAPII recruitment and elongation**

BRD4 was recently shown to occupy and regulate enhancer function (Liu et al., 2013; Zhang et al., 2012a). Thus, we examined BRD4 occupancy at distal EREs and observed that BRD4 is recruited to distal EREs in an E2-dependent manner and correlated with H3K27ac, ER $\alpha$ , FOXA1, RNAPII, and DHS (Figure 2.I.4D, 2.I.4E, 2.I.4H, 2.I.S4G and 2.I.S4I–S4L). Surprisingly, nascent RNA transcription on enhancers correlated with BRD4 occupancy to a greater extent than the other investigated profiles (Figure 2.I.4E–4H). RNAPII occupancy is also well associated with BRD4 on enhancers (Figure 2.I.4E). Interestingly, high eRNA-producing EREs exhibited high E2-induced RNAPII recruitment that extended to more than 5 kb upstream and downstream of the ERE summits, suggesting a tight association



between RNAPII recruitment and elongation at eRNA-producing enhancers (Figure 2.I.4I and 2.I.S4N). ChIP analyses confirmed that E2-induced RNAPII recruitment and elongation at the GREB1 ERE are decreased by JQ1 treatment (Figure 2.I.4J, 2.I.4K, and 2.I.S4O). Altogether, these studies suggest that in addition to its role in transcriptional elongation, BRD4 affects both recruitment and elongation of RNAPII on ER $\alpha$ -dependent enhancers.

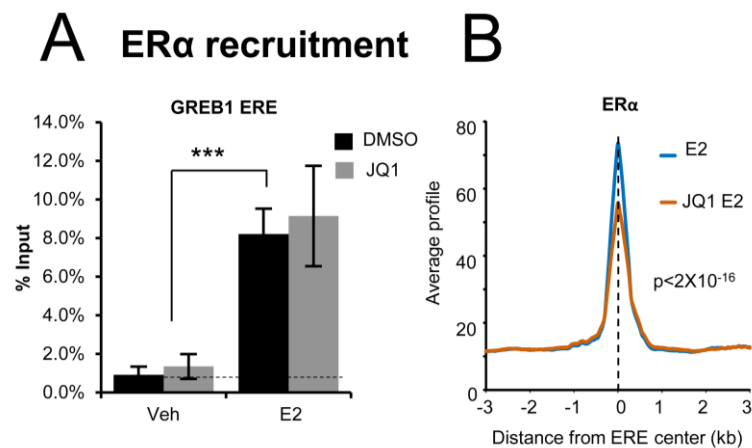


**Figure 2.I.4A,B. BRD4 binds to ER $^+$  enhancers after ER $\alpha$  recruitment and H3K27ac.** (A) ChIP-quantitative PCR (ChIP-qPCR) analyses of ER $\alpha$  occupancy on GREB1 ERE after DMSO or JQ1 treatment with Veh or E2 induction. \*\*\* $p \leq 0.001$ . Data are represented as mean  $\pm$  SD ( $n = 3$ ). Dotted line indicates background. (B) Aggregate plot showing genomic binding profiles of ER $\alpha$  on distal EREs upon E2-treated and JQ1 as well as E2 (JQ1 E2)-treated conditions. x axis shows the distance from the center of ERE in kilobase pairs. y axis shows the average ER $\alpha$  signal of the reads normalized per hundred million base pairs. Weighted averages for each ERE  $\pm 100$  bp were used to calculate the p values using ANOVA with repeated measures with ANOVA with multiple-regression model. p value is mentioned in the plot.

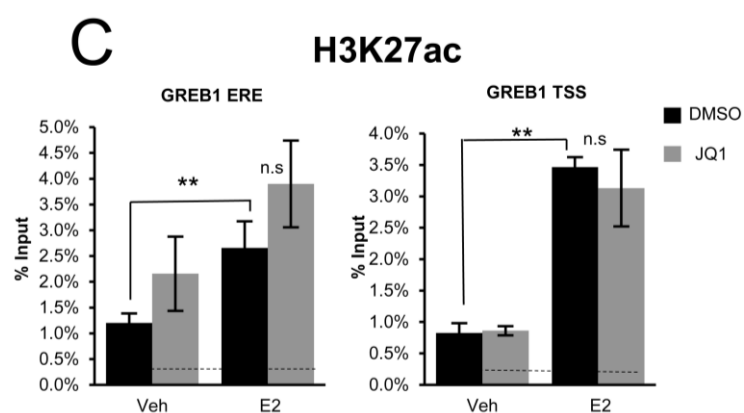


**Figure 2.I.4C. BRD4 binds to ER $^+$  enhancers after ER $\alpha$  recruitment and H3K27ac.** ChIP-qPCR analyses of H3K27ac after DMSO or JQ1 treatment with Veh or E2 induction on GREB1 ERE

overlapping region and GREB1 TSS. The data are represented as mean  $\pm$  SD (n = 3). \*\*p  $\leq$  0.01; n.s., not significant.

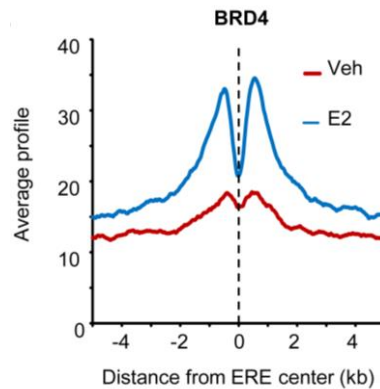


**Figure 2.I.4D. BRD4 binds to ER+ enhancers after ER $\alpha$  recruitment.** Aggregate plot showing genomic binding profiles of BRD4 on distal EREs upon Veh and E2-treated conditions.

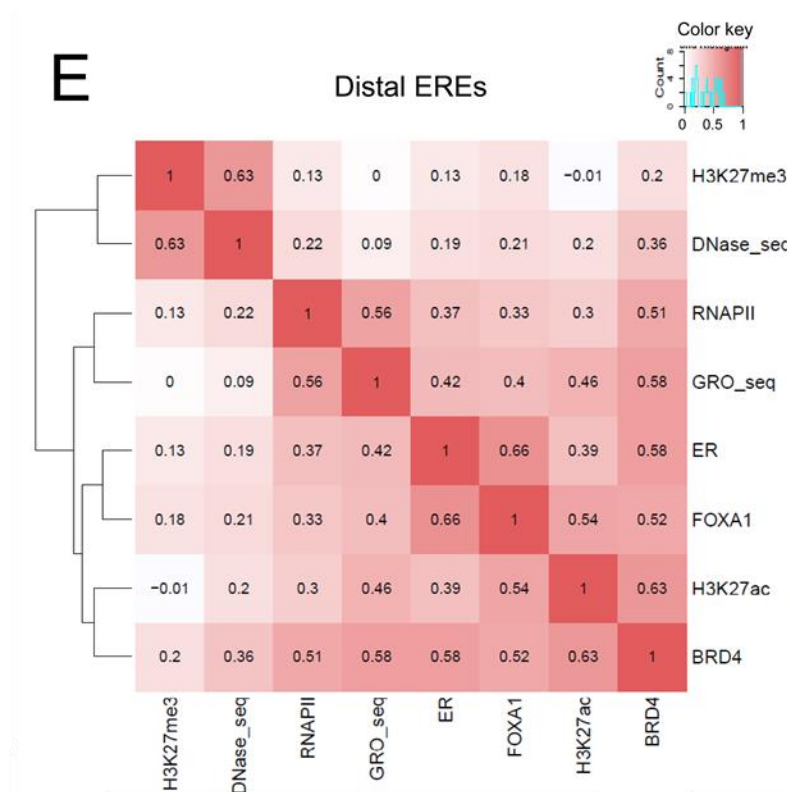


**Figure 2.I.4E. BRD4 binds to ER+ enhancers after ER $\alpha$  recruitment and H3K27ac and regulates eRNA synthesis.** Correlation plot on distal EREs  $\pm$ 1.5 kb showing the association of BRD4, H3K27ac, ER $\alpha$ , FOXA1, nascent RNA transcription (GRO-seq), RNAPII, DNase-seq, and H3K27me3.

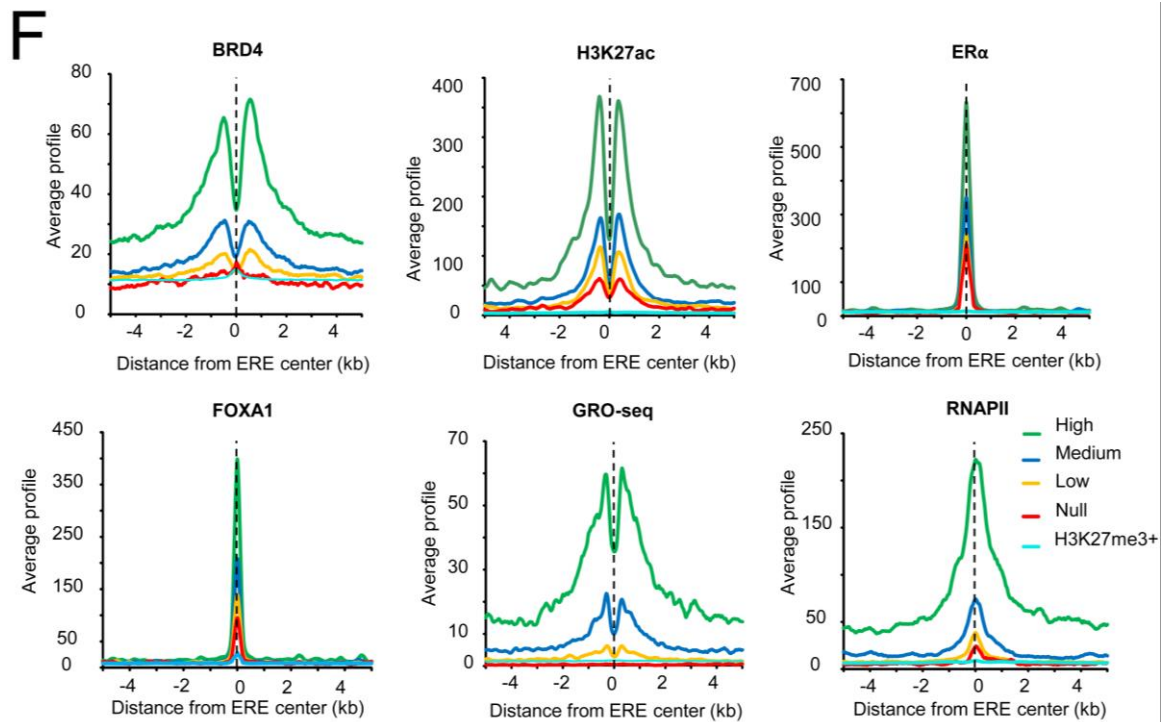


**Figure 2.1.4F. BRD4 binds to ER<sup>+</sup> enhancers after ER $\alpha$  recruitment and H3K27ac and regulates eRNA synthesis.** Aggregate plot analyses of BRD4, H3K27ac, ER $\alpha$ , FOXA1, and RNAPII occupancy on GRO-seq-based classified distal EREs. “High” group corresponds to distal EREs having a weighted average  $>0.45$ , “medium”  $>0.25 <0.45$ , “low”  $>0 <0.25$ , and “null” with no value of average.

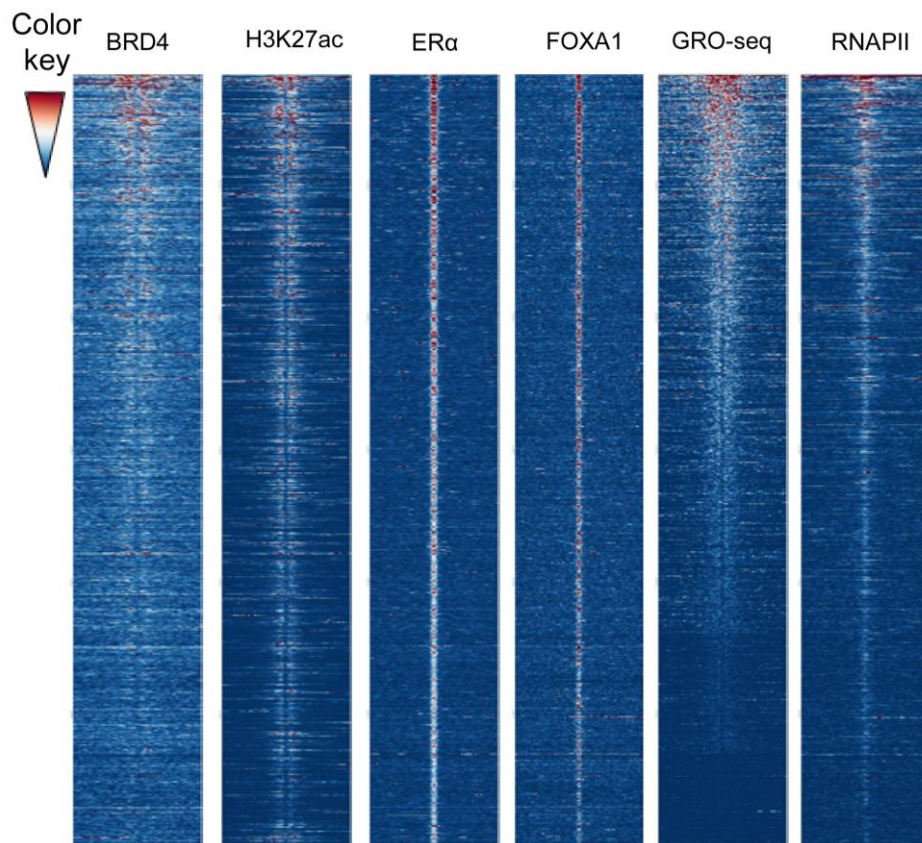


**Figure 2.I.4G. BRD4 binds to ER<sup>+</sup> enhancers after ER $\alpha$  recruitment and H3K27ac and regulates eRNA synthesis.** Heatmap profiles of BRD4, H3K27ac, ER $\alpha$ , FOXA1, nascent RNA transcription (GRO-seq), and RNAPII occupancy on  $\pm 5$  kb of distal EREs aligned from high to null GRO-seq signals. Center of each heatmap denotes center of distal EREs.

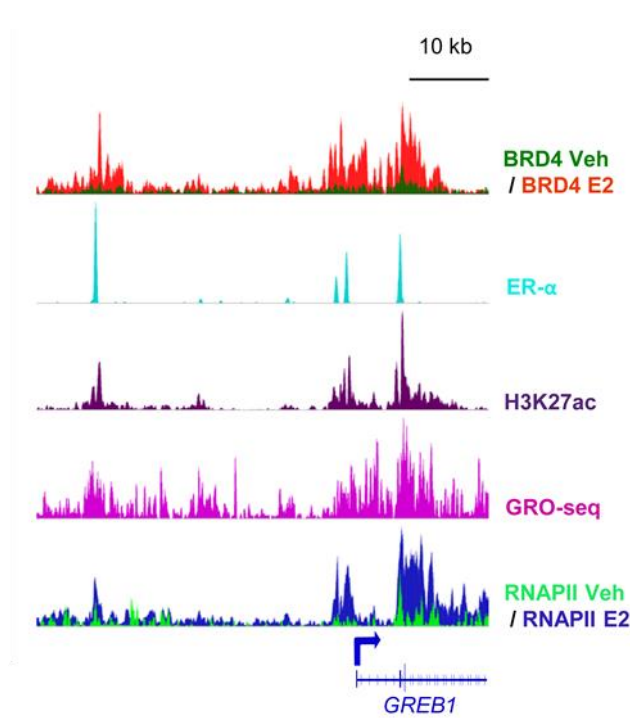


**Figure 2.I.4H. BRD4 binds to ER<sup>+</sup> enhancers after ER $\alpha$  recruitment and H3K27ac and regulates eRNA synthesis.** Binding profiles of BRD4, H3K27ac, ER $\alpha$ , GRO-seq, and RNAPII on GREB1 proximal and distal EREs and promoter. BRD4 with red peaks indicates E2-treated and green indicates Veh-treated conditions. RNAPII with blue peaks indicates E2-treated and light green indicates Veh-treated conditions.

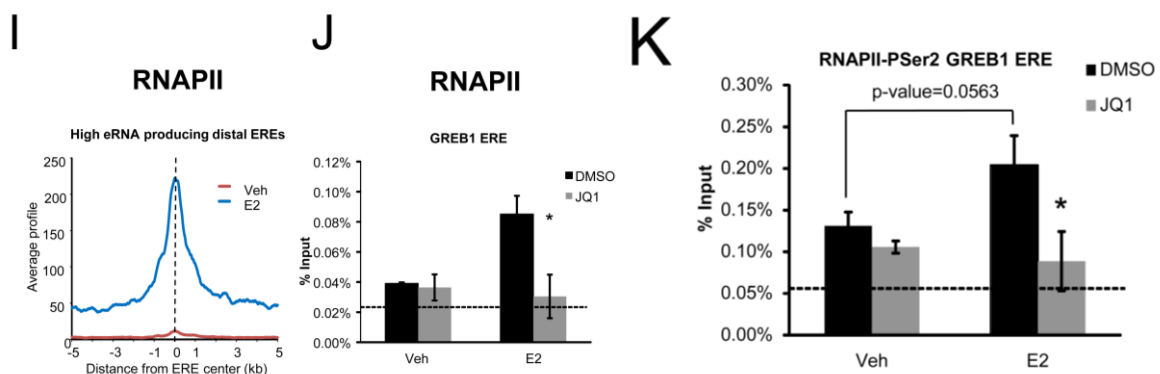


**Figure 2.I.4I,J,K. BRD4 binds to ER<sup>+</sup> enhancers after ER $\alpha$  recruitment and H3K27ac and regulates eRNA synthesis.** (I) Aggregate plot showing genomic binding profiles of RNAPII on distal EREs that produce high eRNA (GRO-seq group “high”) upon Veh and E2-treated conditions. (J and K) ChIP-qPCR analyses of RNAPII (J) and RNAPII-PSer2 (K) occupancy on GREB1 ERE after DMSO or JQ1 treatment with Veh or E2 induction. \* $p \leq 0.05$ . Data are represented as mean  $\pm$  SD ( $n = 3$ ). Dotted line indicates background.

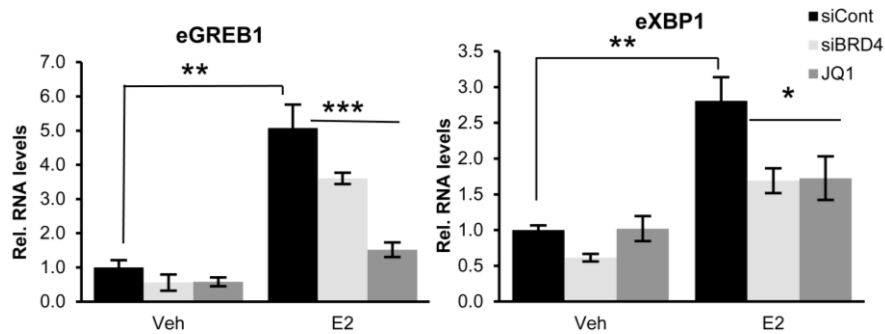


**Figure 2.I.4L. BRD4 binds to ER+ enhancers after ER $\alpha$  recruitment and H3K27ac and regulates eRNA synthesis.** (L) eRNA-qPCR results showing E2-induced eRNA (eGREB1 and eXBP1) upon negative siCont, siBRD4, or JQ1 treatment with Veh or E2 induction. Relative RNA levels are shown as “Rel. RNA levels.” Data are represented as mean  $\pm$  SD (n = 3).

Importantly, BRD4 depletion or inhibition significantly decreased eRNA synthesis from E2-regulated enhancers (Figure 2.I.4L). This suggests that in addition to its reported cis-regulatory function, BRD4 may stimulate E2-induced mRNA transcription by promoting eRNA production at distal EREs.

## Discussion

The hierarchical epigenetic regulation of transcriptional activation involves an intricate network of interactions among various transcription factors, histone-modifying enzymes, epigenetic readers, and the transcriptional machinery. In this study, we investigated the function of the epigenetic reader BRD4 in controlling E2-regulated gene transcription. Our findings support a model in which ER $\alpha$  recruits histone acetyltransferases to a subset of EREs enriched for FOXA1 to facilitate histone acetylation and subsequent recruitment of BRD4 and RNAPII in order to promote eRNA synthesis (Figure 3.1).

To date, most studies have focused largely on the role of BRD4 as a promoter proximal regulator of mRNA synthesis by increasing P-TEFb recruitment. Consistent with a direct function of BRD4 on target gene transcription, we show that BRD4 promotes elongation-associated phosphorylation of RNAPII and monoubiquitination of histone H2B. These results are consistent with an established essential role for H2Bub1 in E2-stimulated transcription (Prenzel et al., 2011) and the dependence of H2Bub1 upon CDK9 (Pirngruber et al., 2009a). In addition to a cis-regulatory function of BRD4, our results uncover a role for BRD4 on enhancers. This is

consistent with a previous finding that CDK9 is recruited by BRD4 to distal intergenic enhancer regions marked by H3K27ac (Lovén et al., 2013). Notably, we show that BRD4 co-occupies eRNA-producing enhancers with ER $\alpha$ , FOXA1, and H3K27ac, regulates RNAPII recruitment on ER $\alpha$ -bound enhancers, and is required for the production of eRNA transcripts. These findings support a role for BRD4 in hormone-dependent cancers (Asangani et al., 2014) and suggest a model in which eRNA synthesis requires a coordinated epigenetic hierarchy that culminates in the recruitment of BRD4 and RNAPII and subsequent transcription from a select subset of distal EREs.

The importance of BRD4 in E2-regulated transcription is consistent with previously identified interactions between BRD4 and ER $\alpha$  (Wu et al., 2013) as well as ER $\alpha$  and CDK9 (Sharp et al., 2006) or cyclin T1 (Wittmann et al., 2005). Furthermore, the 7SK component HEXIM1, which suppresses P-TEFb activity, negatively regulates ER $\alpha$  transcriptional activity (Wittmann et al., 2005), and its overexpression induces tamoxifen resistance (Ketchart et al., 2011). Importantly, recent data showed that CDK9 activity is required for the production of eRNAs at distal EREs (Hah et al., 2013) and the role of eRNA and MED1 in regulating AR-dependent transcription and looping (Hsieh et al., 2014). Thus, consistent with our model, P-TEFb and BRD4 likely promote ER $\alpha$ -mediated transcriptional activation at least in part by promoting eRNA transcription.

ER $\alpha$  functions together with Cohesin to nucleate chromosomal looping that promotes E2-regulated transcription (Fullwood et al., 2009; Schmidt et al., 2010). Our previous study showed that proteasomal inhibition specifically decreases ER $\alpha$ -regulated transcription by decreasing H2Bub1 and transcriptional elongation without affecting long-range chromosomal interactions (Prenzel et al., 2011). Consistently, CDK9 inhibition decreased ER $\alpha$ -dependent gene expression without affecting ER $\alpha$  occupancy, coactivator recruitment, or chromosomal looping (Hah et al., 2013). Similarly, our data show that BRD4 inhibition had little or no effect on ER $\alpha$  recruitment, E2-stimulated H3K27 acetylation, or Cohesin recruitment, indicating that BRD4 functions along with CDK9 downstream of early enhancer activation events but precedes RNAPII recruitment and elongation.

Numerous recent studies have shown a substantial therapeutic potential for BRD4 inhibition in various malignant diseases (Zuber et al., 2011; Herrmann et al., 2012; Lockwood et al., 2012; Asangani et al., 2014; Ott et al., 2012; Filippakopoulos et al., 2010; Zhang et al., 2012b), leading to the testing of several BET domain inhibitors in a clinical setting for certain types of tumors (Filippakopoulos and Knapp, 2014). However, the utility of BET inhibitors in ER $\alpha$ + breast cancer has not been investigated. Here, we describe a function of BRD4 in specifically controlling E2-dependent gene transcription in ER $\alpha$ + normal and malignant cells in vitro and in vivo. We provide mechanistic insight to support a previously unknown mechanism by which BRD4 controls distal enhancer activity and target gene expression by promoting eRNA synthesis. We hypothesize that this BRD4-dependent mechanism likely controls other enhancer-driven transcriptional programs directing processes such as lineage specification during cell differentiation and development. Moreover, these findings may potentially serve to provide a mechanistic-based approach to the treatment of ER $\alpha$ + breast cancer.

## Experimental Procedures

### Cell Culture, Transfections, Inhibitors, and siRNAs

MCF7 cells were provided by K. Pantel (University Medical Center, Hamburg-Eppendorf), Ishikawa from T. Spelsberg (Mayo Clinic, Rochester), and H1299 from M. Dobbstein (University Medical Center, Göttingen). They were grown in phenol red-free high-glucose Dulbecco's modified Eagle's media (DMEMs; Invitrogen) supplemented with 10% bovine growth serum (Thermo Scientific), 1% sodium pyruvate, and 1% penicillin/streptomycin (Sigma-Aldrich). Forward and reverse transfections were performed using DharmaFECT 1 (Thermo Scientific) for small interfering RNAs (siRNAs) according to the manufacturer's instructions. Nontargeting (negative control) and BRD4 siRNAs (siBRD4s) were obtained from Dharmacon (Thermo Scientific). BRD4 SmartPool siRNA (Dharmacon) contained the sequences 5'-AGCUGAACCUCUCCUGAUUA-3', 5'-UGAGAAAUCUGCCAGUAAU-3', 5'-UAAAUGAGCUACCCACAGA-3', and 5'-GAACCUCUCCUGAUUACUUAU-3'. JQ1 (150 nM) was used to pretreat the cells 30 min before E2 induction. 17  $\beta$ -estradiol and ethinyl estradiol (Sigma-Aldrich) were used at the concentration of 10 nM. DMSO or



ethanol was used as Veh. ICI182780 (Fulvestrant) was used at the concentration of 1  $\mu$ M. TGF- $\beta$ 1 (2 ng/ml) treatment was done on H1299 cells for 90 min.

E2-induction experiments were carried out by changing the media to DMEM supplemented with 5% charcoal-dextran-treated fetal bovine serum (CSS; Sigma-Aldrich), 1% sodium pyruvate, and 1% penicillin/streptomycin after 24 hr of cell growth. After 48 hr of hormone deprivation, they were treated with 17  $\beta$ -estradiol for 2, 6, or 24 hr. Ethinyl estradiol was used for proliferation assays in Ishikawa cells. TGF- $\beta$ 1 treatment in H1299 cells was given after growing the cells in serum-free media for 48 hr.

MCF-7 cells were harvested for RNA upon Veh or E2 treatment, and negative control siRNA (siCont), siBRD4, or JQ1 transfection. JQ1-treated cells were also transfected with negative siCont. Ishikawa and H1299 cells were harvested for RNA under Veh or E2 treatment, or TGF- $\beta$ 1 treatment and negative siCont or siBRD4.

### **RNA-Seq**

RNA integrity was checked using Bioanalyzer 2100 (Agilent Technologies). A total of 500 ng of total RNA was used for preparing libraries using TruSeq RNA Sample Preparation Kit (Illumina), and the size range was checked to be 280 bp using Bioanalyzer. These samples were amplified and sequenced by using cBot and HiSeq 2000 from Illumina, respectively, for 51 bp single-ended tags with single indexing. Images from the sequencing results were processed using BaseCaller to bcl files function in Illumina software. These were demultiplexed to fastq files using CASAVA 1.8.2 and mapped to the human reference transcriptome (UCSC HG19) using Bowtie 2 (version 2.1.0) (Langmead and Salzberg, 2012). Read counts for each sample and each gene were aggregated using a custom Ruby script. DESeq (version 1.14.0) was used for measuring differential expression (Anders and Huber, 2010).

### **Gene Set Enrichment Analysis**

Pathway enrichment scores were calculated by GSEA (Subramanian et al., 2005). The gene expression data from RNA sequencing (RNA-seq) analyses are sorted by correlation with log<sub>2</sub>-fold changes between different conditions. This sorted

expression data set was compared with C2-curated gene sets that include published gene sets from pathways of chemical and genetic perturbations, canonical pathways, BIOCARTA, Reactome, and KEGG. WILLIAMS\_ESR1\_TARGETS\_UP (Williams et al., 2008), FRASOR\_RESPONSE\_TO ESTRADIOL\_UP (Frasor et al., 2004), MASSERWEH\_RESPONSE\_TO ESTRADIOL (Massarweh et al., 2008), BHAT\_ESR1\_TARGETS\_NOT\_VIA\_AKT1\_UP (Bhat-Nakshatri et al., 2008), DUTERTRE ESTRADIOL\_RESPONSE\_6HR\_UP (Dutertre et al., 2010), PID\_HNF3A\_PATHWAY (Schaefer et al., 2009), STEIN\_ESR1\_TARGETS (Stein et al., 2008), MASSERWEH\_TAMOXIFEN\_RESISTANCE\_DN (Massarweh et al., 2008), and CREIGHTON\_ENDOCRINE\_THERAPY\_RESISTANCE\_4 (Creighton et al., 2008) are shown as E2-related topmost enriched pathways under BRD4 perturbation.

## ChIP

ChIP and subsequent real-time PCR analyses with specific primers (Table S3) were performed as before (Bedi et al., 2015; Prenzel et al., 2011) for BRD4, ER $\alpha$ , RAD21, H3K27ac, and H2Bub1. ChIP-seq was performed for BRD4, ER $\alpha$ , and H2Bub1. BRD4 ChIP was performed by crosslinking the chromatin for 20 min in 1% formaldehyde. Other antibodies and their dilutions were used as described before (Table S1) (Bedi et al., 2015; Prenzel et al., 2011).

## ChIP-Seq and Bioinformatic Analyses

Prior to library preparation, immunoprecipitated DNA was sonicated an additional time to ensure fragment sizes less than 200 bp. Libraries were prepared using the NEBNext Ultra DNA library preparation kit according to the manufacturer's instructions. Size range was verified to be 280–300 bp using Bioanalyzer 2100. A total of 50 cycles were used for amplification in cBot, and 101 bp single-ended tags for BRD4 and 51 bp single-ended tags for other ChIP samples were sequenced with single indexing using Illumina HiSeq 2500. Raw data for FOXA1, H3K4me3, H3K27me3 (Joseph et al., 2010), H3K27ac (Theodorou et al., 2013), RNAPII (Welboren et al., 2009), DNase sequencing (DNase-seq) (Thurman et al., 2012), and global run-on (GRO) sequencing (GRO-seq) (Hah et al., 2013) were downloaded from the European Nucleotide Archive, and their accession numbers are listed in

Table S4. The reads were mapped to the human reference genome (UCSC HG19) using Bowtie (version 1.0.0) (Langmead et al., 2009). Peak calling was done by Model-based Analysis of ChIP-Seq (version 1.4.2) (Zhang et al., 2008). Coverage was determined by normalizing the total number of mapped reads per hundred million. For plotting correlation, aggregation, ChIP enrichment signals over specific genomic features, and heatmaps, Cistrome (Liu et al., 2011) based on the Galaxy framework was used. Data were visualized in Integrative Genomics Viewer (version 2.3.14) (Thorvaldsdóttir et al., 2013). Common TSS and gene body coordinates were obtained from UCSC Table Browser (Karolchik et al., 2004). Distal EREs were defined as ER $\alpha$  binding sites not within gene bodies or regions 5 kb upstream or downstream thereof. Regions covering the TSS and 3 kb downstream of it were used for TSS-oriented correlation plots and 1.5 kb up- and downstream to distal EREs for distal ERE-oriented correlation plots. Average signals of GRO-seq data with E2 treatment were calculated using assign weighted average function in Cistrome surrounding TSS (plus 3 kb) or ERE ( $\pm 1.5$  kb). These values were used to group the TSS or ERE coordinates as high, medium, low, and null. For distal EREs, the “high” group corresponds to distal EREs having a weighted average greater than 0.45, “medium” has  $>0.25 <0.45$ , “low” has  $>0 \leq 0.25$ , and “null” has a zero (0) average. For TSSs, the “high” group corresponds to distal EREs having a weighted average greater than 0.3, “medium” has  $\geq 0.15 <0.3$ , “low” has  $>0 <0.15$ , “null” has a zero (0) average. The range for these groups was chosen according to the similar number of TSSs or EREs in each group and adequate GRO-seq enrichment signal defined for each group. H3K27me3-positive coordinates were obtained using the summits of H3K27me3 ChIP-seq signal (Joseph et al., 2010). For measuring statistical significance of aggregate plots, weighted averages for each E2-upregulated gene, 1.5–2.5 kb downstream of each TSS or distal ERE  $\pm 100$  bp, were used to compute a multiple-linear regression model. Within the multiple-linear regression model, the weighted average within a 1 kb window was used as a dependent variable, given the independent variables of condition and gene. The condition variable was tested for significant impact using an ANOVA. Groups of E2-upregulated genes based on RNAPII occupancy (RNAPII recruited de novo, RNAPII preloaded and recruited, and RNAPII constitutively bound) were kindly provided by W. Lee Kraus. E2 up- ( $\geq 1.5$ -fold), down- ( $\leq 0.8$ -fold), and nonregulated genes were retrieved from RNA-seq data.

## In Vivo Experiments in JQ1-Injected Mice

Three-week-old C57BL/6 female mice were injected intraperitoneally with JQ1 (50 mg/kg) or Veh (5% DMSO in 5% dextrose) for 3 weeks (n = 8 for each group). Mice were sacrificed via CO<sub>2</sub> inhalation, and uteri were collected to examine differences in their size and weight. Difference in the uterine weight between control (DMSO) and JQ1-injected mice was calculated by normalizing the uterine wet weight (in milligrams) with respect to body weight (in grams). Uteri (n = 4 for each group) were homogenized using beads by FastPrep FP120 homogenizer (Thermo Scientific), and RNA was isolated using TRIzol (QIAGEN) according to manufacturer's instructions. Normalization was done using starting quantity values of glyceraldehyde 3-phosphate dehydrogenase. Relative mRNA expression analyses were done as mentioned before (but not normalized for control conditions) using gene-specific primers for the E2-dependent and cell-cycle-related genes *Ran* and *Mad2l1* (Suzuki et al., 2007) and the reproduction-related gene *Il1b* (Weihua et al., 2000). Primers are listed in Table S2. Statistical significance was analyzed using Student's t test. All animal studies were performed in compliance with the requirements of the German Animal Welfare Act.

## Author Contributions

S.N. and S.A.J. designed the experiments and wrote the manuscript. S.N. and T.H. performed the experiments. S.N. and M.A. performed bioinformatic analyses. Z.N., H.T., I.B.-B., and M.S. performed mouse injection and dissection. D.I. and A.G. performed next-generation sequencing. S.K. provided JQ1. C.-M.C. generated the BRD4 antibody for ChIP-seq. All authors provided intellectual input and edited the manuscript.

## Acknowledgments

The authors thank G. Salinas-Riester for performing RNA-seq, F. Kramer, T. Beissbarth, and S. Joosse for help in statistical analysis, W.L. Kraus for the list of RNAPII groups, members of the S.A.J. group for thoughtful discussions, and V. Manickam for help with graphic design. This work was funded by the German Academic Exchange Service (to S.N.); the SGC, a registered charity (1097737) that

receives funds from the Canadian Institutes for Health Research, the Canada Foundation for Innovation, Genome Canada, AbbVie, Boehringer Ingelheim, Bayer, Janssen, GlaxoSmithKline, Pfizer, Eli Lilly, the Novartis Research Foundation, Takeda, the Ontario Ministry of Research and Innovation, and the Wellcome Trust (092309/Z/10/Z to S.K.); NIH (CA103867), CPRIT (RP110471), and Welch Foundation (I-1805) (to C.-M.C.); German Research Foundation HE 5208/2-1 (to E.H.); the Alexander-von-Humboldt Foundation and EMBO (to H.T.); and the Deutsche Krebshilfe (109088 to S.A.J.).

## **Accession Numbers**

The NCBI Gene Expression Omnibus accession number for RNA- and ChIP-seq data reported in this paper is GSE55923.

## 2.1.1. Supplemental Information

### 2.1.1.1. Supplemental tables

#### Supplemental Table S1 related to Experimental procedures

Antibodies used for Western Blot and ChIP/ChIP-seq

Target Protein	Clone	Cat.No.	ChIP	WB	Source
Beta-Actin	I-19	sc1616	-	1:5000	Santa Cruz
ER $\alpha$	HC-20	sc-543	1 $\mu$ g	1:1,000	Santa Cruz
H2B		ab1790	-	1:15,000	Abcam
H2Bub1	D11	5546	1.5 $\mu$ L	-	Cell signaling
H2Bub1	7B4		-	1:10	Hybridoma (Prenzel et al., 2011)
H3K27ac		pAb-196-050	1 $\mu$ g	-	Diagenode
RAD21		ab992	1 $\mu$ g	-	Abcam
HSC70	B-6	sc-7298	-	1:25,000	Santa Cruz
RNAPII	N-20	sc-899	1 $\mu$ g		Santa Cruz
RNAPII P-Ser2	3E10		-	1:10	Hybridoma (Prenzel et al., 2011)
RNAPII P-Ser2		A300-654A	0.4 $\mu$ g		Bethyl (Prenzel et al., 2012)
BRD4		5716-1	-	1:5000	Epitomics
BRD4(N-term)			4 $\mu$ L	-	(Wu et al., 2006)

#### Supplemental Table S2 related to Experimental procedures

Primers used for qPCR in 5' to 3' orientation. Primers were designed using PRIMER BLAST in these studies.

Gene	Forward Primer (5' to 3')	Reverse Primer (5' to 3')	Source
GREB1	GTGGTAGCCGAGTGGACAAT	ATTTGTTCCAGCCCTCCTT	(Prenzel et al., 2011)
TFF1	CCCAGCACGGTGATTAGTCC	GTCAATCTGTGTTGTGAGCCG	This study
BRD4	GCCGTCCACACTGCGTGAGC	TCCCGGGGTGCCCTTCTTT	This study
18SrRNA	AACTGAGCCATGATTA	GGAACACGACGGTATCTGA	(Bedi et al., 2015)
DHFR	ATGGTTGGTTCGCTAACT	TGAAGAGTTGTGGTCATTC	(Pirngruber et al., 2009b)
TGF- $\alpha$	GCCTTCAAAACTCTGTCAAG	CACATGTGGACTCAGACACC	This study
KLF10	TAGCAGCCAGTCAGCTTG	AGTCTGCTGGAGAGAGGC	This study
SERPINE1	CTCTCTGCCCCTACCAAC	GGTCATGTTGCCCTTCCAGT	This study
SMAD7	CCAACTGCAGACTGTCCAGA	CAGGCTCCAGAAGAAGTTGG	This study
Ran	ACTCTTCTGGAAGGATCCGC	TCTTCTCAAACCTCGCCCGTC	This study
Mad21	GTCCAGAAAGCCATACAGGA	TCAGCAGATCAAAGGAACAAGAA	This study
Il1b	TGAAGAAGAGCCCATCCTCTG	GGAGCCTGTAGTGCAGTTGT	This study
Gapdh	GGCAAATTCACGGCACAGT	CCTTTTGGCTCCACCCTTCA	This study
eGREB1	GCTAACCATGCTGCAAATGA	ACACAGTCAGGGCAAAGGAC	(Li et al., 2013)
eXBP1	TGTGAGCACTTGGCATCCAT	ACAGGGCCTCATTCTCCTCT	This study

#### Supplemental Table S3 related to Experimental procedures

Primers used in ChIP studies in 5' to 3' orientation.

Gene	Forward Primer (5' to 3')	Reverse Primer (5' to 3')	Source
GREB1 TSS	GCCAAATGGAAGAAGGACAG	ACCACCTACCTCCAGTCACC	(Prenzel et al., 2011)
GREB1 ERE	GCTGACCTTGTGGTAGGCAC	CAGGGGCTGACAACTGAAAT	(Prenzel et al., 2011)
GREB1 ERE (RNAPII P-Ser2)	GCTAACCATGCTGCAAATGA	ACACAGTCAGGGCAAAGGAC	(Li et al., 2013)
GREB1 H3K27ac+ ERE	CACGTCCCCACCTCACTG	TGTTAGCTTCGGGACACC	This study
GREB1 TR	CCCAAGCCTTCTCTGGGTTC	AGCAGACGAGAAGTAGGGCT	This study
GREB1 3' end	GGGTGCCAAGTCGCTGCTGT	CTGGATGGCAGAGGCGCCG	(Prenzel et al., 2011)
XBP1 TSS	ATCCCCAGCTCTGGTCATCT	GCCCAGGGCTCTTTCTGTGA	This study
XBP1 ERE	TAGATTCCTTGCCCCGTGTC	GAAAGAGGGGGTTGCCTGAG	This study
XBP1 H3K27ac+ ERE	TGCTGTCCCTAAAGCAGTGG	ATCCCAGCTCCTGATCCCAA	This study
TFF1 TSS	CCTGGATTAAGGTCAGGTTGGA	TCTTGGCTGAGGGATCTGAGA	(Prenzel et al., 2011)
TFF1 ERE	GACAGAGACGACATGTGGTGAGGTCA	CACCCCGTGAGCCACTGTTGTC	(Prenzel et al., 2011)
TFF1 H3K27ac+ ERE	GTGGTTCACTCCCCTGTGTC	GAGGCATGGTACAGGAGAGC	This study
TFF1 TR	CCACTCCCTAGAAGGACCCA	GCTGGCAACCCATATTCCCT	(Bedi et al., 2015)
GAPDH TR	CCGGGAGAAGCTGAGTCATG	TTTGGGTGGAAATGTCCTT	This study

**Supplemental Table S4 related to Experimental procedures**  
Published genomic datasets

Dataset	NCBI accession numbers	Source
H3K27ac+E2	GSM986077	(Theodorou et al., 2013)
GRO-seq+E2	GSM1067414, GSM1067415	(Hah et al., 2013)
RNAPII+E2	GSM365930	(Welboren et al., 2009)
DNase seq	GSM816627	(Thurman et al., 2012)
H3K4me3+E2	GSE23701	(Joseph et al., 2010)
H3K27me3+E2	GSM588564	(Joseph et al., 2010)
FOXA1+E2	GSM659787	(Joseph et al., 2010)

## 2.1.1.2. Supplemental experimental procedures

### Western blot

Protein lysates were prepared by incubating the cells with Radio Immunoprecipitation buffer (RIPA buffer - 1% (v/v) NP-40, 0.5% sodium deoxycholate and 0.1% SDS in 1X PBS along with protease inhibitors: 1 mM Pefabloc, 1 ng/ $\mu$ L Aprotinin/Leupeptin, 10 mM  $\beta$ -glycerophosphate and 1 mM N-ethylmaleimide) for 10 minutes. After brief sonication to release the chromatin associated proteins, 6X loading dye was added to the samples. These were boiled at 95 °C for 5 -10 minutes and run in a SDS-PAGE. Proteins of interest were analyzed by Western blotting with antibodies and dilutions as described in Supplemental Table S1 (Bedi et al., 2015; Prenzel et al., 2011). Hsc70 and  $\beta$ -actin were used as loading control for cytoplasmic proteins and RNA polymerase II (total) and histone H2B for nuclear proteins. Quantification of proteins in Western Blot was done using ImageJ and H2Bub1 was normalized with H2B and ER $\alpha$  with HSC70.

### Quantification of gene expression and eRNA levels by quantitative real-time PCR

RNA isolation and cDNA synthesis were performed as described before (Bedi et al., 2015; Prenzel et al., 2011). RNA isolation was done using TRIzol reagent (Qiagen) according to manufacturer's instructions. 1  $\mu$ g of total RNA was reverse-transcribed using random nonamer primers (Metabion and Sigma). Quantitative real time PCR (qPCR) reaction mix was prepared as follows: 75 mM Tris-HCl (pH 8.8), 20 mM (NH<sub>4</sub>)<sub>2</sub>SO<sub>4</sub>, 0.01% (v/v) Tween-20, 3 mM MgCl<sub>2</sub>, 200  $\mu$ M dNTPs, 0.5 U/reaction Taq DNA Polymerase (Prime Tech, Minsk, Belarus), 0.25% (v/v) Triton X 100, 1:80,000 SYBR Green I (Roche, Mannheim, Germany) and 300 mM Trehalose. After reverse transcription, qPCR was done using 1  $\mu$ L of each sample, 1.5  $\mu$ L of 5

$\mu$ M gene-specific primers (listed in supplemental table S2) and 14  $\mu$ L of qPCR reaction mix and made up for the final volume of 25  $\mu$ L. PCR was done using C1000<sup>TM</sup> Thermal Cycler and CFX96<sup>TM</sup> Optical Reaction Module (Bio-Rad, München, Germany) with 40 cycles of two-step amplification (95°C for 15 s and 60°C for 1 min) for each primer pair. A standard curve was determined from the dilutions of all cDNA samples for gene specific primers. This curve was used for the quantification of samples. Relative quantification was done by normalizing with starting quantity values of 18S ribosomal RNA in case of human cell-derived samples and Gapdh for mice samples. Expression levels of the samples were relatively determined with the vehicle-treated control samples and this relative mRNA expression is denoted as “Rel. mRNA exp.”. eRNA levels were tested by eRNA-specific primers (supplemental table S2) using qPCR and relative eRNA levels were calculated as mentioned above and denoted as “Rel. RNA levels”. Statistical significance was analyzed using ANOVA-single factor test.

### **Cell proliferation assays**

For cell counting based proliferation assays, 10,000 MCF7 cells were plated in normal growth medium which was replaced by hormone-deprived medium after 8 hours. In case of siRNAs, reverse transfection was done. Cells were treated with 17- $\beta$ -estradiol, and or with siRNAs or inhibitors for 3, 5 and 7 days. Transfection was repeated after 72 hours in order to sustain the knockdown efficiency. The counting was performed using Neubauer’s chamber. For statistical significance, one way ANOVA was performed with Tukey HSD based multiple comparisons using SPSS package and p-values were calculated.

For Crystal violet based proliferation assays, 20,000 Ishikawa cells were plated in normal growth medium which was replaced by hormone-deprived medium after 8 hours. In case of siRNAs, reverse transfection was done. Cells were treated with ethinyl estradiol, and or with siRNAs or inhibitors for 7-9 days. Transfection was repeated after 72 hours in order to sustain the knockdown efficiency. On confluency, colonies were fixed with 4 % paraformaldehyde for 5 minutes before staining with 0.1 % crystal violet solution for 1 hour. Percentage of intensity covered by the cells after 7-9 days of growth was quantified using ImageJ with a plugin ColonyArea (Guzmán et al., 2014).



## Chromatin Immunoprecipitation (ChIP)

ChIP assays were performed as follows: Culture medium was removed from the cells and crosslinking of chromatin was performed by adding 1% formaldehyde (in PBS) for 10 minutes (20 minutes for BRD4 ChIP) at room temperature. Formaldehyde was quenched by adding 125 mM glycine at final concentration for 5 minutes. After crosslinking, cells were washed with ice-cold PBS twice and then ice cold nuclear preparation buffer (150 mM NaCl, 20 mM EDTA (pH 8.0), 50 mM Tris (pH 7.5), 0.5% (v/v) NP-40, 1% (v/v) Triton X 100 and 20 mM Sodium Fluoride with protease inhibitors: 10  $\mu$ M indole acetamide, 1mM nickel chloride, 1 mM Pefabloc, 1 ng/ $\mu$ L aprotinin/leupeptin, 10 mM  $\beta$ -glycerophosphate and 1 mM N-ethylmaleimide) was added and the cells were scraped. The harvested cells were centrifuged and the nuclear pellet obtained was resuspended in 300  $\mu$ L of sonication buffer-I (50 mM Tris-HCl (pH 8.0), 10 mM EDTA (pH 8.0), 1% SDS, with protease inhibitors mentioned above), incubated at 4 °C on a rotating wheel for 15 minutes and suspended in an equal volume of sonication buffer-II (150 mM NaCl, 20 mM EDTA (pH 8.0), 50 mM Tris-HCl (pH 8.0), 1% (v/v) NP-40, 20 mM Sodium Fluoride, with protease inhibitors). Sonication was done around 30 cycles using a Bioruptor Plus (Diagenode SA, Liège, Belgium) with high power for alternating 30 seconds of on and off. Sonicated samples were checked for shearing of fragment length ranging 200-400 bp and proceeded further. These were diluted with 600  $\mu$ L of dilution buffer (150 mM NaCl, 20 mM EDTA (pH 8.0), 0.5 % sodium deoxycholate, 50 mM Tris-HCl (pH 8.0), 1% (v/v) NP-40, 20 mM Sodium Fluoride, with protease inhibitors). Pre-clearing was done with 100  $\mu$ L of 50% Sepharose 4B (GE Healthcare, Uppsala, Sweden) slurry in dilution buffer containing 0.1% SDS (with protease inhibitors) for 1 hour at 4 °C.

Pre-cleared chromatin was centrifuged and supernatant was further diluted with dilution buffer to reduce final SDS concentration to 0.1 % and incubated with corresponding antibody (Table S1) overnight at 4°C. 30  $\mu$ L of BSA-blocked 50% Protein-A Sepharose slurry (GE Healthcare) were added to capture the specific chromatin complexes and incubated for 2 hours at 4°C.

ChIP immune complexes were washed twice with dilution buffer with 0.1% SDS, thrice with wash buffer (500 mM LiCl, 20 mM EDTA (pH 8.0), 1 % sodium

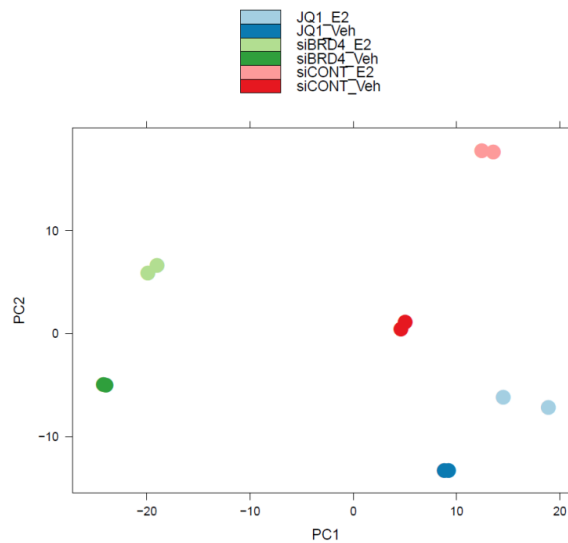
deoxycholate, 100 mM Tris-Cl (pH 8.5), 1% (v/v) NP-40, 20 mM Sodium Fluoride, with protease inhibitors), twice with dilution buffer with 0.1% SDS and finally twice with 1 X TE buffer. Number of washes was reduced one time in each buffer for BRD4 ChIP.

For ChIP-qPCR, washed beads and the input samples (stored after pre-clearing) were added with 100  $\mu$ L of 10% (w/v) Chelex 100 slurry (Bio-Rad) and vortexed for 10 sec, and incubated at 95 °C for 10 minutes. Reverse-crosslinking was done by incubating with Proteinase K (20  $\mu$ g/ $\mu$ L, Invitrogen) at 55°C at 1,000 rpm for 30 minutes and the enzyme was heat-inactivated at 95 °C for 10 minutes. After final centrifugation, immunoprecipitated DNA can be recovered.

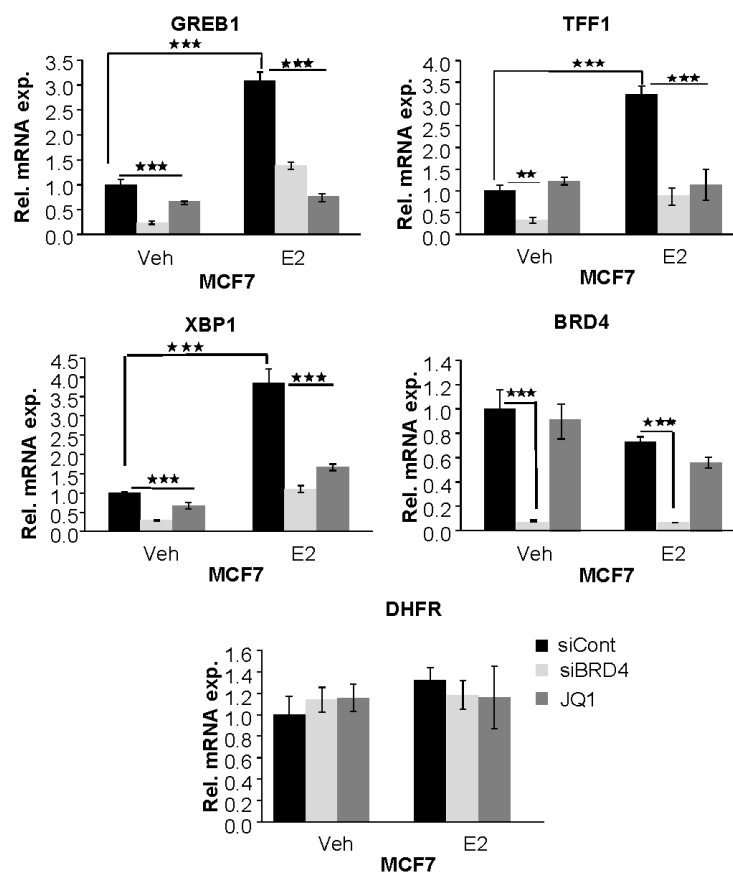
For ChIP-seq, RNase treatment was done by adding 0.2  $\mu$ g/ $\mu$ L of RNase A (Qiagen) in Tris 10 mM pH 8 and incubating the samples for 30 minutes at 37 °C. After diluting the immunoprecipitated complexes by a buffer containing 20 mM EDTA, 100 mM Tris-HCl (pH 8) and 2% SDS without any protease inhibitors, reverse crosslinking was performed by adding 1  $\mu$ L of Proteinase K (20 mg/ml) and incubating overnight at 65 °C for 800 rpm. After adding LiCl and linear polyacrylamide to precipitate DNA, DNA was isolated using phenol-chloroform-isoamyl alcohol mediated extraction.

qPCRs were done for amplicons covering gene-specific TSS, transcribed regions (TR) or ERE specific ChIP primers (Supplemental table S3) using 45 cycles of amplification. For H3K27ac and BRD4, primers were designed adjacent to EREs according to published H3K27ac data (Theodorou et al., 2013). Standard curve was made using DNA from input samples and used for quantification of the samples. Background DNA was detected using a ChIP assay with blocked protein-A sepharose. For normalizing ChIP samples, input DNA was used. The readings were mentioned in the graph as percentage of input.

### 2.1.1.3. Supplementary figures

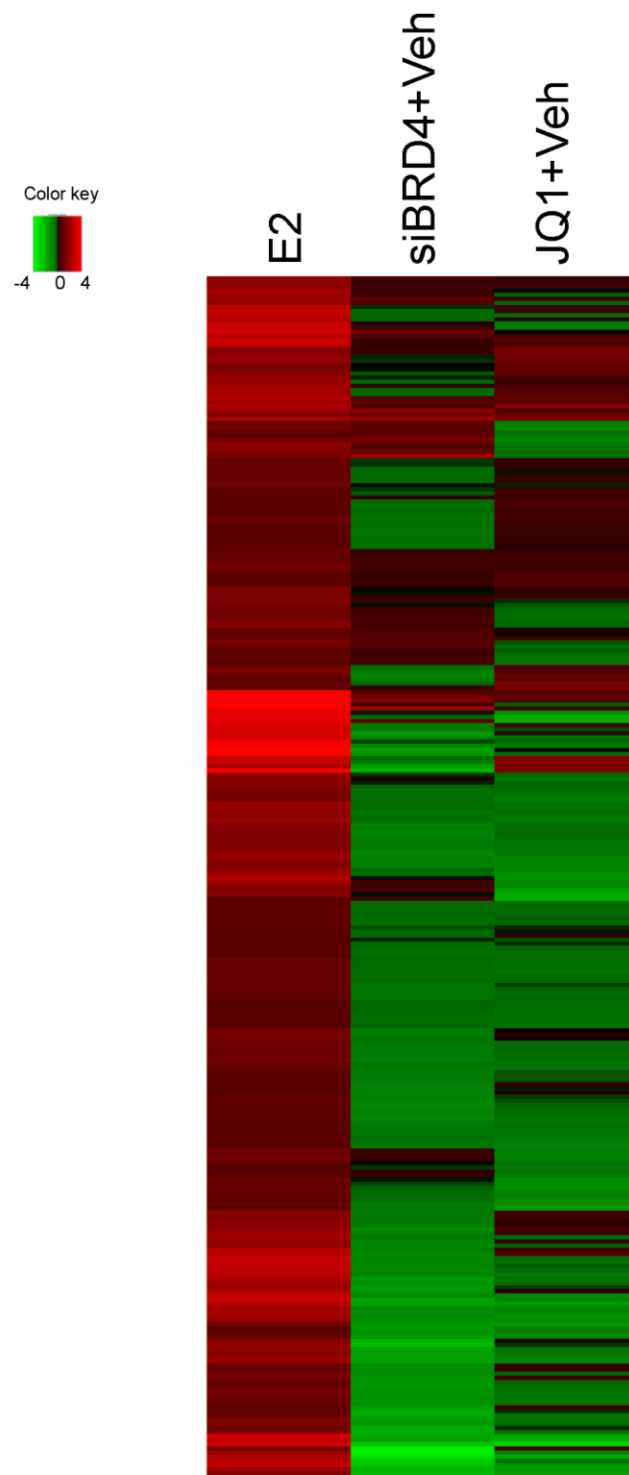


**Figure 2.I.S1A.** Principal Component Analysis (PCA) plot showing the correlation between the replicates and conditions of RNA-sequencing. 12 samples of six different conditions are shown in the 2D plane spanned by their first two principal components.



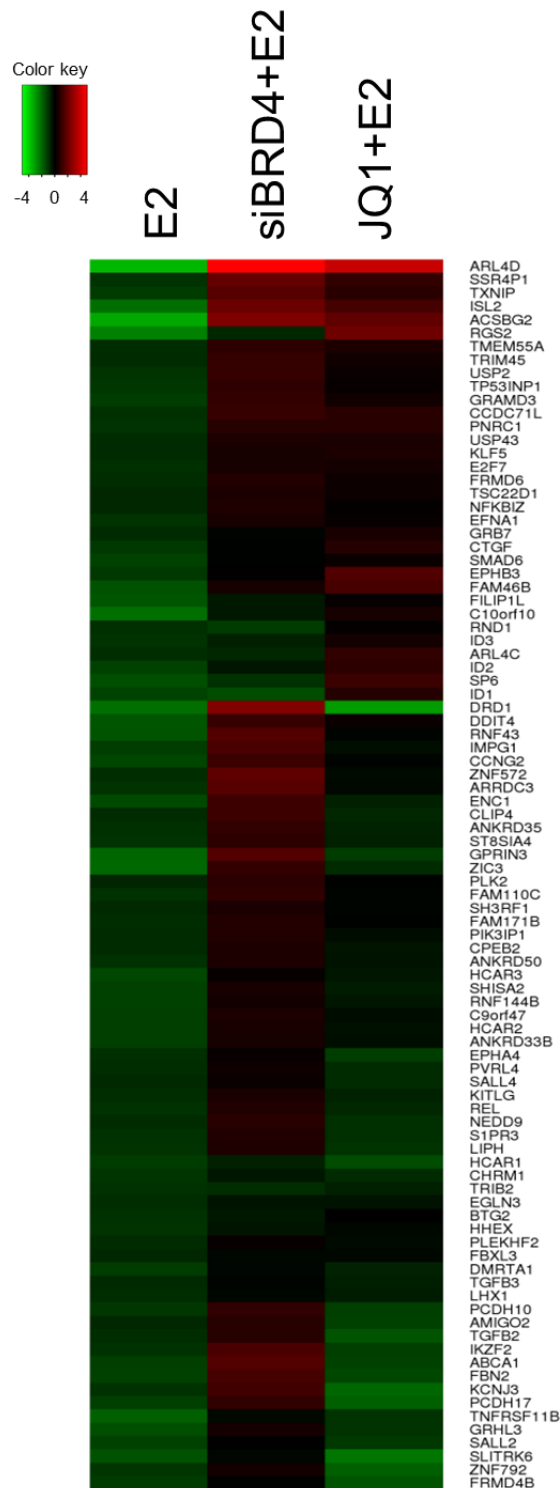
**Figure 2.I.S1B.** Single gene-specific qPCR analyses in MCF-7 showing relative mRNA expression of GREB1, TFF1, XBP1, BRD4 and DHFR (house-keeping gene) upon negative control siRNA (siCont),

BRD4 siRNA (siBRD4) or JQ1 treatment with vehicle (Veh) or estrogen (E2) induction. Relative mRNA expression was shown as "Rel. mRNA exp.". \* indicates  $p \leq 0.05$ , \*\*  $p \leq 0.01$ , \*\*\*  $p \leq 0.001$ . Data are represented as mean  $\pm$  standard deviation. n=3.



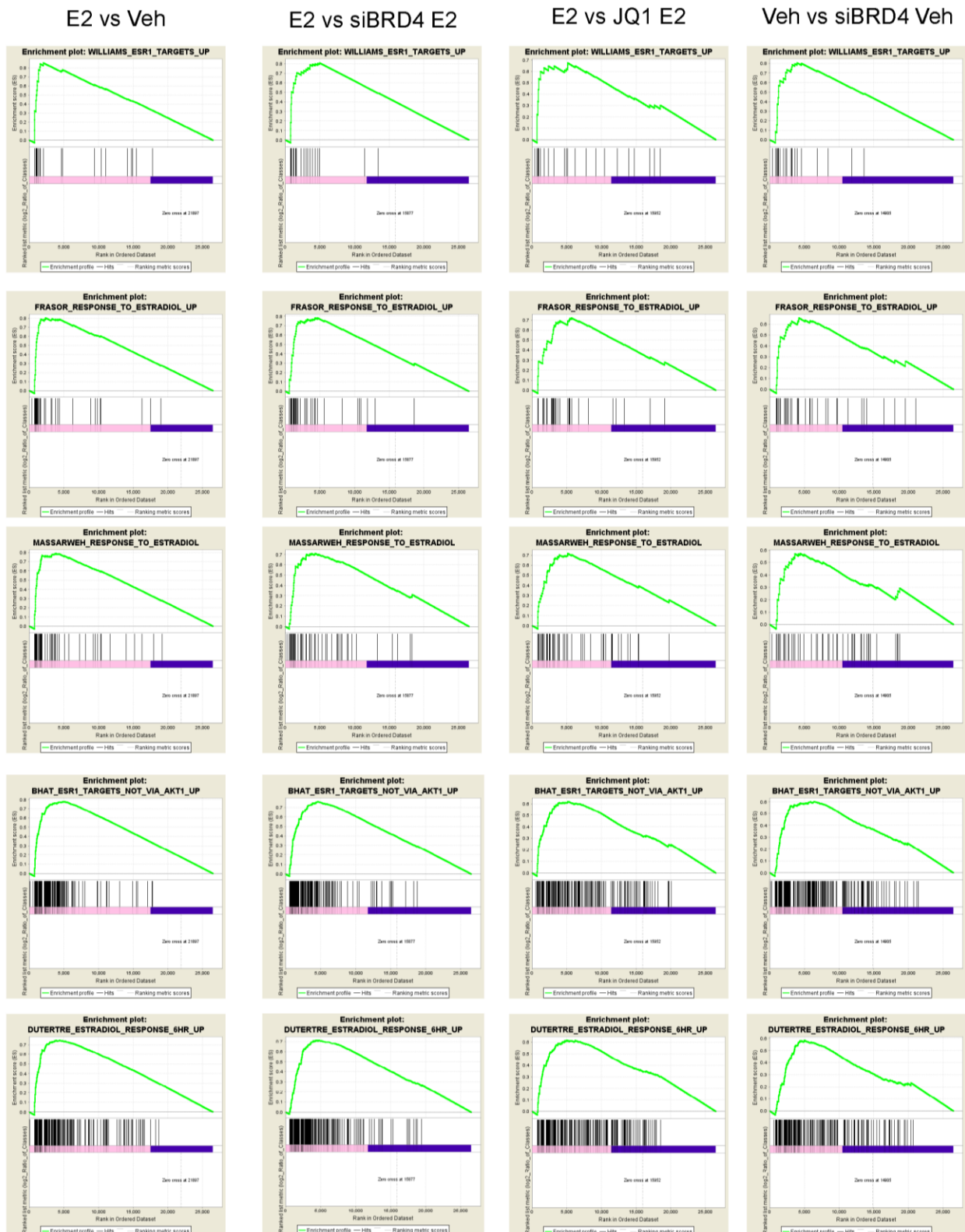
**Figure 2.I.S1C.** Heatmap made with log<sub>2</sub>-fold changes from RNA-sequencing of MCF-7 cells transfected with control, BRD4 siRNA or control siRNA with JQ1 treatment and induced with estrogen (E2). E2 denotes control siRNA and E2 treated samples relative to cells transfected with control

siRNA and vehicle treated. siBRD4+Veh denote BRD4 siRNA and vehicle treated samples relative to control siRNA with vehicle treatment. JQ1+Veh denotes control siRNA, JQ1 and vehicle treated samples relative to negative control siRNA with vehicle treatment. Only estrogen upregulated genes higher than 1.5 fold are shown. Adjusted p-value  $\leq 0.05$ .



**Figure 2.I.S1D.** Heatmap made with log<sub>2</sub>-fold changes from RNA-sequencing of MCF-7 cells transfected with control, BRD4 siRNA or control siRNA with JQ1 treatment and downregulated with

estrogen (E2). E2 denotes control siRNA and E2 treated samples relative to control siRNA with vehicle treatment. siBRD4+E2 denote BRD4 siRNA and vehicle treated samples relative to control siRNA with estrogen treatment. JQ1+E2 denotes control siRNA, JQ1 and vehicle treated samples relative to negative control siRNA with estrogen treatment. Only estrogen-downregulated genes lower than 0.8 fold are shown. Adjusted p-value  $\leq 0.05$ .



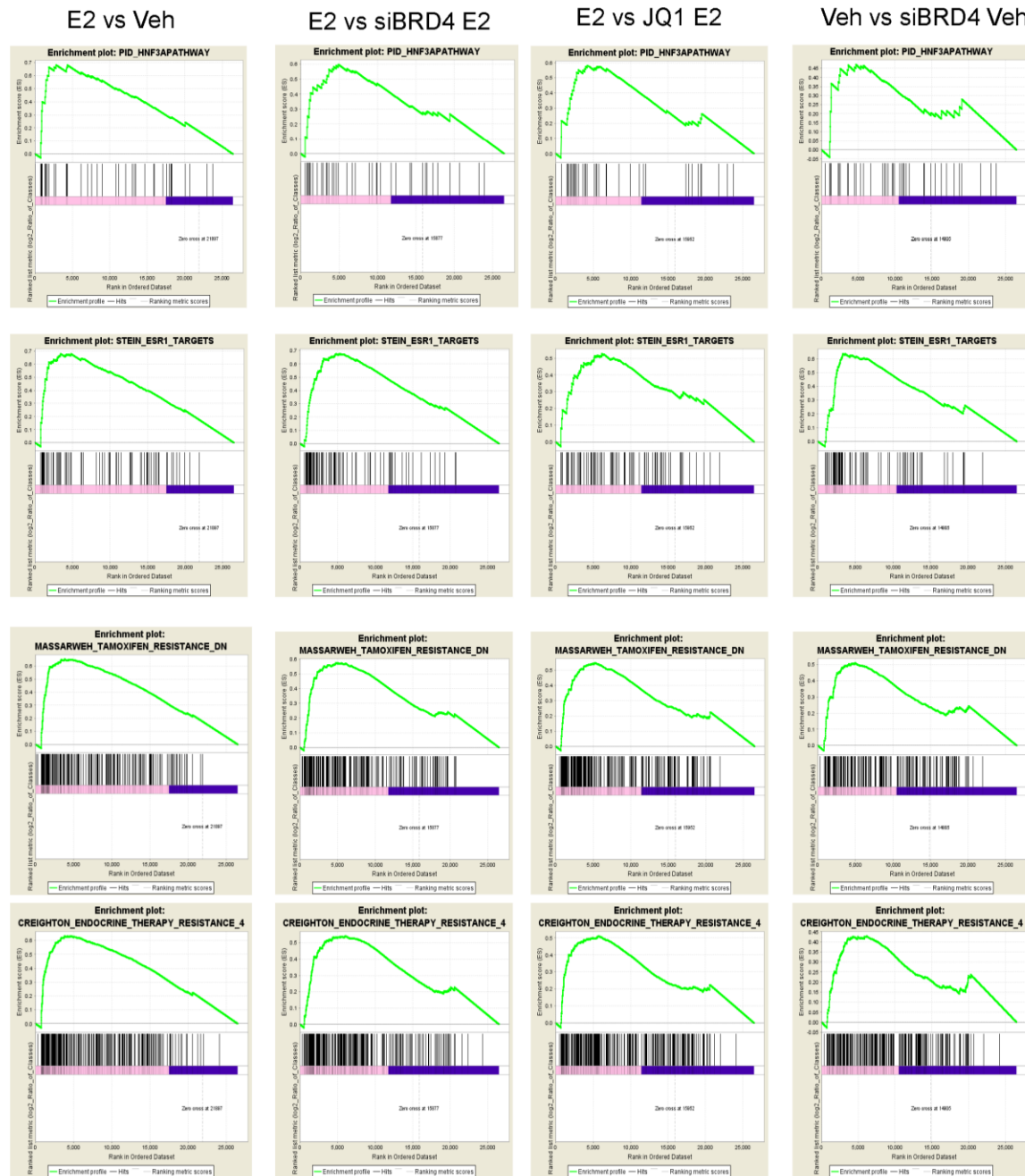


**Figure 2.I.S1E.** Gene Set Enrichment Analysis (GSEA) of mRNA expression data from RNA-seq. X-axes show the enrichment scores of each topmost gene sets of Molecular Signature Database (MSigDB - C2) of GSEA under each conditions. Nominal p-value  $\leq 0.05$ , FDR  $\leq 25\%$ . Y-axes show the location of each gene in the complete gene set. They are sorted by correlation with log2 fold changes comparing different conditions. Rank of each gene in the ordered gene set is also mentioned in Y-axes in the bottom part.

siCont_E2 vs Veh	SIZE	ES	NES	NOM p-val	FDR q-val
BHAT_ESR1_TARGETS_NOT_VIA_AKT1_UP	200	0.77737	2.349227	0	0
BHAT_ESR1_TARGETS_VIA_AKT1_UP	268	0.756114	2.296358	0	0
DUTERTRE ESTRADIOL_RESPONSE_6HR_UP	215	0.744167	2.246275	0	0
MASSARWEH_RESPONSE_TO ESTRADIOL	59	0.788324	2.180643	0	0
WILLIAMS_ESR1_TARGETS_UP	25	0.853848	2.153418	0	0
FRASOR_RESPONSE_TO ESTRADIOL_UP	37	0.805491	2.137869	0	1.67E-04
STOSSI_RESPONSE_TO ESTRADIOL	50	0.766867	2.130182	0	1.44E-04
MASSARWEH_TAMOXIFEN_RESISTANCE_DN	236	0.653726	1.963541	0	0.003643
DALESSIO_TSA_RESPONSE	23	0.786871	1.962876	0	0.003239
STEIN_ESR1_TARGETS	83	0.679738	1.938982	0	0.00593
MASRI_RESISTANCE_TO_TAMOXIFEN_AND_AROMATASE_INHIBITORS_UP	20	0.786553	1.926356	0	0.007308
CREIGHTON_ENDOCRINE_THERAPY_RESISTANCE_4	276	0.631735	1.926256	0	0.006699
MATZUK_EMBRYONIC_GERM_CELL	19	0.799361	1.911452	0	0.009585
STEIN_ESTROGEN_RESPONSE_NOT_VIA_ESRRA	18	0.801374	1.897912	0	0.012274
MAHADEVAN_IMATINIB_RESISTANCE_DN	19	0.776987	1.884905	0	0.01581
BIOCARTA_NO2IL12_PATHWAY	17	0.799528	1.880474	0	0.01614
STEIN_ESRRA_TARGETS_RESPONSIVE_TO_ESTROGEN_UP	31	0.720591	1.862184	0.001004016	0.022402
SUZUKI_AMPLIFIED_IN_ORAL_CANCER	16	0.783862	1.845964	0.002094241	0.029254
MARSON_FOXP3_CORE_DIRECT_TARGETS	19	0.759435	1.839263	0	0.030624
RIGGINS_TAMOXIFEN_RESISTANCE_UP	64	0.651282	1.838491	0	0.029595
SARTIPY_NORMAL_AT_INSULIN_RESISTANCE_UP	32	0.704474	1.835175	0.001008065	0.030004
MARZEC_IL2_SIGNALING_UP	109	0.622787	1.82242	0	0.035631
PID_HNF3APATHWAY	42	0.680523	1.816607	0.001006036	0.037882
PID_IL6_7PATHWAY	44	0.672811	1.815335	0	0.037601

siContE2 vs SiBRD4 E2	SIZE	ES	NES	NOM p-val	FDR q-val
BHAT_ESR1_TARGETS_NOT_VIA_AKT1_UP	2000	0.76053905	3.131201	0	0
BHAT_ESR1_TARGETS_VIA_AKT1_UP	2680	0.734698063	0.748098	0	0
DUTERTRE ESTRADIOL_RESPONSE_6HR_UP	215	0.71270552	2.9384253	0	0
DUTERTRE ESTRADIOL_RESPONSE_24HR_UP	301	0.64888252	2.7355871	0	0
SOTIRIOU_BREAST_CANCER_GRADE_1_VS_3_UP	138	0.6682781	2.675094	0	0
ROSTY_CERVICAL_CANCER_PROLIFERATION_CLUSTER	1290	0.67658865	2.671732	0	0
MANALO_HYPOXIA_DN	264	0.62733392	2.6129906	0	0
FRASOR_RESPONSE_TO ESTRADIOL_UP	37	0.78252432	2.5869553	0	0
STEIN_ESR1_TARGETS	83	0.67636362	2.5490239	0	0
GRAHAM_NORMAL QUIESCENT_VS_NORMAL_DIVIDING_DN	800	0.67546266	2.539488	0	0
MASSARWEH_RESPONSE_TO ESTRADIOL	590	0.70951676	2.528032	0	0
WONG_EMBRYONIC_STEM_CELL_CORE	314	0.5909258	2.492312	0	0
ELVIDGE_HYPOXIA_DN	1360	0.629178352	2.4880753	0	0
CROONQUIST_IL6_DEPRIVATION_DN	960	0.641422752	2.4665902	0	7.44E-05
ZHANG_TLX_TARGETS_60HR_DN	2570	0.59295446	2.464522	0	6.94E-05
MORI_LARGE_PRE_BII_LYMPHOCYTE_UP	80	0.6583836	2.453662	0	6.51E-05
ELVIDGE_HYPOXIA_BY_DMOG_DN	56	0.68882842	2.4328387	0	6.12E-05
CROONQUIST_NRAS_SIGNALING_DN	68	0.66311232	2.4322226	0	5.78E-05
STEIN_ESRRA_TARGETS_RESPONSIVE_TO_ESTROGEN_DN	40	0.73123042	2.4288318	0	5.48E-05
GRAHAM_CML_DIVIDING_VS_NORMAL QUIESCENT_UP	166	0.60391652	2.4222484	0	5.21E-05
MITSIADES_RESPONSE_TO_APLIDIN_DN	232	0.58531582	2.4170249	0	4.96E-05
WILLIAMS_ESR1_TARGETS_UP	250	0.809152662	2.4112246	0.00122549	4.73E-05
ZHAN_MULTIPLE_MYELOMA_PR_UP	430	0.706307232	2.4091768	0	4.53E-05
FRASOR_RESPONSE_TO_SERM_OR_FULVESTRANT_DN	47	0.70188442	2.4064696	0	8.62E-05



siCont Veh vs siBRD4 Veh	SIZE	ES	NES	NOM p-val	FDR q-val
ROSTY_CERVICAL_CANCER_PROLIFERATION_CLUSTER	129	0.7554562	3.1447787	0	0
CROONQUIST_IL6_DEPRIVATION_DN	96	0.75288653	3.0514975	0	0
KOBAYASHI_EGFR_SIGNALING_24HR_DN	232	0.6872548	2.9890876	0	0
DUTERTRE ESTRADIOL_RESPONSE_24HR_UP	301	0.67073053	2.972512	0	0
CROONQUIST_NRAS_SIGNALING_DN	68	0.77253234	2.9631977	0	0
SOTIRIOU_BREAST_CANCER_GRADE_1_VS_3_UP	138	0.6964254	2.9320428	0	0
CHANG_CYCLING_GENES	139	0.6797935	2.8719358	0	0
ZHANG_TLX_TARGETS_UP	85	0.7239937	2.8614352	0	0
BENPORATH_PROLIFERATION	126	0.66662	2.7793763	0	0
ZHOU_CELL_CYCLE_GENES_IN_IR_RESPONSE_6HR	78	0.7045884	2.7772913	0	0
GRAHAM_NORMAL_QUIESCENT_VS_NORMAL_DIVIDING_DN	80	0.69683254	2.7695696	0	0
GRAHAM_CML_DIVIDING_VS_NORMAL_QUIESCENT_UP	166	0.64656204	2.7632775	0	0
KAUFFMANN_MELANOMA_RELAPSE_UP	55	0.739735	2.757882	0	0
ZHAN_MULTIPLE_MYELOMA_PR_UP	43	0.7809228	2.7515335	0	0
ZHANG_TLX_TARGETS_60HR_DN	257	0.61842483	2.713085	0	0
WINNEPENNINCKX_MELANOMA_METASTASIS_UP	145	0.6406073	2.7076862	0	0
STEIN_ESRRA_TARGETS_RESPONSIVE_TO_ESTROGEN_DN	40	0.7696113	2.698512	0	0
ISHIDA_E2F_TARGETS	49	0.739043	2.6719766	0	0
WHITEFORD_PEDIATRIC_CANCER_MARKERS	109	0.64757484	2.6602173	0	0
AMUNDSON_GAMMA_RADIATION_RESPONSE	39	0.7662029	2.6576457	0	0
HOFFMANN_LARGE_TO_SMALL_PRE_BII_LYMPHOCYTE_UP	149	0.63202643	2.655566	0	0
PUJANA_BRCA_CENTERED_NETWORK	110	0.6456967	2.6534736	0	0
MANALO_HYPOXIA_DN	264	0.60161823	2.649204	0	0
KANG_DOXORUBICIN_RESISTANCE_UP	52	0.71361727	2.6285622	0	0

siCont E2 vs JQ1 E2	SIZE	ES	NES	NOM p-val	FDR q-val
MASSARWEH_RESPONSE_TO ESTRADIOL	59	0.71549064	2.5384789	0	0
DACOSTA_UV_RESPONSE_VIA_ERCC3_COMMON_DN	453	0.5869554	2.498534	0	0
DUTERTRE ESTRADIOL_RESPONSE_6HR_UP	215	0.61588156	2.487698	0	0
BHAT_ESR1_TARGETS_NOT_VIA_AKT1_UP	200	0.6173828	2.4722798	0	2.29E-04
DAZARD_UV_RESPONSE_CLUSTER_G6	138	0.62467754	2.4417944	0	3.68E-04
BHAT_ESR1_TARGETS_VIA_AKT1_DN	77	0.64871377	2.4023495	0	6.15E-04
DAZARD_RESPONSE_TO_UV_NHEK_DN	295	0.5775019	2.385174	0	7.91E-04
BHAT_ESR1_TARGETS_VIA_AKT1_UP	268	0.5783704	2.370834	0	8.07E-04
FRASOR_RESPONSE_TO ESTRADIOL_UP	37	0.72050685	2.342595	0	0.001532561
BHAT_ESR1_TARGETS_NOT_VIA_AKT1_DN	85	0.62239504	2.3374982	0	0.001379305
REACTOME_CHEMOKINE_RECEPTORS_BIND_CHEMOKINES	50	0.6760867	2.2896569	0	0.004096103
BIOCARTA_NKT_PATHWAY	26	0.7553289	2.2810843	0	0.004597125
REACTOME_LIGAND_GATED_ION_CHANNEL_TRANSPORT	20	0.8100897	2.2767363	0	0.004455225
DACOSTA_UV_RESPONSE_VIA_ERCC3_XPCS_DN	82	0.6085627	2.267605	0	0.004793383
GABRIELY_MIR21_TARGETS	270	0.5528928	2.2588477	0	0.005271983
MASSARWEH_TAMOXIFEN_RESISTANCE_DN	236	0.54690456	2.244952	0	0.005802476
REACTOME_AMINE_LIGAND_BINDING_RECEPTORS	34	0.70331544	2.2330241	0	0.006271695
DAWSON_METHYLATED_IN_LYMPHOMA_TCL1	54	0.6305694	2.2128468	0	0.008427626
XU_GH1_AUTOCRINE_TARGETS_DN	135	0.5618327	2.1977618	0	0.010110091
WINZEN_DEGRADED_VIA_KHSRP	97	0.572317	2.157775	0	0.018243486
SEKI_INFLAMMATORY_RESPONSE_LPS_UP	69	0.5898828	2.1203454	0.001035197	0.03155982
RODRIGUES_THYROID_CARCINOMA_DN	68	0.58948743	2.1141522	0	0.03242452
ZHENG_FOXP3_TARGETS_IN_T_LYMPHOCYTE_DN	35	0.65810335	2.1074293	0	0.033732098
BILD_CTNNB1_ONCOGENIC_SIGNATURE	75	0.5730551	2.1057093	0.001029866	0.033627305

siCont Veh vs JQ1 Veh	SIZE	ES	NES	NOM p-val	FDR q-val
REACTOME_DEFENSINS	41	0.6796378	2.7609951	0	0
REACTOME_BETA_DEFENSINS	34	0.6933237	2.7132173	0	5.45E-04
REACTOME_CHEMOKINE_RECEPTORS_BIND_CHEMOKINES	50	0.5490659	2.2963414	0	0.014366189
BIOCARTA_NKT_PATHWAY	26	0.6004894	2.2393486	0	0.018044466
DEBOSSCHER_NFKB_TARGETS_REPRESSED_BY_GLUCOCORTICOIDS	22	0.58775836	2.1552618	0	0.031020135
MOSERLE_IFNA_RESPONSE	25	0.5535619	2.0779119	0	0.055686608
BHAT_ESR1_TARGETS_VIA_AKT1_DN	77	0.45446214	1.985265	0	0.09582544
REACTOME_AMINE_LIGAND_BINDING_RECEPTORS	34	0.4946886	1.9541703	0	0.1063371
MIKKELSEN_MCV6_LCP_WITH_H3K27ME3	29	0.507249	1.9480784	0	0.0989576
REACTOME_LIGAND_GATED_ION_CHANNEL_TRANSPORT	20	0.551872	1.9396627	0.001626016	0.09531598
HONRADO_BREAST_CANCER_BRCA1_VS_BRCA2	18	0.55550534	1.9070691	0	0.10840696
SA_MMP_CYTOKINE_CONNECTION	15	0.58328354	1.8897389	0.001715266	0.11284291
SHIN_B_CELL_LYMPHOMA_CLUSTER_5	16	0.5768539	1.8859048	0.005076142	0.10698174
WANG_TNF_TARGETS	22	0.51762974	1.8482577	0.001572327	0.13046929
KEGG_PROTEASOME	36	0.46135208	1.8421545	0.001390821	0.12688814
REACTOME_VIF_MEDIATED_DEGRADATION_OF_APOBEC3G	39	0.44333953	1.7919956	0	0.17045225
PEDERSEN_METASTASIS_BY_ERBB2_ISOFORM_6	27	0.47050405	1.7790515	0.004716981	0.17431973
PID_IL27PATHWAY	25	0.47843313	1.7762812	0.001592357	0.1683523
REACTOME_AUTODEGRADATION_OF_THE_E3_UBIQUITIN_LIGASE_COPI	37	0.44329327	1.7751285	0	0.16051246
TSAI_RESPONSE_TO_RADIATION_THERAPY	32	0.4475077	1.7590309	0	0.16882983
CHEMELLO_SOLEUS_VS_EDL_MYOFIBERS_UP	31	0.45222646	1.7481539	0.001515152	0.17322586
MARKS_HDAC_TARGETS_DN	15	0.54893583	1.741878	0.007194245	0.17241904
REACTOME_P53_INDEPENDENT_G1_S_DNA_DAMAGE_CHECKPOINT	38	0.43154877	1.7322242	0.00143472	0.17598443
BIOCARTA_IL17_PATHWAY	16	0.516217	1.7155629	0.00660066	0.18959087

**Figure 2.I.S1F.** Top 25 pathways of GSEA analyses under each condition are shown. Each pathway enriched is shown with size of the geneset, Enrichment Score (ES), Normalised Enrichment Score (NES) Nominal p-value (NOM p-val) and FDR (False Discovery Rate) q-value.

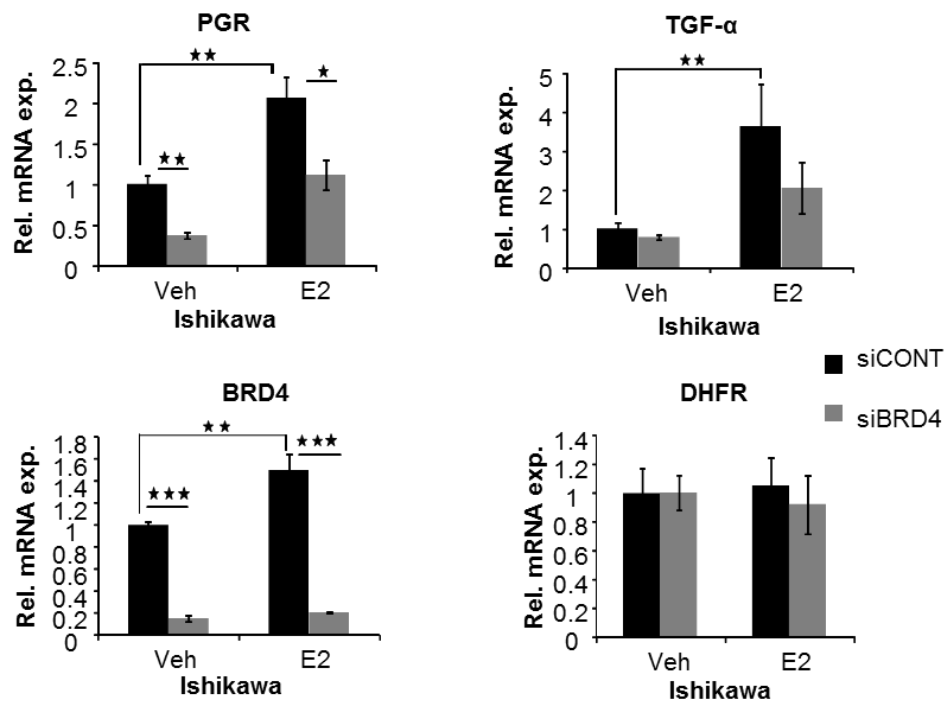


**Figure 2.I.S1G.** Single gene-specific qPCR analyses in Ishikawa showing relative mRNA expression of PGR, TGF- $\alpha$ , BRD4 and DHFR (house-keeping gene) upon negative control siRNA, (siCont) or BRD4 siRNA (siBRD4) treatment with vehicle (Veh) or estrogen (E2) induction. Relative mRNA expression was shown as “Rel. mRNA exp.”. \* indicates  $p \leq 0.05$ , \*\*  $p \leq 0.01$ , \*\*\*  $p \leq 0.001$ . Data are represented as mean +/- standard deviation. n=3.

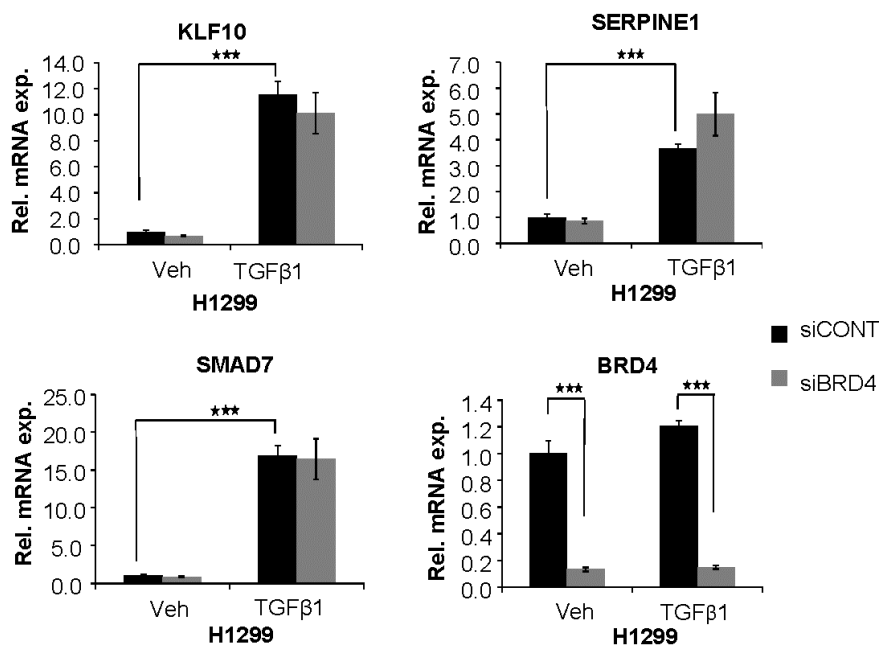


**Figure 2.I.S1H.** Single gene-specific qPCR analyses in H1299 cells showing relative mRNA expression of KLF10, SERPINE1, SMAD7 and BRD4 upon negative control siRNA (siCont) or BRD4 siRNA (siBRD4) treatment with vehicle (Veh) or TGF- $\beta$ 1 induction. Relative mRNA expression was



after BRD4 knockdown. Relative mRNA expression was shown as “Rel. mRNA exp.”. \* for  $p \leq 0.05$ , \*\* for  $p \leq 0.01$ , \*\*\* for  $p \leq 0.001$ . Data are represented as mean +/- standard deviation. n=3.

Multiple Comparisons			
Tukey HSD			
No. of days			Significance (p-values)
3 days	siCont Veh	siBRD4 Veh	0.98001991
		siCont + JQ1 Veh	0.99819060
		siCont +ICI Veh	1.00000000
		siCont E2	0.28687023
		siBRD4 E2	0.28687023
		siCont + JQ1 E2	1.00000000
		siCont+ICI E2	0.99998130
	siCont E2	siCont Veh	0.28687023
		siBRD4 Veh	0.78419937
		siCont + JQ1 Veh	0.61094806
		siCont +ICI Veh	0.28687023
		siBRD4 E2	1.00000000
		siCont + JQ1 E2	0.28687023
		siCont+ICI E2	0.17830028
5 days	siCont Veh	siBRD4 Veh	.99999924
		siCont + JQ1 Veh	.99999924
		siCont +ICI Veh	.56008758
		siCont E2	.00000004
		siBRD4 E2	.00001149
		siCont + JQ1 E2	.19753455
		siCont+ICI E2	.99875794
	siCont E2	siCont Veh	.00000004
		siBRD4 Veh	.00000006
		siCont + JQ1 Veh	.00000006
		siCont +ICI Veh	.00000001
		siBRD4 E2	.01710835
		siCont + JQ1 E2	.00000150
		siCont+ICI E2	.00000002
7 days	siCont Veh	siBRD4 Veh	.39844088
		siCont + JQ1 Veh	.39844088
		siCont +ICI Veh	.36329803
		siCont E2	.00000267
		siBRD4 E2	.01729712
		siCont + JQ1 E2	.55485365
		siCont+ICI E2	.19585105
	siCont E2	siCont Veh	.00000267
		siBRD4 Veh	.00000027
		siCont + JQ1 Veh	.00000027
		siCont +ICI Veh	.00000025
		siBRD4 E2	.00268939
		siCont + JQ1 E2	.00000035
		siCont+ICI E2	.00000017

**Figure 2.I.S2A.** Statistical significance of proliferation based cell counting assay in MCF7 after negative control siRNA (siCont), BRD4 siRNA (siBRD4), JQ1 and ICI182780 (ICI) with vehivle (Veh) or estrogen treatment (E2) after 3, 5 and 7 days shown in Fig 2A. One way ANOVA was performed with Tukey HSD based multiple comparisons using SPSS package and p-values were calculated. Second and third columns show the pattern of comparisons.

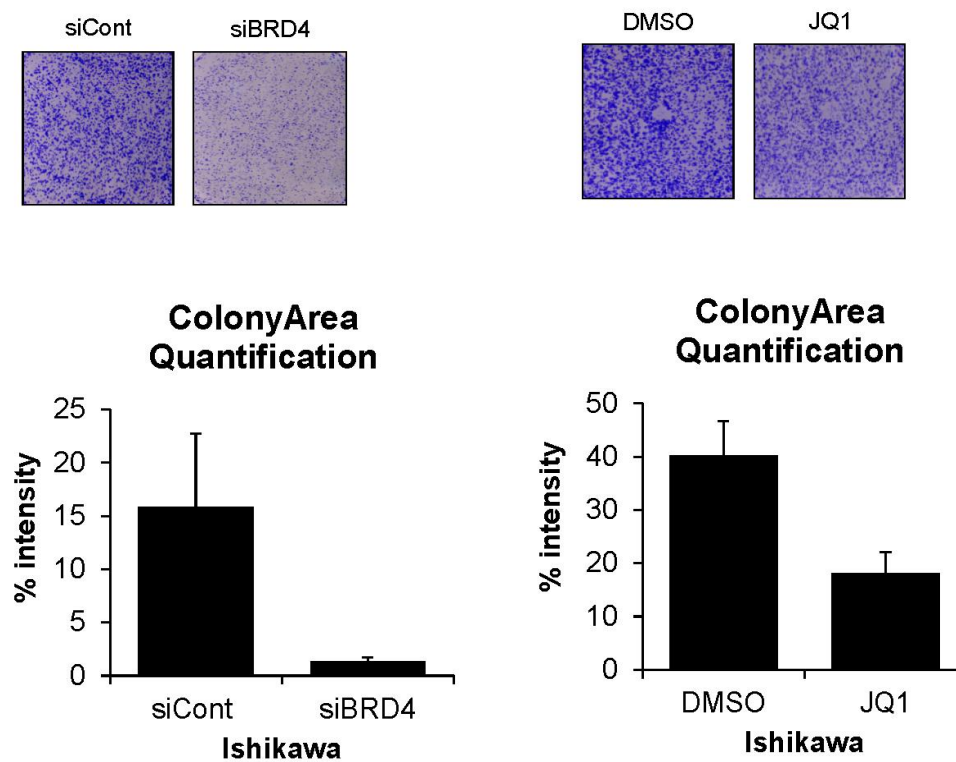


**Figure 2.I.S2B.** Proliferation based crystal violet assays in Ishikawa showing the proliferation defect under estrogen induced conditions with negative control siRNA (siCont) or BRD4 siRNA (siBRD4) and DMSO or JQ1 treatment. Percentage of intensity (area and density) covered by the cells after 7-9 days of growth were quantified using ImageJ with a plugin ColonyArea. The data is represented as mean +/- standard deviation. n=2.

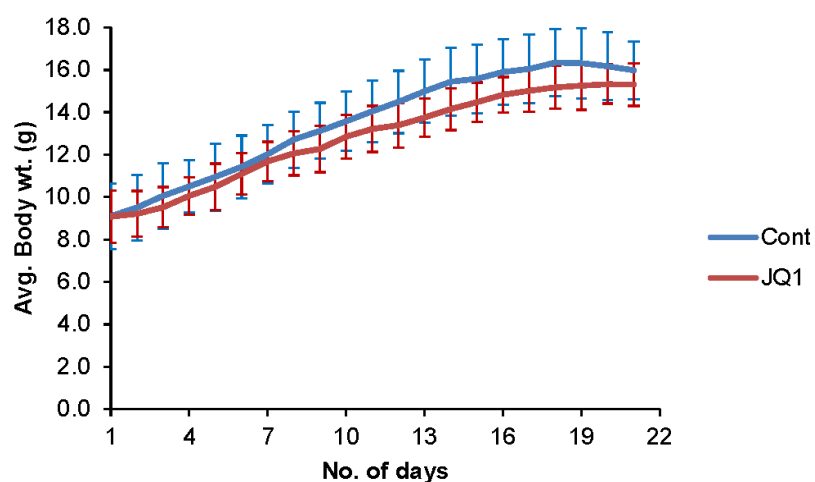


**Figure 2.I.S2C.** Three week-old mice injected with vehicle (Cont) or JQ1 for 3 weeks were analyzed for their difference in body weight. X-axis shows the time-course of treatment in days and Y-axis shows the average body weight in grams. The data is represented as mean +/- standard deviation. n=8 for each group.

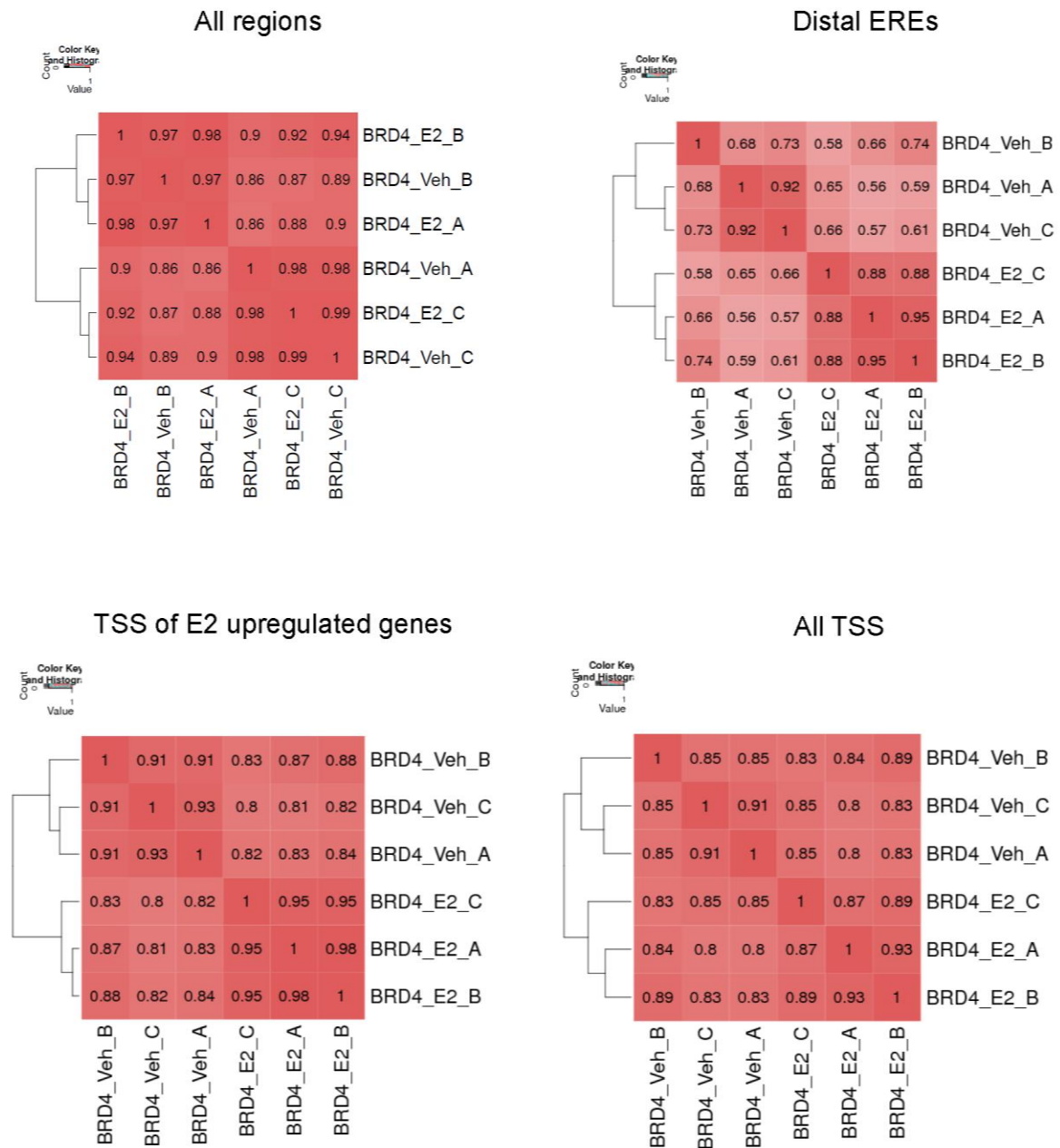


**Figure 2.I.S3A.** Correlation plots of BRD4 ChIP signals of different replicates and conditions - vehicle (veh) and estrogen (E2) on all regions and specifically on distal EREs, estrogen upregulated gene-specific TSS and all TSS.

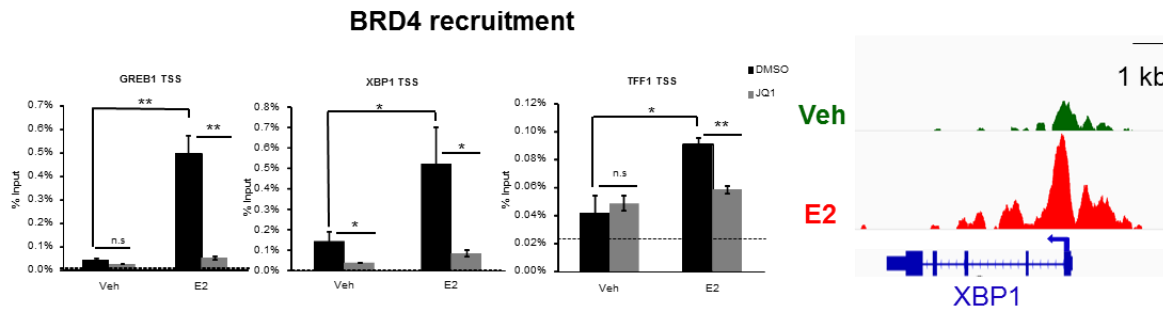


**Figure 2.I.S3B.** ChIP-qPCR analyses of BRD4 recruitment to GREB1, XBP1 and TFF1 TSS after DMSO or JQ1 treatment with vehicle (Veh) or estrogen (E2) induction. \* indicates  $p \leq 0.05$ , \*\*  $p \leq 0.01$ , \*\*\*  $p \leq 0.001$ . Data are represented as mean +/- standard deviation.  $n=3$ . Dotted line indicates background. The right panel shows the genomic profile of BRD4 on XBP1 after vehicle (Veh) or estrogen (E2) induction.

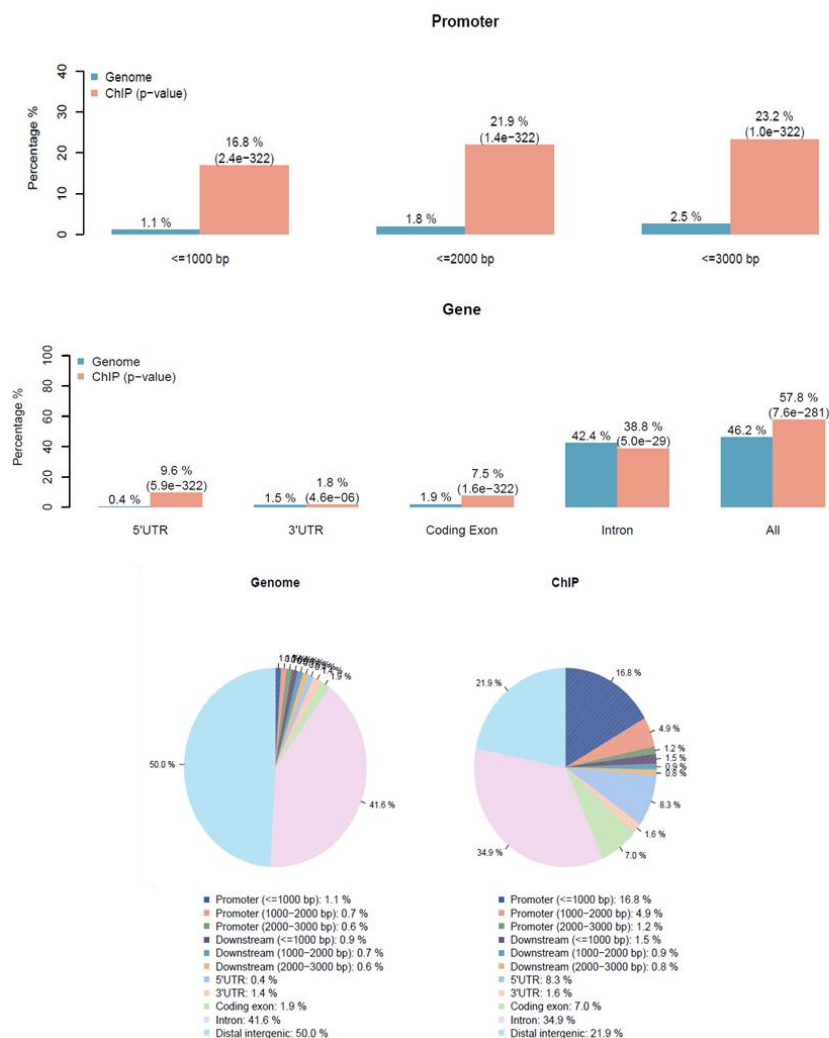


**Figure 2.I.S3C.** Average percentage of BRD4 ChIP enrichment signals over specific genomic features like promoters, 5' UTR, 3' UTR, Coding exon, introns and distal regions. Significance of enrichment was mentioned as p-values. Both genome and ChIP enrichments were compared.

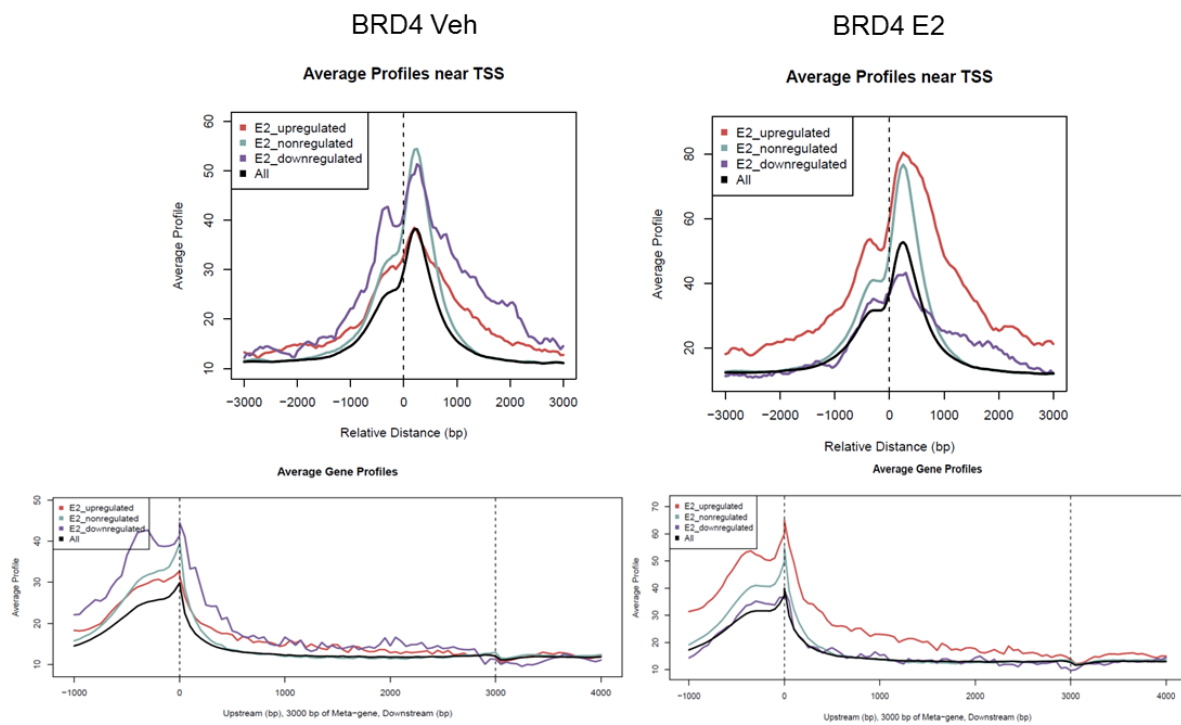


**Figure 2.I.S3D.** Average BRD4 ChIP enrichment profiles were compared for all TSS, E2 upregulated, downregulated and nonregulated gene-specific TSS under vehicle (Veh) and estrogen (E2) treated conditions. X-axis shows the distance from TSS in base pairs. TSS is marked with a black dotted line. Y-axis shows the average BRD4 signal of the reads normalized per hundred million base pairs.

E2 upregulated gene-specific TSS

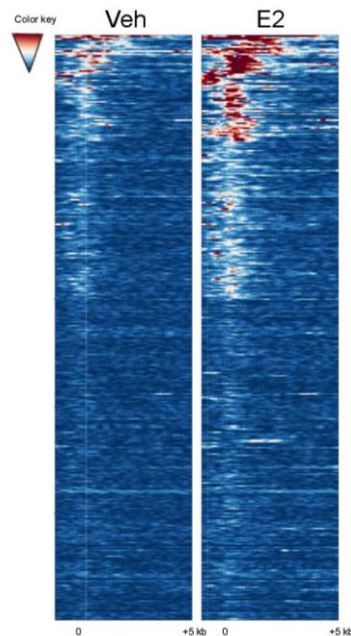


**Figure 2.I.S3E.** Heatmap profiles of BRD4 after vehicle (Veh) and estrogen (E2) treatment on regions 1 kb upstream and 5 kb downstream of estrogen upregulated gene-specific TSS. TSS and +5 kb are marked.



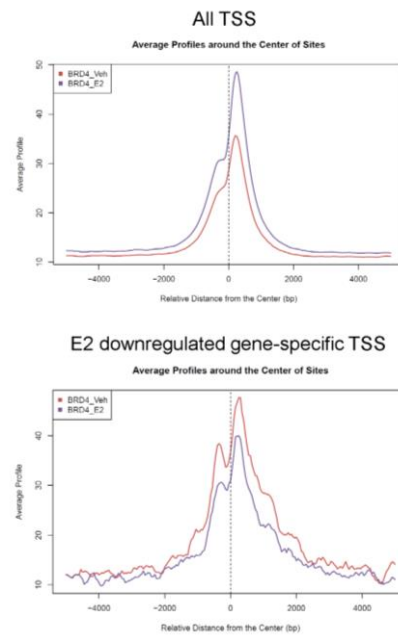


**Figure 2.I.S3F.** Aggregate plots showing genomic binding profiles of BRD4 on all TSS and estrogen-downregulated genes upon vehicle (Veh) and estrogen (E2) treated conditions. X-axis shows the distance from TSS in base pairs. Y-axis shows the average BRD4 signal of the reads normalized per hundred million base pairs. TSS is marked with a black dotted line.

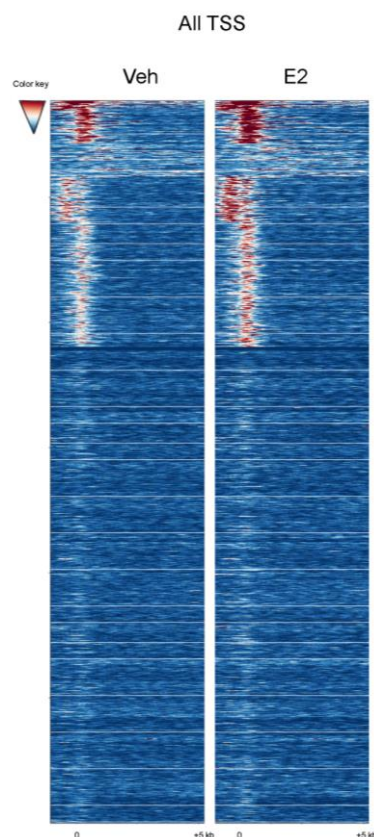


**Figure 2.I.S3G.** Heatmap profiles of BRD4 after vehicle (Veh) and estrogen (E2) treatment on regions 1 kb upstream and 5 kb downstream of all TSS. TSS and +5 kb are marked.

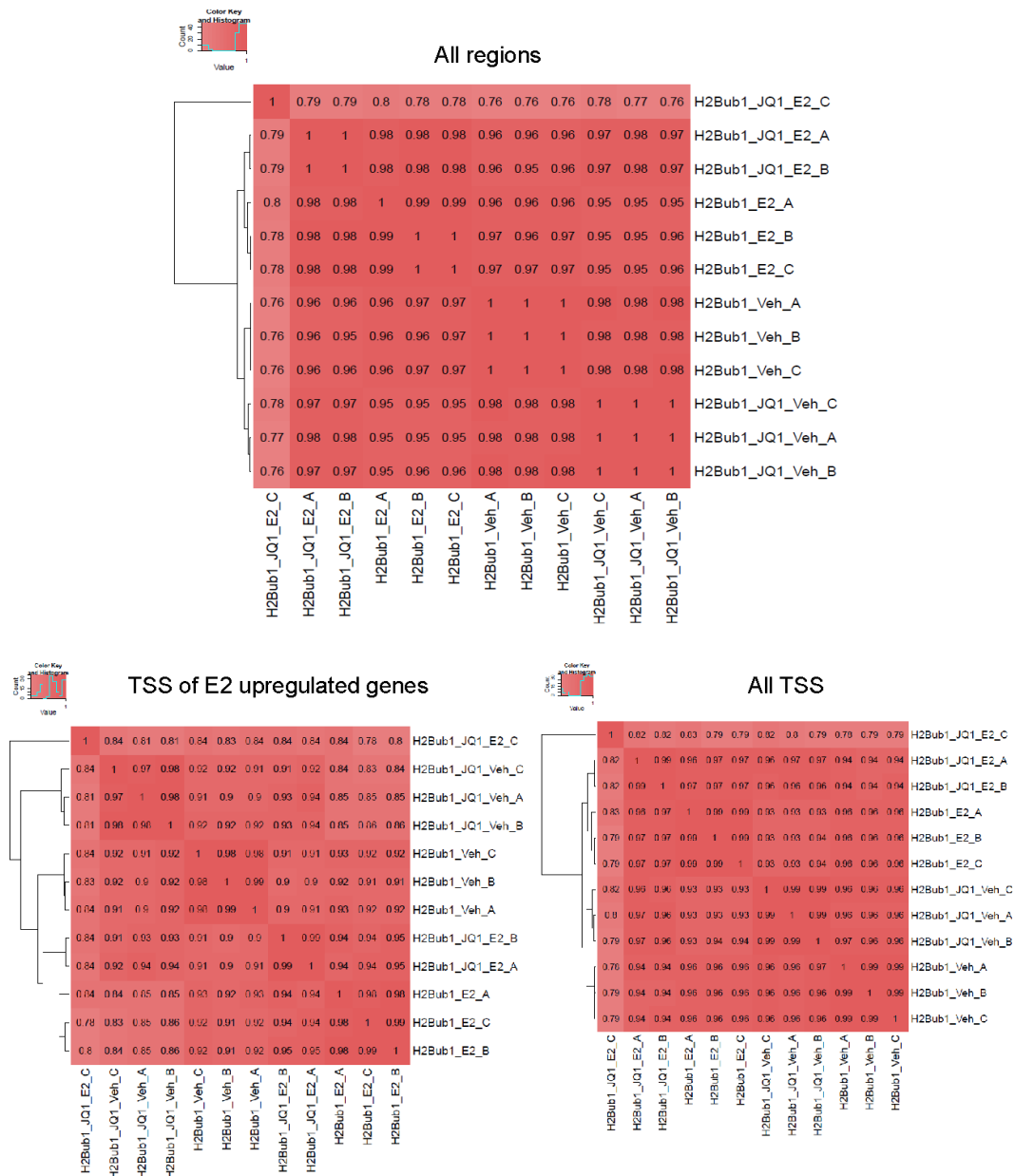


**Figure 2.I.S3H.** Correlation plots of H2Bub1 ChIP signals of different replicates and conditions - vehicle (veh) and estrogen (E2) on all regions and specifically on distal EREs, estrogen upregulated gene-specific TSS and all TSS.

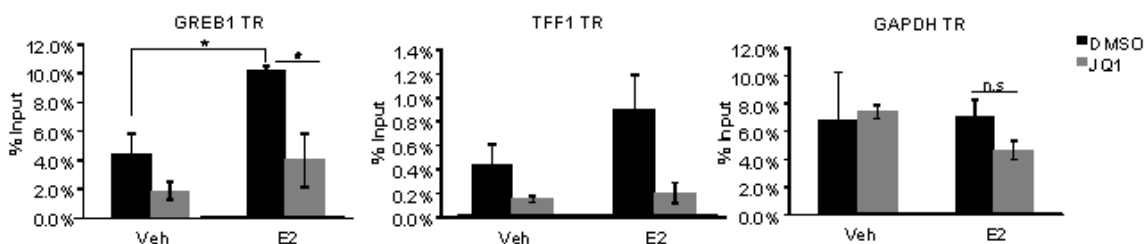


**Figure 2.I.S3I.** ChIP-qPCR analyses of H2Bub1 on GREB1, TFF1 and GAPDH transcribed regions (TR) after DMSO or JQ1 treatment with vehicle (Veh) or estrogen (E2) induction. \* indicates  $p \leq 0.05$ , n.s. indicates not significant.

\*\*  $p \leq 0.01$ , \*\*\*  $p \leq 0.001$ . Data are represented as mean +/- standard deviation. n=3. Dotted line indicates background.

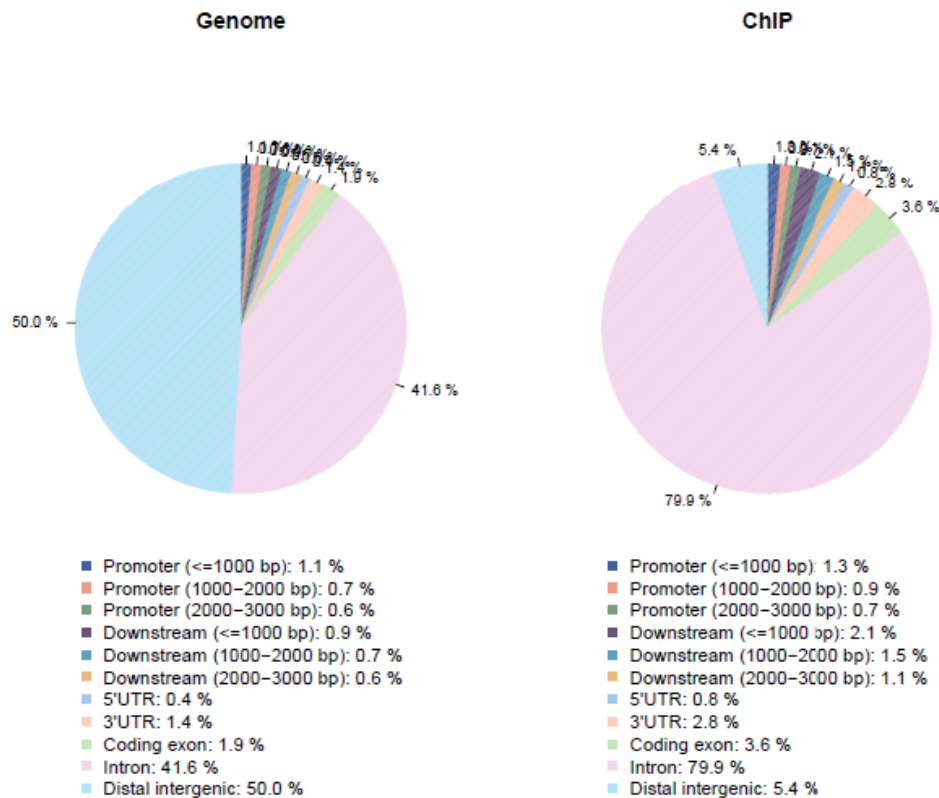


**Figure 2.I.S3J.** Average percentage of H2Bub1 ChIP enrichment signals over specific genomic features like promoters, 5' UTR, 3' UTR, Coding exon, introns and distal regions. Both genome and CHIP enrichments were compared.

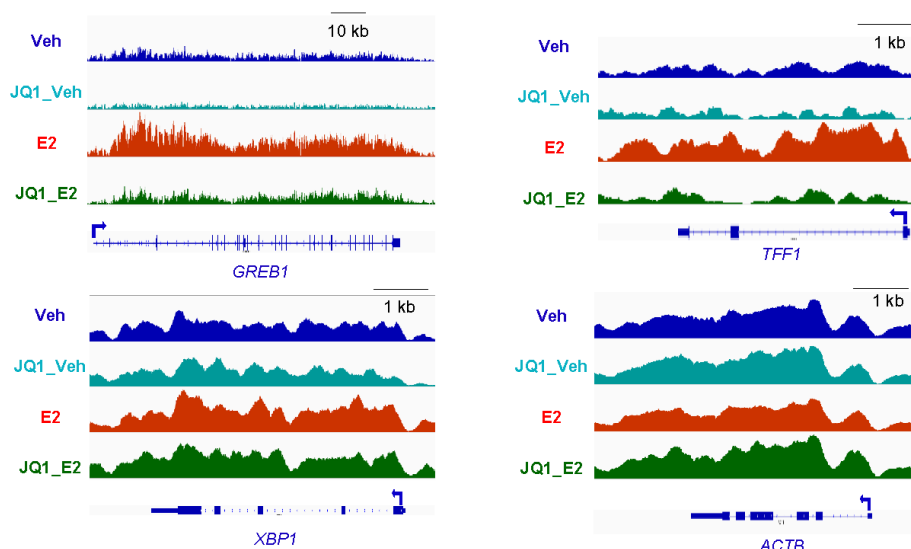


**Figure 2.I.S3K.** Single gene profiles of H2Bub1 on estrogen induced genes (GREB1, XBP1 and TFF1) and house-keeping gene ACTB after DMSO or JQ1 treatment with vehicle (Veh) or estrogen (E2) induction.

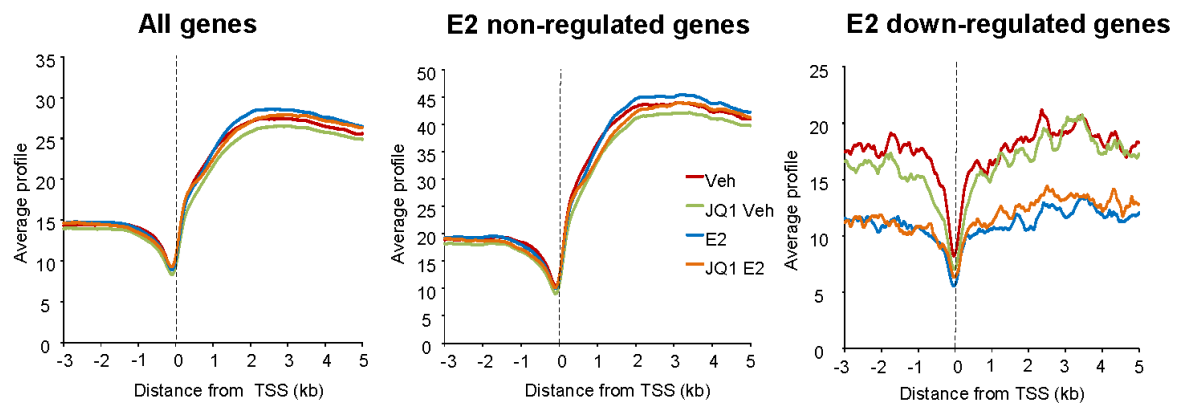


**Figure 2.I.S3L.** Aggregate plots showing genomic profiles of H2Bub1 on all TSS, estrogen-nonregulated and downregulated genes upon vehicle (Veh), JQ1 as well as vehicle (JQ1 Veh), estrogen (E2) and JQ1 as well as estrogen (JQ1 E2) treated conditions. X-axis shows the distance from TSS in kilobase pairs. Y-axis shows the average H2Bub1 signal of the reads normalized per hundred million base pairs. TSS is marked with a black dotted line.

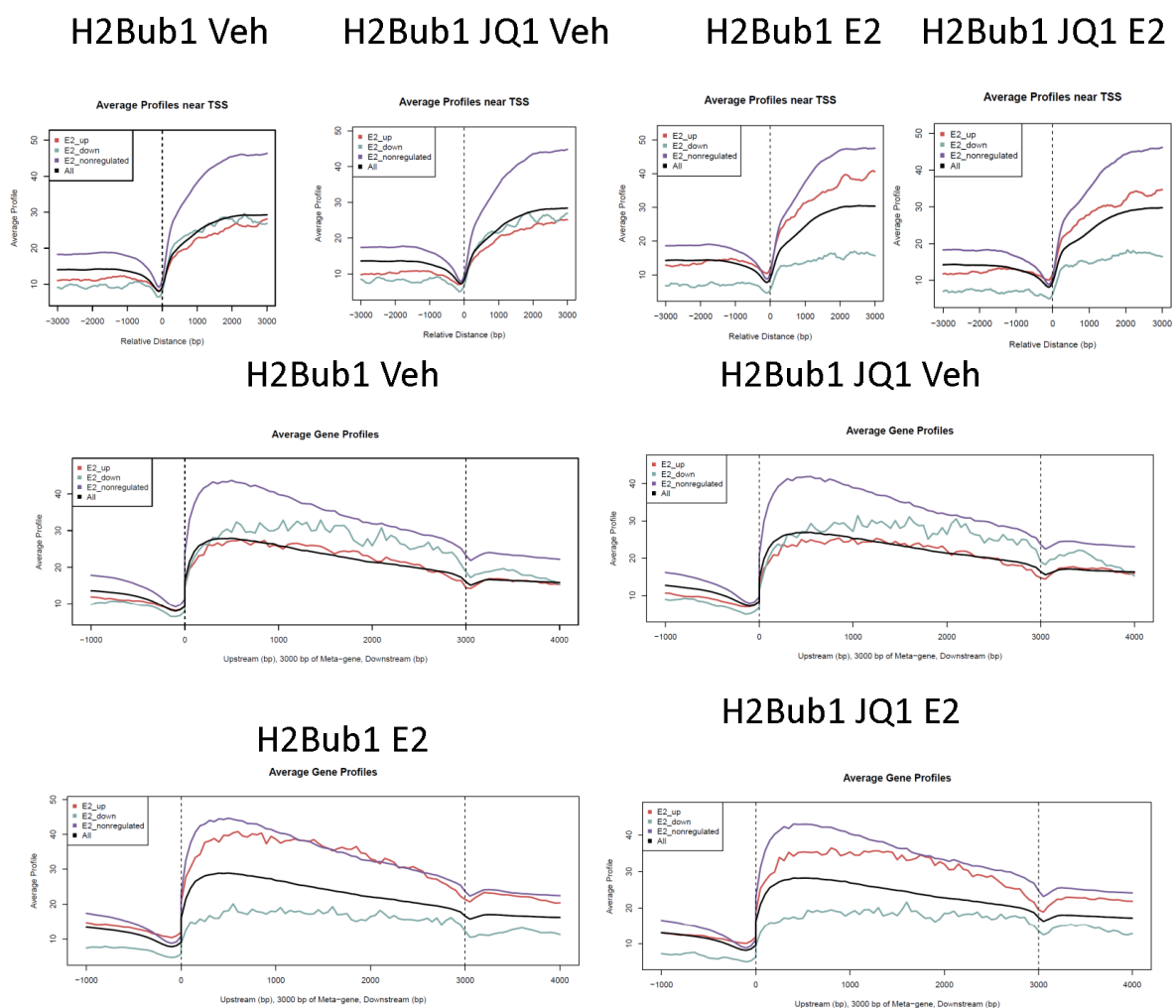


**Figure 2.I.S3M.** Average ChIP enrichment profiles of H2Bub1 were compared for all TSS, E2 upregulated, downregulated and nonregulated gene-specific TSS under vehicle (Veh) and estrogen

(E2) treated conditions. X-axis shows the distance from TSS in base pairs. TSS and gene end are marked with a black dotted line. Y-axis shows the average H2Bub1 signal of the reads normalized per hundred million base pairs.

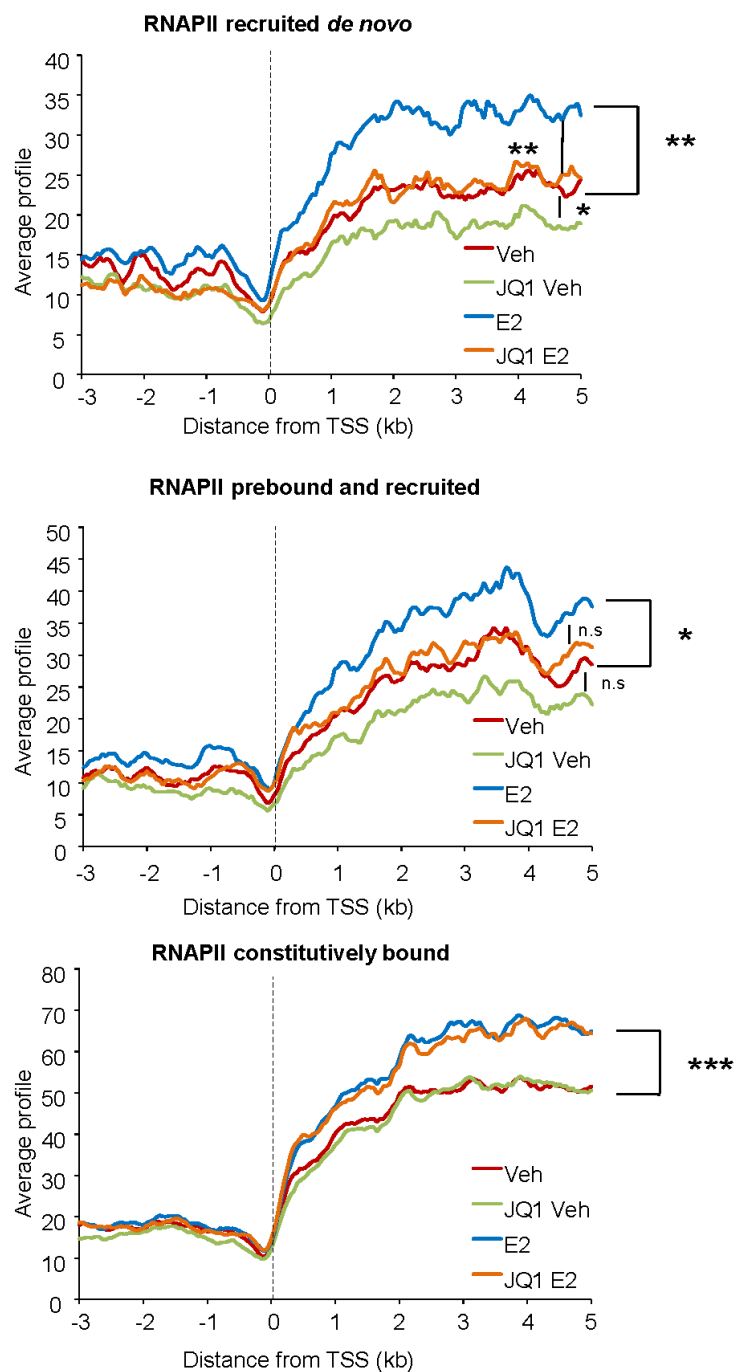


**Figure 2.I.S3N.** Aggregate plots showing genomic profiles of H2Bub1 on estrogen-upregulated genes grouped according to RNAPII occupancy (RNAPII recruited *de novo*, RNAPII prebound and recruited and RNAPII constitutively bound) upon vehicle (Veh), JQ1 as well as vehicle (JQ1 Veh), estrogen (E2) and JQ1 as well as estrogen (JQ1 E2) treated conditions. X-axis shows the distance from TSS in kilobase pairs. Y-axis shows the average H2Bub1 signal of the reads normalized on hundred million base pairs. TSS is marked with a black dotted line. Weighted averages for each estrogen-upregulated

gene - 1.5 to 2.5 kb downstream of each TSS were used to calculate the p-values using ANOVA with multiple regression models between conditions. \* indicates  $p \leq 0.05$ , \*\*  $p \leq 0.01$ , \*\*\*  $p \leq 0.001$ , n.s - not significant.

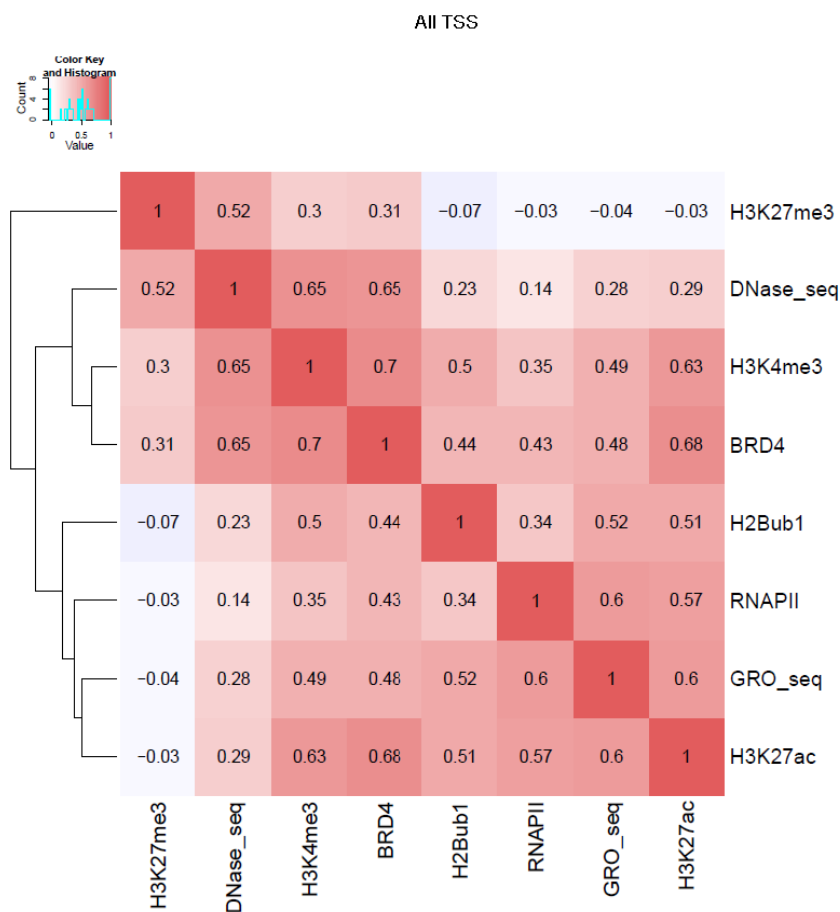


**Figure 2.I.S30.** Correlation plot on all TSS + 3 kb showing the association of BRD4, H3K27ac, H3K4me3, nascent RNA transcription (GRO-seq), RNAPII, H2Bub1 and DNaseI hypersensitivity sites (DNase-seq) and H3K27me3.

E2 upregulated gene-specific TSS

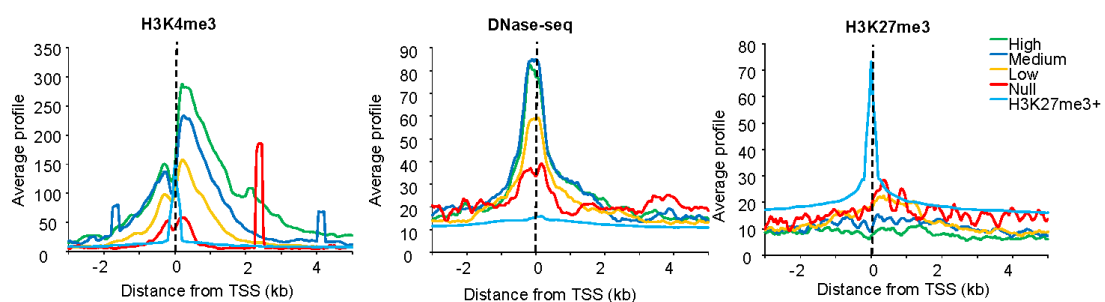


**Figure 2.I.S3P.** Aggregate plot analyses of H3K4me3, DNaseI hypersensitivity sites (DNase-seq) and H3K27me3 on GRO-seq based classified (High, Medium, Low and Null) TSS sites on estrogen

regulated genes. “High” group corresponds to estrogen-upregulated TSS having weighted average of GRO-seq signal greater than 0.3; “medium”  $\geq 0.15 < 0.3$ ; “low”  $> 0 < 0.15$ ; “null” with no value of average.

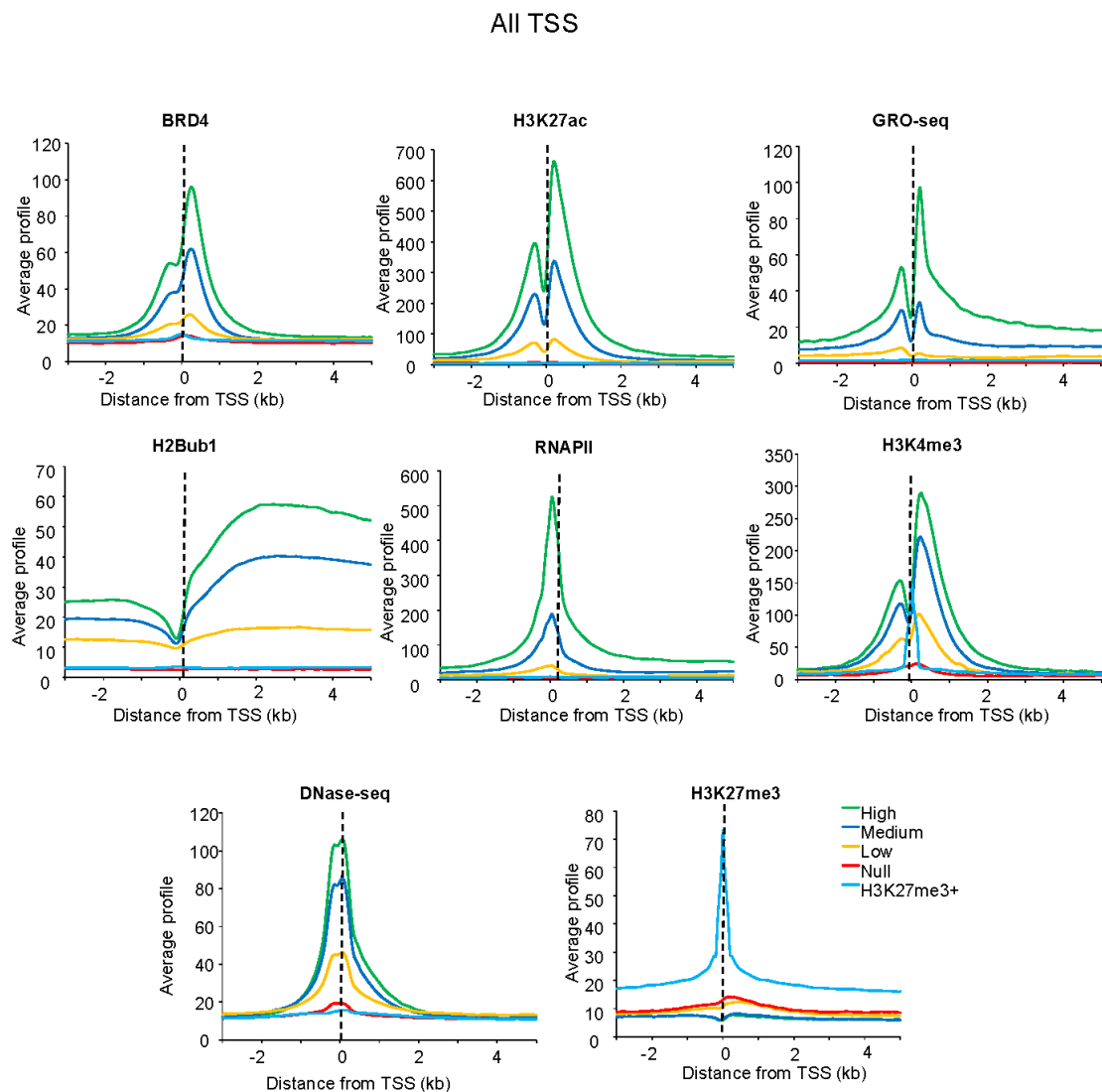


**Figure 2.I.S3Q.** Aggregate plot analyses of BRD4, H3K27ac, RNA expression (GRO-seq), RNAPII occupancy, H2Bub1, H3K4me3, DNaseI hypersensitivity sites (DNase-seq) and H3K27me3 on GRO-seq based classified (High, Medium, Low and Null) all TSS sites. “High” group corresponds to all TSS having weighted average of GRO-seq signal greater than 0.3; “medium”  $\geq 0.15 < 0.3$ ; “low”  $> 0 < 0.15$ ; “null” with no value of average. A class of H3K27me3-positive summits was examined as a negative control of active transcription.

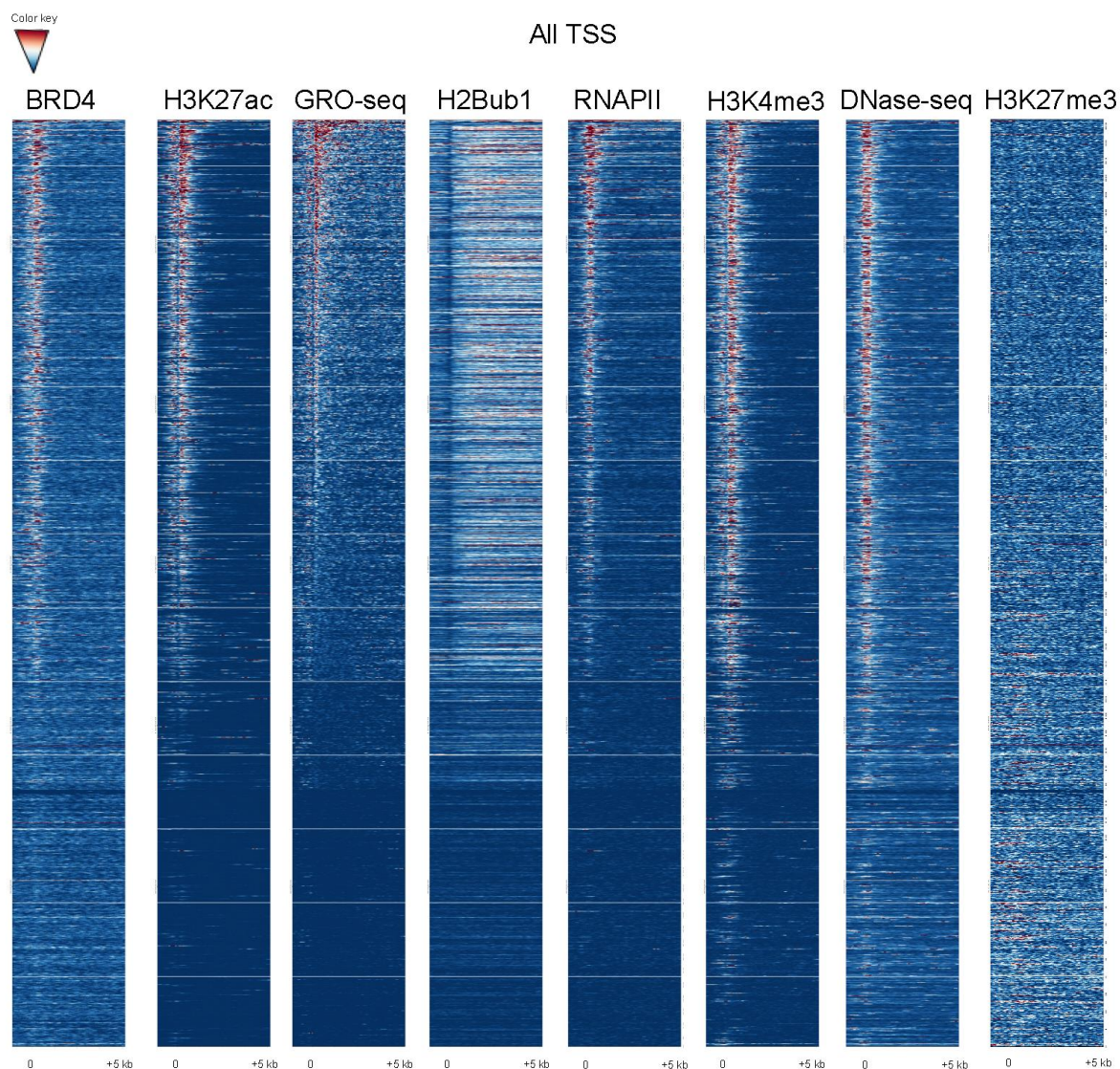


**Figure 2.I.S3R.** Heatmap profiles of BRD4 and H3K27ac, nascent RNA transcription (GRO-seq), RNAPII, H2Bub1, H3K4me3, DNaseI hypersensitivity sites (DNase-seq) and H3K27me3 on 1 kb upstream and 5 kb downstream of all TSS aligned from high to null GRO-seq signals. TSS and +5 kb are marked.



**Figure 2.I.S4A.** Western blot analyses with ERα and β-actin specific antibodies on whole MCF-7 protein extracts after DMSO (-) or JQ1 and or E2 induction for 2 hours.



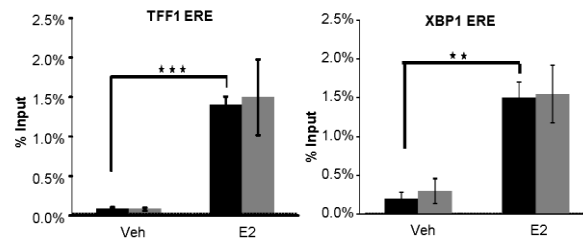


**Figure 2.I.S4B.** ChIP-qPCR analyses of ER $\alpha$  recruitment to XBP1 and TFF1 ERE after DMSO or JQ1 treatment with vehicle (Veh) or estrogen (E2) induction. \* indicates  $p \leq 0.05$ , \*\*  $p \leq 0.01$ , \*\*\*  $p \leq 0.001$ . Data are represented as mean  $\pm$  standard deviation.  $n=3$ . Dotted line indicates background.

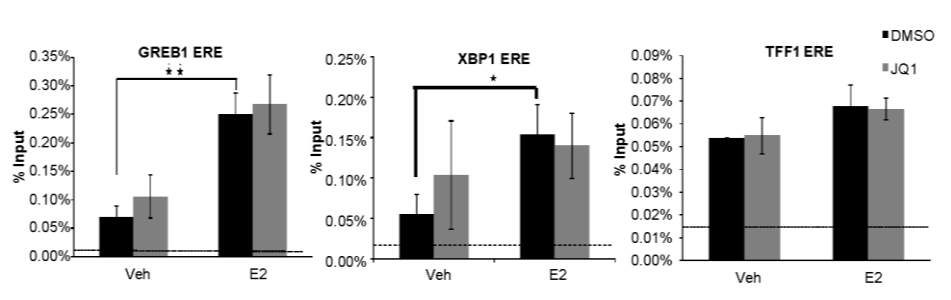


**Figure 2.I.S4C.** ChIP-qPCR analyses of RAD21 recruitment to GREB1, XBP1 and TFF1 ERE after DMSO or JQ1 treatment with vehicle (Veh) or estrogen (E2) induction. \* indicates  $p \leq 0.05$ , \*\*  $p \leq 0.01$ , \*\*\*  $p \leq 0.001$ . Data are represented as mean  $\pm$  standard deviation.  $n=3$ . Dotted line indicates background.

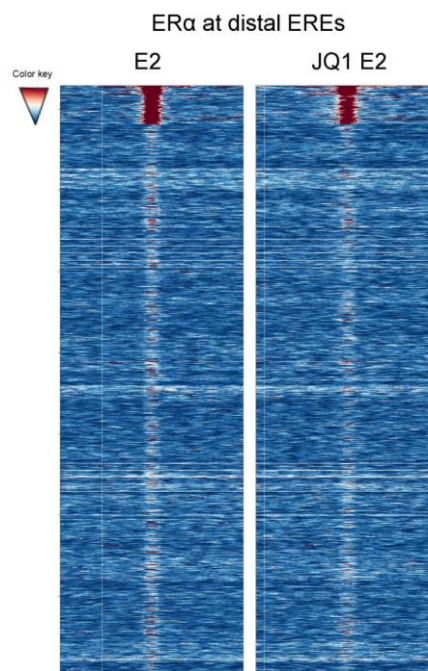


**Figure 2.I.S4D.** Heatmap profiles of ER $\alpha$  under estrogen (E2) and JQ1 as well as estrogen (JQ1 E2) treatment on distal EREs  $\pm$  5 kb. Center of each heatmap denotes center of distal EREs.

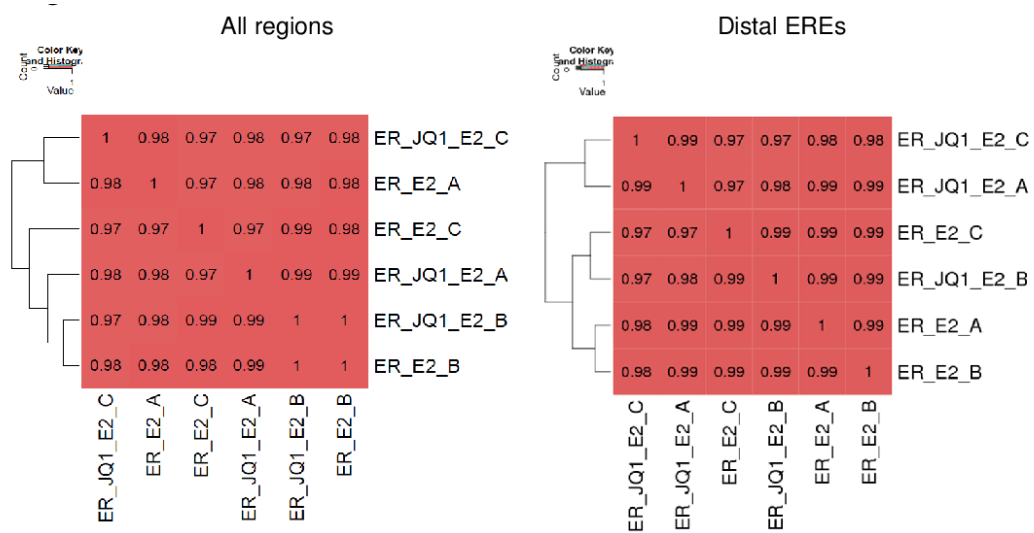


**Figure 2.I.S4E.** Correlation plots of ERα ChIP signals of different replicates and conditions - estrogen (E2) and JQ1 as well as estrogen (JQ1 E2) on all regions and specifically on distal EREs.

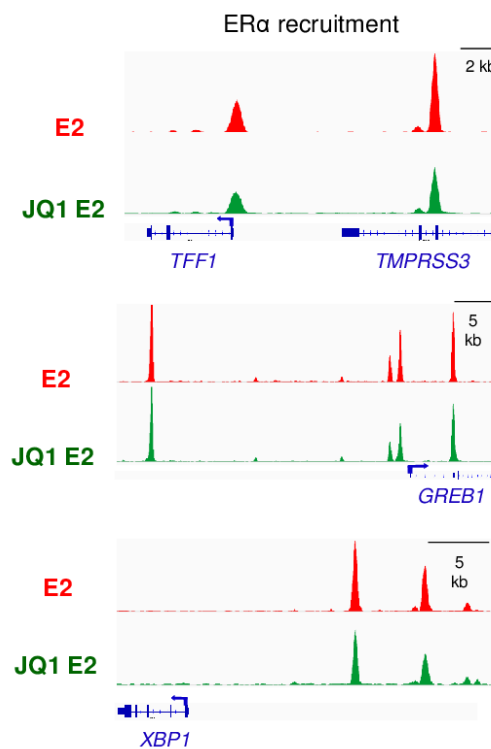


**Figure 2.I.S4F.** Genomic binding profiles of ERα on estrogen induced genes (GREB1, XBP1 and TFF1) after estrogen (E2) and JQ1 as well as estrogen (JQ1 E2) treatment.



**Figure 2.I.S4G.** Venn diagram showing overlap in binding regions of ER $\alpha$  and BRD4. The number of regions is written inside the circles.

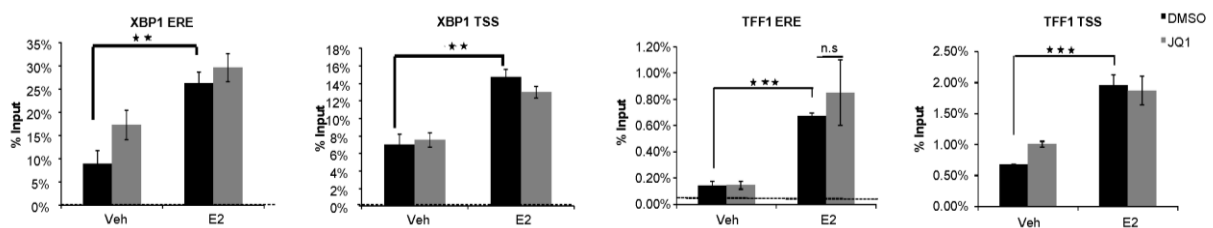


**Figure 2.I.S4H.** ChIP-qPCR analyses of H3K27ac on XBP1 and TFF1 ERE overlapping region and TSS after DMSO or JQ1 treatment with vehicle (Veh) or estrogen (E2) induction. \* indicates  $p \leq 0.05$ , \*\*  $p \leq 0.01$ , \*\*\*  $p \leq 0.001$ . Data are represented as mean  $\pm$  standard deviation.  $n=3$ . Dotted line indicates background.

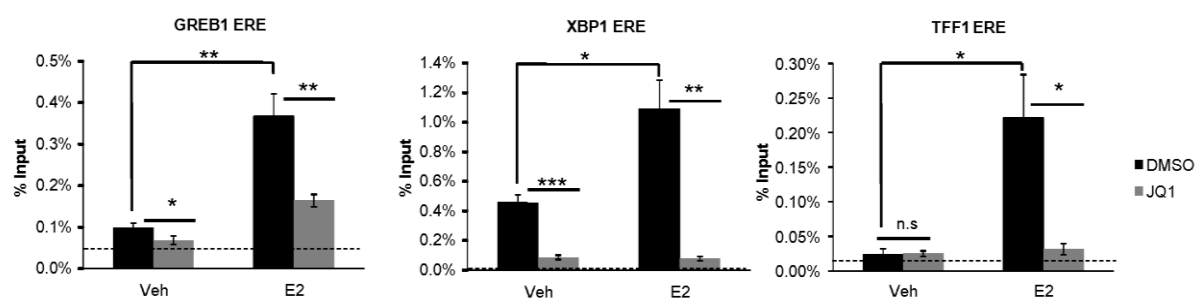


**Figure 2.I.S4I.** ChIP-qPCR analyses of BRD4 recruitment to GREB1, XBP1 and TFF1 ERE after DMSO or JQ1 treatment with vehicle (Veh) or estrogen (E2) induction. \* indicates  $p \leq 0.05$ , \*\*  $p \leq 0.01$ , \*\*\*  $p \leq 0.001$ . Data are represented as mean  $\pm$  standard deviation.  $n=3$ . Dotted line indicates background.

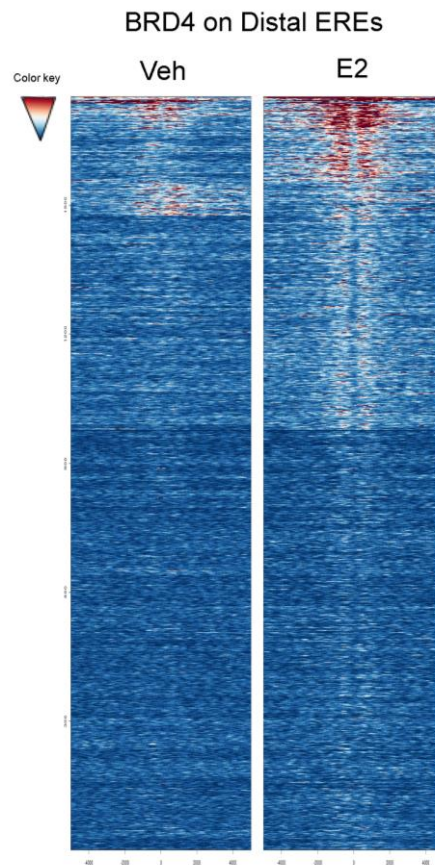


**Figure 2.I.S4J.** Heatmap profiles of BRD4 under estrogen (E2) and JQ1 as well as estrogen (JQ1 E2) treatment on distal EREs +/- 5 kb. Center of each heatmap denotes center of distal EREs.

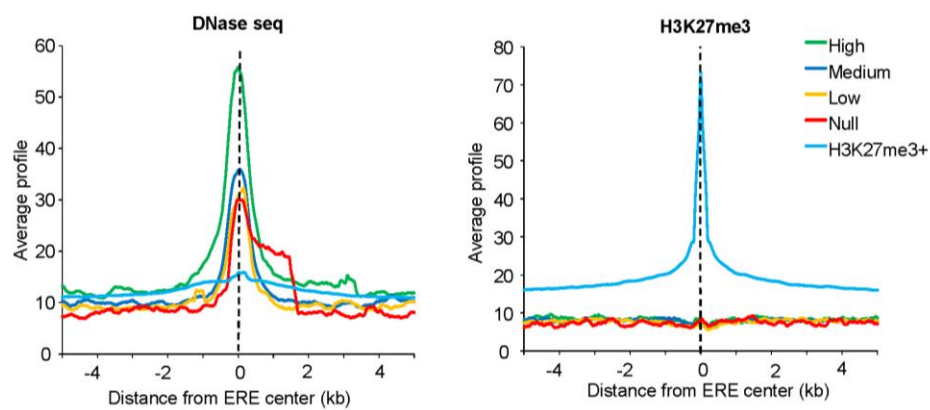


**Figure 2.I.S4K.** Aggregate plot analyses of DNase I hypersensitivity sites (DNase-seq) and H3K27me3 on GRO-seq based classified (High, Medium, Low and Null) TSS sites on distal EREs. “High” group corresponds to distal EREs having weighted average greater than 0.45; “medium”  $> 0.25 < 0.45$ ; “low”  $> 0 \leq 0.25$ ; “null” with no value of average. A class of H3K27me3-positive summits was examined as a negative control of active transcription.

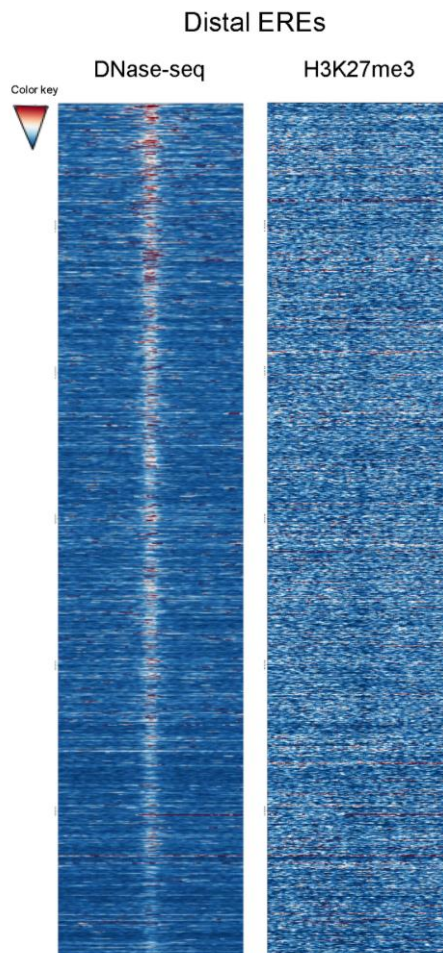


**Figure 2.I.S4L.** Heatmap profiles of DNase I hypersensitivity sites (DNase-seq) and H3K27me3 on distal EREs aligned from high to null GRO-seq signals. Center of each heatmap denotes center of distal EREs.

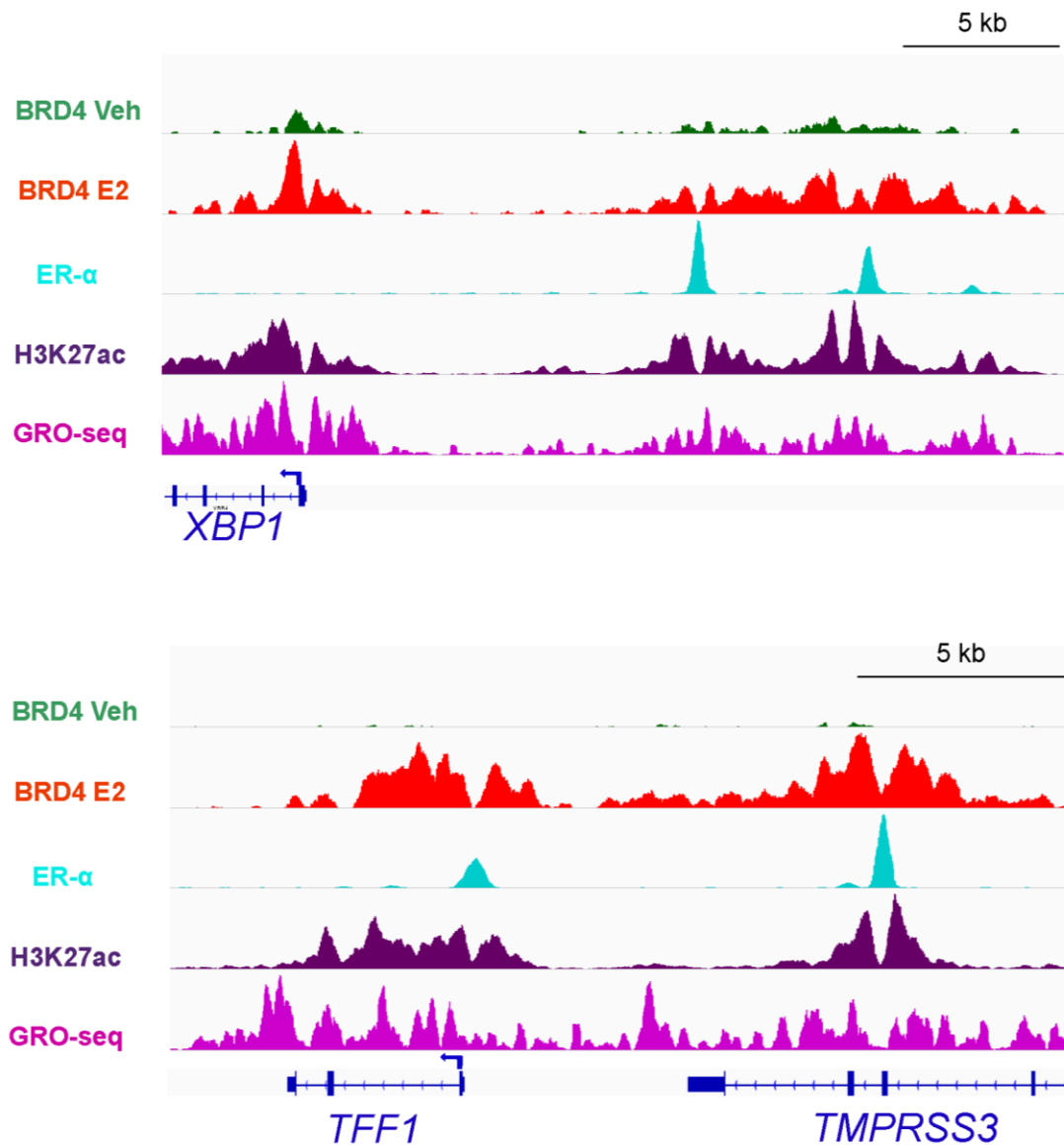


**Figure 2.I.S4M.** Binding profiles of BRD4, H3K27ac (purple), ER $\alpha$  (light blue) and GRO-seq (pink) on XBP1 and TFF1 distal EREs and promoter. BRD4 with red peaks indicates estrogen (E2) treated and green indicates vehicle (Veh) treated conditions.

## RNAPII on high BRD4 bound and high eRNA producing distal EREs

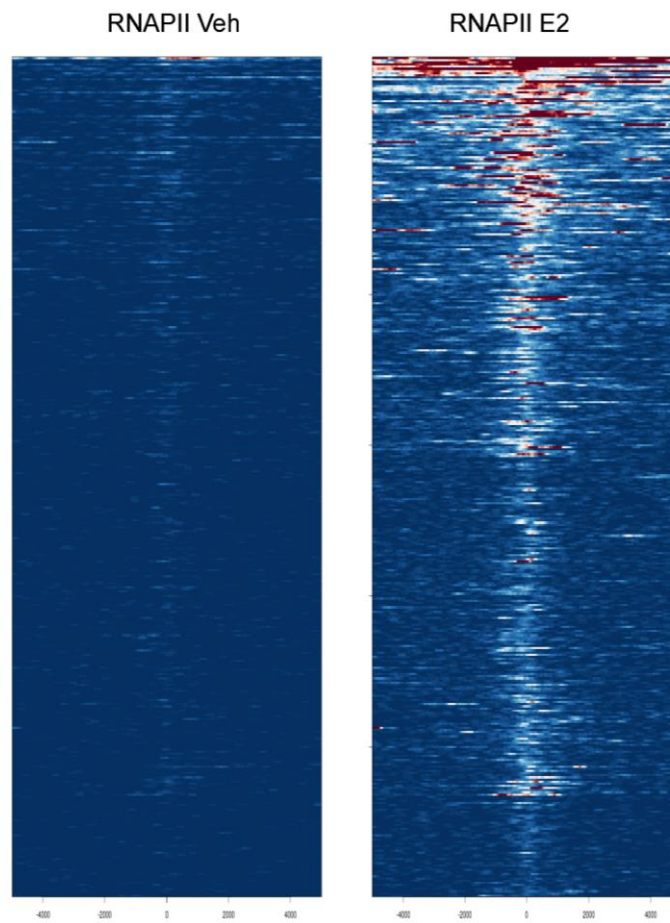


**Figure 2.I.S4N.** Heatmap showing genomic binding profiles of RNAPII on distal EREs which produce high eRNA (GRO-seq group “high”) upon vehicle (veh) and estrogen (E2) treated conditions.

## RNAPII P<sub>Ser2</sub>

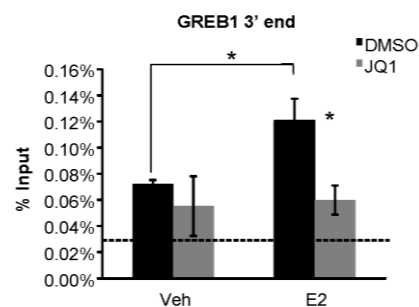


**Figure 2.I.S4O.** ChIP-qPCR analyses of RNAPII P<sub>Ser2</sub> occupancy on GREB1 3' end after DMSO or JQ1 treatment with vehicle (Veh) or estrogen (E2) induction. \* indicates  $p \leq 0.05$ , \*\*  $p \leq 0.01$ , \*\*\*  $p \leq 0.001$ . Data are represented as mean  $\pm$  standard deviation.  $n=3$ . Dotted line indicates background.

## 2.1. Publication II

### **H4K12ac is regulated by estrogen receptor-alpha and is associated with BRD4 function and inducible transcription**

#### **Citation**

Sankari Nagarajan, Eva Benito, Andre Fischer and Steven A. Johnsen

H4K12ac is regulated by estrogen receptor-alpha and is associated with BRD4 function and inducible transcription

*Oncotarget* 5 (2015), Advanced Online Publication, Retrieved from

<http://www.impactjournals.com/oncotarget/index.php?journal=oncotarget&page=article&op=view&path%5B%5D=3439&path%5B%5D=6743>

#### **Own contribution**

Experiments and data analyses for accomplishing all the figures and the supplementary figures, bioinformatic analyses, complete figure arrangements and writing the manuscript.



## Abstract

Hormone-dependent gene expression requires dynamic and coordinated epigenetic changes. Estrogen receptor-positive (ER<sup>+</sup>) breast cancer is particularly dependent upon extensive chromatin remodeling and changes in histone modifications for the induction of hormone-responsive gene expression. Our previous studies established an important role of bromodomain-containing protein-4 (BRD4) in promoting estrogen-regulated transcription and proliferation of ER<sup>+</sup> breast cancer cells. Here, we investigated the association between genome-wide occupancy of histone H4 acetylation at lysine 12 (H4K12ac) and BRD4 in the context of estrogen-induced transcription. Similar to BRD4, we observed that H4K12ac occupancy increases near the transcription start sites (TSS) of estrogen-induced genes as well as at distal ER $\alpha$  binding sites in an estrogen-dependent manner. Interestingly, H4K12ac occupancy highly correlates with BRD4 binding and enhancer RNA production on ER $\alpha$ -positive enhancers. Consistent with an importance in estrogen-induced gene transcription, H4K12ac occupancy globally increased in ER-positive cells relative to ER-negative cells and these levels were further increased by estrogen treatment in an ER $\alpha$ -dependent manner. Together, these findings reveal a strong correlation between H4K12ac and BRD4 occupancy with estrogen-dependent gene transcription and further suggest that modulators of H4K12ac and BRD4 may serve as new therapeutic targets for hormone-dependent cancers.

## Introduction

The estrogen receptor-alpha (ER $\alpha$ ) plays a central role in determining a luminal epithelial phenotype and tumor progression in a large fraction of breast cancers. Notably, interfering with ER $\alpha$ -regulated gene transcription represents a major therapeutic target in breast cancers where anti-estrogen therapies are the primary indicated therapy for patients with ER $\alpha$ -positive tumors. Estrogen-mediated gene induction is tightly and dynamically regulated. Stimulation with estrogen induces the binding of ER $\alpha$  to estrogen response elements (EREs), which act as enhancers in a manner largely dependent upon the pioneer factor, Forkhead protein A-1 (FOXA1) (Carroll et al., 2005; Hurtado et al., 2011). Upon activation, ER $\alpha$  further recruits coactivator proteins of the p160 family of histone acetyltransferases (HATs)

including SRC1/NCOA1 (Liu et al., 1999). SRC1 further interacts with and recruits additional HATs such as p300 and CBP (Demarest et al., 2002; Kamei et al., 1996). Additionally, ER $\alpha$  also recruits another HAT, p300/CBP-associated factor (PCAF) (Blanco et al., 1998). Recruitment of HATs to EREs promotes histone acetylation and thereby leads to gene induction (Green and Carroll, 2007). In particular, acetylation of H3K27 and H4K16 are found near transcriptional start sites (TSS) as well as on active enhancer regions where their occupancy is tightly associated with the recruitment of bromodomain protein-4 (BRD4) (Creyghton et al., 2010; Zhang et al., 2012a; Nagarajan et al., 2014; Zippo et al., 2009; Belikov et al., 2012).

BRD4 belongs to the bromo- and extraterminal (BET) domain protein family and serves as a major epigenetic reader of histone acetylation. BRD4 preferentially binds to multiple acetylated lysine residues including K5, K8, K12 and K16 of histone H4 (Jung et al., 2014; Zhang et al., 2012a) and functions to recruit and activate Cyclin-Dependent Kinase-9 (CDK9), the kinase component of Positive Transcription Elongation Factor-b (P-TEFb) (Yang et al., 2005). CDK9 in turn promotes transcriptional elongation by phosphorylating serine 2 of the C-terminal heptapeptide repeat of RNA polymerase (RNAPII) as well as subunits of the Negative Elongation Factor (NELF) and DRB Sensitivity-Inducing Factor (DSIF) complexes (Ping and Rana, 2001; Pirngruber et al., 2009a; Yamaguchi et al., 1999). Notably, RNAPII Ser2 phosphorylation serves as a hallmark for transcriptional elongation and serves as a platform for the co-transcriptional recruitment of chromatin-modifying enzymes including the RNF20/40 ubiquitin ligase complex, which catalyzes the monoubiquitination of histone H2B at lysine 120 (H2Bub1) in the transcribed region of active genes (Karpiuk et al., 2012; Minsky et al., 2008; Pirngruber et al., 2009a). Addition of ubiquitin is hypothesized to topologically open chromatin structure (Fierz et al., 2011) and promote transcriptional elongation (Karpiuk et al., 2012; Pavri et al., 2006; Pirngruber et al., 2009a). In addition to its role in recruiting CDK9 to acetylated chromatin, BRD4 has also been reported to exhibit intrinsic kinase activity and directly phosphorylate RNAPII-PSer2 (Devaiah et al., 2012). These findings support a role for BRD4 in promoting gene expression by binding to acetylated histones and promoting RNAPII elongation in a chromatin context. This effect appears to be, at least in part, dependent upon CDK9 and BRD4 recruitment to enhancers (Lovén et al., 2013; Nagarajan et al., 2014) where they promote the transcription of noncoding

RNAs from enhancer elements (eRNAs) which are required for induced gene transcription and chromosomal looping (Hah et al., 2013; Kaikkonen et al., 2013; Li et al., 2013; Nagarajan et al., 2014; Kanno et al., 2014).

A number of studies have uncovered an essential role for BRD4 in various malignancies including Myc-driven cancers (Delmore et al., 2011; Ott et al., 2012), leukemia (Herrmann et al., 2012; Lockwood et al., 2012), lymphoma (Chapuy et al., 2013), lung adenocarcinoma (Lockwood et al., 2012), prostate (Asangani et al., 2014) and breast cancers (Crawford et al., 2008; Feng et al., 2014; Nagarajan et al., 2014). BRD4 was also reported to regulate metastasis in breast cancer (Alsarraj et al., 2011). Consistently, a BRD4-regulated gene signature was reported to predict outcome and survival in breast cancer, especially ER-positive breast cancer (Alsarraj et al., 2011; Crawford et al., 2008). Moreover, BRD4 is required for the growth of ER $\alpha$ -positive tamoxifen-resistant breast cancer where it functions to promote ER $\alpha$ -dependent gene transcription (Feng et al., 2014). In addition to these findings, our recent studies also show that BRD4 and downstream histone H2B monoubiquitination are central regulators of estrogen-responsive transcription (Bedi et al., 2015; Nagarajan et al., 2014; Prenzel et al., 2011). BRD4 is recruited to promoters and enhancers of ER $\alpha$ -dependent genes following estrogen stimulation to regulate estrogen-induced transcription and is required for estrogen-dependent proliferation (Nagarajan et al., 2014). However, the epigenetic mechanisms controlling BRD4 recruitment to estrogen responsive genes and EREs is poorly understood.

In this study, we examined the association of H4K12ac with BRD4 occupancy genome-wide and analyzed its function in estrogen-regulated transcription. We show that H4K12ac occupies estrogen-responsive gene promoters and EREs in an inducible manner (Nagarajan et al., 2014) where its occupancy significantly correlates with BRD4 binding, H2Bub1 occupancy, mRNA expression as well as eRNA synthesis. We also observed higher global levels of H4K12ac in ER $\alpha$ -positive breast cancer cells compared to ER $\alpha$ -negative mammary epithelial cells and a further estrogen-dependent increase in ER $\alpha$ -positive cells which was decreased by anti-estrogen treatment. Together these results identify H4K12ac as a potential important epigenetic mediator of ER $\alpha$  activity, possibly via the recruitment of BRD4.

## Results

### H4K12ac correlates with BRD4 binding and active transcription on estrogen-induced genes

In order to determine whether H4K12ac may play a role in estrogen-responsive gene expression, we performed genome-wide ChIP-sequencing analyses of H4K12ac with or without estrogen treatment in the ER $\alpha$ -positive MCF7 luminal breast cancer cell line. Aggregate profiles and heatmap analyses showed that estrogen induction increases H4K12ac occupancy near the transcription start sites (TSS) (Figure 2.II.1A-B, 2.II.S1A-B). Interestingly, this resembled the increased recruitment of BRD4 adjacent to TSS of estrogen-responsive genes (Nagarajan et al., 2014). We further performed correlation and heatmap analyses to determine whether H4K12ac occupancy is correlated with BRD4 (Nagarajan et al., 2014) recruitment, RNAPII (Welboren et al., 2009) occupancy as well as various other histone modifications. Specifically, we compared H4K12ac occupancy to that of H3K27ac (Theodorou et al., 2013) and H3K4me3 (Joseph et al., 2010) which are both active marks of transcription initiation, H2Bub1 (Nagarajan et al., 2014) which correlates with transcriptional elongation and is dependent upon BRD4 activity (Nagarajan et al., 2014) and GRO-seq (Global run on-sequencing) (Hah et al., 2013) which represents nascent RNA transcription. H3K27me3 (Joseph et al., 2010) was used as a negative control and a repressive mark for transcription. Heatmaps were arranged in descending order according to the H3K27ac signals near TSS (TSS and 3 kb downstream). These analyses revealed a high correlation between H4K12ac and BRD4 occupancy and to a lesser extent with H3K27ac occupancy (Figure 2.II.1C-D, 2.II.S1C-D). Furthermore, consistent with their common association with active gene transcription, H3K4me3 and H2Bub1 displayed highest correlations with H4K12ac and BRD4. Interestingly, H4K12ac levels did not decrease near the TSS of estrogen-downregulated genes (Figure 2.II.S1D-E). These effects are consistent with the negligible change in BRD4 binding on estrogen-repressed genes after estrogen treatment and indicate that histone deacetylase-mediated removal of H4K12ac may occur slower than the transcriptional repression of these genes (Nagarajan et al., 2014). Altogether these results uncover a high correlation between H4K12ac and BRD4 occupancy at TSS following estrogen treatment.

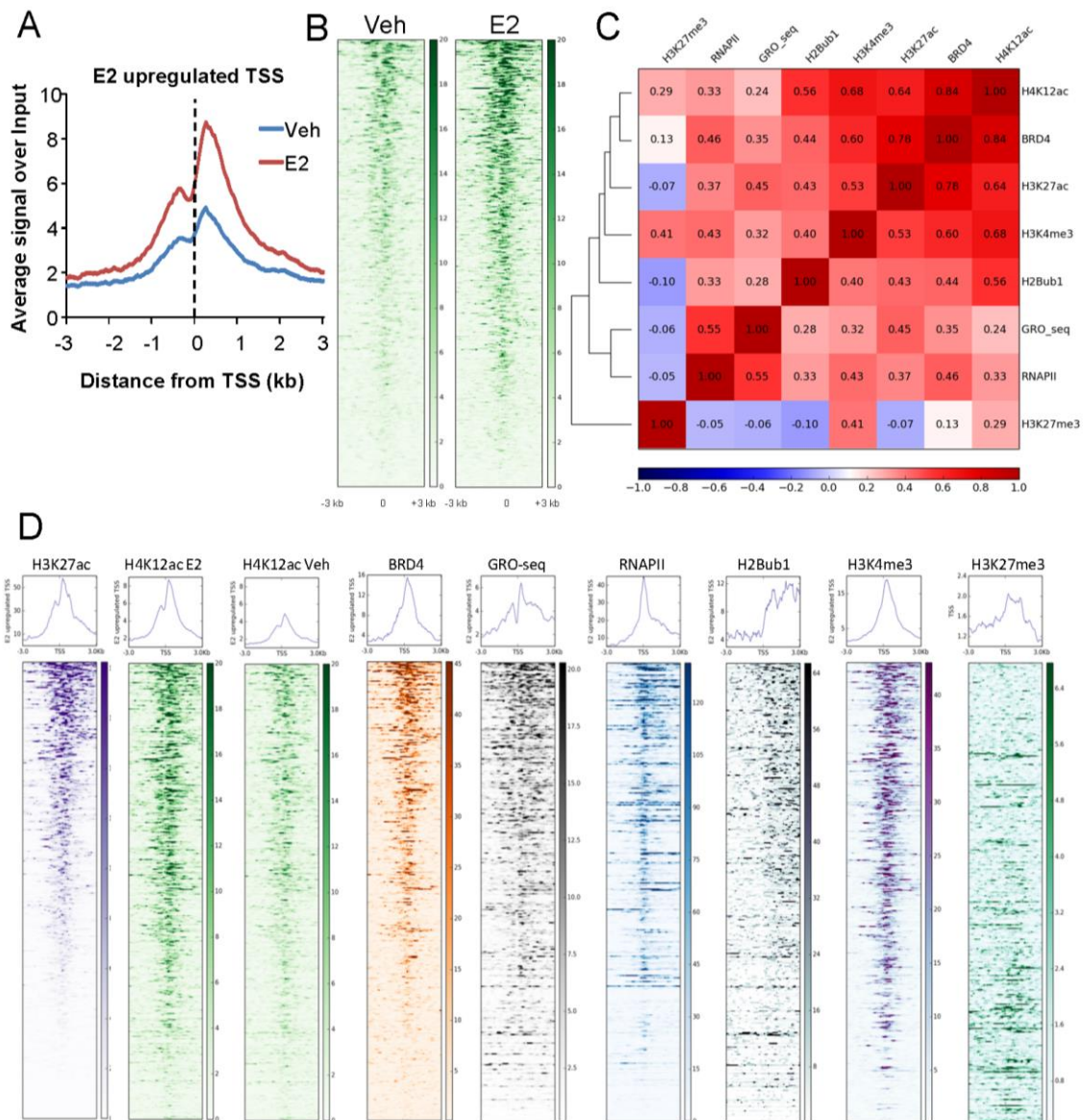


**Figure 2.II.1: H4K12ac correlates with BRD4 binding in estrogen-induced transcription.** (A) Average genomic binding profiles of H4K12ac around TSS and 3 kb upstream and downstream of estrogen-induced genes under vehicle (Veh) and estrogen-treated (E2) conditions. The X-axis shows the distance from the TSS of the genes in kilobase pairs. TSS is indicated by a black dotted line. (B) Heatmaps showing genomic binding profiles of H4K12ac around TSS and 3 kb upstream and downstream of estrogen-induced genes under vehicle (Veh) and estrogen-treated (E2) conditions. Center of the heatmap represents TSS. Color key of the heatmaps is shown on the side. (C) Correlation plot showing the heatmap with the Pearson's correlation coefficient values for H4K12ac, BRD4, H3K27ac, H3K4me3, H2Bub1, GRO-seq, RNAPII and H3K27me3 on TSS and 3 kb downstream region of estrogen-upregulated genes. Color key of the heatmap is shown at the bottom of the plot. (D) Heatmaps showing genomic binding profiles of H3K27ac, H4K12ac with estrogen treatment (H4K12ac E2) and without estrogen treatment (H4K12ac Veh), BRD4, nascent RNA transcription (GRO-seq), RNAPII, H2Bub1, H3K4me3 and H3K27me3 around TSS and 3 kb upstream and downstream of estrogen-induced genes. Density of the signals is arranged according to average

H3K27ac signals from high to low. Center of the heatmap represents TSS. Color key of the heatmaps is shown at their side.

### **H4K12ac is associated with enhancer function**

Given the association of BRD4 with enhancers (Chapuy et al., 2013; Lovén et al., 2013) and its recently established role in promoting eRNA transcription (Kaikkonen et al., 2013; Nagarajan et al., 2014; Kanno et al., 2014), we examined whether H4K12ac occupancy is also preferentially enriched on ER $\alpha$ - and FOXA1-bound enhancers. Indeed, we observed H4K12ac enrichment on distal EREs and this enrichment significantly increased following estrogen treatment as shown in aggregate plot and heatmap analyses (Figure 2.II.2A-B). To further examine the association of H4K12ac at distal ER $\alpha$ -bound enhancers, correlation plot and heatmaps were generated for BRD4, as well as ER $\alpha$ , FOXA1 and H3K27ac on these regions (Figure 2.II.2C, 2.II.S2A). We observed that BRD4 and H3K27ac occupancy correlated with H4K12ac on distal enhancers. Notably, apart from its association with FOXA1 and BRD4, ER $\alpha$  binding correlated particularly well with H4K12ac and lesser with H3K27ac. Interestingly, RNAPII occupancy and nascent RNA transcription on enhancers, which are indicative of eRNA production, also correlated with H4K12ac occupancy. Genomic Regions Enrichment of Annotations Tool (GREAT) analyses (McLean et al., 2010) on distal intergenic regions which exhibited overlapping peaks of H3K27ac, H4K12ac and BRD4 demonstrated an enrichment of estrogen and breast cancer luminal upregulated and basal downregulated-related pathways (Figure 2.II.S2B-C). These findings support a strong association among H4K12ac, H3K27ac, BRD4 and ER $\alpha$  function on distal enhancer regions.

To further evaluate the association of H4K12ac with distal enhancer function, distal EREs were grouped into four classes (high, medium, low and null) according to the enrichment of H4K12ac around EREs. Consistent with their potential function as active enhancers, these groups of distal regions also correlated with BRD4 and RNAPII occupancy as well as nascent RNA transcription (Figure 2.II.2D). Together these findings demonstrate that H4K12ac occupies active EREs which are bound by ER $\alpha$ , FOXA1, BRD4 and H3K27ac and produce eRNAs.

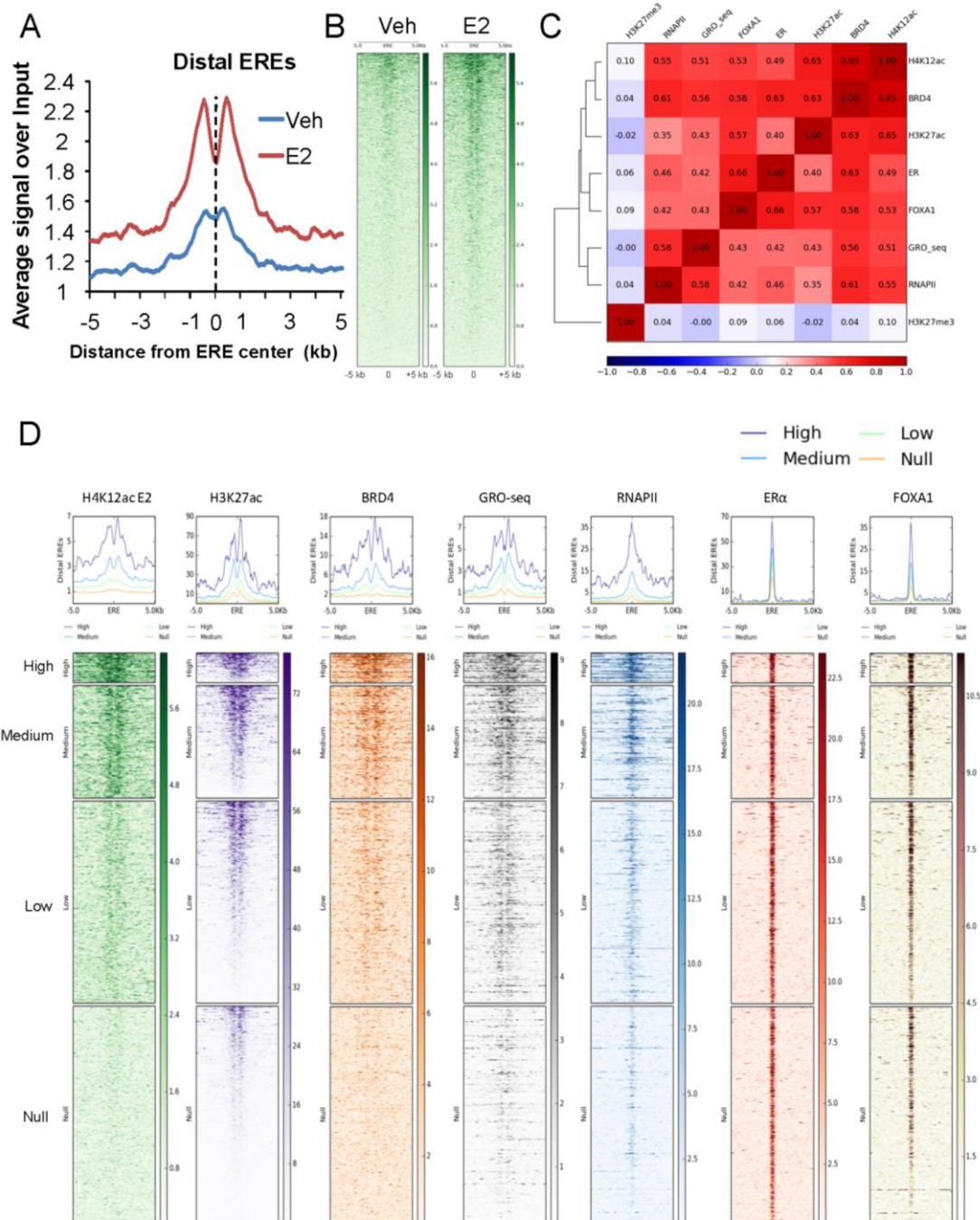


**Figure 2.II.2: H4K12ac correlates with BRD4 binding in estrogen-induced enhancer function.**

(A) Average genomic binding profiles of H4K12ac around distal EREs and 5 kb upstream and downstream under vehicle (Veh) and estrogen-treated (E2) conditions. X-axis shows the distance from distal EREs in kilobase pairs. Center of ERE is marked with black dotted line. (B) Heatmaps showing genomic binding profiles of H4K12ac around ERE and 5 kb upstream and downstream under vehicle (Veh) and estrogen-treated (E2) conditions. Center of the heatmap represents center of ERE. Color key of the heatmaps is shown on the side. (C) Correlation plot showing the heatmap with the Pearson's correlation coefficient values for H4K12ac, BRD4, H3K27ac, ER $\alpha$ , FOXA1, GRO-seq, RNAPII and H3K27me3 on distal EREs and 1.5 kb upstream and downstream region of estrogen-

induced genes. Color key of the heatmap is shown at the bottom of the plot. (D) High, medium, low and null groups were classified according to the H4K12ac signal under estrogen-treated conditions and then heatmaps were plotted for various ChIP-seq signals (H4K12ac E2, BRD4, nascent RNA transcription (GRO-seq), RNAPII, ER $\alpha$ , FOXA1 and H3K27me3) around distal EREs and 5 kb upstream and downstream. Center of the heatmap represents center of the distal ERE region. Color key of the heatmaps is shown on the side.

### H4K12ac correlates with BRD4 function in gene regulation

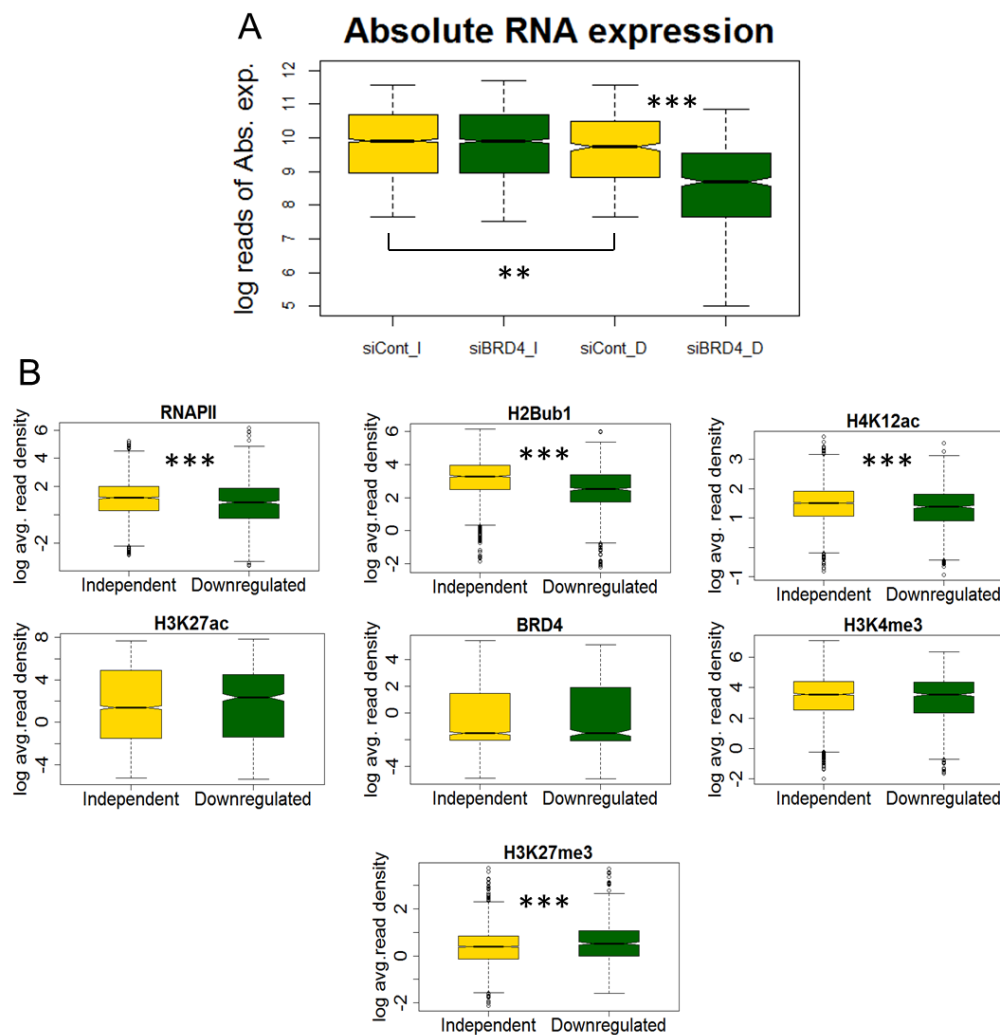


**Figure 2.II.3: H4K12ac correlates with BRD4 function in regulating gene expression.** (A) Boxplot showing the absolute gene expression in logarithmic values of normalized counts (log reads of Abs. exp.) under vehicle treated conditions. Genes which are independent (I) and downregulated (D) following BRD4 depletion (siBRD4) are shown. siCont refers to negative control siRNA treated samples. p-values were calculated using Mann-Whitney test and are shown only for significant changes. \*\*\* $p \leq 0.001$ ; \*\* $p \leq 0.01$ ; \* $p \leq 0.05$ ; (B) Boxplots showing the average ChIP-seq signal in logarithmic values (log avg. read density) of RNAPII, H2Bub1, H4K12ac, H3K27ac, BRD4, H3K4me3 and H3K27me3 under vehicle-treated conditions. Genes which are independent (I) and



downregulated (D) following BRD4 depletion (siBRD4) are shown. siCont refers to negative control siRNA treated samples. p-values were calculated using Mann-Whitney test were shown only for significant changes. \*\*\* $p \leq 0.001$ ; \*\* $p \leq 0.01$ ; \* $p \leq 0.05$ .

In order to investigate a potential association with the function of BRD4, the average intensity of BRD4, H4K12ac, H3K27ac, H3K4me3, H2Bub1 and RNAPII downstream of the TSS (TSS and 3 kb downstream) were calculated on genes whose expression either decreased (“downregulated”) or was unaffected (“independent”) upon BRD4 depletion under vehicle treated conditions from our previously published RNA sequencing data. Interestingly, genes whose expression decreased following BRD4 depletion were lower expressed than non-regulated genes prior to knockdown (Figure 2.II.3A) and also displayed lower levels of RNAPII (Figure 2.II.3B). Consistent with lower RNAPII occupancy, H4K12ac and H2Bub1 occupancy were also lower on BRD4-dependent genes compared to BRD4-independent genes (Figure 2.II.3B). These results further suggest a cooperative function between H4K12ac and BRD4 in controlling RNAPII and co-transcriptional H2B monoubiquitination to regulate a defined subset of inducible genes.

### **H4K12ac occupancy correlates with gene expression levels**

In order to further validate the association of H4K12ac with active gene transcription, average signals of the active transcription marks around TSS were compared with the normalized counts of expression for each gene. As shown in scatterplots along with the respective correlation coefficients, H2Bub1, RNAPII, H3K4me3 and H4K12ac significantly correlated with mRNA expression (Figure 2.II.4, 2.II.S3-4). Together these results support a model in which a H4K12ac-BRD4-RNAPII-H2Bub1 axis directs overall gene expression, especially in estrogen-induced transcription.

### **Estrogen promotes global H4K12ac**

As H4K12ac occupancy is closely associated with ER $\alpha$ -dependent gene activity, we also compared H4K12ac occupancy in ER $\alpha$ -positive MCF7 breast cancer cells to that in the ER-negative MCF10A normal mammary epithelial cell line both in ChIP and in whole cell protein lysates. Both single gene ChIP-qPCRs as well as genome-wide ChIP-seq analyses displayed induced H4K12ac occupancy in MCF7

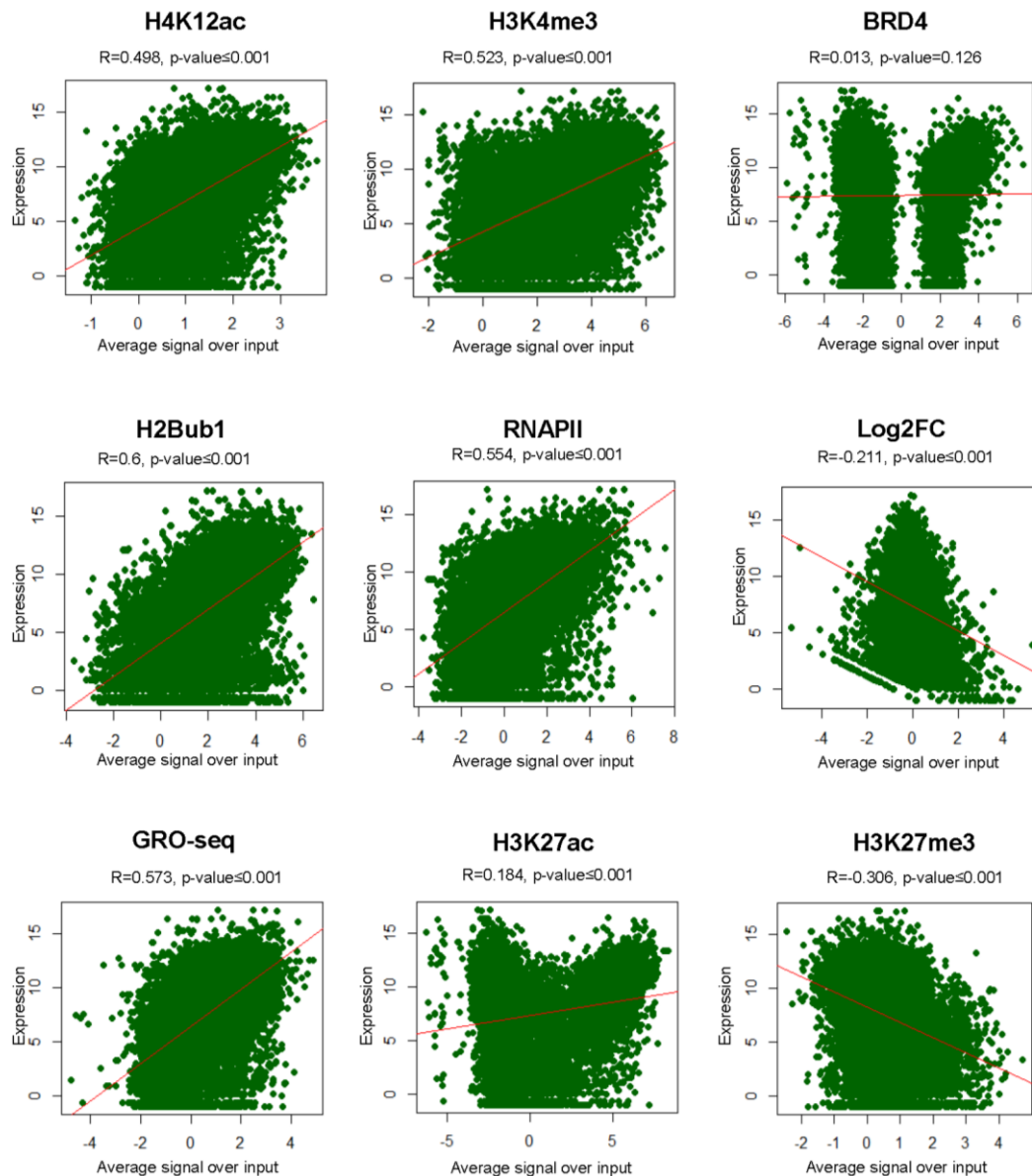


**Figure 2.II.4: H4K12ac positively correlates with gene expression.** Scatterplots showing the relationship between various ChIP-seq signals (average signal over input of H4K12ac, H3K4me3, BRD4, H2Bub1, RNAPII, GRO-seq, H3K27ac, H3K27me3, logarithmic fold changes of siBRD4 compared to siCont (Log2FC)) and absolute gene expression in logarithmic values. Pearson correlation coefficient (R) values and two-tailed p-values were shown above the plot. Each dot in the plot represents a single gene. Red line indicates the correlation.

comparing to MCF10A around TSS of estrogen-dependent genes (Figure 2.II.5A-B). Surprisingly, this effect was also observed near the TSS of estrogen-independent genes (Figure 2.II.5C-D) as well as at both distal H3K27ac-positive regions from MCF7 and MCF10A and regions occupied by H3K27ac, but not ER $\alpha$  (Figure 2.II.5F-G). These effects required ER $\alpha$  activity, since treatment of MCF7 cells with the anti-

estrogen fulvestrant, which rapidly reduces ER $\alpha$  protein levels via proteosomal degradation (Eckert et al., 1984; Wakeling and Bowler, 1992), decreases H4K12ac occupancy on estrogen-dependent and independent genes (Figure 2.II.5B, 2.II.5.D). Together, these studies suggested that H4K12ac levels may globally depend upon ER $\alpha$  activity. Consistently, Western blot analyses confirmed that H4K12ac globally increased after estrogen treatment in MCF7 cells and decreased following fulvestrant treatment (Figure 2.II.5E). Notably, H4K12ac levels were the lowest in ER-negative MCF10A cells. These results suggest a potential specific role of H4K12ac in estrogen-induced transcription and correlation with ER $\alpha$  status.

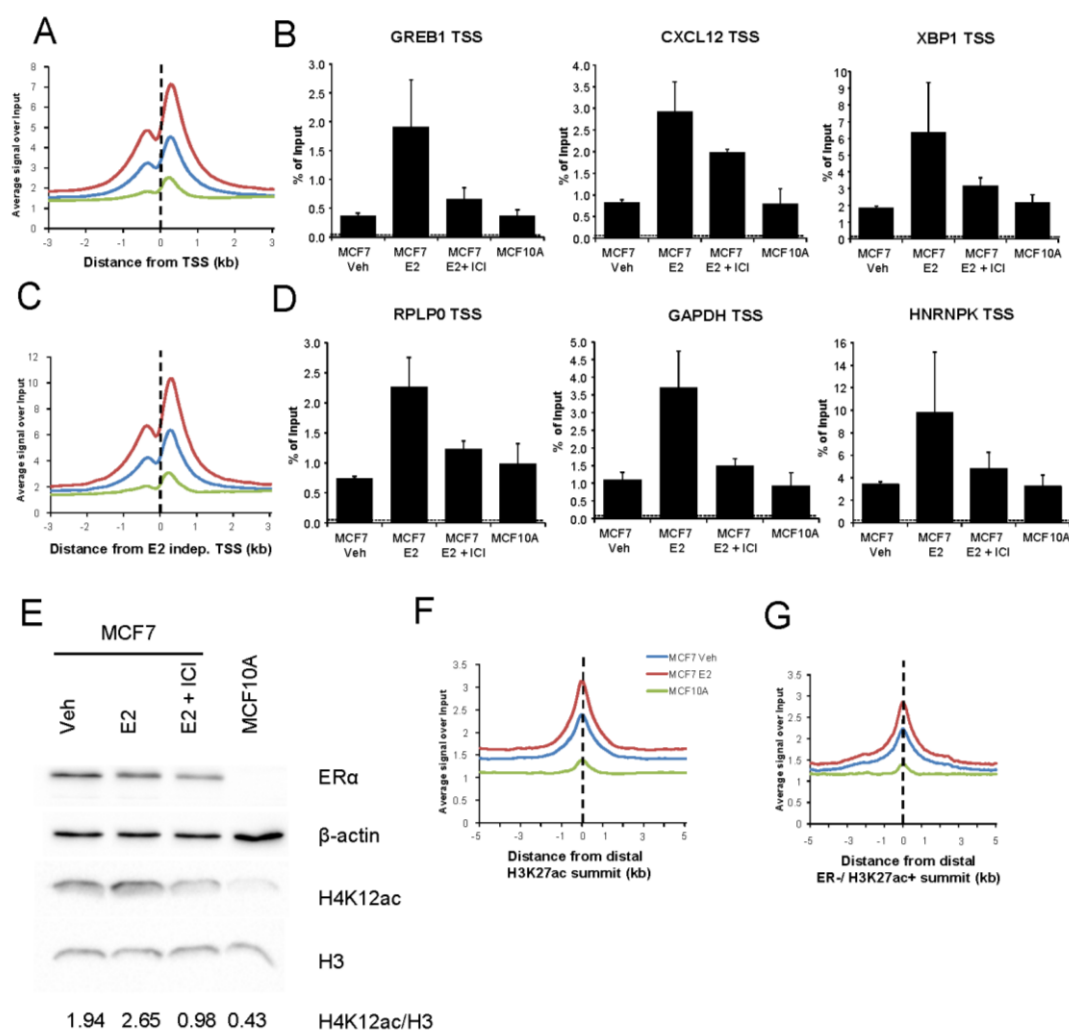


**Figure 2.II.5: H4K12ac depends upon ER $\alpha$  activity.** (A, C, F, G) Average genomic binding profiles of H4K12ac in vehicle- (Veh) and estrogen-treated (E2) MCF7 or MCF10A cells around TSS and 3 kb upstream and downstream of estrogen upregulated genes (A), TSS and 3 kb upstream and downstream of estrogen-independent genes (C) distal H3K27ac-positive regions and 5 kb upstream and downstream of them (F), and distal H3K27ac-positive regions which don't possess ER $\alpha$  binding

(ER negative (-ve)) and 5 kb upstream and downstream of them (G). X-axis shows the distance from the TSS (A, C) or center of the distal H3K27ac-positive region (B, D) in kilobase pairs. TSS or center of H3K27ac peak is indicated by a black dotted line. (B, D) ChIP-qPCR analyses of H4K12ac in vehicle- (Veh), estrogen-treated (E2) and/or ICI-182,780 (ICI) treated MCF7 or MCF10A cells on TSS of respective estrogen-dependent (GREB1, CXCL12 and XBP1) (B) and estrogen-independent genes (RPLP0, GAPDH and HNRNPK) (D). H4K12ac enrichment is denoted by percentage of input values. Dotted line indicates background DNA precipitated by negative control IgG antibody. (E) Western blot analyses showing ER $\alpha$ ,  $\beta$ -actin, H4K12ac and H3 levels in vehicle- (Veh), estrogen-treated (E2) and/or ICI-182,780 (ICI) treated MCF7 or MCF10A cells. H4K12ac levels were normalized with H3 and the values were shown under the blot.

## Discussion

Signal-induced transcription requires a highly coordinated and complex interplay between various transcription factors, post-translational histone modifications, epigenetic readers and chromatin remodelers in order to induce gene expression in a proper temporal and spatial manner. Dysregulation of these mechanisms frequently results in disorders such as cancer. Positive association of H4K12ac with estrogen-induced gene transcription reveals a potentially important and specific role of this modification in promoting ER $\alpha$ -induced gene transcription. According to our model, ER $\alpha$ -directed H4K12 acetylation facilitates the recruitment of BRD4 to both enhancers and promoters. Subsequently, BRD4 recruits CDK9 in order to promote eRNA synthesis at enhancers and transcriptional elongation of ER $\alpha$ -dependent mRNAs. The latter occurs, at least in part via phosphorylation of RNAPII at serine-2 and the subsequent monoubiquitination of histone H2B, which may help to open chromatin structure and facilitate the activity of other chromatin-associated elongation factors (Bedi et al., 2015; Nagarajan et al., 2014; Pavri et al., 2006; Prenzel et al., 2011).

Transcriptional activation is tightly coupled with histone acetylation (Allfrey et al., 1964; Grunstein, 1997; Struhl, 1998). However, the mechanisms linking histone acetylation and ER $\alpha$ -dependent transcriptional activation are not completely understood. Here, we show that H4K12ac is globally increased across the ER $\alpha$  cistrome in response to estrogen induction. This supports the dynamic nature of histone acetylation including H4K12ac upon estrogen treatment (Sun et al., 2001; Eeckhoutte et al., 2007; Lupien et al., 2009, 2010). H4K12ac may be catalyzed by

p300/CBP (Bowers et al., 2010; Ogryzko et al., 1996), which is a critical determinant of ER $\alpha$ -regulated transcription (Kim et al., 2001; Liu et al., 1999). Thus, our findings not only validate the role of histone acetyltransferases like p300 in hormone-dependent systems (Kim et al., 2001; Liu et al., 1999), but also provide a further potential mechanistic explanation linking H4K12ac to BRD4 recruitment to estrogen-responsive enhancers and TSS. Thus, H4K12ac may play a central role in transcriptional activation which links ER $\alpha$  binding to the subsequent recruitment of other epigenetic regulators like BRD4, which are essential for ER $\alpha$  activity.

The transcriptional mechanisms controlling stimuli-induced gene expression is tightly coupled to the rapid association and disassociation of transcriptional factor and cofactor complexes as well as dynamic changes in chromatin remodeling and histone modifications (Green and Carroll, 2007; Johnsen, 2012; Métivier et al., 2006; Voss and Hager, 2014). Interestingly, we show that the genes which are dependent upon BRD4 exhibit reduced expression and lower RNAPII occupancy than BRD4-independent genes. This could support the possibility that these genes may have a higher turnover of the transcriptional activation complexes. Consistent with the lower expression and RNAPII occupancy, H4K12ac and H2Bub1 occupancy on these genes were also lower compared to BRD4-independent genes and their levels were highly dynamic during estrogen-induced transcription. Pathway analyses of BRD4-regulated genes (Nagarajan et al., 2014) as well as genes associated with enhancer regions which are co-bound by H3K27ac, H4K12ac and BRD4 revealed a specific enrichment of estrogen-induced genes. Consistently, estrogen-responsive genes display a highly dynamic and ER $\alpha$ -dependent assembly and disassembly of transcription factor and co-factor complexes which determine the magnitude and duration of gene induction (Métivier et al., 2006). Together these results suggest that estrogen-inducible genes may differentially depend upon BRD4 and its associated up- and downstream epigenetic regulatory mechanisms are based on a necessity for dynamic recruitment of transcriptional cofactors, RNAPII, post-translational modification of histones and chromatin remodeling.

Previous studies have suggested that BRD4 predominantly binds to histone H4 acetylated at lysine residues 5, 8, 12 and 16 (Jung et al., 2014; Zhang et al., 2012a). However, the close relationship between histone acetylation and BRD4 in

regulating transcriptional activity is less established (Zippo et al., 2009). Our studies demonstrate a strong link between the dynamic nature of H4K12ac and BRD4 and their association with RNAPII and H2Bub1 during target gene activation.

Induced occupancy of H4K12ac at both TSS and enhancers in cancer cells support a role for histone acetylation and enhancer activity in ER $\alpha$ -dependent cancer progression. Moreover, we describe a significant correlation between histone acetylation and eRNA production, which can control targeted gene induction in various disease-specific conditions (Hah et al., 2013; Kaikkonen et al., 2013; Li et al., 2013; Nagarajan et al., 2014). Notably, given the potential utility of BET domain inhibitors for the treatment of various cancers (Chapuy et al., 2013; Delmore et al., 2011; Herrmann et al., 2012; Lockwood et al., 2012; Lovén et al., 2013; Ott et al., 2012), these findings provide additional insight into the molecular mechanisms by which BRD4 functions in ER $\alpha$ -regulated gene transcription. Considering the recent demonstration of the utility of BET inhibition in the treatment of tamoxifen-resistant and hormone-dependent cancers (Asangani et al., 2014; Feng et al., 2014; Nagarajan et al., 2014), our studies provide a better understanding into the mechanism controlling BRD4 activity in this system. Importantly, BRD4 inhibition along with Fulvestrant sensitizes tumors for their growth inhibition in tamoxifen-resistant xenograft models (Feng et al., 2014) and our studies show that Fulvestrant rapidly reduces H4K12ac. This opens up a possibility of significant H4K12ac occupancy in tamoxifen-resistant breast cancers bringing up the therapeutic importance of H4K12ac and combined therapies with BRD4 inhibition and anti-estrogens in these cancers. Combination of HDAC inhibitors with tamoxifen is implicated in reversing tamoxifen/aromatase inhibitor-resistance in ER-positive breast cancers and HDAC inhibitors were shown to increase the sensitivity of cells to BRD4 inhibition for blocking cell growth and promoting apoptosis in leukemia and lymphoma (Bhadury et al., 2014; Fiskus et al., 2014; Munster et al., 2011). This may potentially provide a rationale for testing specific modulators of BRD4 recruitment to chromatin (e.g., inhibitors of histone deacetylases or histone acetyltransferases which particularly modulate H4K12ac) in regulating hormone-dependent gene expression.

## Methods

### Cell culture

MCF7 cells were kindly provided by K. Effenberger (University Medical Center, Hamburg-Eppendorf) and were grown in phenol red-free high-glucose Dulbecco's modified Eagle's media (DMEM, Invitrogen) supplemented with 10% fetal bovine serum (Thermo Scientific), 1% sodium pyruvate, and 1% penicillin/streptomycin (Sigma-Aldrich) at 37°C. For estrogen induction, cells were deprived of hormones by treating them with DMEM media supplemented with 5% charcoal-dextran-treated fetal bovine serum (CSS; Biochrome), 1% sodium pyruvate, and 1% penicillin/streptomycin after 24 hr of growth. After 48 hr, cells were treated with 10 nM 17  $\beta$ -estradiol (Sigma-Aldrich) and/or 1  $\mu$ M ICI-182,780 (Fulvestrant) for 2 hr. MCF10A cells were kindly provided by M. Oren (Weizmann Institute of Science, Israel) and were grown in phenol-red free DMEM/F12 medium supplemented with 5% horse serum, 20 ng/mL epidermal growth factor, 0.1  $\mu$ g/mL Cholera toxin, 10  $\mu$ g/mL insulin, 0.5  $\mu$ g/mL hydrocortisone, 1% penicillin/streptomycin at 37°C.

### Protein isolation and Western blotting

As mentioned previously (Bedi et al., 2015; Nagarajan et al., 2014), whole cell protein lysates were prepared from MCF7 and MCF10A by incubating the cells in Radioimmuno-precipitation buffer (RIPA buffer - 1% (v/v) NP-40, 0.5% sodium deoxycholate and 0.1% SDS in 1X PBS along with protease inhibitors: 1 mM Pefabloc, 1 ng/ $\mu$ L Aprotinin/Leupeptin, 10 mM  $\beta$ -glycerophosphate and 1 mM N-ethylmaleimide) for 10 minutes and scraping the cells if required. Samples were briefly sonicated to release the chromatin associated proteins. Samples were heated along with SDS loading dye by incubating them at 95°C for 5 -10 minutes. These samples were run in a SDS- Polyacrylamide Gel Electrophoresis (PAGE). Proteins were visualized by Western blotting with following antibodies and dilutions:  $\beta$ -actin, I-19, sc1616, HRP-conjugated, 1:5000, Santa Cruz; ER $\alpha$ , HC-20, sc-543, rabbit polyclonal, 1:1,000, Santa Cruz; H4K12ac, ab61238, rabbit polyclonal, 1:1000, abcam; H3, ab10799, mouse monoclonal, 1:5000, abcam.  $\beta$ -actin was used as loading control for ER $\alpha$  and histone H3 for H4K12ac. Quantification of proteins in

Western blot was done using Biorad Image Lab 5.2 software and H4K12ac was normalized with H3.

### ChIP-Seq, RNA-seq and raw data information

Chromatin immunoprecipitation of H4K12ac was performed as described previously (Nagarajan et al., 2014) using anti-acetyl-histone H4 (Lys12) (07-595; EMD Millipore) and negative control IgG (ab37415; abcam) with 10 min crosslinking with 1% formaldehyde. The following primers were used for ChIP-qPCR analyses: GREB1 TSS Forward - 5'-GCCAAATGGAAGAAGGACAG-3', Reverse - 5'-ACCACCTACCTCCAGTCACC-3'; CXCL12 TSS Forward - 5'-GCAGTGCGCTCCGGCCTTT-3', Reverse - 5'-CCTCACTGCAGACCGGGCCA-3'; XBP1 TSS Forward - 5'-ATCCCCAGCTCTGGTCATCT-3', Reverse- 5'-GCCCAGGGCTCTTTTCTGTA-3'; RPLP0 TSS Forward - 5'-CTTCGCGACCCTACTTAAAGG-3', Reverse - CAATCAGAAACCGCGGATAG-3'; GAPDH TSS Forward - 5'-CGGCTACTAGCGGTTTTACG-3', Reverse - 5'-AAGAAGATGCGGCTGACTGT-3'; hnRNPK adjacent to TSS Forward- 5'-TCCACGAGGTCCCTAGTTCC-3', reverse - 5'-GCCATTTCCCTGAGCGTGTA-3'.

ChIP-seq libraries were made using the NEBNext Ultra DNA library preparation kit according to the manufacturer's instructions (Nagarajan et al., 2014). The size range of the libraries was verified to be 250-600 bp using Bioanalyzer 2100. 75 bp single-ended tags were sequenced with single indexing using Illumina NextSeq 500 (XCelris Genomics, Ahmedabad, India). Previously published data for BRD4, H2Bub1 and ER $\alpha$  ChIP-seq as well as RNA-seq are available from the NCBI Gene Expression Omnibus (GEO) (GSE55921, GSE55922) (Nagarajan et al., 2014). Raw data for FOXA1, H3K4me3, H3K27me3 (Joseph et al., 2010), H3K27ac (Theodorou et al., 2013), RNAPII (Welboren et al., 2009), and GRO-seq (Hah et al., 2013) were downloaded from the European Nucleotide Archive. Normalization of RNA-sequencing read counts for each gene was performed using DESeq (Anders and Huber, 2010).

### Bioinformatic analyses

ChIP-seq reads were mapped to the human reference genome (UCSC HG19) using Bowtie (version 1.0.0) (Langmead et al., 2009). Sam files from Bowtie were



converted into bam files by SAMtools (Li et al., 2009). DeepTools (Ramírez et al., 2014) was used to create bigwigs by normalizing the ChIP-seq sample with the input samples of each cell line and obtaining the ratio of the reads using bamCompare function. Normalization was done using read counts of each ChIP-seq sample. Average density was calculated using computeMatrix function in deepTools surrounding TSS (plus 3 kb) or ERE ( $\pm 1.5$  kb). The Heatmapper function from deepTools was used to create heatmaps and average profiles. TSS and gene body coordinates for hg19 were obtained from UCSC Table Browser (Karolchik et al., 2004). Estrogen-upregulated, downregulated and BRD4 siRNA downregulated and BRD4-independent genes were categorized from our previously published RNA seq datasets (Nagarajan et al., 2014). Distal EREs or H3K27ac-positive regions were obtained from ER $\alpha$  and H3K27ac binding sites respectively which were not within gene bodies and regions 5 kb upstream or downstream of them. TSS and 3 kb downstream regions were used for TSS-based correlation plots and 1.5 kb up- and downstream of distal EREs for distal ERE-based correlation plots. Correlation plots were made using the bamCorrelate function in deepTools. Groups based on H4K12ac signals were determined using k-means clustering in heatmapper function of deepTools. Molecular signature database (MSigDB) (Liberzon et al., 2011) pathways whose target genes are enriched for BRD4 or specific histone modifications were identified using the Genomic Regions Enrichment of Annotations Tool (GREAT) (McLean et al., 2010). Boxplots and scatterplots were made using R for statistical computing. The Mann-Whitney test was used to calculate the statistical significance for boxplots. Pearson correlation coefficient values were calculated using R for scatter plots and p-values were calculated using two-tailed probability test.

## Accession Numbers

The NCBI Gene Expression Omnibus accession number for H4K12ac ChIP-seq data reported in this paper is GSE65886.

## Conflict of Interest

The authors declare no conflict of interest.

## Acknowledgements

The authors acknowledge W. Xie, Z. Najafova and T. Hossan for scientific discussions and suggestions. We would also like to thank U. Bedi and Z. Najafova for providing raw data for sequencing of H3K27ac in MCF10A cells. This work was funded by the German Academic Exchange Service (DAAD) (to S.N.) and the Deutsche Krebshilfe (109088 and 111600 to S.A.J.).

## 2.2.1. Supplementary information

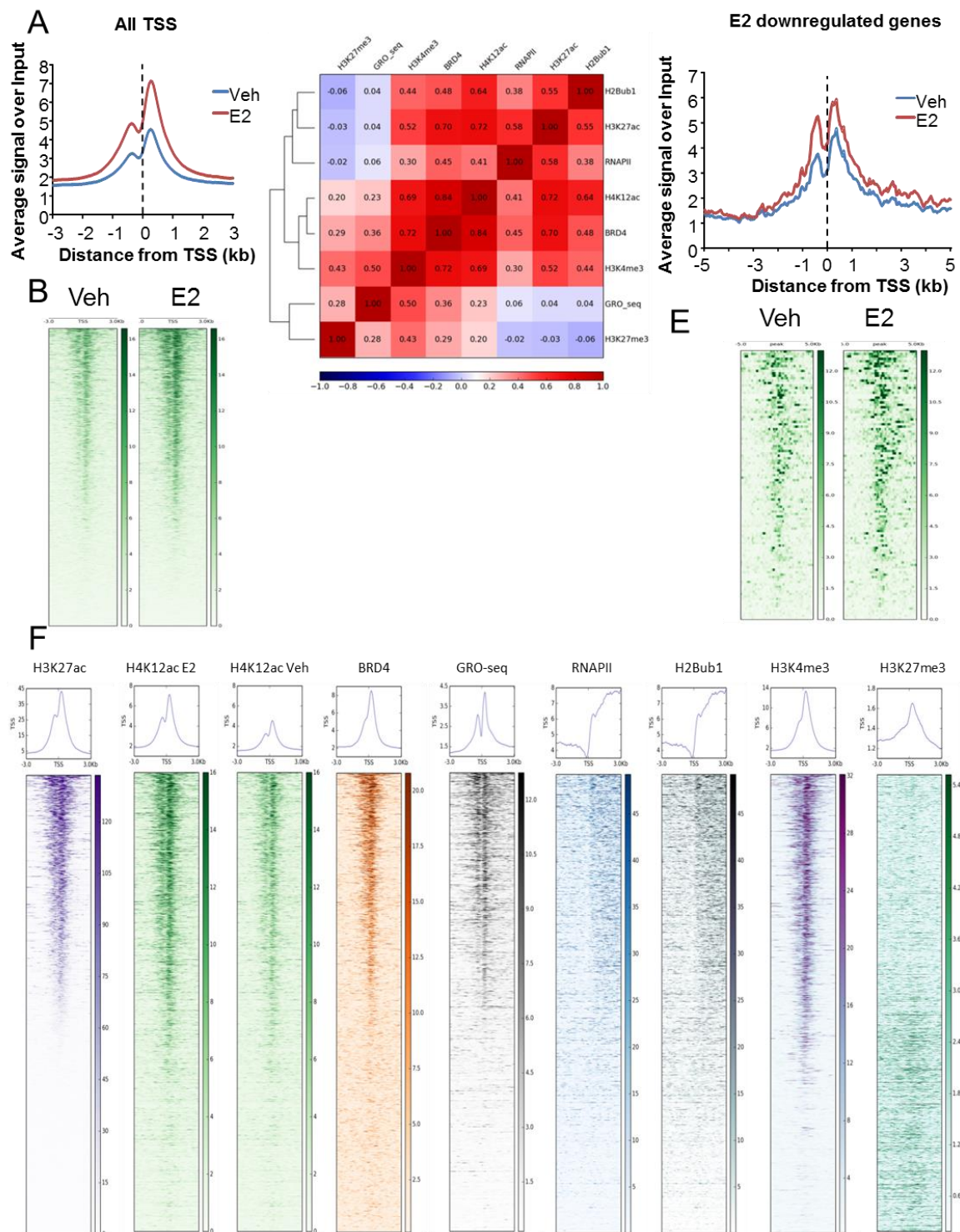


**Figure 2.II.S1.** (A) Average genomic binding profiles of H4K12ac around TSS and 3 kb upstream and downstream of all the genes under vehicle (Veh) and estrogen-treated (E2) conditions. The X-axis shows the distance from the TSS of the genes in kilobase pairs. TSS is indicated by a black dotted line. (B) Heatmaps showing genomic binding profiles of H4K12ac around TSS and 3 kb upstream and downstream of all genes under vehicle (Veh) and estrogen-treated (E2) conditions. Center of the

heatmap represents TSS. Color key of the heatmaps is shown on the side. (C) Correlation plot showing the heatmap with the Pearson's correlation coefficient values for H4K12ac, BRD4, H3K27ac, H3K4me3, H2Bub1, GRO-seq, RNAPII and H3K27me3 on TSS and 3 kb downstream region of all genes. Color key of the heatmap is shown at the bottom of the plot. (D) Average genomic binding profiles of H4K12ac around TSS and 3 kb upstream and downstream of estrogen-downregulated genes under vehicle (Veh) and estrogen-treated (E2) conditions. The X-axis shows the distance from the TSS of the genes in kilobase pairs. TSS is indicated by a black dotted line. (E) Heatmaps showing genomic binding profiles of H4K12ac around TSS and 3 kb upstream and downstream of all genes under vehicle (Veh) and estrogen-treated (E2) conditions. Center of the heatmap represents TSS. Color key of the heatmaps is shown on the side. (F) Heatmaps showing genomic binding profiles of H3K27ac, H4K12ac with estrogen treatment (H4K12ac E2) and without estrogen treatment (H4K12ac Veh), BRD4, nascent RNA transcription (GRO-seq), RNAPII, H2Bub1, H3K4me3 and H3K27me3 around TSS and 3 kb upstream and downstream of estrogen-induced genes. Density of the signals is arranged according to average H3K27ac signals from high to low. Center of the heatmap represents TSS. Color key of the heatmaps is shown at their side.

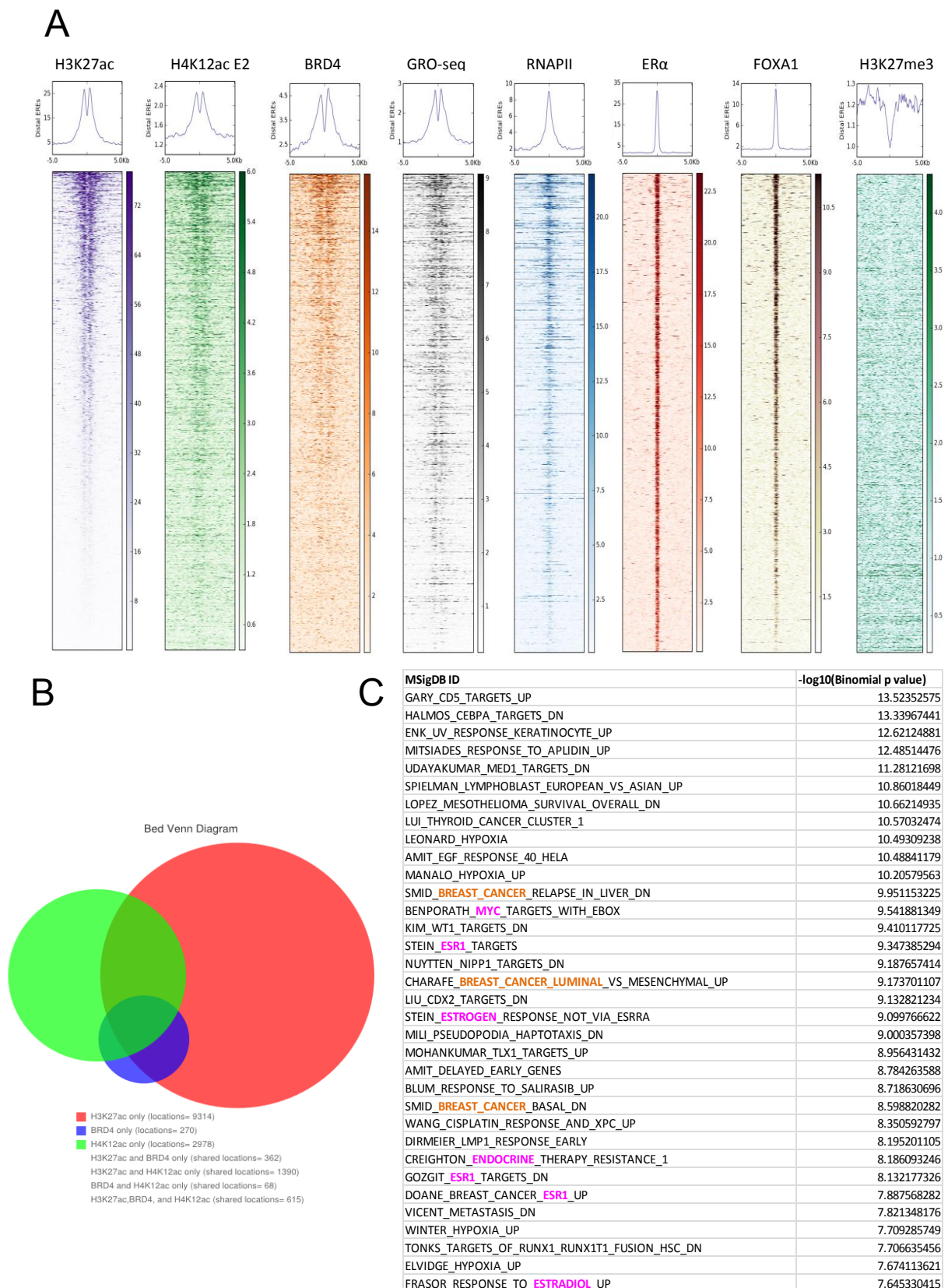


**Figure 2.II.S2:** (A) Heatmaps showing genomic binding profiles of H3K27ac, H4K12ac with estrogen treatment (H4K12ac E2) and without estrogen treatment (H4K12ac Veh), BRD4, nascent RNA

transcription (GRO-seq), RNAPII, ER $\alpha$ , FOXA1 and H3K27me3 around distal EREs and 5 kb upstream and downstream with all estrogen-treated (E2) conditions. Density of the signals is arranged according to H3K27ac signals from high to low. Center of the heatmap represents center of the distal ERE region. Color key of the heatmaps is shown on the side. (B) Venn diagram showing the overlap of distal binding regions of H3K27ac (red), H4K12ac (green) and BRD4 (blue). (C) GREAT analyses on distal regions which overlap with H3K27ac, H4K12ac and BRD4 occupancy. The names of the Molecular signature database (MSigDB) pathways are denoted with their  $-\log_{10}$  binomial p-values. Estrogen-specific pathways are highlighted in pink and other breast cancer-related pathways in brown.

### E2 upregulated genes

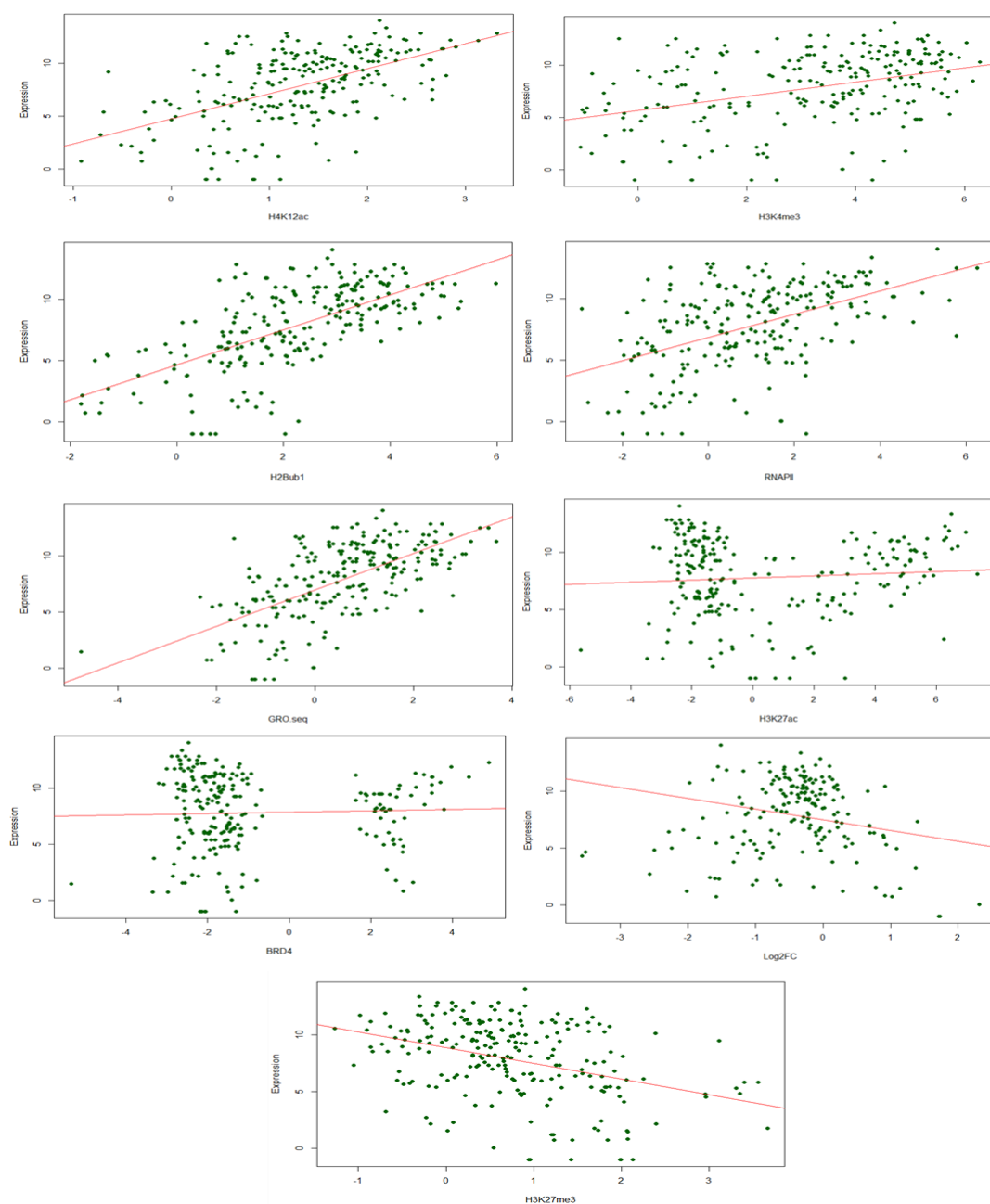


**Figure 2.II.S3.** Scatterplots showing the relationship between various ChIP-seq signals (H4K12ac, H3K4me3, BRD4, H2Bub1, RNAPII, GRO-seq, H3K27ac, H3K27me3, logarithmic fold changes of siBRD4 compared to siCont (Log2FC)) and absolute gene expression in logarithmic values for estrogen upregulated genes. Each dot in the plot represents a single gene. Red line indicates the correlation.

### All genes

	GRO.seq	H2Bub1	H3K4me3	RNAPII	H3K27me3	BRD4	H3K27ac	H4K12ac	Expression	Log2FC
GRO.seq	1	0.737716	0.607588	0.740766	-0.16243	0.109476	0.29921	0.59734	0.573008	-0.07581
H2Bub1	0.737716	1	0.604958	0.617574	-0.02786	0.093484	0.262579	0.69864	0.600286	-0.08857
H3K4me3	0.607588	0.604958	1	0.623692	0.181553	0.085577	0.288095	0.749786	0.521682	-0.12752
RNAPII	0.740766	0.617574	0.623692	1	-0.165	0.018243	0.206677	0.635878	0.553889	-0.09979
H3K27me3	-0.16243	-0.02786	0.181553	-0.165	1	0.074421	-0.01146	0.069792	-0.30611	0.010353
BRD4	0.109476	0.093484	0.085577	0.018243	0.074421	1	0.675574	0.036245	0.011641	-0.01329
H3K27ac	0.29921	0.262579	0.288095	0.206677	-0.01146	0.675574	1	0.224662	0.183565	-0.04418
H4K12ac	0.59734	0.69864	0.749786	0.635878	0.069792	0.036245	0.224662	1	0.497749	-0.09188
Expression	0.573008	0.600286	0.521682	0.553889	-0.30611	0.011641	0.183565	0.497749	1	-0.21114
Log2FC	-0.07581	-0.08857	-0.12752	-0.09979	0.010353	-0.01329	-0.04418	-0.09188	-0.21114	1

### E2 regulated genes

	GRO.seq	H2Bub1	H3K4me3	RNAPII	H3K27me3	BRD4	H3K27ac	H4K12ac	Expression	Log2FC
GRO.seq	1	0.677545	0.536808	0.703225	-0.22096	0.040218	0.112583	0.510785	0.629388	-0.09888
H2Bub1	0.677545	1	0.555719	0.496261	-0.05379	0.136138	0.189556	0.686092	0.640592	-0.02342
H3K4me3	0.536808	0.555719	1	0.572254	0.242915	0.018732	0.233546	0.721774	0.375121	0.029958
RNAPII	0.703225	0.496261	0.572254	1	-0.19608	-0.0191	0.091506	0.540041	0.490185	-0.0855
H3K27me3	-0.22096	-0.05379	0.242915	-0.19608	1	0.050236	0.040627	0.068655	-0.36606	0.081474
BRD4	0.040218	0.136138	0.018732	-0.0191	0.050236	1	0.591603	0.008577	0.038346	-0.21605
H3K27ac	0.112583	0.189556	0.233546	0.091506	0.040627	0.591603	1	0.161019	0.07871	-0.04206
H4K12ac	0.510785	0.686092	0.721774	0.540041	0.068655	0.008577	0.161019	1	0.540699	-0.10892
Expression	0.629388	0.640592	0.375121	0.490185	-0.36606	0.038346	0.07871	0.540699	1	-0.24406
Log2FC	-0.09888	-0.02342	0.029958	-0.0855	0.081474	-0.21605	-0.04206	-0.10892	-0.24406	1

**Figure 2.II.S4.** Pearson correlation coefficient (R) values were shown in tables representing the relationship between various ChIP-seq signals (H4K12ac, H3K4me3, BRD4, H2Bub1, RNAPII, GRO-seq, H3K27ac, H3K27me3, logarithmic fold changes of siBRD4 compared to siCont (Log2FC)) and absolute gene expression for all genes and estrogen-induced genes.

### 3. Discussion

Efficient transcription requires a complex integration of several chromatin-associated factors, histone modifications and transcriptional machinery in order to facilitate its temporal and spatial regulation. Several transcription factors have been shown to be important in stimulus-dependent transcription and these factors were observed to be recruited by specific stimuli. The recruitment of transcription factors determines cell type-specific function. The binding of these factors can also regulate or be regulated by the presence of histone marks. The tight cross-regulation of the histone marks may coordinate active transcription in response to various signaling pathways and inducible gene expression systems. Thus the histone marks and transcription factors can efficiently modulate stimulus-associated transcription.

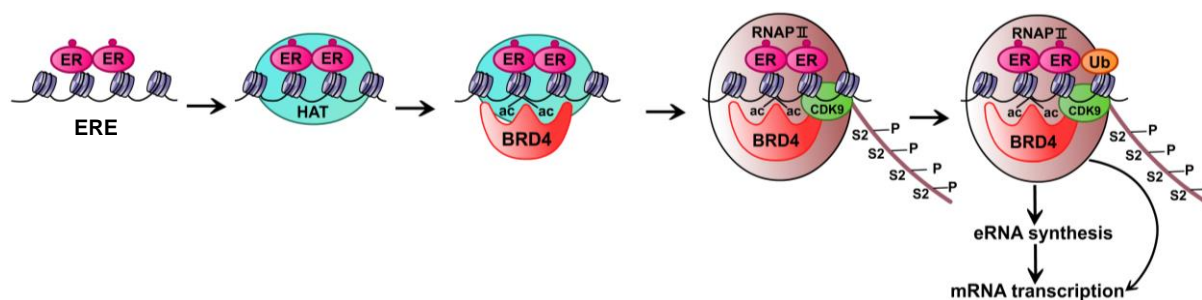


**Figure 3.1. Mechanism of histone acetylation and BRD4 in regulating estrogen-induced transcription.** Binding of ER $\alpha$  to EREs recruits HATs to promote BRD4 binding to the chromatin. This activates CDK9 to phosphorylate RNAPII at Ser2 residues and subsequently histone monoubiquitination. ER – ER $\alpha$ ; HAT - histone acetyltransferase; ac - histone acetylation; S2P - RNAPII p-Ser2; Ub - H2Bub1.

In our study, we demonstrated the importance and the association of H4K12ac and BRD4 in regulating estrogen-dependent transcription (Figure 3.1) (Nagarajan et al., 2014, 2015). Notably, we attempted to elucidate the mechanisms stimulated by the association of H4K12ac and BRD4 in estrogen induction. According to our model, estrogen treatment induces the ER $\alpha$ -dependent recruitment of histone acetyltransferases (HATs), which promote H4K12 acetylation and subsequent BRD4 recruitment to promoters and conserved EREs, especially on ER $\alpha$ -stimulated genes. This further leads to the estrogen-induced elongation-



dependent phosphorylation of RNAPII and monoubiquitination of H2B across gene bodies. More importantly, H4K12ac and BRD4 associate with the occupancy of ER $\alpha$ , FOXA1, RNAPII and H3K27ac on active distal enhancers and regulate the production of eRNAs from these regions. Our findings significantly support the recent evidences showing the importance of BRD4 in controlling the nuclear hormone-dependent transcriptional function in castration-resistant prostate cancer and tamoxifen-resistant breast cancer which were published while our manuscript was under review (Asangani et al., 2014; Feng et al., 2014). Deeper analyses of these mechanisms underlying the regulation of estrogen-dependent transcription improve our understanding of transcriptional machinery involved in stimulus-induced transcription and the cell-type specific role of histone acetylation and BRD4 in promoting signal-induced transcription.

### **3.1. Mechanisms of H4K12ac and BRD4 in regulating transcription**

#### **3.1.1. The BRD4 , CDK9 and RNF40 axis in estrogen-induced transcription**

Our studies identified a novel association of H4K12ac and BRD4 in regulating RNAPII recruitment and/or phosphorylation and H2B monoubiquitination during estrogen-induced transcription. Hence this supports a tight coupling of histone acetylation, BRD4 recruitment, P-TEFb, RNF20/40 and H2Bub1 in a coordinated axis in the transcription of estrogen-stimulated genes. This hierarchical pathway is partially shown to be associated with several signal-induced transcriptional mechanisms or cellular differentiation (Ai et al., 2011; Karpiuk et al., 2012; Lamoureux et al., 2014). However, its complete association is mostly unknown in other contexts. The established paradigm in our study supports the association of P-TEFb and H2Bub1 in regulating the transcriptional outcome during estrogen stimulation (Wittmann et al., 2005; Ogba et al., 2008; Prenzel et al., 2011; Mitra et al., 2012; Sengupta et al., 2014). Moreover, our results further support a role of BRD4 in promoting the cell-fate specific decisions or processes via regulating transcriptional pathways (Chiang, 2014; Liu et al., 2014; Micco et al., 2014; Xu and Vakoc, 2014).

CDK9 phosphorylates RNAPII at Ser2 residues and facilitates transcription elongation. The phosphorylated RNAPII serves as a platform for the recruitment of

the WAC/RNF20/40 complex and leads to H2B monoubiquitination across gene bodies. Decreased RNAPII phosphorylation and H2B monoubiquitination following BRD4 depletion/inhibition and the positive correlation of H4K12ac with H2Bub1 illustrate H4K12ac and BRD4 as upstream regulators of CDK9- and RNF20/40-associated transcriptional elongation and further confirms their importance in the involvement of the H4K12ac – BRD4 – P-TEFb – RNF40 – H2Bub1 model. Furthermore, this supports the role of transcriptional elongation in mediating estrogen-regulated transcription (Aiyar et al., 2004; Kininis et al., 2009). Interestingly, our study also uncovers an important role of BRD4 in the recruitment of RNAPII on enhancers and histone monoubiquitination on the gene bodies which exhibit *de novo* recruitment of RNAPII upon estrogen treatment.

A previous study from our group showed that RNF40 depletion stimulates estrogen-independent growth by activating EGFR-dependent kinase pathways (Prenzel et al., 2011). Moreover, overexpression of Ubiquitin-Specific Protease-22 (USP22), which possesses H2B deubiquitinase activity, was also shown to promote androgen-dependent as well as androgen-independent growth in castration-resistant prostate cancer cell lines by facilitating AR expression and its activity and USP22 is also highly expressed in castration-resistant prostate cancer (Schrecengost et al., 2014). Interestingly, our work highlights the involvement of BRD4 in ER $\alpha$ -dependent growth *in vitro* and *in vivo* (Figure 2.1.2). Altogether these suggest a strong connection between BRD4 and H2B ubiquitination in determining estrogen dependency by the cells.

An important role of CDK9 and Cyclin T1 was shown to be important for estrogen-regulated gene expression (Wittmann et al., 2005; Sharp et al., 2006; Mitra et al., 2012). This supports a mechanism whereby BRD4 could potentially associate with and activate a P-TEFb-ER $\alpha$  complex and thus promote ER $\alpha$ -associated transcriptional pathways. An examination of the amino acid sequence of BRD4 shows that BRD4 contains a possible estrogen Receptor Interaction Domain, LXXLL motif (LQYLL from 63-67 amino acid residues) within its first bromodomain (Results unpublished). Consistently, a weak BRD4-ER $\alpha$  interaction was reported using biochemical overexpression and immunoprecipitation analyses (Wu et al., 2013). Moreover, reduced occupancy of H4K12ac in ER-negative cell lines and a rapid

decrease of H4K12ac following treatment with a pure ER $\alpha$ -antagonist (Figure 2.II.5) strongly suggests a coordinated functional interaction of H4K12ac and physical interaction between BRD4 with ER $\alpha$ . Altogether these results support a direct or indirect association/interaction of H4K12ac-BRD4-CDK9 with ER $\alpha$  to elicit their effect on the estrogen-specific gene expression.

### **3.1.2. BRD4 recruitment is associated with histone acetylation downstream of initial active enhancer events**

Global histone acetylation was previously shown to correlate with the tumor phenotype and survival in breast cancer (Elsheikh et al., 2009). BRD4 is tightly associated with binding to acetylated chromatin via bromodomains. Several studies show that BRD4 specifically recognizes histone acetylation at H4K5, 8, 12 and 16 (Chiang, 2009; Umehara et al., 2010; Filippakopoulos et al., 2012; Zhang et al., 2012a). Structural and biochemical analyses demonstrated the differential binding of BD1 and BD2 of BRD4 to histone acetylation (Filippakopoulos et al., 2012). Interestingly, H4K12ac is bound by both the bromodomains. Even though the mechanistic link between H4K12ac and BRD4 is well established, their functional relevance was poorly known. Our study shows a clear correlation of H4K12ac and BRD4 occupancy on estrogen-dependent promoters as well as enhancers to regulate target gene expression.

H4K12ac was previously shown to be dynamically regulated upon estrogen treatment on various estrogen-induced genes (Eeckhoute et al., 2007; Lupien et al., 2009, 2010). This mark can be catalyzed by several HATs including p300 and CBP which are considered to be important coactivators of ER $\alpha$ -regulated transcription. Furthermore, signal-induced H4K12ac has been implicated in the enhancer activity along with H4K16ac (Zippo et al., 2009). Our findings further validate the importance of H4K12ac in estrogen-regulated gene induction via occupying enhancers and suggest a possibility of a general function in stimulus-dependent transcriptional regulation. Further analyses of the association of H4K12ac with RNAPII recruitment and H2Bub1 reveal a potential role of H4K12ac in regulating the transcriptional elongation by associating with BRD4.

Even though BRD4 preferentially binds to H4 acetylated residues, the strong correlation of BRD4 and H4K12ac with H3K27ac and increased enrichment of both H4K12ac and H3K27ac after estrogen treatment infers a possible functional cross-talk between H3K27ac and H4K12ac in promoting estrogen-dependent transcription. Our studies show that BRD4 and H4K12ac correlate with H3K27ac on both promoters and enhancers. This supports the previously reported link between BRD4 and H3K27ac in facilitating gene transcriptional activity (Zhang et al., 2012a). Consistent with the importance of H4K12ac in regulating the recruitment of BRD4 rather than H3K27ac, our results show that BRD4 occupancy is more closely correlated with H4K12ac than H3K27ac (Figure 2.II.1-2). Moreover, the increased occupancy of H3K27ac after estrogen treatment is not affected by the inhibition of BRD4 binding which supports the fact that BRD4 binding occurs downstream of histone acetylation events. More importantly, ER $\alpha$  binding is more closely associated with H4K12ac and BRD4 than with H3K27ac. This may further support an essential function of BRD4 and H4K12ac in regulating the enhancer activity in estrogen-responsive systems.

### **3.1.3. H4K12ac and BRD4 correlate with enhancer activity and eRNA production**

Apart from the involvement of BRD4 and CDK9 in transcriptional elongation, these proteins have also been shown to be associated with enhancer activity (Hah et al., 2013; Lovén et al., 2013). H4K12ac occupancy at EREs was also shown of both conventional ER $\alpha$  binding sites as well as for tamoxifen-resistant binding (Lupien et al., 2009, 2010). Our results show that H4K12ac and BRD4 are essential for promoting the enhancer activity of EREs. More importantly, we show that BRD4 depletion or inhibition results in decreased eRNA transcription particularly from ER $\alpha$ /FOXA1-bound EREs which are enriched for H4K12ac as well as RNAPII and BRD4. This supports a previously reported role of CDK9 and BRD4 inhibition in controlling the transcription of estrogen-induced and active macrophage associated eRNAs respectively (Hah et al., 2013; Kaikkonen et al., 2013). Our results further provide a mechanistic insight into the regulation of enhancer activity by histone acetylation and BRD4. Interestingly, another study showed that inhibition of eRNA production affects the transcriptional initiation-associated RNAPII phosphorylation

(RNAPII P<sup>Ser5</sup>) and MED1 occupancy on androgen receptor-bound enhancers (Hsieh et al., 2014). Given the tight association of the Mediator complex and BRD4 (Wu and Chiang, 2007; Chiang, 2009; Lovén et al., 2013), this study supports our data and suggests that BRD4 plays a central role in regulating nuclear hormone receptor-dependent eRNA production. The observed BRD4-specific regulation of eRNA synthesis and polymerase recruitment on ER $\alpha$ -bound enhancers was also further verified by another recent study which shows that BRD4 is required for the elongation of eRNA transcripts from the enhancers with hyperacetylated nucleosomes (Kanno et al., 2014). Overall H4K12ac and BRD4 can very likely regulate genome-wide production of enhancer-derived transcripts and facilitate the enhancer activity to help in the determination of cell-specific functions.

A recent study elucidated eRNA transcription as a very early response following induction with various stimuli (Arner et al., 2015). However, our studies show that BRD4 inhibition does not affect the early chromatin-associated events of enhancer activation, but inhibit estrogen-induced eRNA transcription. Another study shows that establishment of an enhancer (ie., H3K4me2 occupancy) is regulated at the level of elongation of eRNA transcription by CDK9 and BRD4 inhibition, but inhibition of eRNA transcription did not affect H3K4me2 deposition (Kaikkonen et al., 2013). This suggests a hierarchical mechanism of BRD4 and CDK9 activity in regulating eRNA transcription which could be an intermediate event which must be further elucidated to achieve a clear understanding of eRNA-driven establishment of enhancers and regulation of enhancer activity.

#### **3.1.4. BRD4 recruits RNAPII and can release pausing of RNAPII**

Previous evidences described the coordinated function of BRD4 and CDK9 in regulating the phosphorylation events of RNAPII across gene bodies in order to control and coordinate transcriptional elongation with cotranscriptional processes (Zhang et al., 2012a; Patel et al., 2013). Consistently, our results uncover a likely role of BRD4 in the release of paused polymerase and efficient elongation in the context of ER $\alpha$ -dependent transcription. As described before, estrogen-regulated transcription is controlled by the phosphorylation of RNAPII and NELF complex proteins (Aiyar et al., 2004; Kininis et al., 2009). However, the regulatory mechanisms controlling the coordinated recruitment of RNAPII and release of

pausing on enhancers are poorly understood. We showed that inhibition of enhancer-associated BRD4 binding affects RNAPII phosphorylation on individual EREs (Figure 2.1.4K). This was also supported by recent studies which show that BRD4 association on enhancers is involved in the transcriptional pause release of polymerase on the proximal promoter regions as well as enhancers and helps in the efficient transcription of mRNAs and eRNAs (Liu et al., 2013; Kanno et al., 2014). In addition to the effect on elongation-specific phosphorylation of RNAPII on enhancers, our studies surprisingly show that the recruitment of RNAPII to a subset of EREs is affected by BRD4 inhibition which further affects eRNA production at these distal regions (Figure 2.1.4J-L). Altogether, these findings suggest a novel mechanism where apart from releasing poised polymerase from the proximal promoters, BRD4 is involved in both the recruitment of RNAPII as well as its release from transcriptional pausing on enhancers and thereby promotes elongation of eRNA transcripts following estrogen stimulation. Considering the absence of RNAPII phosphorylation at Ser2 residues (Koch et al., 2011; Lam et al., 2014) and H2Bub1 on enhancers which was observed in our study (unpublished results), these findings also proposes a unique process of transcriptional elongation which can likely be involved in the activation of enhancers.

### **3.1.5. BRD4 acts downstream of initial enhancer activation events**

ER $\alpha$ -dependent transcription is influenced by the occupancy of active enhancer marks like H3K27ac and recruitment of several transcription factors and cofactors like FOXA1, ER $\alpha$ , p300/CBP, Cohesin complex, etc., on the corresponding EREs upon estrogen treatment. These events can happen very early before or during estrogen treatment and play an essential role in promoting enhancer-driven transcription probably by mediating enhancer-promoter interactions. Interestingly, our report shows that BRD4 is not required for these events. This suggests a downstream function of BRD4 in regulating ER $\alpha$ -dependent transcriptional pathways which does not affect the initial events which are important for epigenetically activating enhancers.

An important mechanism by which ER $\alpha$  promotes transcription via enhancers is that it nucleates changes in higher order chromatin structure and brings enhancers and promoter regions into proximity with one another (Fullwood et al., 2009; Schmidt

et al., 2010). BRD4 and CDK9 were shown to be associated with Mediator complex proteins suggesting an important role in long range chromosomal interactions (Wu and Chiang, 2007; Chiang, 2009; Donner et al., 2010; Lovén et al., 2013; Allen and Taatjes, 2015). The CDK8 subunit of the Mediator complex interacts with CDK9 and promotes the recruitment of P-TEFb to facilitate RNAPII phosphorylation (Donner et al., 2010; Ebmeier and Taatjes, 2010; Galbraith et al., 2013; Allen and Taatjes, 2015). Surprisingly, on a subset of ER $\alpha$ - and H3K27ac-occupied EREs, BRD4 inhibition does not affect the estrogen-induced occupancy of the Cohesin complex subunit RAD21. This is consistent with another study which utilized 3C analyses to show that CDK9 inhibition does not impair the estrogen-induced chromosomal looping and other initiation events associated with eRNA-producing enhancers (Hah et al., 2013). Moreover, proteasomal inhibition using Bortezomib decreased estrogen-regulated transcription, whereas it had no effect on estrogen-induced looping events (Prenzel et al., 2011). All these studies further validate our data showing that BRD4 binding occurs downstream of early events of enhancer activation and probably does not affect chromosomal looping despite its association with the Mediator complex.

### 3.1.6. BRD4 can facilitate chromatin opening

A significant correlation of BRD4 with DNase hypersensitive sites occupying estrogen-responsive gene promoters and enhancers opens the possibility that BRD4 could be involved in the opening of the chromatin (Figure 2.1.3E, 2.1.4E). Our studies reveal a potential role of BRD4 in bringing the chromatin to an elongation-favorable open state by promoting histone monoubiquitination across gene bodies in order to facilitate transcription (Figure 2.1.3C). Furthermore, Formaldehyde-Assisted Isolation of Regulatory Elements (FAIRE) analyses on MCF7 cells revealed that BRD4 inhibition results in less frequency of open chromatin on ER $\alpha$ -bound enhancers (unpublished results). This further substantiates the role of BRD4 in regulating the opening of chromatin.

Another possible mechanism which could be involved in the BRD4 associated opening of chromatin is the interaction of BRD4 with the SWI/SNF chromatin remodeling complex and their co-occupancy on enhancers (Shi et al., 2013). The SWI/SNF complex promotes the opening of chromatin by its ATPase subunits.

Binding of the SWI/SNF complex to acetylated chromatin may be coordinated by BRD4 binding because both of these proteins contain bromodomains and H4K12ac may influence the binding of SWI/SNF to the chromatin. Given the important role of SWI/SNF subunits in estrogen-stimulated transcription and their association with H2B monoubiquitination (García-Pedrero et al., 2006; Green and Carroll, 2007; Shema-Yaacoby et al., 2013), BRD4 and the SWI/SNF complex may coordinate with histone acetylation and monoubiquitination to promote chromatin remodeling and estrogen-regulated transcription.

### **3.1.7. Histone acetylation and BRD4 can coordinate transcriptional assembly turnover**

Estrogen-regulated transcription involves rapid and dynamic changes in the assembly of transcriptional machinery in order to regulate the temporal transcriptional activation in estrogen stimulation (Shang et al., 2000; Métivier et al., 2003, 2006; Green and Carroll, 2007). This requires the coordinated activity of an intricate network of complex association and disassociation of transcriptional coactivators, chromatin remodelers and histone marks (Voss and Hager, 2014). Notably, our data uncover a low occupancy of H4K12ac, RNAPII and H2Bub1 adjacent to the gene promoters which are dependent upon BRD4 compared to the genes which do not require BRD4 for their expression (Figure 2.II.3). This may suggest that genes which display rapid regulation of gene expression dependent upon BRD4 have lower occupancy of active marks which may coordinate a faster response. This may enable a dynamic mechanism of transcriptional assembly and its turnover which could be needed for the fast and precise fine-tuning in the temporal transcriptional activation upon estrogen response. Moreover, the rapid reduction of H4K12ac after ER $\alpha$  antagonist treatment further supports the dynamic nature of H4K12ac and BRD4 and their role in determining the extent and the level of increased gene expression.

A complex of proteins exhibiting transcriptionally contradictory functions would be ideally suited to facilitate cyclical activity during transcription. An example is the Spt-Ada-Gcn5 acetyltransferase (SAGA) complex which contains both acetylating activity in GCN5 as well as deubiquitinating activity of H2B via the USP22 subunit (Koutelou et al., 2010). Similarly, the SWI/SNF complex binds to acetylated



chromatin and can also associate with an NCOR-HDAC complex, although this connection is not well-understood (Underhill et al., 2000). Due to their possession of oppositely functioning subunits, these complexes can be involved in the temporal and dynamic regulation of induced gene activity. This effect may help to enable a rapid response to a decreased presence of the activating signal such that when the signal is no longer present, the deubiquitination and deacetylation would enable a pause in the expression by stimulating the cycling of the epigenetic status of the gene. Surprisingly, H2B ubiquitination and deubiquitination may be coordinated during gene activation such that both are required for the activation of some genes (Johnsen, 2012). Consistently, an earlier doctoral student in the Johnsen group demonstrated that depletion of either RNF40 or USP22 elicits a similar phenotype in mammary epithelial cells *in vivo* and *in vitro* (Bedi, 2015 Dissertation). This supports the necessity of addition or removal of active transcriptional marks or factors for the rapid turnover to maintain the subsequent rounds of transcription upon dynamic signaling. Thus, these complexes can coordinate with H4K12ac and H2Bub1 due to their previously studied physical and functional interactions and could be commonly involved in various scenarios in order to control the dynamic nature of gene transcription (Johnsen, 2012; Shema-Yaacoby et al., 2013).

### **3.2. Targeting histone acetylation and BRD4 in the treatment of breast cancer**

Overall our studies describe a potential important role of H4K12ac and BRD4 in coordinating various chromatin-associated during estrogen-induced transcription. Deregulation of these mechanisms results in altered transcriptional responses and control the biological effects of various signaling pathways. BRD4 activity has been implicated in the development of various diseases, most importantly cancer (Zuber et al., 2011; Herrmann et al., 2012; Lockwood et al., 2012; Chapuy et al., 2013; Asangani et al., 2014; Bhadury et al., 2014; Feng et al., 2014; Fiskus et al., 2014). A deeper understanding of the association of histone acetylation and BRD4 in transcriptional regulation could provide a potential rationale for utilizing BRD4 or HAT inhibitors as specific therapeutic targets for various cancers. Given the recent availability of various specific inhibitors of BRD4, such an approach may represent a realistic way to reverse disease-associated transcriptional dysregulation (Figure 3.2).

Therapeutic approach of using BRD4 inhibition as a possible therapeutic approach is supported by the fact that some BRD4 inhibitors have already entered clinical trials. OTX015 is currently in phase 1B trial for advanced solid tumors (Clinicaltrials.gov Identifier: NCT02259114) and in phase 1-associated dose finding study against hematological malignancies (NCT01713582). IBET-762 is in phase 1 trials for NUT-midline carcinoma (NCT01587703) and relapsed, refractory hematologic malignancies (NCT01943851). In another context, RVX-208 successfully completed phase 2 trials against diabetes, coronary artery disease, atherosclerosis and dyslipidemia (NCT01728467, NCT01058018 and NCT00768274). Based on the early use of these inhibitors in clinical trials, our studies utilizing BRD4 inhibition as a strategy to control the estrogen-dependent growth in breast cancer cells *in vitro* and uterine growth *in vivo* may provide a foundation for its use in breast cancer patients (Figure 2.1.2). By developing bromodomain-specific inhibitors, recent evidences demonstrate different functions of BD1 and BD2 of BET family of proteins (Picaud et al., 2013b). The acetylation binding pattern of each bromodomain was also recently shown to be unique for several bromodomain-containing proteins (Filippakopoulos et al., 2012). Thus, understanding the possible distinct functions of different bromodomains in the context of estrogen-dependent transcriptional pathway may further improve the specificity and efficacy of BET inhibitor-based therapeutic approaches.

Similar to the growth inhibitory role of BRD4 inhibition in regulating ER $\alpha$ -dependent transcription in tamoxifen-resistant breast cancers (Feng et al., 2014), another recent study observed the efficient inhibition of proliferation by JQ1 using *in vitro* and *in vivo* models of everolimus (mTOR inhibitor which inhibits estrogen independent growth)-resistant ER-positive breast cancers (Bihani et al., 2015). Moreover, another study reported an interaction of BRD4 with diacetylated TWIST, a transcriptional factor involved in epithelial-to-mesenchymal transition and proposed to play an important role in tumor metastasis (Yang et al., 2004), thereby providing a rationale and independent mechanism for targeting BRD4 in basal-like breast cancers (Shi et al., 2014, 2015).

Differential acetylation pattern on enhancers likely determines cell-specific transcription patterns. Apart from the established role of H3K27ac in estrogen-

induced transcription, our study uncovers the role of H4K12ac in determining estrogen-dependent enhancers. Considering the differential association of acetylation marks with different bromodomain-containing proteins (Filippakopoulos et al., 2012), our study further supports a specific strategy of targeting various diseases. However, using HDAC inhibitors may inappropriately hyperacetylate and activate enhancers which should not be active and thereby lead to adverse effects. A deeper understanding of the specific association of histone acetylation with enhancers and the effect of HDAC inhibition in these cases would be therefore necessary before utilizing HDAC inhibitors for treating ER $\alpha$ -positive breast cancer patients. Our attempt to study a single acetylation mark in a cell-specific function which can be deregulated in disease furthers our knowledge about the role of specific histone acetylation events in facilitating cell-type specific transcriptional programs.

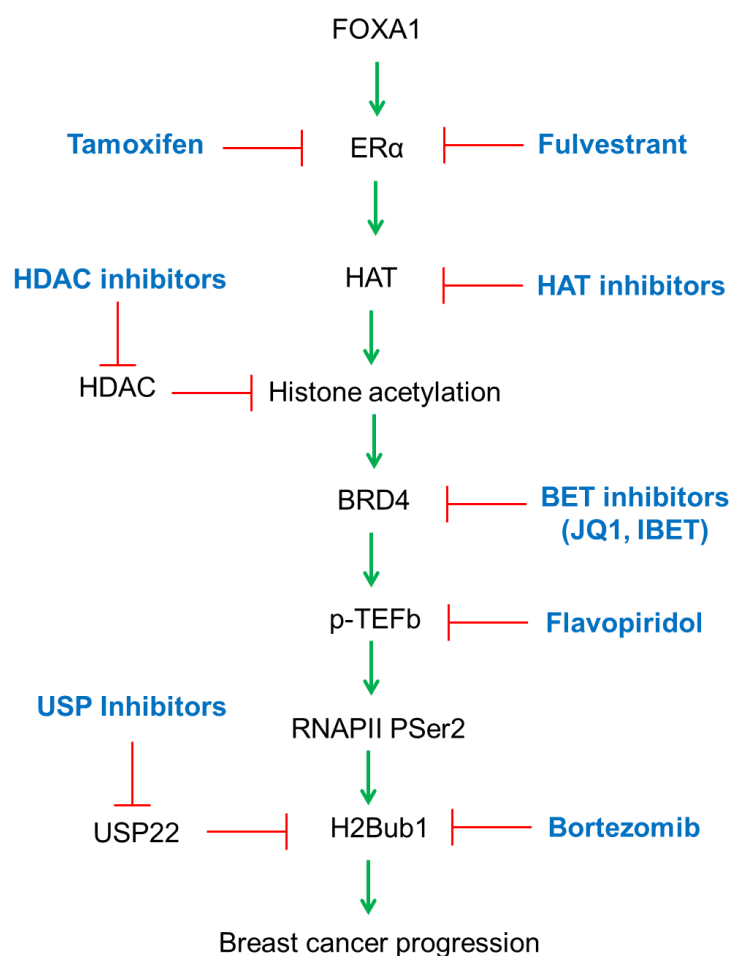


**Figure 3.2. Therapeutic targeting of the ER $\alpha$ -regulated transcriptional pathway by the inhibitors.** Green arrows show the activated pathways and red blocked lines show the steps where

the particular proteins or their inhibitors are involved in the inhibition of the pathway. Inhibitors of these proteins or processes are marked in blue. (Modified from Johnsen, 2012).

In addition to estrogen induction, H4K12ac occupancy was also shown to be induced on the distinct ER $\alpha$  binding sites upon EGF signaling and implicated in the tamoxifen-resistant breast cancers (Lupien et al., 2010). Furthermore, a recent study shows that synergistic ER $\alpha$  degradation could be induced by JQ1 and Fulvestrant. This suggests a combinatorial effect in arresting tumor growth by increasing tumor sensitivity to growth inhibition and results in better survival in tamoxifen-resistant xenograft models (Feng et al., 2014). Similarly, our studies also show that prolonged BRD4 knockdown reduces ER $\alpha$  expression while short term BRD4 inhibition does not affect ER $\alpha$  mRNA or protein levels but still significantly inhibits estrogen-induced transcriptional pathways (Figure 2.I.S1J, 2.I.S4A). Considering the rapid reduction of H4K12ac by Fulvestrant in our study, this suggests a plausible role of H4K12ac occupancy in the progression of tamoxifen-resistance which could be consistent with the role of BRD4 (Feng et al., 2014). Consistently, HDAC inhibitors were shown to reverse tamoxifen/aromatase inhibitor-associated resistance in ER-positive breast cancers (Munster et al., 2011). This further supports an importance of histone acetylation in mediating tamoxifen-sensitivity in breast cancer. Furthermore, recent evidences show that HDAC inhibition acts synergistically with JQ1 in promoting apoptosis and tumor regression by affecting the same subset of gene targets synergistically (Bhadury et al., 2014; Fiskus et al., 2014). Mechanistically, this may mean that HDAC inhibition promotes hyperacetylation and likely makes the transcriptional machinery more sensitive to JQ1 inhibition. Hence, targeting histone acetylation and BRD4 could serve as a potential therapeutic strategy for the cells resistant to various treatments (Figure 3.2).

However, studies also report a role of BRD4 in suppressing metastasis and the progression of advanced breast cancers, thereby suggesting another, opposing tumor-suppressor function of BRD4 (Crawford et al., 2008; Alsarraj et al., 2011; Fernandez et al., 2014). However, BRD4 inhibition by IBET-151 which was previously shown to reduce tumor growth of primary leukemic cell lines in xenograft models did not affect the pulmonary metastasis in metastatic lung models (Dawson et al., 2011; Alsarraj et al., 2013). Further analyses have shown that the short isoform of BRD4 is associated with the nuclear membrane, possesses wider

acetylated histone binding properties and promotes metastasis by interacting with metastasis associated proteins (Alsarraj et al., 2013). Moreover, the short isoform of BRD4 was also shown to inhibit the DNA damage response by interacting with the Condensin complex and maintain a closed chromatin context. Inhibition of BRD4 along with radiation in various cancer cell lines resulted in the enhanced DNA damage response and survival of these cells (Floyd et al., 2013). From these studies, we can hypothesize that the spatial and nuclear distribution of BRD4 isoforms will significantly impact the therapeutic targeting of cancers. Considering the association of loss of H2Bub1 and BRD4 in cancer progression, considerable care should be taken in analyzing the repertoire of BRD2/3/4 isoforms expressed in the tumor before treating them with BRD4 inhibitors.

Overall our studies demonstrate a major attempt to understand the molecular epigenetic mechanisms promoting estrogen-induced transcription and proliferation or growth of breast and endometrial cancer cells. Given the importance of the H4K12ac-BRD4-P-TEFb-RNF40-H2Bub1 axis in estrogen-induced transcription, combination therapies inhibiting the function of individual protein involved in this paradigm may efficiently and specifically affect estrogen-dependent cancer progression (Figure 3.2). Consistently, the inhibitors available against these proteins were found to be effective in *in vitro* or *in vivo* models of induced gene transcription, and interestingly some of them were also successful with the combinatorial administration (Wakeling and Bowler, 1992; Prenzel et al., 2011; Munster et al., 2011; Hah et al., 2013; Nagarajan et al., 2014; Schrecengost et al., 2014; Fiskus et al., 2014; Feng et al., 2014; Bhadury et al., 2014). Xenograft studies in mice using the administration of these inhibitors in combination would further support the utility of targeting histone acetylation and BRD4 in the treatment of breast cancer. Considering the possible CDK9-independent function of BRD4 in regulating ER $\alpha$ -driven cancers, a therapeutic approach combining BRD4 inhibitors with CDK9 inhibitors may potentiate the survival of patients. Altogether, our study would greatly help in the development of combinatorial therapies involving the modulation of histone acetylation and BRD4 inhibition as a potential specific therapeutic strategy for inhibiting the estrogen-dependent growth in ER $\alpha$ -positive breast cancers.

## 4. Reference

- Ai, N., Hu, X., Ding, F., Yu, B., Wang, H., Lu, X., Zhang, K., Li, Y., Han, A., Lin, W., et al. (2011). Signal-induced Brd4 release from chromatin is essential for its role transition from chromatin targeting to transcriptional regulation. *Nucleic Acids Res.* *39*, 9592–9604.
- Aiyar, S.E., Sun, J., Blair, A.L., Moskaluk, C.A., Lu, Y., Ye, Q.-N., Yamaguchi, Y., Mukherjee, A., Ren, D., Handa, H., et al. (2004). Attenuation of estrogen receptor alpha-mediated transcription through estrogen-stimulated recruitment of a negative elongation factor. *Genes Dev.* *18*, 2134–2146.
- Albergaria, A., Paredes, J., Sousa, B., Milanezi, F., Carneiro, V., Bastos, J., Costa, S., Vieira, D., Lopes, N., Lam, E.W., et al. (2009). Expression of FOXA1 and GATA-3 in breast cancer: the prognostic significance in hormone receptor-negative tumours. *Breast Cancer Res.* *11*, R40.
- Allen, B.L., and Taatjes, D.J. (2015). The Mediator complex: a central integrator of transcription. *Nat. Rev. Mol. Cell Biol.* *16*, 155–166.
- Allfrey, V.G., Faulkner, R., and Mirsky, A.E. (1964). Acetylation and methylation of histones and their possible role in the regulation of RNA synthesis. *Proc. Natl. Acad. Sci. U. S. A.* *51*, 786–794.
- Alsarraj, J., Walker, R.C., Webster, J.D., Geiger, T.R., Crawford, N.P.S., Simpson, R.M., Ozato, K., and Hunter, K.W. (2011). Deletion of the proline-rich region of the murine metastasis susceptibility gene Brd4 promotes epithelial-to-mesenchymal transition- and stem cell-like conversion. *Cancer Res.* *71*, 3121–3131.
- Alsarraj, J., Faraji, F., Geiger, T.R., Mattaini, K.R., Williams, M., Wu, J., Ha, N.-H., Merlino, T., Walker, R.C., Bosley, A.D., et al. (2013). BRD4 Short Isoform Interacts with RRP1B, SIPA1 and Components of the LINC Complex at the Inner Face of the Nuclear Membrane. *PLoS ONE* *8*, e80746.
- Anand, P., Brown, J.D., Lin, C.Y., Qi, J., Zhang, R., Artero, P.C., Alaiti, M.A., Bullard, J., Alazem, K., Margulies, K.B., et al. (2013). BET Bromodomains Mediate Transcriptional Pause Release in Heart Failure. *Cell* *154*, 569–582.
- Anders, S., and Huber, W. (2010). Differential expression analysis for sequence count data. *Genome Biol.* *11*, R106.
- Arner, E., Daub, C.O., Vitting-Seerup, K., Andersson, R., Lilje, B., Drabløs, F., Lennartsson, A., Rönnblad, M., Hrydziszko, O., Vitezic, M., et al. (2015). Transcribed enhancers lead waves of coordinated transcription in transitioning mammalian cells. *Science* *347*, 1010–1014.
- Arpino, G., Weiss, H., Lee, A.V., Schiff, R., De Placido, S., Osborne, C.K., and Elledge, R.M. (2005). Estrogen receptor-positive, progesterone receptor-negative breast cancer: association with growth factor receptor expression and tamoxifen resistance. *J. Natl. Cancer Inst.* *97*, 1254–1261.
- Asangani, I.A., Dommeti, V.L., Wang, X., Malik, R., Cieslik, M., Yang, R., Escara-Wilke, J., Wilder-Romans, K., Dhanireddy, S., Engelke, C., et al. (2014). Therapeutic targeting of BET bromodomain proteins in castration-resistant prostate cancer. *Nature* *510*, 278–282.
- Baniahmad, C., Nawaz, Z., Baniahmad, A., Gleeson, M.A., Tsai, M.J., and O'Malley, B.W. (1995). Enhancement of human estrogen receptor activity by SPT6: a potential coactivator. *Mol. Endocrinol. Baltim. Md* *9*, 34–43.

- Baratta, M.G., Schinzel, A.C., Zwang, Y., Bandopadhyay, P., Bowman-Colin, C., Kutt, J., Curtis, J., Piao, H., Wong, L.C., Kung, A.L., et al. (2015). An in-tumor genetic screen reveals that the BET bromodomain protein, BRD4, is a potential therapeutic target in ovarian carcinoma. *Proc. Natl. Acad. Sci. U. S. A.* *112*, 232–237.
- Barbieri, I., Cannizzaro, E., and Dawson, M.A. (2013). Bromodomains as therapeutic targets in cancer. *Brief. Funct. Genomics* *elt007*.
- Barnett, D.H., Sheng, S., Charn, T.H., Waheed, A., Sly, W.S., Lin, C.-Y., Liu, E.T., and Katzenellenbogen, B.S. (2008). Estrogen Receptor Regulation of Carbonic Anhydrase XII through a Distal Enhancer in Breast Cancer. *Cancer Res.* *68*, 3505–3515.
- Bauer, U.-M., Daujat, S., Nielsen, S.J., Nightingale, K., and Kouzarides, T. (2002). Methylation at arginine 17 of histone H3 is linked to gene activation. *EMBO Rep.* *3*, 39–44.
- Beatson, G. (1896). On the treatment of inoperable cases of carcinoma of the mamma: Suggestions for a new method of treatment, with illustrative cases.1. *The Lancet* *148*, 104–107.
- Bedi, U. (2015). Regulation of H2B Monoubiquitination Pathway in Breast cancer. Georg August University Göttingen.
- Bedi, U., Scheel, A.H., Hennion, M., Begus-Nahrman, Y., Rüschoff, J., and Johnsen, S.A. (2015). SUPT6H controls estrogen receptor activity and cellular differentiation by multiple epigenomic mechanisms. *Oncogene* *34*, 465–473.
- Belandia, B., Orford, R.L., Hurst, H.C., and Parker, M.G. (2002). Targeting of SWI/SNF chromatin remodelling complexes to estrogen-responsive genes. *EMBO J.* *21*, 4094–4103.
- Belikov, S., Holmqvist, P.-H., Astrand, C., and Wrangé, Ö. (2012). FoxA1 and glucocorticoid receptor crosstalk via histone H4K16 acetylation at a hormone regulated enhancer. *Exp. Cell Res.* *318*, 61–74.
- Bhadury, J., Nilsson, L.M., Muralidharan, S.V., Green, L.C., Li, Z., Gesner, E.M., Hansen, H.C., Keller, U.B., McLure, K.G., and Nilsson, J.A. (2014). BET and HDAC inhibitors induce similar genes and biological effects and synergize to kill in Myc-induced murine lymphoma. *Proc. Natl. Acad. Sci.* *111*, E2721–E2730.
- Bhat-Nakshatri, P., Wang, G., Appaiah, H., Luktuke, N., Carroll, J.S., Geistlinger, T.R., Brown, M., Badve, S., Liu, Y., and Nakshatri, H. (2008). AKT alters genome-wide estrogen receptor alpha binding and impacts estrogen signaling in breast cancer. *Mol. Cell. Biol.* *28*, 7487–7503.
- Biçaku, E., Marchion, D.C., Schmitt, M.L., and Münster, P.N. (2008). Selective inhibition of histone deacetylase 2 silences progesterone receptor-mediated signaling. *Cancer Res.* *68*, 1513–1519.
- Bihani, T., Ezell, S.A., Ladd, B., Grosskurth, S.E., Mazzola, A.M., Pietras, M., Reimer, C., Zinda, M., Fawell, S., and D’Cruz, C.M. (2015). Resistance to everolimus driven by epigenetic regulation of MYC in ER+ breast cancers. *Oncotarget* *6*, 2407–2420.
- Blanco, J.C.G., Minucci, S., Lu, J., Yang, X.-J., Walker, K.K., Chen, H., Evans, R.M., Nakatani, Y., and Ozato, K. (1998). The histone acetylase PCAF is a nuclear receptor coactivator. *Genes Dev.* *12*, 1638–1651.

- Bonéy-Montoya, J., Ziegler, Y.S., Curtis, C.D., Montoya, J.A., and Nardulli, A.M. (2010). Long-range transcriptional control of progesterone receptor gene expression. *Mol. Endocrinol. Baltim. Md* **24**, 346–358.
- Bowers, E.M., Yan, G., Mukherjee, C., Orry, A., Wang, L., Holbert, M.A., Crump, N.T., Hazzalin, C.A., Liszczak, G., Yuan, H., et al. (2010). Virtual Ligand Screening of the p300/CBP Histone Acetyltransferase: Identification of a Selective Small Molecule Inhibitor. *Chem. Biol.* **17**, 471–482.
- Bretschneider, N., Kangaspeska, S., Seifert, M., Reid, G., Gannon, F., and Denger, S. (2008). E2-mediated cathepsin D (CTSD) activation involves looping of distal enhancer elements. *Mol. Oncol.* **2**, 182–190.
- Brisken, C., and O'Malley, B. (2010). Hormone Action in the Mammary Gland. *Cold Spring Harb. Perspect. Biol.* **2**, a003178.
- Britton, D.J., Hutcheson, I.R., Knowlden, J.M., Barrow, D., Giles, M., McClelland, R.A., Gee, J.M.W., and Nicholson, R.I. (2006). Bidirectional cross talk between ERalpha and EGFR signalling pathways regulates tamoxifen-resistant growth. *Breast Cancer Res. Treat.* **96**, 131–146.
- Carroll, J.S., Liu, X.S., Brodsky, A.S., Li, W., Meyer, C.A., Szary, A.J., Eeckhoute, J., Shao, W., Hestermann, E.V., Geistlinger, T.R., et al. (2005). Chromosome-wide mapping of estrogen receptor binding reveals long-range regulation requiring the forkhead protein FoxA1. *Cell* **122**, 33–43.
- Carroll, J.S., Meyer, C.A., Song, J., Li, W., Geistlinger, T.R., Eeckhoute, J., Brodsky, A.S., Keeton, E.K., Fertuck, K.C., Hall, G.F., et al. (2006). Genome-wide analysis of estrogen receptor binding sites. *Nat. Genet.* **38**, 1289–1297.
- Casa, A.J., Dearth, R.K., Litzenburger, B.C., Lee, A.V., and Cui, X. (2008). The type I insulin-like growth factor receptor pathway: a key player in cancer therapeutic resistance. *Front. Biosci. J. Virtual Libr.* **13**, 3273–3287.
- Chapuy, B., McKeown, M.R., Lin, C.Y., Monti, S., Roemer, M.G.M., Qi, J., Rahl, P.B., Sun, H.H., Yeda, K.T., Doench, J.G., et al. (2013). Discovery and Characterization of Super-Enhancer-Associated Dependencies in Diffuse Large B Cell Lymphoma. *Cancer Cell* **24**, 777–790.
- Chen, D., Ma, H., Hong, H., Koh, S.S., Huang, S.-M., Schurter, B.T., Aswad, D.W., and Stallcup, M.R. (1999). Regulation of Transcription by a Protein Methyltransferase. *Science* **284**, 2174–2177.
- Chen, D., Huang, S.-M., and Stallcup, M.R. (2000). Synergistic, p160 Coactivator-dependent Enhancement of Estrogen Receptor Function by CARM1 and p300. *J. Biol. Chem.* **275**, 40810–40816.
- Chiang, C.-M. (2009). Brd4 engagement from chromatin targeting to transcriptional regulation: selective contact with acetylated histone H3 and H4. *F1000 Biol. Rep.* **1**.
- Chiang, C.-M. (2014). Nonequivalent response to bromodomain-targeting BET inhibitors in oligodendrocyte cell fate decision. *Chem. Biol.* **21**, 804–806.
- Cicatiello, L., Mutarelli, M., Grober, O.M.V., Paris, O., Ferraro, L., Ravo, M., Tarallo, R., Luo, S., Schroth, G.P., Seifert, M., et al. (2010). Estrogen Receptor  $\alpha$  Controls a Gene Network in Luminal-Like Breast Cancer Cells Comprising Multiple Transcription Factors and MicroRNAs. *Am. J. Pathol.* **176**, 2113–2130.



- Cirillo, L.A., McPherson, C.E., Bossard, P., Stevens, K., Cherian, S., Shim, E.Y., Clark, K.L., Burley, S.K., and Zaret, K.S. (1998). Binding of the winged-helix transcription factor HNF3 to a linker histone site on the nucleosome. *EMBO J.* *17*, 244–254.
- Cirillo, L.A., Lin, F.R., Cuesta, I., Friedman, D., Jarnik, M., and Zaret, K.S. (2002). Opening of compacted chromatin by early developmental transcription factors HNF3 (FoxA) and GATA-4. *Mol. Cell* *9*, 279–289.
- Clark, K.L., Halay, E.D., Lai, E., and Burley, S.K. (1993). Co-crystal structure of the HNF-3/fork head DNA-recognition motif resembles histone H5. *Nature* *364*, 412–420.
- Clayton, A.L., Hazzalin, C.A., and Mahadevan, L.C. (2006). Enhanced Histone Acetylation and Transcription: A Dynamic Perspective. *Mol. Cell* *23*, 289–296.
- Coude, Marie M., Berrou, J., Bertrand, S., Riveiro, E., Herait, P., Baruchel, A., Dombret, H., and Gardin, C. (2013). Preclinical Study Of The Bromodomain Inhibitor OTX015 In Acute Myeloid (AML) and Lymphoid (ALL) Leukemias. *Blood* *122*, 4218–4218.
- Cowley, S.M., Hoare, S., Mosselman, S., and Parker, M.G. (1997). Estrogen Receptors  $\alpha$  and  $\beta$  Form Heterodimers on DNA. *J. Biol. Chem.* *272*, 19858–19862.
- Crawford, N.P.S., Alsarraj, J., Lukes, L., Walker, R.C., Officewala, J.S., Yang, H.H., Lee, M.P., Ozato, K., and Hunter, K.W. (2008). Bromodomain 4 activation predicts breast cancer survival. *Proc. Natl. Acad. Sci. U. S. A.* *105*, 6380–6385.
- Creighton, C.J., Massarweh, S., Huang, S., Tsimelzon, A., Hilsenbeck, S.G., Osborne, C.K., Shou, J., Malorni, L., and Schiff, R. (2008). Development of resistance to targeted therapies transforms the clinically associated molecular profile subtype of breast tumor xenografts. *Cancer Res.* *68*, 7493–7501.
- Creighton, M.P., Cheng, A.W., Welstead, G.G., Kooistra, T., Carey, B.W., Steine, E.J., Hanna, J., Lodato, M.A., Frampton, G.M., Sharp, P.A., et al. (2010). Histone H3K27ac separates active from poised enhancers and predicts developmental state. *Proc. Natl. Acad. Sci. U. S. A.* *107*, 21931–21936.
- Dawson, M.A., Prinjha, R.K., Dittmann, A., Giotopoulos, G., Bantscheff, M., Chan, W.-I., Robson, S.C., Chung, C., Hopf, C., Savitski, M.M., et al. (2011). Inhibition of BET recruitment to chromatin as an effective treatment for MLL-fusion leukaemia. *Nature* *478*, 529–533.
- Dekker, J. (2006). The three “C” s of chromosome conformation capture: controls, controls, controls. *Nat. Methods* *3*, 17–21.
- Delmore, J.E., Issa, G.C., Lemieux, M.E., Rahl, P.B., Shi, J., Jacobs, H.M., Kastiris, E., Gilpatrick, T., Paranal, R.M., Qi, J., et al. (2011). BET Bromodomain Inhibition as a Therapeutic Strategy to Target c-Myc. *Cell* *146*, 904–917.
- Demarest, S.J., Martinez-Yamout, M., Chung, J., Chen, H., Xu, W., Dyson, H.J., Evans, R.M., and Wright, P.E. (2002). Mutual synergistic folding in recruitment of CBP/p300 by p160 nuclear receptor coactivators. *Nature* *415*, 549–553.
- Deroo, B.J., and Korach, K.S. (2006). Estrogen receptors and human disease. *J. Clin. Invest.* *116*, 561–570.

- Devaiah, B.N., Lewis, B.A., Cherman, N., Hewitt, M.C., Albrecht, B.K., Robey, P.G., Ozato, K., Sims, R.J., and Singer, D.S. (2012). BRD4 is an atypical kinase that phosphorylates Serine2 of the RNA Polymerase II carboxy-terminal domain. *Proc. Natl. Acad. Sci.* *109*, 6927–6932.
- Donner, A.J., Ebmeier, C.C., Taatjes, D.J., and Espinosa, J.M. (2010). CDK8 is a positive regulator of transcriptional elongation within the serum response network. *Nat. Struct. Mol. Biol.* *17*, 194–201.
- Dover, J., Schneider, J., Boateng, M.A., Wood, A., Dean, K., Johnston, M., and Shilatifard, A. (2002). Methylation of histone H3 by COMPASS requires ubiquitination of histone H2B by RAD6. *J. Biol. Chem.*
- Dutertre, M., Gratadou, L., Dardenne, E., Germann, S., Samaan, S., Lidereau, R., Driouch, K., de la Grange, P., and Auboeuf, D. (2010). Estrogen regulation and physiopathologic significance of alternative promoters in breast cancer. *Cancer Res.* *70*, 3760–3770.
- Ebmeier, C.C., and Taatjes, D.J. (2010). Activator-Mediator binding regulates Mediator-cofactor interactions. *Proc. Natl. Acad. Sci.* *107*, 11283–11288.
- Eckert, R.L., Mullick, A., Rorke, E.A., and Katzenellenbogen, B.S. (1984). Estrogen Receptor Synthesis and Turnover in MCF-7 Breast Cancer Cells Measured by a Density Shift Technique. *Endocrinology* *114*, 629–637.
- Eeckhoutte, J., Keeton, E.K., Lupien, M., Krum, S.A., Carroll, J.S., and Brown, M. (2007). Positive Cross-Regulatory Loop Ties GATA-3 to Estrogen Receptor  $\alpha$  Expression in Breast Cancer. *Cancer Res.* *67*, 6477–6483.
- Elsheikh, S.E., Green, A.R., Rakha, E.A., Powe, D.G., Ahmed, R.A., Collins, H.M., Soria, D., Garibaldi, J.M., Paish, C.E., Ammar, A.A., et al. (2009). Global Histone Modifications in Breast Cancer Correlate with Tumor Phenotypes, Prognostic Factors, and Patient Outcome. *Cancer Res.* *69*, 3802–3809.
- Feng, Q., Zhang, Z., Shea, M.J., Creighton, C.J., Coarfa, C., Hilsenbeck, S.G., Lanz, R., He, B., Wang, L., Fu, X., et al. (2014). An epigenomic approach to therapy for tamoxifen-resistant breast cancer. *Cell Res.* *24*, 809–819.
- Ferlay, J., Soerjomataram, I., Dikshit, R., Eser, S., Mathers, C., Rebelo, M., Parkin, D.M., Forman, D., and Bray, F. (2015). Cancer incidence and mortality worldwide: Sources, methods and major patterns in GLOBOCAN 2012. *Int. J. Cancer* *136*, E359–E386.
- Fernandez, P., Scaffidi, P., Markert, E., Lee, J.-H., Rane, S., and Misteli, T. (2014). Transformation resistance in a premature aging disorder identifies a tumor-protective function of BRD4. *Cell Rep.* *9*, 248–260.
- Fierz, B., Chatterjee, C., McGinty, R.K., Bar-Dagan, M., Raleigh, D.P., and Muir, T.W. (2011). Histone H2B ubiquitylation disrupts local and higher-order chromatin compaction. *Nat. Chem. Biol.* *7*, 113–119.
- Filippakopoulos, P., and Knapp, S. (2014). Targeting bromodomains: epigenetic readers of lysine acetylation. *Nat. Rev. Drug Discov.* *13*, 337–356.
- Filippakopoulos, P., Qi, J., Picaud, S., Shen, Y., Smith, W.B., Fedorov, O., Morse, E.M., Keates, T., Hickman, T.T., Felletar, I., et al. (2010). Selective inhibition of BET bromodomains. *Nature* *468*, 1067–1073.

- Filippakopoulos, P., Picaud, S., Mangos, M., Keates, T., Lambert, J.-P., Barsyte-Lovejoy, D., Felletar, I., Volkmer, R., Müller, S., Pawson, T., et al. (2012). Histone Recognition and Large-Scale Structural Analysis of the Human Bromodomain Family. *Cell* *149*, 214–231.
- Fiskus, W., Sharma, S., Qi, J., Valenta, J.A., Schaub, L.J., Shah, B., Peth, K., Portier, B.P., Rodriguez, M., Devaraj, S.G.T., et al. (2014). Highly active combination of BRD4 antagonist and histone deacetylase inhibitor against human acute myelogenous leukemia cells. *Mol. Cancer Ther.* *13*, 1142–1154.
- Floyd, S.R., Pacold, M.E., Huang, Q., Clarke, S.M., Lam, F.C., Cannell, I.G., Bryson, B.D., Rameseder, J., Lee, M.J., Blake, E.J., et al. (2013). The bromodomain protein Brd4 insulates chromatin from DNA damage signalling. *Nature* *498*, 246–250.
- Frasor, J., Stossi, F., Danes, J.M., Komm, B., Lyttle, C.R., and Katzenellenbogen, B.S. (2004). Selective estrogen receptor modulators: discrimination of agonistic versus antagonistic activities by gene expression profiling in breast cancer cells. *Cancer Res.* *64*, 1522–1533.
- French, C.A., Miyoshi, I., Aster, J.C., Kubonishi, I., Kroll, T.G., Dal Cin, P., Vargas, S.O., Perez-Atayde, A.R., and Fletcher, J.A. (2001). BRD4 bromodomain gene rearrangement in aggressive carcinoma with translocation t(15;19). *Am. J. Pathol.* *159*, 1987–1992.
- French, C.A., Ramirez, C.L., Kolmakova, J., Hickman, T.T., Cameron, M.J., Thyne, M.E., Kutok, J.L., Toretsky, J.A., Tadavarthy, A.K., Kees, U.R., et al. (2008). BRD-NUT oncoproteins: a family of closely related nuclear proteins that block epithelial differentiation and maintain the growth of carcinoma cells. *Oncogene* *27*, 2237–2242.
- Fullwood, M.J., Liu, M.H., Pan, Y.F., Liu, J., Xu, H., Mohamed, Y.B., Orlov, Y.L., Velkov, S., Ho, A., Mei, P.H., et al. (2009). An oestrogen-receptor- $\alpha$ -bound human chromatin interactome. *Nature* *462*, 58–64.
- Galbraith, M.D., Allen, M.A., Bensard, C.L., Wang, X., Schwinn, M.K., Qin, B., Long, H.W., Daniels, D.L., Hahn, W.C., Dowell, R.D., et al. (2013). HIF1A Employs CDK8-Mediator to Stimulate RNAPII Elongation in Response to Hypoxia. *Cell* *153*, 1327–1339.
- García-Pedrero, J.M., Kiskinis, E., Parker, M.G., and Belandia, B. (2006). The SWI/SNF chromatin remodeling subunit BAF57 is a critical regulator of estrogen receptor function in breast cancer cells. *J. Biol. Chem.* *281*, 22656–22664.
- Green, K.A., and Carroll, J.S. (2007). Oestrogen-receptor-mediated transcription and the influence of co-factors and chromatin state. *Nat. Rev. Cancer* *7*, 713–722.
- Grunstein, M. (1997). Histone acetylation in chromatin structure and transcription. *Nature* *389*, 349–352.
- Hah, N., Murakami, S., Nagari, A., Danko, C.G., and Kraus, W.L. (2013). Enhancer transcripts mark active estrogen receptor binding sites. *Genome Res.* *23*, 1210–1223.
- Heintzman, N.D., Hon, G.C., Hawkins, R.D., Kheradpour, P., Stark, A., Harp, L.F., Ye, Z., Lee, L.K., Stuart, R.K., Ching, C.W., et al. (2009). Histone modifications at human enhancers reflect global cell-type-specific gene expression. *Nature* *459*, 108–112.
- Heinz, S., Romanoski, C.E., Benner, C., and Glass, C.K. (2015). The selection and function of cell type-specific enhancers. *Nat. Rev. Mol. Cell Biol.* *16*, 144–154.

- Herrmann, H., Blatt, K., Shi, J., Gleixner, K.V., Cerny-Reiterer, S., Müllauer, L., Vakoc, C.R., Sperr, W.R., Horny, H.-P., Bradner, J.E., et al. (2012). Small-molecule inhibition of BRD4 as a new potent approach to eliminate leukemic stem- and progenitor cells in acute myeloid leukemia AML. *Oncotarget* 3, 1588–1599.
- Ho, Y., Elefant, F., Liebhaber, S.A., and Cooke, N.E. (2006). Locus Control Region Transcription Plays an Active Role in Long-Range Gene Activation. *Mol. Cell* 23, 365–375.
- Hodges-Gallagher, L., Valentine, C.D., Bader, S.E., and Kushner, P.J. (2006). Inhibition of histone deacetylase enhances the anti-proliferative action of antiestrogens on breast cancer cells and blocks tamoxifen-induced proliferation of uterine cells. *Breast Cancer Res. Treat.* 105, 297–309.
- Hohmann, A.F., and Vakoc, C.R. (2014). A rationale to target the SWI/SNF complex for cancer therapy. *Trends Genet.* 30, 356–363.
- Hsieh, C.-L., Fei, T., Chen, Y., Li, T., Gao, Y., Wang, X., Sun, T., Sweeney, C.J., Lee, G.-S.M., Chen, S., et al. (2014). Enhancer RNAs participate in androgen receptor-driven looping that selectively enhances gene activation. *Proc. Natl. Acad. Sci. U. S. A.* 111, 7319–7324.
- Hu, Q., Luo, Z., Xu, T., Zhang, J.-Y., Zhu, Y., Chen, W.-X., Zhong, S.-L., Zhao, J.-H., and Tang, J.-H. (2014). FOXA1: a promising prognostic marker in breast cancer. *Asian Pac. J. Cancer Prev. APJCP* 15, 11–16.
- Hu, Y., Zhou, J., Ye, F., Xiong, H., Peng, L., Zheng, Z., Xu, F., Cui, M., Wei, C., Wang, X., et al. (2015). BRD4 Inhibitor Inhibits Colorectal Cancer Growth and Metastasis. *Int. J. Mol. Sci.* 16, 1928–1948.
- Hudelist, G., Czerwenka, K., Kubista, E., Marton, E., Pischinger, K., and Singer, C.F. (2003). Expression of sex steroid receptors and their co-factors in normal and malignant breast tissue: AIB1 is a carcinoma-specific co-activator. *Breast Cancer Res. Treat.* 78, 193–204.
- Hurtado, A., Holmes, K.A., Geistlinger, T.R., Hutcheson, I.R., Nicholson, R.I., Brown, M., Jiang, J., Howat, W.J., Ali, S., and Carroll, J.S. (2008). Regulation of ERBB2 by oestrogen receptor–PAX2 determines response to tamoxifen. *Nature* 456, 663–666.
- Hurtado, A., Holmes, K.A., Ross-Innes, C.S., Schmidt, D., and Carroll, J.S. (2011). FOXA1 is a critical determinant of Estrogen Receptor function and endocrine response. *Nat. Genet.* 43, 27–33.
- Ilott, N.E., Heward, J.A., Roux, B., Tsitsiou, E., Fenwick, P.S., Lenzi, L., Goodhead, I., Hertz-Fowler, C., Heger, A., Hall, N., et al. (2014). Long non-coding RNAs and enhancer RNAs regulate the lipopolysaccharide-induced inflammatory response in human monocytes. *Nat. Commun.* 5.
- Jenuwein, T., and Allis, C.D. (2001). Translating the histone code. *Science* 293, 1074–1080.
- Johnsen, S.A. (2012). The enigmatic role of H2Bub1 in cancer. *FEBS Lett.* 586, 1592–1601.
- Joseph, R., Orlov, Y.L., Huss, M., Sun, W., Kong, S.L., Ukil, L., Pan, Y.F., Li, G., Lim, M., Thomsen, J.S., et al. (2010). Integrative model of genomic factors for determining binding site selection by estrogen receptor- $\alpha$ . *Mol. Syst. Biol.* 6, 456.
- Jozwik, K.M., and Carroll, J.S. (2012). Pioneer factors in hormone-dependent cancers. *Nat. Rev. Cancer* 12, 381–385.

- Jung, M., Philpott, M., Müller, S., Schulze, J., Badock, V., Eberspächer, U., Moosmayer, D., Bader, B., Schmees, N., Fernández-Montalván, A., et al. (2014). Affinity Map of Bromodomain Protein 4 (BRD4) Interactions with the Histone H4 Tail and the Small Molecule Inhibitor JQ1. *J. Biol. Chem.* *289*, 9304–9319.
- Kagey, M.H., Newman, J.J., Bilodeau, S., Zhan, Y., Orlando, D.A., van Berkum, N.L., Ebmeier, C.C., Goossens, J., Rahl, P.B., Levine, S.S., et al. (2010). Mediator and cohesin connect gene expression and chromatin architecture. *Nature* *467*, 430–435.
- Kaikkonen, M.U., Spann, N.J., Heinz, S., Romanoski, C.E., Allison, K.A., Stender, J.D., Chun, H.B., Tough, D.F., Prinjha, R.K., Benner, C., et al. (2013). Remodeling of the enhancer landscape during macrophage activation is coupled to enhancer transcription. *Mol. Cell* *51*, 310–325.
- Kamei, Y., Xu, L., Heinzl, T., Torchia, J., Kurokawa, R., Gloss, B., Lin, S.C., Heyman, R.A., Rose, D.W., Glass, C.K., et al. (1996). A CBP integrator complex mediates transcriptional activation and AP-1 inhibition by nuclear receptors. *Cell* *85*, 403–414.
- Kanno, T., Kanno, Y., LeRoy, G., Campos, E., Sun, H.-W., Brooks, S.R., Vahedi, G., Heightman, T.D., Garcia, B.A., Reinberg, D., et al. (2014). BRD4 assists elongation of both coding and enhancer RNAs by interacting with acetylated histones. *Nat. Struct. Mol. Biol.* *21*, 1047–1057.
- Karolchik, D., Hinrichs, A.S., Furey, T.S., Roskin, K.M., Sugnet, C.W., Haussler, D., and Kent, W.J. (2004). The UCSC Table Browser data retrieval tool. *Nucleic Acids Res.* *32*, D493–D496.
- Karpiuk, O., Najafova, Z., Kramer, F., Hennion, M., Galonska, C., König, A., Snaidero, N., Vogel, T., Shchebet, A., Begus-Nahrman, Y., et al. (2012). The Histone H2B Monoubiquitination Regulatory Pathway Is Required for Differentiation of Multipotent Stem Cells. *Mol. Cell* *46*, 705–713.
- Katoh, M., and Katoh, M. (2004). Human FOX gene family (Review). *Int. J. Oncol.* *25*, 1495–1500.
- Ketchart, W., Ogba, N., Kresak, A., Albert, J.M., Pink, J.J., and Montano, M.M. (2011). HEXIM1 is a critical determinant of the response to tamoxifen. *Oncogene* *30*, 3563–3569.
- Kim, M.Y., Hsiao, S.J., and Kraus, W.L. (2001). A role for coactivators and histone acetylation in estrogen receptor  $\alpha$ -mediated transcription initiation. *EMBO J.* *20*, 6084–6094.
- Kim, T.-K., Hemberg, M., Gray, J.M., Costa, A.M., Bear, D.M., Wu, J., Harmin, D.A., Laptewicz, M., Barbara-Haley, K., Kuersten, S., et al. (2010). Widespread transcription at neuronal activity-regulated enhancers. *Nature* *465*, 182–187.
- Kininis, M., Isaacs, G.D., Core, L.J., Hah, N., and Kraus, W.L. (2009). Postrecruitment regulation of RNA polymerase II directs rapid signaling responses at the promoters of estrogen target genes. *Mol. Cell. Biol.* *29*, 1123–1133.
- Kobayashi, Y., Kitamoto, T., Masuhiro, Y., Watanabe, M., Kase, T., Metzger, D., Yanagisawa, J., and Kato, S. (2000). p300 Mediates Functional Synergism between AF-1 and AF-2 of Estrogen Receptor  $\alpha$  and  $\beta$  by Interacting Directly with the N-terminal A/B Domains. *J. Biol. Chem.* *275*, 15645–15651.
- Koch, F., Fenouil, R., Gut, M., Cauchy, P., Albert, T.K., Zacarias-Cabeza, J., Spicuglia, S., de la Chapelle, A.L., Heidemann, M., Hintermair, C., et al. (2011). Transcription initiation platforms and GTF recruitment at tissue-specific enhancers and promoters. *Nat. Struct. Mol. Biol.* *18*, 956–963.

- Korzus, E., Torchia, J., Rose, D.W., Xu, L., Kurokawa, R., McInerney, E.M., Mullen, T.-M., Glass, C.K., and Rosenfeld, M.G. (1998). Transcription Factor-Specific Requirements for Coactivators and Their Acetyltransferase Functions. *Science* 279, 703–707.
- Koutelou, E., Hirsch, C.L., and Dent, S.Y.R. (2010). Multiple faces of the SAGA complex. *Curr. Opin. Cell Biol.* 22, 374–382.
- Kumar, R., Zakharov, M.N., Khan, S.H., Miki, R., Jang, H., Toraldo, G., Singh, R., Bhasin, S., and Jasuja, R. (2011). The Dynamic Structure of the Estrogen Receptor. *J. Amino Acids* 2011, e812540.
- Lam, M.T.Y., Li, W., Rosenfeld, M.G., and Glass, C.K. (2014). Enhancer RNAs and regulated transcriptional programs. *Trends Biochem. Sci.* 39, 170–182.
- Lamoureux, F., Baud'huin, M., Rodriguez Calleja, L., Jacques, C., Berreur, M., Rédini, F., Lecanda, F., Bradner, J.E., Heymann, D., and Ory, B. (2014). Selective inhibition of BET bromodomain epigenetic signalling interferes with the bone-associated tumour vicious cycle. *Nat. Commun.* 5, 3511.
- Langmead, B., and Salzberg, S.L. (2012). Fast gapped-read alignment with Bowtie 2. *Nat. Methods* 9, 357–359.
- Langmead, B., Trapnell, C., Pop, M., and Salzberg, S.L. (2009). Ultrafast and memory-efficient alignment of short DNA sequences to the human genome. *Genome Biol.* 10, R25.
- Lee, A., and Yee, D. (1995). Insulin-like growth factors and breast cancer. *Biomed. Pharmacother.* 49, 415–421.
- Li, H., Handsaker, B., Wysoker, A., Fennell, T., Ruan, J., Homer, N., Marth, G., Abecasis, G., Durbin, R., and 1000 Genome Project Data Processing Subgroup (2009). The Sequence Alignment/Map format and SAMtools. *Bioinforma. Oxf. Engl.* 25, 2078–2079.
- Li, W., Notani, D., Ma, Q., Tanasa, B., Nunez, E., Chen, A.Y., Merkurjev, D., Zhang, J., Ohgi, K., Song, X., et al. (2013). Functional roles of enhancer RNAs for oestrogen-dependent transcriptional activation. *Nature* 498, 516–520.
- Li, X., Huang, J., Yi, P., Bambara, R.A., Hilf, R., and Muyan, M. (2004). Single-Chain Estrogen Receptors (ERs) Reveal that the ER $\alpha$ / $\beta$  Heterodimer Emulates Functions of the ER $\alpha$  Dimer in Genomic Estrogen Signaling Pathways. *Mol. Cell. Biol.* 24, 7681–7694.
- Liberzon, A., Subramanian, A., Pinchback, R., Thorvaldsdóttir, H., Tamayo, P., and Mesirov, J.P. (2011). Molecular signatures database (MSigDB) 3.0. *Bioinforma. Oxf. Engl.* 27, 1739–1740.
- Ling, J., Ainol, L., Zhang, L., Yu, X., Pi, W., and Tuan, D. (2004). HS2 enhancer function is blocked by a transcriptional terminator inserted between the enhancer and the promoter. *J. Biol. Chem.* 279, 51704–51713.
- Liu, M.H., and Cheung, E. (2014). Estrogen receptor-mediated long-range chromatin interactions and transcription in breast cancer. *Mol. Cell. Endocrinol.* 382, 624–632.
- Liu, L., Xu, Y., He, M., Zhang, M., Cui, F., Lu, L., Yao, M., Tian, W., Benda, C., Zhuang, Q., et al. (2014). Transcriptional pause release is a rate-limiting step for somatic cell reprogramming. *Cell Stem Cell* 15, 574–588.

- Liu, T., Ortiz, J.A., Taing, L., Meyer, C.A., Lee, B., Zhang, Y., Shin, H., Wong, S.S., Ma, J., Lei, Y., et al. (2011). Cistrome: an integrative platform for transcriptional regulation studies. *Genome Biol.* *12*, R83.
- Liu, W., Ma, Q., Wong, K., Li, W., Ohgi, K., Zhang, J., Aggarwal, A.K., and Rosenfeld, M.G. (2013). Brd4 and JMJD6-associated anti-pause enhancers in regulation of transcriptional pause release. *Cell* *155*, 1581–1595.
- Liu, Z., Wong, J., Tsai, S.Y., Tsai, M.-J., and O'Malley, B.W. (1999). Steroid receptor coactivator-1 (SRC-1) enhances ligand-dependent and receptor-dependent cell-free transcription of chromatin. *Proc. Natl. Acad. Sci. U. S. A.* *96*, 9485–9490.
- Lockwood, W.W., Zejnullahu, K., Bradner, J.E., and Varmus, H. (2012). Sensitivity of human lung adenocarcinoma cell lines to targeted inhibition of BET epigenetic signaling proteins. *Proc. Natl. Acad. Sci. U. S. A.* *109*, 19408–19413.
- Lovén, J., Hoke, H.A., Lin, C.Y., Lau, A., Orlando, D.A., Vakoc, C.R., Bradner, J.E., Lee, T.I., and Young, R.A. (2013). Selective Inhibition of Tumor Oncogenes by Disruption of Super-Enhancers. *Cell* *153*, 320–334.
- Luger, K., Mäder, A.W., Richmond, R.K., Sargent, D.F., and Richmond, T.J. (1997). Crystal structure of the nucleosome core particle at 2.8 Å resolution. *Nature* *389*, 251–260.
- Lumachi, F., Brunello, A., Maruzzo, M., Basso, U., and Basso, S. (2013). Treatment of Estrogen Receptor-Positive Breast Cancer. *Curr. Med. Chem.* *20*, 596–604.
- Lupien, M., Eeckhoute, J., Meyer, C.A., Krum, S.A., Rhodes, D.R., Liu, X.S., and Brown, M. (2009). Coactivator Function Defines the Active Estrogen Receptor Alpha Cistrome. *Mol. Cell. Biol.* *29*, 3413–3423.
- Lupien, M., Meyer, C.A., Bailey, S.T., Eeckhoute, J., Cook, J., Westerling, T., Zhang, X., Carroll, J.S., Rhodes, D.R., Liu, X.S., et al. (2010). Growth factor stimulation induces a distinct ER $\alpha$  cistrome underlying breast cancer endocrine resistance. *Genes Dev.* *24*, 2219–2227.
- Ma, H., Baumann, C.T., Li, H., Strahl, B.D., Rice, R., Jelinek, M.A., Aswad, D.W., Allis, C.D., Hager, G.L., and Stallcup, M.R. (2001). Hormone-dependent, CARM1-directed, arginine-specific methylation of histone H3 on a steroid-regulated promoter. *Curr. Biol.* *11*, 1981–1985.
- Mariño-Ramírez, L., Kann, M.G., Shoemaker, B.A., and Landsman, D. (2005). Histone structure and nucleosome stability. *Expert Rev. Proteomics* *2*, 719–729.
- Massarweh, S., Osborne, C.K., Creighton, C.J., Qin, L., Tsimelzon, A., Huang, S., Weiss, H., Rimawi, M., and Schiff, R. (2008). Tamoxifen resistance in breast tumors is driven by growth factor receptor signaling with repression of classic estrogen receptor genomic function. *Cancer Res.* *68*, 826–833.
- McLean, C.Y., Bristol, D., Hiller, M., Clarke, S.L., Schaar, B.T., Lowe, C.B., Wenger, A.M., and Bejerano, G. (2010). GREAT improves functional interpretation of cis-regulatory regions. *Nat. Biotechnol.* *28*, 495–501.
- Métivier, R., Penot, G., Hübner, M.R., Reid, G., Brand, H., Koš, M., and Gannon, F. (2003). Estrogen Receptor- $\alpha$  Directs Ordered, Cyclical, and Combinatorial Recruitment of Cofactors on a Natural Target Promoter. *Cell* *115*, 751–763.

- Métivier, R., Reid, G., and Gannon, F. (2006). Transcription in four dimensions: nuclear receptor-directed initiation of gene expression. *EMBO Rep.* *7*, 161–167.
- Micco, R.D., Fontanals-Cirera, B., Low, V., Ntziachristos, P., Yuen, S.K., Lovell, C.D., Dolgalev, I., Yonekubo, Y., Zhang, G., Rusinova, E., et al. (2014). Control of Embryonic Stem Cell Identity by BRD4-Dependent Transcriptional Elongation of Super-Enhancer-Associated Pluripotency Genes. *Cell Rep.* *9*, 234–247.
- Minsky, N., Shema, E., Field, Y., Schuster, M., Segal, E., and Oren, M. (2008). Monoubiquitinated H2B is associated with the transcribed region of highly expressed genes in human cells. *Nat. Cell Biol.* *10*, 483–488.
- Mirguet, O., Gosmini, R., Toum, J., Clément, C.A., Barnathan, M., Brusq, J.-M., Mordaunt, J.E., Grimes, R.M., Crowe, M., Pineau, O., et al. (2013). Discovery of epigenetic regulator I-BET762: lead optimization to afford a clinical candidate inhibitor of the BET bromodomains. *J. Med. Chem.* *56*, 7501–7515.
- Mitra, P., Pereira, L.A., Drabsch, Y., Ramsay, R.G., and Gonda, T.J. (2012). Estrogen receptor- $\alpha$  recruits P-TEFb to overcome transcriptional pausing in intron 1 of the MYB gene. *Nucleic Acids Res.* *40*, 5988–6000.
- Mochizuki, K., Nishiyama, A., Jang, M.K., Dey, A., Ghosh, A., Tamura, T., Natsume, H., Yao, H., and Ozato, K. (2008). The bromodomain protein Brd4 stimulates G1 gene transcription and promotes progression to S phase. *J. Biol. Chem.* *283*, 9040–9048.
- Morinière, J., Rousseaux, S., Steuerwald, U., Soler-López, M., Curtet, S., Vitte, A.-L., Govin, J., Gaucher, J., Sadoul, K., Hart, D.J., et al. (2009). Cooperative binding of two acetylation marks on a histone tail by a single bromodomain. *Nature* *461*, 664–668.
- Mosselman, S., Polman, J., and Dijkema, R. (1996). ER $\beta$ : Identification and characterization of a novel human estrogen receptor. *FEBS Lett.* *392*, 49–53.
- Muller, S., Filippakopoulos, P., and Knapp, S. (2011). Bromodomains as therapeutic targets. *Expert Rev. Mol. Med.* *13*, e29.
- Munster, P.N., Thurn, K.T., Thomas, S., Raha, P., Lacevic, M., Miller, A., Melisko, M., Ismail-Khan, R., Rugo, H., Moasser, M., et al. (2011). A phase II study of the histone deacetylase inhibitor vorinostat combined with tamoxifen for the treatment of patients with hormone therapy-resistant breast cancer. *Br. J. Cancer* *104*, 1828–1835.
- Nagarajan, S., Hossan, T., Alawi, M., Najafova, Z., Indenbirken, D., Bedi, U., Taipaleenmäki, H., Ben-Batalla, I., Scheller, M., Loges, S., et al. (2014). Bromodomain Protein BRD4 Is Required for Estrogen Receptor-Dependent Enhancer Activation and Gene Transcription. *Cell Rep.* *8*, 460–469.
- Nagarajan, S., Benito, E., Fischer, A., and Johnsen, S.A. (2015). H4K12ac is regulated by estrogen receptor-alpha and is associated with BRD4 function and inducible transcription. *Oncotarget* *5*.
- Nakshatri, H., and Badve, S. (2007). FOXA1 as a therapeutic target for breast cancer. *Expert Opin. Ther. Targets* *11*, 507–514.
- Narendra, V., Rocha, P.P., An, D., Raviram, R., Skok, J.A., Mazzoni, E.O., and Reinberg, D. (2015). CTCF establishes discrete functional chromatin domains at the Hox clusters during differentiation. *Science* *347*, 1017–1021.



- Natoli, G., and Andrau, J.-C. (2012). Noncoding transcription at enhancers: general principles and functional models. *Annu. Rev. Genet.* *46*, 1–19.
- Nicholson, R.I., Hutcheson, I.R., Knowlden, J.M., Jones, H.E., Harper, M.E., Jordan, N., Hiscox, S.E., Barrow, D., and Gee, J.M.W. (2004). Nonendocrine Pathways and Endocrine Resistance Observations with Antiestrogens and Signal Transduction Inhibitors in Combination. *Clin. Cancer Res.* *10*, 346s – 354s.
- Ogba, N., Chaplin, L.J., Doughman, Y.Q., Fujinaga, K., and Montano, M.M. (2008). HEXIM1 regulates 17beta-estradiol/estrogen receptor-alpha-mediated expression of cyclin D1 in mammary cells via modulation of P-TEFb. *Cancer Res.* *68*, 7015–7024.
- Ogryzko, V.V., Schiltz, R.L., Russanova, V., Howard, B.H., and Nakatani, Y. (1996). The Transcriptional Coactivators p300 and CBP Are Histone Acetyltransferases. *Cell* *87*, 953–959.
- Omoto, Y., Eguchi, H., Yamamoto-Yamaguchi, Y., and Hayashi, S. (2003). Estrogen receptor (ER) beta1 and ERbeta2 inhibit ERalpha function differently in breast cancer cell line MCF7. *Oncogene* *22*, 5011–5020.
- Onitilo, A.A., Engel, J.M., Greenlee, R.T., and Mukesh, B.N. (2009). Breast Cancer Subtypes Based on ER/PR and Her2 Expression: Comparison of Clinicopathologic Features and Survival. *Clin. Med. Res.* *7*, 4–13.
- Ott, C.J., Kopp, N., Bird, L., Paranal, R.M., Qi, J., Bowman, T., Rodig, S.J., Kung, A.L., Bradner, J.E., and Weinstock, D.M. (2012). BET bromodomain inhibition targets both c-Myc and IL7R in high-risk acute lymphoblastic leukemia. *Blood* *120*, 2843–2852.
- Pace, P., Taylor, J., Suntharalingam, S., Coombes, R.C., and Ali, S. (1997). Human estrogen receptor beta binds DNA in a manner similar to and dimerizes with estrogen receptor alpha. *J. Biol. Chem.* *272*, 25832–25838.
- Pan, Y.F., Wansa, K.D.S.A., Liu, M.H., Zhao, B., Hong, S.Z., Tan, P.Y., Lim, K.S., Bourque, G., Liu, E.T., and Cheung, E. (2008). Regulation of Estrogen Receptor-mediated Long Range Transcription via Evolutionarily Conserved Distal Response Elements. *J. Biol. Chem.* *283*, 32977–32988.
- Patel, M.C., Debrosse, M., Smith, M., Dey, A., Huynh, W., Sarai, N., Heightman, T.D., Tamura, T., and Ozato, K. (2013). BRD4 coordinates recruitment of pause release factor P-TEFb and the pausing complex NELF/DSIF to regulate transcription elongation of interferon-stimulated genes. *Mol. Cell. Biol.* *33*, 2497–2507.
- Pavri, R., Zhu, B., Li, G., Trojer, P., Mandal, S., Shilatifard, A., and Reinberg, D. (2006). Histone H2B monoubiquitination functions cooperatively with FACT to regulate elongation by RNA polymerase II. *Cell* *125*, 703–717.
- Peng, B., Lu, B., Leygue, E., and Murphy, L.C. (2003). Putative functional characteristics of human estrogen receptor-beta isoforms. *J. Mol. Endocrinol.* *30*, 13–29.
- Perillo, B., Ombra, M.N., Bertoni, A., Cuozzo, C., Sacchetti, S., Sasso, A., Chiariotti, L., Malorni, A., Abbondanza, C., and Avvedimento, E.V. (2008). DNA Oxidation as Triggered by H3K9me2 Demethylation Drives Estrogen-Induced Gene Expression. *Science* *319*, 202–206.
- Peterlin, B.M., and Price, D.H. (2006). Controlling the elongation phase of transcription with P-TEFb. *Mol. Cell* *23*, 297–305.

- Phillips, J.E., and Corces, V.G. (2009). CTCF: master weaver of the genome. *Cell* *137*, 1194–1211.
- Picaud, S., Da Costa, D., Thanasopoulou, A., Filippakopoulos, P., Fish, P.V., Philpott, M., Fedorov, O., Brennan, P., Bunnage, M.E., Owen, D.R., et al. (2013a). PFI-1, a highly selective protein interaction inhibitor, targeting BET Bromodomains. *Cancer Res.* *73*, 3336–3346.
- Picaud, S., Wells, C., Felletar, I., Brotherton, D., Martin, S., Savitsky, P., Diez-Dacal, B., Philpott, M., Bountra, C., Lingard, H., et al. (2013b). RVX-208, an inhibitor of BET transcriptional regulators with selectivity for the second bromodomain. *Proc. Natl. Acad. Sci. U. S. A.* *110*, 19754–19759.
- Ping, Y.-H., and Rana, T.M. (2001). DSIF and NELF Interact with RNA Polymerase II Elongation Complex and HIV-1 Tat Stimulates P-TEFb-mediated Phosphorylation of RNA Polymerase II and DSIF during Transcription Elongation. *J. Biol. Chem.* *276*, 12951–12958.
- Pirngruber, J., Shchebet, A., Schreiber, L., Shema, E., Minsky, N., Chapman, R.D., Eick, D., Aylon, Y., Oren, M., and Johnsen, S.A. (2009a). CDK9 directs H2B monoubiquitination and controls replication-dependent histone mRNA 3'-end processing. *EMBO Rep.* *10*, 894–900.
- Pirngruber, J., Shchebet, A., and Johnsen, S.A. (2009b). Insights into the function of the human P-TEFb component CDK9 in the regulation of chromatin modifications and co-transcriptional mRNA processing. *Cell Cycle Georget. Tex* *8*, 3636–3642.
- Prenzel, T., Begus-Nahrmann, Y., Kramer, F., Hennion, M., Hsu, C., Gorsler, T., Hintermair, C., Eick, D., Kremmer, E., Simons, M., et al. (2011). Estrogen-Dependent Gene Transcription in Human Breast Cancer Cells Relies upon Proteasome-Dependent Monoubiquitination of Histone H2B. *Cancer Res.* *71*, 1–15.
- Prenzel, T., Kramer, F., Bedi, U., Nagarajan, S., Beissbarth, T., and Johnsen, S.A. (2012). Cohesin is required for expression of the estrogen receptor-alpha (ESR1) gene. *Epigenetics Chromatin* *5*, 13.
- Rahman, S., Sowa, M.E., Ottinger, M., Smith, J.A., Shi, Y., Harper, J.W., and Howley, P.M. (2011). The Brd4 Extraterminal Domain Confers Transcription Activation Independent of pTEFb by Recruiting Multiple Proteins, Including NSD3. *Mol. Cell. Biol.* *31*, 2641–2652.
- Ramakrishnan, V. (1997). Histone structure and the organization of the nucleosome. *Annu. Rev. Biophys. Biomol. Struct.* *26*, 83–112.
- Ramírez, F., Dündar, F., Diehl, S., Grüning, B.A., and Manke, T. (2014). deepTools: a flexible platform for exploring deep-sequencing data. *Nucleic Acids Res.* gku365.
- Rhodes, J.M., McEwan, M., and Horsfield, J.A. (2011). Gene Regulation by Cohesin in Cancer: Is the Ring an Unexpected Party to Proliferation? *Mol. Cancer Res.* *9*, 1587–1607.
- Robinson, J.L.L., Holmes, K.A., and Carroll, J.S. (2013). FOXA1 mutations in hormone-dependent cancers. *Front. Oncol.* *3*, 20.
- Ross-Innes, C.S., Brown, G.D., and Carroll, J.S. (2011). A co-ordinated interaction between CTCF and ER in breast cancer cells. *BMC Genomics* *12*, 593.
- Ross-Innes, C.S., Stark, R., Teschendorff, A.E., Holmes, K.A., Ali, H.R., Dunning, M.J., Brown, G.D., Gojis, O., Ellis, I.O., Green, A.R., et al. (2012). Differential oestrogen receptor binding is associated with clinical outcome in breast cancer. *Nature* *481*, 389–393.

- Russo, J., and Russo, I.H. (2006). THE ROLE OF ESTROGEN IN THE INITIATION OF BREST CANCER. *J. Steroid Biochem. Mol. Biol.* *102*, 89–96.
- Sabnis, G.J., Goloubeva, O., Chumsri, S., Nguyen, N., Sukumar, S., and Brodie, A.M.H. (2011). Functional Activation of the Estrogen Receptor- $\alpha$  and Aromatase by the HDAC Inhibitor Entinostat Sensitizes ER-Negative Tumors to Letrozole. *Cancer Res.* *71*, 1893–1903.
- Sahai, V., Kumar, K., Knab, L.M., Chow, C.R., Raza, S.S., Bentrem, D.J., Ebine, K., and Munshi, H.G. (2014). BET bromodomain inhibitors block growth of pancreatic cancer cells in three-dimensional collagen. *Mol. Cancer Ther.* *13*, 1907–1917.
- Schaefer, C.F., Anthony, K., Krupa, S., Buchoff, J., Day, M., Hannay, T., and Buetow, K.H. (2009). PID: the Pathway Interaction Database. *Nucleic Acids Res.* *37*, D674–D679.
- Schmidt, D., Schwalie, P.C., Ross-Innes, C.S., Hurtado, A., Brown, G.D., Carroll, J.S., Flicek, P., and Odom, D.T. (2010). A CTCF-independent role for cohesin in tissue-specific transcription. *Genome Res.* *20*, 578–588.
- Schrecengost, R.S., Dean, J.L., Goodwin, J.F., Schiewer, M.J., Urban, M.W., Stanek, T.J., Sussman, R.T., Hicks, J.L., Birbe, R.C., Draganova-Tacheva, R.A., et al. (2014). USP22 regulates oncogenic signaling pathways to drive lethal cancer progression. *Cancer Res.* *74*, 272–286.
- Schröder, S., Cho, S., Zeng, L., Zhang, Q., Kaehlcke, K., Mak, L., Lau, J., Bisgrove, D., Schnölzer, M., Verdin, E., et al. (2012). Two-pronged binding with bromodomain-containing protein 4 liberates positive transcription elongation factor b from inactive ribonucleoprotein complexes. *J. Biol. Chem.* *287*, 1090–1099.
- Schurter, B.T., Koh, S.S., Chen, D., Bunick, G.J., Harp, J.M., Hanson, B.L., Henschen-Edman, A., Mackay, D.R., Stallcup, M.R., and Aswad, D.W. (2001). Methylation of Histone H3 by Coactivator-Associated Arginine Methyltransferase 1 $\dagger$ . *Biochemistry (Mosc.)* *40*, 5747–5756.
- Sengupta, S., Biarnes, M.C., and Jordan, V.C. (2014). Cyclin dependent kinase-9 mediated transcriptional de-regulation of cMYC as a critical determinant of endocrine-therapy resistance in breast cancers. *Breast Cancer Res. Treat.* *143*, 113–124.
- Sewack, G.F., Ellis, T.W., and Hansen, U. (2001). Binding of TATA Binding Protein to a Naturally Positioned Nucleosome Is Facilitated by Histone Acetylation. *Mol. Cell. Biol.* *21*, 1404–1415.
- Shang, Y., Hu, X., DiRenzo, J., Lazar, M.A., and Brown, M. (2000). Cofactor dynamics and sufficiency in estrogen receptor-regulated transcription. *Cell* *103*, 843–852.
- Sharp, Z.D., Mancini, M.G., Hinojos, C.A., Dai, F., Berno, V., Szafran, A.T., Smith, K.P., Lele, T.P., Lele, T.T., Ingber, D.E., et al. (2006). Estrogen-receptor- $\alpha$  exchange and chromatin dynamics are ligand- and domain-dependent. *J. Cell Sci.* *119*, 4101–4116.
- Shema, E., Tirosh, I., Aylon, Y., Huang, J., Ye, C., Moskovits, N., Raver-Shapira, N., Minsky, N., Pirngruber, J., Tarcic, G., et al. (2008). The histone H2B-specific ubiquitin ligase RNF20/hBRE1 acts as a putative tumor suppressor through selective regulation of gene expression. *Genes Dev.* *22*, 2664–2676.
- Shema-Yaacoby, E., Nikolov, M., Haj-Yahya, M., Siman, P., Allemand, E., Yamaguchi, Y., Muchardt, C., Urlaub, H., Brik, A., Oren, M., et al. (2013). Systematic identification of proteins binding to

- chromatin-embedded ubiquitylated H2B reveals recruitment of SWI/SNF to regulate transcription. *Cell Rep.* **4**, 601–608.
- Shi, J., Whyte, W.A., Zepeda-Mendoza, C.J., Milazzo, J.P., Shen, C., Roe, J.-S., Minder, J.L., Mercan, F., Wang, E., Eckersley-Maslin, M.A., et al. (2013). Role of SWI/SNF in acute leukemia maintenance and enhancer-mediated Myc regulation. *Genes Dev.* **27**, 2648–2662.
- Shi, J., Wang, Y., Zeng, L., Wu, Y., Deng, J., Zhang, Q., Lin, Y., Li, J., Kang, T., Tao, M., et al. (2014). Disrupting the interaction of BRD4 with diacetylated Twist suppresses tumorigenesis in basal-like breast cancer. *Cancer Cell* **25**, 210–225.
- Shi, J., Cao, J., and Zhou, B.P. (2015). Twist-BRD4 Complex: Potential Drug Target for Basal-like Breast Cancer. *Curr. Pharm. Des.* **21**, 1256–1261.
- Shiau, A.K., Barstad, D., Loria, P.M., Cheng, L., Kushner, P.J., Agard, D.A., and Greene, G.L. (1998). The structural basis of estrogen receptor/coactivator recognition and the antagonism of this interaction by tamoxifen. *Cell* **95**, 927–937.
- Shlyueva, D., Stampfel, G., and Stark, A. (2014). Transcriptional enhancers: from properties to genome-wide predictions. *Nat. Rev. Genet.* **15**, 272–286.
- Shou, J., Massarweh, S., Osborne, C.K., Wakeling, A.E., Ali, S., Weiss, H., and Schiff, R. (2004). Mechanisms of Tamoxifen Resistance: Increased Estrogen Receptor-HER2/neu Cross-Talk in ER/HER2-Positive Breast Cancer. *J. Natl. Cancer Inst.* **96**, 926–935.
- Sommer, S., and Fuqua, S.A.W. (2001). Estrogen receptor and breast cancer. *Semin. Cancer Biol.* **11**, 339–352.
- Spencer, T.E., Jenster, G., Burcin, M.M., Allis, C.D., Zhou, J., Mizzen, C.A., McKenna, N.J., Onate, S.A., Tsai, S.Y., Tsai, M.-J., et al. (1997). Steroid receptor coactivator-1 is a histone acetyltransferase. *Nature* **389**, 194–198.
- Stein, R.A., Chang, C.-Y., Kazmin, D.A., Way, J., Schroeder, T., Wergin, M., Dewhirst, M.W., and McDonnell, D.P. (2008). Estrogen-related receptor alpha is critical for the growth of estrogen receptor-negative breast cancer. *Cancer Res.* **68**, 8805–8812.
- Strahl, B.D., and Allis, C.D. (2000). The language of covalent histone modifications. *Nature* **403**, 41–45.
- Struhl, K. (1998). Histone acetylation and transcriptional regulatory mechanisms. *Genes Dev.* **12**, 599–606.
- Subramanian, A., Tamayo, P., Mootha, V.K., Mukherjee, S., Ebert, B.L., Gillette, M.A., Paulovich, A., Pomeroy, S.L., Golub, T.R., Lander, E.S., et al. (2005). Gene set enrichment analysis: a knowledge-based approach for interpreting genome-wide expression profiles. *Proc. Natl. Acad. Sci. U. S. A.* **102**, 15545–15550.
- Sun, J.M., Chen, H.Y., and Davie, J.R. (2001). Effect of estradiol on histone acetylation dynamics in human breast cancer cells. *J. Biol. Chem.* **276**, 49435–49442.
- Suzuki, A., Urushitani, H., Watanabe, H., Sato, T., Iguchi, T., Kobayashi, T., and Ohta, Y. (2007). Comparison of estrogen responsive genes in the mouse uterus, vagina and mammary gland. *J. Vet. Med. Sci. Jpn. Soc. Vet. Sci.* **69**, 725–731.

- Tamkun, J.W., Deuring, R., Scott, M.P., Kissinger, M., Pattatucci, A.M., Kaufman, T.C., and Kennison, J.A. (1992). *brahma*: a regulator of *Drosophila* homeotic genes structurally related to the yeast transcriptional activator SNF2/SWI2. *Cell* *68*, 561–572.
- Tan, S.K., Lin, Z.H., Chang, C.W., Varang, V., Chng, K.R., Pan, Y.F., Yong, E.L., Sung, W.K., and Cheung, E. (2011). AP-2 $\gamma$  regulates oestrogen receptor-mediated long-range chromatin interaction and gene transcription. *EMBO J.* *30*, 2569–2581.
- Theodorou, V., Stark, R., Menon, S., and Carroll, J.S. (2013). GATA3 acts upstream of FOXA1 in mediating ESR1 binding by shaping enhancer accessibility. *Genome Res.* *23*, 12–22.
- Thomas, S., Thurn, K.T., Biçaku, E., Marchion, D.C., and Münster, P.N. (2011). Addition of a histone deacetylase inhibitor redirects tamoxifen-treated breast cancer cells into apoptosis, which is opposed by the induction of autophagy. *Breast Cancer Res. Treat.* *130*, 437–447.
- Thomas, S., Thurn, K.T., Raha, P., Chen, S., and Munster, P.N. (2013). Efficacy of Histone Deacetylase and Estrogen Receptor Inhibition in Breast Cancer Cells Due to Concerted down Regulation of Akt. *PLoS ONE* *8*, e68973.
- Thorvaldsdóttir, H., Robinson, J.T., and Mesirov, J.P. (2013). Integrative Genomics Viewer (IGV): high-performance genomics data visualization and exploration. *Brief. Bioinform.* *14*, 178–192.
- Thurman, R.E., Rynes, E., Humbert, R., Vierstra, J., Maurano, M.T., Haugen, E., Sheffield, N.C., Stergachis, A.B., Wang, H., Vernot, B., et al. (2012). The accessible chromatin landscape of the human genome. *Nature* *489*, 75–82.
- Tuan, D., Kong, S., and Hu, K. (1992). Transcription of the hypersensitive site HS2 enhancer in erythroid cells. *Proc. Natl. Acad. Sci.* *89*, 11219–11223.
- Tzeng, D.Z., and Klinge, C.M. (1996). Phosphorylation of purified estradiol-liganded estrogen receptor by casein kinase II increases estrogen response element binding but does not alter ligand stability. *Biochem. Biophys. Res. Commun.* *223*, 554–560.
- Umehara, T., Nakamura, Y., Jang, M.K., Nakano, K., Tanaka, A., Ozato, K., Padmanabhan, B., and Yokoyama, S. (2010). Structural basis for acetylated histone H4 recognition by the human BRD2 bromodomain. *J. Biol. Chem.* *285*, 7610–7618.
- Underhill, C., Qutob, M.S., Yee, S.-P., and Torchia, J. (2000). A Novel Nuclear Receptor Corepressor Complex, N-CoR, Contains Components of the Mammalian SWI/SNF Complex and the Corepressor KAP-1. *J. Biol. Chem.* *275*, 40463–40470.
- Vietri Rudan, M., Barrington, C., Henderson, S., Ernst, C., Odom, D.T., Tanay, A., and Hadjur, S. (2015). Comparative Hi-C Reveals that CTCF Underlies Evolution of Chromosomal Domain Architecture. *Cell Rep.* *10*, 1297–1309.
- Vogel, V.G., Costantino, J.P., Wickerham, D.L., Cronin, W.M., Cecchini, R.S., Atkins, J.N., Bevers, T.B., Fehrenbacher, L., Pajon, E.R., Wade, J.L., et al. (2006). Effects of tamoxifen vs raloxifene on the risk of developing invasive breast cancer and other disease outcomes: the NSABP Study of Tamoxifen and Raloxifene (STAR) P-2 trial. *JAMA* *295*, 2727–2741.
- Voss, T.C., and Hager, G.L. (2014). Dynamic regulation of transcriptional states by chromatin and transcription factors. *Nat. Rev. Genet.* *15*, 69–81.

- Wagner, S., Weber, S., Kleinschmidt, M.A., Nagata, K., and Bauer, U.-M. (2006). SET-mediated Promoter Hypoacetylation Is a Prerequisite for Coactivation of the Estrogen-responsive pS2 Gene by PRMT1. *J. Biol. Chem.* *281*, 27242–27250.
- Wakeling, A.E., and Bowler, J. (1992). ICI 182,780, a new antioestrogen with clinical potential. *J. Steroid Biochem. Mol. Biol.* *43*, 173–177.
- Wang, D., Garcia-Bassets, I., Benner, C., Li, W., Su, X., Zhou, Y., Qiu, J., Liu, W., Kaikkonen, M.U., Ohgi, K.A., et al. (2011). Reprogramming transcription by distinct classes of enhancers functionally defined by eRNA. *Nature* *474*, 390–394.
- Wang, Y.-H., Sui, Y.-N., Yan, K., Wang, L.-S., Wang, F., and Zhou, J.-H. (2015). BRD4 promotes pancreatic ductal adenocarcinoma cell proliferation and enhances gemcitabine resistance. *Oncol. Rep.* *33*, 1699–1706.
- Webb, P., Nguyen, P., Shinsako, J., Anderson, C., Feng, W., Nguyen, M.P., Chen, D., Huang, S.-M., Subramanian, S., McKinerney, E., et al. (1998). Estrogen Receptor Activation Function 1 Works by Binding p160 Coactivator Proteins. *Mol. Endocrinol.* *12*, 1605–1618.
- Weihua, Z., Saji, S., Mäkinen, S., Cheng, G., Jensen, E.V., Warner, M., and Gustafsson, J.A. (2000). Estrogen receptor (ER) beta, a modulator of ERalpha in the uterus. *Proc. Natl. Acad. Sci. U. S. A.* *97*, 5936–5941.
- Welboren, W.-J., van Driel, M.A., Janssen-Megens, E.M., van Heeringen, S.J., Sweep, F.C., Span, P.N., and Stunnenberg, H.G. (2009). ChIP-Seq of ERalpha and RNA polymerase II defines genes differentially responding to ligands. *EMBO J.* *28*, 1418–1428.
- Williams, C., Edvardsson, K., Lewandowski, S.A., Ström, A., and Gustafsson, J.-A. (2008). A genome-wide study of the repressive effects of estrogen receptor beta on estrogen receptor alpha signaling in breast cancer cells. *Oncogene* *27*, 1019–1032.
- Wittmann, B.M., Fujinaga, K., Deng, H., Ogba, N., and Montano, M.M. (2005). The breast cell growth inhibitor, estrogen down regulated gene 1, modulates a novel functional interaction between estrogen receptor alpha and transcriptional elongation factor cyclin T1. *Oncogene* *24*, 5576–5588.
- Wrenn, C.K., and Katzenellenbogen, B.S. (1993). Structure-function analysis of the hormone binding domain of the human estrogen receptor by region-specific mutagenesis and phenotypic screening in yeast. *J. Biol. Chem.* *268*, 24089–24098.
- Wu, S.-Y., and Chiang, C.-M. (2007). The double bromodomain-containing chromatin adaptor Brd4 and transcriptional regulation. *J. Biol. Chem.* *282*, 13141–13145.
- Wu, S.-Y., Lee, A.-Y., Hou, S.Y., Kemper, J.K., Erdjument-Bromage, H., Tempst, P., and Chiang, C.-M. (2006). Brd4 links chromatin targeting to HPV transcriptional silencing. *Genes Dev.* *20*, 2383–2396.
- Wu, S.-Y., Lee, A.-Y., Lai, H.-T., Zhang, H., and Chiang, C.-M. (2013). Phospho switch triggers Brd4 chromatin binding and activator recruitment for gene-specific targeting. *Mol. Cell* *49*, 843–857.
- Xiao, X., Cai, M., Chen, J., Guan, X., Kung, H., Zeng, Y., and Xie, D. (2011). High Expression of p300 in Human Breast Cancer Correlates with Tumor Recurrence and Predicts Adverse Prognosis. *Chin. J. Cancer Res.* *23*, 201–207.

- Xu, Y., and Vakoc, C.R. (2014). Brd4 is on the move during inflammation. *Trends Cell Biol.* *24*, 615–616.
- Xu, W., Cho, H., Kadam, S., Banayo, E.M., Anderson, S., Yates, J.R., Emerson, B.M., and Evans, R.M. (2004). A methylation-mediator complex in hormone signaling. *Genes Dev.* *18*, 144–156.
- Yamaguchi, Y., Takagi, T., Wada, T., Yano, K., Furuya, A., Sugimoto, S., Hasegawa, J., and Handa, H. (1999). NELF, a Multisubunit Complex Containing RD, Cooperates with DSIF to Repress RNA Polymerase II Elongation. *Cell* *97*, 41–51.
- Yang, J., Mani, S.A., Donaher, J.L., Ramaswamy, S., Itzykson, R.A., Come, C., Savagner, P., Gitelman, I., Richardson, A., and Weinberg, R.A. (2004). Twist, a Master Regulator of Morphogenesis, Plays an Essential Role in Tumor Metastasis. *Cell* *117*, 927–939.
- Yang, Z., Yik, J.H.N., Chen, R., He, N., Jang, M.K., Ozato, K., and Zhou, Q. (2005). Recruitment of P-TEFb for stimulation of transcriptional elongation by the bromodomain protein Brd4. *Mol. Cell* *19*, 535–545.
- Yi, P., Wang, Z., Feng, Q., Pintilie, G.D., Foulds, C.E., Lanz, R.B., Ludtke, S.J., Schmid, M.F., Chiu, W., and O'Malley, B.W. (2015). Structure of a Biologically Active Estrogen Receptor-Coactivator Complex on DNA. *Mol. Cell* *57*, 1047–1058.
- Zhang, F., and Yu, X. (2011). WAC, a functional partner of RNF20/40, regulates histone H2B ubiquitination and gene transcription. *Mol. Cell* *41*, 384–397.
- Zhang, W., Prakash, C., Sum, C., Gong, Y., Li, Y., Kwok, J.J.T., Thiessen, N., Pettersson, S., Jones, S.J.M., Knapp, S., et al. (2012a). Bromodomain-containing protein 4 (BRD4) regulates RNA polymerase II serine 2 phosphorylation in human CD4+ T cells. *J. Biol. Chem.* *287*, 43137–43155.
- Zhang, Y., Liu, T., Meyer, C.A., Eeckhoute, J., Johnson, D.S., Bernstein, B.E., Nusbaum, C., Myers, R.M., Brown, M., Li, W., et al. (2008). Model-based analysis of ChIP-Seq (MACS). *Genome Biol.* *9*, R137.
- Zhang, Y., Liang, J., Li, Y., Xuan, C., Wang, F., Wang, D., Shi, L., Zhang, D., and Shang, Y. (2010). CCCTC-binding factor acts upstream of FOXA1 and demarcates the genomic response to estrogen. *J. Biol. Chem.* *285*, 28604–28613.
- Zhang, Y., Chen, A., Yan, X.-M., and Huang, G. (2012b). Disordered epigenetic regulation in MLL-related leukemia. *Int. J. Hematol.* *96*, 428–437.
- Zhou, Q., Atadja, P., and Davidson, N.E. (2007). Histone deacetylase inhibitor LBH589 reactivates silenced estrogen receptor alpha (ER) gene expression without loss of DNA hypermethylation. *Cancer Biol. Ther.* *6*, 64–69.
- Zhou, V.W., Goren, A., and Bernstein, B.E. (2011). Charting histone modifications and the functional organization of mammalian genomes. *Nat. Rev. Genet.* *12*, 7–18.
- Zippo, A., Serafini, R., Rocchigiani, M., Pennacchini, S., Krepelova, A., and Oliviero, S. (2009). Histone Crosstalk between H3S10ph and H4K16ac Generates a Histone Code that Mediates Transcription Elongation. *Cell* *138*, 1122–1136.

Zou, Z., Huang, B., Wu, X., Zhang, H., Qi, J., Bradner, J., Nair, S., and Chen, L.-F. (2014). Brd4 maintains constitutively active NF- $\kappa$ B in cancer cells by binding to acetylated RelA. *Oncogene* 33, 2395–2404.

Zuber, J., Shi, J., Wang, E., Rappaport, A.R., Herrmann, H., Sison, E.A., Magoon, D., Qi, J., Blatt, K., Wunderlich, M., et al. (2011). RNAi screen identifies Brd4 as a therapeutic target in acute myeloid leukaemia. *Nature* 478, 524–528.



## 5. Acknowledgement

I sincerely convey my heartfelt gratitude to Prof. Dr. Steven A Johnsen, Clinic for General, Visceral and Pediatric surgery, University Medical center Gottingen, for allowing me to work in his excellent and well equipped laboratory, and giving an extraordinary scientific environment. It was a great honor to work with him and I am really privileged to have his support, love and guidance in everything needed for my graduate studies.

I also take this opportunity to convey my heartfelt thanks to my thesis committee members, Prof. Dr. Dieter Kube and Dr. Halyna Shcherbata for their kind suggestions and guidance throughout the project.

I would like to thank German Academic Exchange Service (DAAD) for supporting me financially throughout the end of my degree and Göttingen Graduate School for Neurosciences, Biophysics, and Molecular Biosciences (GGNB) for giving me the opportunity to do my Ph.D. studies in Germany.

I thank Tareq Hossan, Zeynab Najafova, Dr. Upasana Bedi, Dr. Vijayalakshmi Kari and Dr. Tanja Prenzel for providing me an excellent guidance and discussions during my experiments and a great moral support in the laboratory. I am deeply thankful to Dr. Malik Alawi for their careful guidance and suggestions for bioinformatics analyses during my project. I am thankful to Prof. Dr. Hans Will and all my lab members for their love and cooperation.

I would like to thank our collaborators, Prof. Dr. Sonja Loges, Prof. Dr. Eric Hesse, Prof. Dr. Adam Grundhoff and Prof. Dr. Andre Fischer for timely help, cooperation and support. I would like to convey my deepest gratitude to Prof. Stefan Knapp and Dr. Cheng-Ming Chiang for the timely help with reagents.

It is very hard to mention all my friends as a list. I am very grateful to Mrs. Katja Shivani, Oliva Saldanha, Nekkanti Yelha Phanikumar, Priyadarshini Arunachalam, Vinodh Ilangovan, Karthikeyan Annamalai, Zulfaquar Ahmad Arfi, Mrs. Mandira Sen, Vijaybabu Manickam and other friends for their love, efforts, caring,

invaluable help, blessings, support and encouragement during all the situations and at every step of my stay in Germany.

I will be failing my duty if I do not mention about my mother, Mrs. Dhanalakshmi Nagarajan, and my special and cute sisters, Mrs. Saranya Nagarajan and Iswarya Ramu, who taught me to handle the difficult situations. My special thanks to all my teachers and well-wishers who taught me to work hard and supported me during my work.

Last but not least I thank the divine soul of my father for showing his blessings on me always and for making everything possible.

## 6. Curriculum Vitae

### SANKARI NAGARAJAN

Rosenbachweg 12-311, 37075 Göttingen, Germany.

Email : [snagara1@gwdg.de](mailto:snagara1@gwdg.de) , [sankari.nam10san@gmail.com](mailto:sankari.nam10san@gmail.com)

Mobile: +4915171357766

#### EDUCATION:

- **Ph.D.** Molecular Biology of Cells 2011 - Present  
Göttingen Graduate School for Neurosciences, Biophysics, and Molecular Biosciences (**GGNB**), Georg-August-Universität Göttingen, Germany.
- **M.Sc., Bio-Medical Science**, 2010 (Five year Integrated) CGPA: 8.31  
Bharathidasan University, Trichy, India. **First Rank Holder**

#### COMPETITIVE FELLOWSHIPS HELD:

- German Academic Exchange Service (**DAAD**) PhD scholarship – October 2011 to March 2015.
- **JRF-UGC: CSIR** (Junior research Fellowship-United Grants Commission: Council of Scientific and Industrial Research) test in June 2010. All India Rank **266**.
- **93.3** percentile in Graduate Aptitude Test in Engineering (**GATE-2010**) in Biotechnology.

#### RESEARCH EXPERIENCE:

- **10/2011 - Present** **Ph.D.**  
5/2014 – Present Department of General, Visceral and Pediatric Surgery, University Medical Center Göttingen, Germany.  
7/2012 – 4/2014 Institute for Tumor Biology, University Hospital Hamburg-Eppendorf, Hamburg, Germany  
10/2011 – 6/2012 Department of Molecular Oncology, University Medical Center Göttingen, Germany  
**Supervisor:** Prof. Dr. Steven A. Johnsen  
**Project:** Investigation into the Epigenetic Role of histone acetylation and BRD4 in Breast Cancers.
- 07/2010 – 12/2010 **Junior Research Fellow**  
10/2009 – 03/2010 **Project Trainee, M.Sc., Dissertation**  
**Supervisor:** Prof. Ramaswamy Subramanian, Institute for Stem Cell Biology and Regenerative Medicine, Bangalore, India  
**Project:** Structural and Functional Studies of Caenorhabditis elegans' Rieske Oxygenase System

#### PUBLICATIONS:

- **Nagarajan S**, Benito E, Fischer A, Johnsen SA, H4K12ac is regulated by estrogen receptor-alpha and is associated with BRD4 function and inducible transcription, **Oncotarget**, 2015 (Epub ahead of print).
- Chen NM, Singh G, Koenig A, Liou GY, Storz P, Zhang JS, Regul L, **Nagarajan S**, Kühnemuth B, Johnsen SA, Hebrok M, Siveke J, Billadeau DD, Ellenrieder V, Hessmann E, NFATC1 Links EGFR Signaling to Induction of Sox9 Transcription and Acinar-Ductal Transdifferentiation in the Pancreas, **Gastroenterology**, 2015 (Epub ahead of print).

- **Nagarajan S**, Hossan T, Alawi M, Najafova Z, Indenbirken D, Bedi U, Taipaleenmäki H, Ben-Batalla I, Scheller M, Loges S, Knapp S, Hesse E, Chiang C-M, Grundhoff A, Johnsen SA, Bromodomain Protein BRD4 Is Required for Estrogen Receptor-Dependent Enhancer Activation and Gene Transcription, *Cell Reports* 2014, **8** (2), 460-469.
- Prenzel T, Kramer F, Bedi U, **Nagarajan S**, Beissbarth T, Johnsen SA, Cohesin is required for expression of the estrogen receptor-alpha (*ESR1*) gene, *Epigenetics & Chromatin* 2012, **5**:13.

**PRESENTATIONS:**

- **Invited speaker**, 7<sup>th</sup> PhD Minisymposium, Epigenetic reader proteins in differentiation and malignancies, Integrated Research Training Group, "Epigenetics and Chromatin" TRR81, Marburg, Germany, 20 November 2014.  
Title: BRD4 is essential for estrogen receptor-mediated transcription in breast cancers.
- **Poster presentation**, 11<sup>th</sup> EMBL conference on Transcription and Chromatin, Heidelberg, Germany, 23-26 August, 2014.
- **Oral presentation**, Collaborative Research Centre 992 Medical Epigenetics Symposium, Freiburg, Germany, 7-9 April, 2014.  
Title: BRD4 is essential for estrogen-induced transcription in ER<sup>+</sup> breast cancers.
- **Poster presentation**, Keystone Symposia: Nuclear Receptors - Biological Networks, Genome Dynamics and Disease, Taos, New Mexico, USA, 10-15 January, 2014.
- **Poster presentation**, 10<sup>th</sup> EMBL conference on Transcription and Chromatin, Heidelberg, Germany, 25-28 August, 2012.

**LABORATORY TECHNIQUES KNOWN****Molecular Biology and Bioinformatics:**

- Chromatin immunoprecipitation and sequencing (ChIP-seq), RNA sequencing, library preparation for Illumina, chromosomal conformation capture (3C), chromatin fractionation
- Conventional PCR, quantitative PCR, cloning techniques
- SDS-PAGE, 2D gel electrophoresis, Western blotting
- RNA-seq and ChIP-seq analysis tools- Linux and R tools, GSEA, DAVID, Galaxy, Cistrome, CLC genomics workbench, UCSC Genome Browser, IGV, RSA tools- peak-motifs.

**PERSONAL PROFILE:**

**Gender** : Female  
**Date of Birth** : 19.05.1988  
**Nativity** : Indian

**REFERENCE:**

Prof. Dr. Steven A Johnsen,  
 Department of General, Visceral and Pediatric  
 Surgery, University Medical Center Göttingen,  
 37075 Göttingen, Germany.  
 E.mail ID: [steven.johnsen@med.uni-goettingen.de](mailto:steven.johnsen@med.uni-goettingen.de)

Prof. Dr. Hans Will,  
 Institute for Tumor Biology,  
 University Hospital Hamburg-Eppendorf,  
 20246 Hamburg, Germany.  
 E.mail ID: [hanskilianwill@gmail.com](mailto:hanskilianwill@gmail.com)

Prof. Ramaswamy Subramanian,  
 Dean, inSTEM,  
 National Centre for Biological Sciences,  
 Bangalore-560065, India.  
 E.mail ID: [ramas@ncbs.res.in](mailto:ramas@ncbs.res.in)

Dr. Sashidhar Mulugu, Associate Professor,  
 Department of Bio Medical Science,  
 Chair, School of Basic Medical Sciences,  
 Bharathidasan University, Trichy- 620024, India.  
 E.mail ID: [sashibms@yahoo.com](mailto:sashibms@yahoo.com)